

**Synaptic modulation in the dorsal cochlear nucleus:  
a biological substrate of tinnitus**

Thesis submitted for the degree of

Doctor of Philosophy

at the University of Leicester

by

**Thomas Tagoe**

Department of Cell Physiology and Pharmacology

University of Leicester

2013

# Synaptic modulation in the dorsal cochlear nucleus: a biological substrate of tinnitus

Thomas Tagoe

Acoustic over exposure (AOE) triggers hearing loss alongside a decreased excitability in the dorsal cochlear nucleus (DCN) within 3 to 5 days post exposure. On a longer time scale (from 6 weeks onwards) AOE can also generate phantom auditory perceptions known as tinnitus alongside a spontaneous hyperactivity in the DCN. The delayed onset of this hyperactivity relative to the early onset of hearing loss and decreased excitability suggests intermediate plastic changes in the DCN that remain to be identified.

The first aim of this thesis was to identify *in vitro*, AOE-induced changes in synaptic plasticity within the DCN that could underlie the subsequent development of tinnitus. The second aim was to identify means of reversing the *in vitro* changes in synaptic plasticity triggered by AOE. The final aim was to test whether reversing the identified AOE-induced changes in synaptic plasticity could prevent the onset of tinnitus.

Wistar rats were exposed to a loud (110 dB SPL) single tone (15 kHz) for a period of 9 hours (AOE protocol). Auditory brainstem response recordings performed 3 to 5 days later showed a significant increase of the rat's hearing threshold for frequencies above 8 kHz. Field potential recordings of auditory nerve compound action potentials revealed a decreased amplitude and conduction velocity which was confirmed using computational modelling studies. Whole cell recordings of auditory nerve evoked excitatory post synaptic currents (EPSCs) revealed a decrease in EPSC amplitudes after AOE due to a decreased number of release sites. Field potential recordings of parallel fibre evoked activity performed 3 to 5 days following AOE showed that AOE prevented the induction of long term potentiation (LTP) otherwise observed at multisensory DCN synapses. Whole cell recordings of parallel fibre evoked EPSCs in fusiform cells revealed this to be due to an increased release probability after AOE. Perfusion of D-AP5 (an NMDA receptor antagonist) promoted the induction of LTP otherwise deficient after AOE. Perfusion of D-AP5 or elevating the concentration of magnesium in the extracellular medium decreased the release probability after AOE.

Based on these findings, subsets of rats were placed on a high magnesium diet (in combination with magnesium injections) immediately after AOE. This reduced the behavioural evidence of tinnitus measured as deficits in silent gap detection.

In conclusion, following AOE, the absence of LTP induction in the DCN due to an increased release probability constitutes an *in vitro* deficit prior to the later onset of tinnitus. Decreasing release probability at DCN multisensory synapses after AOE allowed AOE induced tinnitus to be targeted and reversed in an animal model.

## ACKNOWLEDGMENTS

I would first like to thank my supervisor Dr. Martine Hamann for her direction and support, especially at times when this was done at her own personal expense. Without her this project will not be a success. In particular, I would like to thank her for allowing me this opportunity; I have experienced a lot of growth in both knowledge and character over the course of this PhD.

I would also like to thank Prof. Nick Hartell and Prof. Robert Fern for sitting on my supervisory panel and always offering useful suggestions and perspectives on this project.

I am grateful to Dr. Volko Straub and Dr. Jennifer Linden for examining this thesis; I hope it proves to be a good read.

My thanks also go to past and current members of this lab for their vital contributions: Dr. Nadia Pilati, Dr. Bavan Sasikandarajah, Dr. Julie-Myrtille Bourgognon, Matt Barker and especially Daniel Deeping for playing the role of my personal editor.

I am also grateful to Dr. Revers Donga, Prof. Nick Hartell and the Head of Department Dr. Blair Grubb for their advice and support in my time of need. I would like to also express gratitude to Dr. Mike Mulheran for allowing me the use of his equipment.

I will also like to thank 'Action on Hearing Loss' for funding this project. A special thanks also goes to staff of the Biomedical Services, particularly Carl Breacker, Anthony Oakden, Ken White, Dave White and Debbie Bursnall. I would also like to thank David Jones, John Rowley and staff of the Electronic and Mechanical workshop. All these individuals went above and beyond their call of duty.

I want to thank my family for being such a blessing and seeing the silver lining in every dark cloud. Thanks also to all my friends in and out of the Department, particularly Benedicta Gyampem, for continued moral support.

Last but not least I would like to thank God Almighty for helping me defy a few odds to reach the end, I can't take credit for that.

# Table of Contents

---

List of figures .....	ix
-----------------------	----

Abbreviations list .....	xiv
--------------------------	-----

## INTRODUCTION

<b>I.1. The auditory system .....</b>	<b>2</b>
I.1.1. Physical properties of sound.....	2
I.1.2. The peripheral auditory system.....	3
I.1.3. The central auditory system .....	6
<b>I.2. The dorsal cochlear nucleus .....</b>	<b>8</b>
I.2.1. Structural organisation of the dorsal cochlear nucleus.....	8
I.2.2. Synaptic integration in the dorsal cochlear nucleus.....	10
<b>I.3. Deficits related to the auditory system.....</b>	<b>13</b>
I.3.1. Hearing loss.....	13
I.3.2. Tinnitus .....	15
<b>I.4. The dorsal cochlear nucleus and its role in tinnitus.....</b>	<b>18</b>
I.4.1. Synaptic plasticity in the central nervous system .....	18
I.4.2. Role of DCN in hearing loss and tinnitus.....	19

## MATERIALS AND METHODS

<b>II.1. Subjects.....</b>	<b>24</b>
<b>II. 2. <i>In vitro</i> methodology .....</b>	<b>24</b>
II.2.1. Cresyl violet staining.....	24
II.2.2. Dissection and slicing.....	25
II.2.3. Electrophysiological recording setup .....	27
II.2.4. Stimulating and recording electrodes .....	29
II.2.5. Perfusion of solutions .....	29
II.2.6. Extracellular field potential recordings .....	30
II. 2.6.1. Analysis of field potentials .....	30
II.2.6.2. Separation of the pre- and postsynaptic components .....	31
II.2.6.3. Determination of the conduction velocity.....	32

II.2.6.4. Stimulus intensity relationships.....	33
II.2.6.5. Paired pulse facilitation .....	34
II.2.6.6. Long term potentiation of field potentials .....	34
II.2.6.7. Pharmacological tests under field potential recordings .....	35
II.2.7. Whole cell recordings .....	35
II.2.7.1. Whole cell voltage clamp technique .....	35
II.2.7.2. Intracellular solutions .....	37
II.2.7.3. Recording excitatory postsynaptic currents .....	37
II.2.7.4. Functional segregation of synaptic pathways .....	37
II.2.7.5. Stimulation of synaptic inputs .....	39
II.2.7.6. Quantal analysis .....	39
<b>II.3. <i>In vivo</i> methodology .....</b>	<b>42</b>
II.3.1. Anaesthesia and sedation.....	42
II.3.2. Acoustic overexposure .....	43
II.3.3. Auditory brainstem response recordings .....	44
II.3.3.1. The recording setup.....	44
II.3.3.2. Analysis .....	45
II.3.4. Tinnitus screening via the gap detection method .....	48
II.3.5. The gap detection setup .....	49
II.3.5.1. The Panlab gap detection setup .....	49
II.3.5.2. The Kinder Scientific gap detection setup .....	50
II.3.6. Gap detection protocols .....	51
<b>II.4. Modelling .....</b>	<b>53</b>
<b>II.5. Experimental conditions .....</b>	<b>54</b>
<b>II.6. Calibration of acoustic equipment .....</b>	<b>55</b>
<b>II.7. Statistical tests.....</b>	<b>56</b>

## CHAPTER 1

### **Effects of acoustic overexposure on action potential propagation and synaptic responses evoked by auditory nerve stimulations**

1.1.	INTRODUCTION: Effects of acoustic overexposure .....	59
1.2.	RESULTS.....	60
1.2.1.	A typical effect of acoustic overexposure on ABRs .....	60
1.2.2.	Effect of acoustic overexposure on ABR peak 'I' amplitude.....	62
1.2.3.	Effects of acoustic overexposure on ABR peak 'I' latency.....	63
1.2.4.	Effects of acoustic overexposure on hearing thresholds .....	64
1.2.5.	Effects on auditory nerve compound action potentials.....	65
1.2.6.	Effects on fusiform cell excitatory postsynaptic currents .....	68
1.2.7.	Effects of acoustic overexposure on presynaptic release .....	69
1.3.	DISCUSSION .....	72
1.3.1.	Characteristics of ABR properties in the unexposed condition.....	72
1.3.2.	Changes in auditory brainstem response properties .....	72
1.3.3.	Effect of AOE on the compound action potentials.....	75
1.3.4.	Is hearing loss linked to deficits identified in the DCN? .....	79
1.3.5.	Is tinnitus linked to auditory nerve action potential deficits?.....	83
1.4.	CONCLUSION .....	85

## CHAPTER 2

### **Effects of acoustic overexposure on synaptic responses evoked by multisensory input stimulations**

2.1.	INTRODUCTION .....	88
2.2.	RESULTS.....	89
2.2.1.	Characterisation of field potentials .....	89
2.2.2.	Effect of acoustic overexposure on evoked field potentials and paired pulse facilitation .....	93
2.2.3.	Effect of acoustic overexposure on long term synaptic plasticity.....	96
2.2.4.	Mechanisms underlying long term potentiation.....	97
2.2.5.	Mechanism underlying a lack of LTP after exposure to loud sound .....	102
2.2.6.	Modulation of release probability in the dorsal cochlear nucleus.....	105
2.2.7.	Quantal analysis of evoked excitatory postsynaptic currents.....	107

2.3.	DISCUSSION.....	113
2.3.1.	Interpretation of field potential recordings .....	113
2.3.2.	Plasticity in the dorsal cochlear nucleus.....	114
2.3.3.	Effects of acoustic overexposure on synaptic properties.....	119
2.3.4.	Effects of acoustic overexposure on induction of plasticity.....	124
2.3.5.	Role of NMDA receptors in hearing loss and tinnitus .....	126
2.4.	CONCLUSION .....	129

### **CHAPTER 3**

#### **Modulation of synaptic activity in the dorsal cochlear nucleus: a biomarker for tinnitus?**

3.1.	INTRODUCTION .....	131
3.2.	RESULTS.....	132
3.2.1.	Effects of memantine and MgCl <sub>2</sub> injections in unexposed rats.....	132
3.2.2.	Effect of memantine injections following exposure to loud sound .....	135
3.2.3.	Effects of MgCl <sub>2</sub> injections following exposure to loud sound .....	136
3.2.4.	Effects of magnesium threonate diet .....	137
3.2.5.	Effects of combined delivery of magnesium .....	141
3.2.5.1.	Effects on hearing thresholds .....	141
3.2.5.2.	Effects on gap detection .....	144
3.3.	DISCUSSION.....	152
3.3.1.	Gap detection deficits as a means to quantify tinnitus.....	152
3.3.2.	Age related changes to hearing loss and gap detection.....	153
3.3.3.	Induction of hearing loss and gap detection deficits.....	155
3.3.4.	<i>In vitro</i> markers of tinnitus .....	158
3.4.	CONCLUSION .....	161
	<b>DISCUSSION.....</b>	<b>162</b>
	<b>APPENDICES.....</b>	<b>169</b>
	<b>REFERENCES.....</b>	<b>172</b>

## List of tables

### INTRODUCTION

**Table I.1:** Guidelines of maximum safe exposure times in relation to sound intensity. (Pg.14)

### Materials and methods

**Table II.1:** Acoustic driver calibration. (Pg.56)

### CHAPTER 1

**Table 1.1:** Average hearing thresholds. (Pg. 63)

### CHAPTER 3

**Table 3.1:** Absence of memantine or magnesium injections effects on hearing thresholds of unexposed rats. (Pg. 133)

**Table 3.2:** Gap detection ratios recorded at 12 weeks following AOE protocol (Pg. 138)

## List of figures

### INTRODUCTION

**Figure I.1:** Sound represented as a sinusoidal waveform (Pg.2)

**Figure I.2:** The peripheral auditory system. (Pg.3)

**Figure I.3:** Scanning electron micrograph. (Pg.4)

**Figure I.4:** Functional properties of hair cells. (Pg. 5)

**Figure I.5:** The auditory pathway. (Pg. 7)

**Figure I.6:** Schematic representation of synaptic connections within the dorsal cochlear nucleus. (Pg.9)

### MATERIALS AND METHODS

**Figure II.1:** The slicing procedure. (Pg.26)

**Figure II.2:** Electrophysiological setup. (Pg.28)

**Figure II.3:** Field potential response components. (Pg.30)

**Figure II.4:** Cresyl violet image showing positioning of stimulating and recording electrodes. (Pg.32)

**Figure II.5:** Stimulation of the auditory nerve fibres specifically activates AN synaptic inputs. (Pg.38)

**Figure II.6:** Acoustic overexposure setup. (Pg.43)

**Figure II.7:** Placement of the acoustic driver and the recording electrodes. (Pg.44)

**Figure II.8:** Auditory brainstem response recording setup. (Pg.45)

**Figure II.9:** Identifying the hearing threshold using ABRs. (Pg.46)

**Figure II.10:** Analysis of auditory brainstem responses. (Pg.47)

**Figure II.11:** Attenuation of the acoustic startle reflex. (Pg.49)

**Figure II.12:** Kinder scientific gap detection setup. (Pg.50)

## CHAPTER 1

**Figure 1.1:** Acoustic overexposure raises the hearing threshold. (Pg.61)

**Figure 1.2:** Acoustic overexposure decreases the peak I amplitude at specific frequencies. (Pg.62)

**Figure 1.3:** Acoustic overexposure increases the latency to peak I. (Pg.63)

**Figure 1.4:** Effects of acoustic overexposure on hearing threshold shifts. (Pg.65)

**Figure 1.5:** Acoustic overexposure decreases the size of AN (presynaptic) field potentials. (Pg.66)

**Figure 1.6:** Acoustic overexposure decreases the length for which AN field potentials could be recorded. (Pg.66)

**Figure 1.7:** Acoustic overexposure decreases the conduction velocity of action potentials. (Pg.67)

**Figure 1.8:** Multiple AN morphological deficits contribute towards a decreased conduction velocity. (Pg.68)

**Figure 1.9:** Acoustic overexposure decreases AN evoked EPSCs in fusiform cells. (Pg.68)

**Figure 1.10:** Lack of paired pulse facilitation at AN synapses. (Pg.70)

**Figure 1.11:** Acoustic overexposure decreases the number of release sites at AN synapses. (Pg.71)

**Figure 1.12:** Summary of AOE induced deficits along the auditory nerve. (Pg.85)

## CHAPTER 2

**Figure 2.1:** Identification of field potential response components. (Pg.89)

**Figure 2.2:** Separating field potentials into pre- and post-synaptic components. (Pg.90)

**Figure 2.3:** D-AP5 blocks a delayed response. (Pg.91)

**Figure 2.4:** Recordings from differential positions along the transverse axis of the DCN. (Pg.92)

**Figure 2.5:** Selective recording of the pre-synaptic volley allows the conduction velocity of the parallel fibres to be measured. (Pg.93)

**Figure 2.6:** Effect of stimulation intensity on the pre-and post-synaptic field potentials. (Pg.94)

**Figure 2.7:** Acoustic overexposure abolishes paired pulse facilitation of post-synaptic responses evoked by parallel fibre stimulation. (Pg.95)

**Figure 2.8:** Acoustic overexposure abolishes LTP induction by HFS. (Pg.97)

**Figure 2.9:** Long term potentiation is accompanied by a decrease in the paired pulse ratio of the post-synaptic N2 response. (Pg.98)

**Figure 2.10:** LTP is evoked at sub maximal stimulation intensities. (Pg.99)

**Figure 2.11:** Multiple high frequency stimulations do not induce further potentiation in the unexposed condition. (Pg.100)

**Figure 2.12:** Effect of NBQX on the long term potentiation of postsynaptic field potentials in the unexposed condition. (Pg.100)

**Figure 2.13:** Addition of D-AP5 abolishes the LTP induced by high frequency stimulation. (Pg.101)

**Figure 2.14:** Induction of LTP by high frequency stimulation is independent of NMDA receptor activation. (Pg.102)

**Figure 2.15:** Addition of D-AP5 after HFS restores paired pulse facilitation in the overexposed condition. (Pg.102)

**Figure 2.16:** Perfusing 10 mM Mg<sup>2+</sup> 30 minutes after HFS reduces the normalised N2 amplitude after acoustic overexposure. (Pg.103)

**Figure 2.17:** Multiple HFs do not alter the N2 response in the overexposed condition. (Pg.104)

**Figure 2.18:** Addition of D-AP5 leads to the induction of LTP by high frequency stimulation in the overexposed condition. (Pg.104)

**Figure 2.19:** Modulation of LTP via the alteration of extracellular calcium concentration. (Pg.106)

**Figure 2.20:** Input-output relationships are unaffected by AOE. (Pg.107)

**Figure 2.21:** Paired pulse facilitation of EPSCs evoked by parallel fibre stimulations in unexposed and overexposed conditions. (Pg.108)

**Figure 2.22:** Schematic representation of the two protocols used to measure the release probability. (Pg.109)

**Figure 2.23:** Acoustic overexposure leads to an increased presynaptic release probability. (Pg.110)

**Figure 2.24:** D-AP5 addition after HFS decreases the synaptic release probability. (Pg.111)

### CHAPTER 3

**Figure 3.1:** *In vivo* memantine or Mg<sup>2+</sup> administration leaves the hearing threshold in unexposed animals unaffected. (Pg.132)

**Figure 3.2:** The input-output relationship in the DCN of unexposed animals is unaltered by memantine or magnesium injections. (Pg.134)

**Figure 3.3:** Induction of LTP by HFS persists following *in vivo* memantine or magnesium injections. (Pg.134)

**Figure 3.4:** Hearing threshold shifts and absence of LTP in the DCN after AOE persists following administration of memantine. (Pg.135)

**Figure 3.5:** Partial protection against hearing loss and absence of LTP following Mg<sup>2+</sup> injections. (Pg.137)

**Figure 3.6:** Absence of *in vivo* and *in vitro* effects following a high Mg<sup>2+</sup> diet in unexposed rats. (Pg.139)

**Figure 3.7:** The high MgT diet promotes induction of LTP in the DCN following AOE. (Pg.140)

**Figure 3.8:** Effects of combined magnesium delivery on hearing thresholds of unexposed rats. (Pg.141)

**Figure 3.9:** Effects of combined magnesium delivery on hearing thresholds four days following acoustic overexposure. (Pg.142)

**Figure 3.10:** Effects of combined magnesium treatment on hearing thresholds of rats at multiple times following acoustic overexposure. (Pg.143)

**Figure 3.11:** Effects of combined magnesium delivery on the gap detection within a BBN background. (Pg.144)

**Figure 3.12:** Changes in GDRs overtime in all conditions and at various frequencies. (Pg.146)

**Figure 3.13:** Effects of acoustic overexposure on GDR for specific background frequencies. (Pg.147)

**Figure 3.14:** Gap detection abilities and deficits expressed over time at various frequencies for each animal. **(Pg.148)**

**Figure 3.15:** Gap detection abilities expressed as a percentage of detections per animal. **(Pg.149)**

**Figure 3.16:** Table summarising the effects of the treatments on gap detection ratios using LMM tests of fixed effects. **(Pg.150)**

**Figure 3.17:** Reduced gap detection deficits in AOEMgC rats. **(Pg.151)**

**Figure 3.18:** Lack of correlation between hearing threshold and GDR. **(Pg.152)**

## Abbreviations list

**ABR:** Auditory brainstem responses

**AC:** Auditory cortex

**aCSF:** Artificial cerebrospinal fluid

**ADC:** Analogue to digital converter

**AMPA:**  $\alpha$ -amino-3-hydroxy-5-methyl-4-isoxazolepropionic acid

**AN:** Auditory nerve

**AOE:** Acoustic overexposure

**AOEMem:** Overexposed animals treated with memantine injections

**AOEMg:** Overexposed animals treated with magnesium injections

**AOEMgC:** Overexposed animals treated with magnesium injections and diet

**AOEMgT:** Overexposed animals put on high magnesium diet

**BBN:** Broadband noise

**CAP:** Compound action potential

**CCD:** Charge coupled device

**CV:** Conduction velocity

**CV<sup>2</sup>:** (Coefficient of variation)<sup>2</sup>

**D-AP5:** D-(-)-2-Amino-5-phosphonopentanoic acid

**dB:** Decibels

**dB SIL:** Decibel sound intensity level

**dB SPL:** Decibel sound pressure level

**dB V:** Decibel Volts

**DCN:** Dorsal cochlear nucleus

**DPOAE:** Distortion product otoacoustic emissions

**DPX:** Dibutyl phthalate xylene

**EPSC:** Excitatory postsynaptic current

**FL:** Fusiform layer

**GABA:**  $\gamma$ -Aminobutyric acid

**GDR:** Gap detection ratio

**HFS:** High frequency stimulation

**IC:** Inferior colliculus

**IHC:** Inner hair cells

**LL:** Lateral lemniscus

**LMM:** Linear mixed model

**LSO:** Lateral superior olivary complex

**LTD:** Long term depression

**LTP:** Long term potentiation

**MAPKs:** Mitogen activated protein kinases

**mGluR:** Metabotropic glutamate receptor

**Mem:** Memantine

**MGN:** Medial geniculate nucleus

**MgC:** Combined magnesium treatment

**MgT:** Magnesium threonate

**ML:** Molecular layer

**MNTB:** Medial nucleus of the trapezoid body

**MSO:** Medial superior olivary complex

**NBQX:** 2,3-dioxo-6-nitro-1,2,3,4-tetrahydrobenzo[f]quinoxaline-7-sulfonamide

**NMDA:** N-Methyl-D-aspartic acid

**N:** Number of release sites

**NS:** Non significant

**OHC:** Outer hair cells

**P:** Release probability

**PPF:** Paired pulse facilitation

**PPR:** Paired pulse ratio

**P<sub>ref</sub>:** Sound pressure level in air

**PTP:** Post tetanic potentiation

**Q:** Quantal size

**RM:** Repeated measures

**STIM:** Stimulation electrode

**SEM:** Standard error of the mean

**SNK:** Student-Newman-Keuls

**SR:** Startle response

**STDP:** Spike timing dependent plasticity

**TTX:** Tetrodotoxin

**Un:** Unexposed animals

**UnMem:** Unexposed animals treated with memantine injections

**UnMg:** Unexposed animals treated with magnesium injections

**UnMgC:** Unexposed animals treated with magnesium injections and diet

**UnMgT:** Unexposed animals put on high magnesium diet

**VCN:** Ventral cochlear nucleus

**VGluT:** Vesicular glutamate transporter

**VM:** Variance-Mean

# **I. INTRODUCTION**

## I.1. The auditory system

The auditory pathway is responsible for enabling our perception of sound. It stretches from the pinna of the outer ear to the auditory cortex where sound processing is achieved. The auditory system is divided into two pathways: the peripheral auditory system which is responsible for transforming the mechanical stimulation of the sound waves into action potentials and the central auditory system which processes the generated action potentials and retrieves the information it encodes.

### I.1.1. Physical properties of sound

Sound can exist as a sinusoidal waveform travelling through a medium with two measurable components: The frequency (measured in Hz) which is related to sound pitch and the amplitude which is related to loudness (*Fig. I.1*).

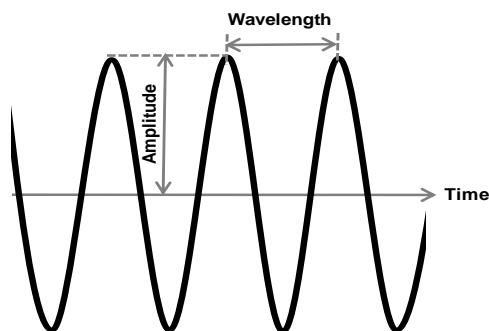


**Figure I.1: Sound represented as a sinusoidal waveform.** The measurable components of the sound wave have been indicated. The sound intensity can be measured as the peak to peak amplitude. The frequency is measured as the number of complete waves per second.

The amplitude of a sound wave is more commonly expressed as decibels (dB) relative to a specific or implied reference level. This can be in volts (dB V), sound intensity level (dB SIL) or sound pressure level (dB SPL). When travelling through air the implied reference is the sound pressure level. Under these circumstances the sound intensity is calculated as shown:

$$dB\ SPL = 20 \times \log \left( \frac{P}{P_{ref}} \right)$$

where 'P' is the pressure exerted by the sound and 'P<sub>ref</sub>' is sound pressure level in air (20 µPascals). All sound measurements in this report will be referred to as dB SPL.

### I.1.2. The peripheral auditory system

The peripheral auditory system is inclusive of all structures involved in sound processing from the pinna of the outer ear to the hair cells of the inner ear (Fig. I.2). Sound channelled into the ear canal by the pinna causes vibrations of the tympanic membrane which transmits these vibrations to the ossicles (malleus, incus and stapes) of the middle ear. These ossicles convert low pressure sound vibrations into high pressure sound vibrations, necessary to progress through the fluid (endolymph and perilymph) filled chambers of the inner ear (Merchant, 1997). The organ of Corti within the cochlea contains inner and outer hair cells lying on a thin basilar membrane which are responsible for the electrical transduction of sound waves.

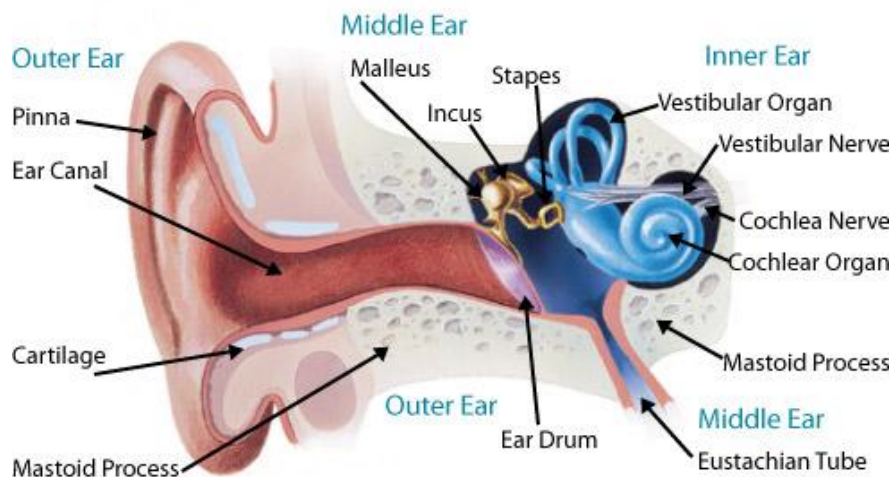


**Figure I.2. The peripheral auditory system.** Sound waves are channelled down the auditory canal and directly vibrate the ear drum (tympanic membrane). Vibrations are transferred via the three ossicles of the middle ear (malleus, incus and stapes) to the cochlea. The organ of Corti is located in the cochlea where inner and outer hair cells respond to mechanical stimulations induced by the sound waves. Glutamate is released at the hair cell roots onto spiral ganglion neurons which propagate action potentials along the auditory nerve (AN). Picture adapted from <http://www.alpinehearingprotection.com/>

Inner hair cells (IHCs) form a single row of cells covering the entire length of the cochlea and are innervated by myelinated spiral ganglion cells also known as type I primary auditory neurons. These neurons represent more than 90% of the spiral ganglion cell population that project to the cochlear nucleus in the central auditory system (Berglund and Ryugo, 1987, Brown, 1987, Echteler, 1992) and are involved in the transduction of sound into action potentials. On the other hand, outer hair cells (OHCs) run parallel to the IHCs in three rows (*Fig. I.3*) and are innervated by unmyelinated spiral ganglion cells also known as type II primary auditory neurons (Berglund and Ryugo, 1987, Brown, 1987, Echteler, 1992). These neurons represent only a small proportion (10%) of the auditory nerve propagating to the cochlear nucleus (Berglund and Ryugo, 1987, Brown, 1987, Echteler, 1992) and have been shown to act as amplifiers, necessary to increase the cochlear sensitivity to sound (Liberman et al., 2002).

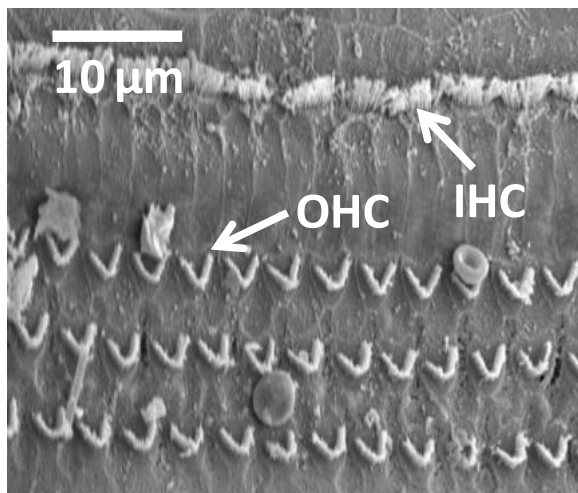


**Figure I.3. Scanning electron micrograph** showing the basal segment of a rat cochlea. The image shows a single row of inner hair cells (IHCs) and three rows of outer hair cells (OHCs). Courtesy of Kathryn Francis and Benjamin Tanner (Dr. Martine Hamann's lab).

The cochlea displays a tonotopic organisation meaning that each hair cell responds to a specific sound frequency dependent on its location. Hair cells at the base of the cochlea respond to high frequencies and those located at the apex respond to low frequencies (Rose et al., 1959). Both IHCs and OHCs have mechanosensitive organelles

called stereocilia which are organised into hair bundles projecting perpendicularly from the apical cellular surface. The length of the stereocilia in the hair bundle increases from one edge to the other, giving it a distinctive slope like appearance (Hudspeth, 1989) (*Fig. 1.4A*).

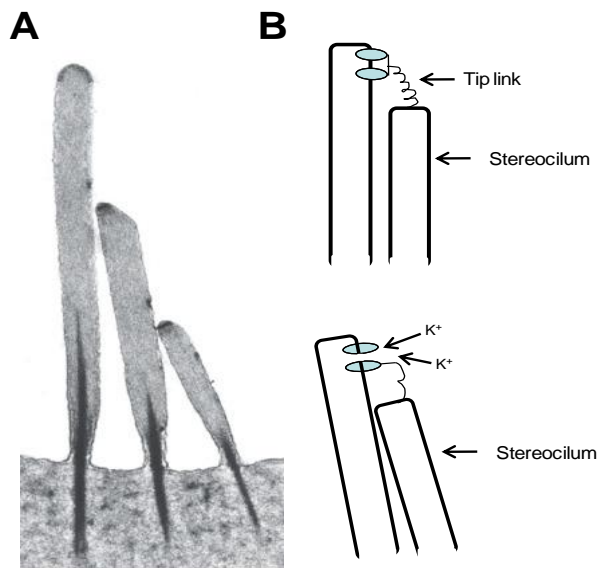


**Figure 1.4: Functional properties of hair cells.** (A) An electron micrograph showing three stereocilia on a guinea pig OHC and revealing its slope-like arrangement. Adapted from (Fettiplace and Hackney, 2006) (B) Schematic representation of the stereocilia connected by tip links. Under resting conditions (above) the tip links are relaxed and the potassium channels are closed. When a positive stimulus deflects the stereocilia towards its tall edge (below), the tension between the tip links is increased and this mechanically opens the ion channels allowing an influx of ions.

The stereocilia are also connected to each other by tip link molecules, and have a potassium permeable, wide diameter pore at one or both tip link ends (*Fig. 1.4B*) (Ohmori, 1985, Tsuprun and Santi, 2002, Farris et al., 2004). The stereocilia are deflected when there is a movement of the endolymph and as such the tension between the tip link molecules is altered (*Fig. 1.4B*). The change in tension physically opens mechanosensitive channels resulting in an influx of positive ions that depolarize the cell. The depolarisation opens voltage gated calcium channels (Tucker and Fettiplace, 1995) resulting in an increase of the intracellular calcium concentration which leads to the release of glutamate from synaptic vesicles and activation of spiral ganglion neurons (Kataoka and Ohmori, 1994). Glutamate released results in the activation of NMDA receptors (NR1 and NR2A-D subunits) (Kuriyama et al., 1993),

AMPA receptors (GluR 2-4 subunits), and kainate receptors (GluR5, GluR6, KA1 and KA2 subunits) (Safieddine and Eybalin, 1992, Niedzielski and Wenthold, 1995, Matsubara et al., 1996). All these receptor types have been identified at the postsynaptic terminal of spiral ganglion neurons (Kuriyama et al., 1993, Matsubara et al., 1996).

### **I.1.3. The central auditory system**

Auditory signals are carried along the auditory nerve (AN) to the first site of neuronal processing, known as the cochlear nucleus which is located in the brainstem and subdivided into the dorsal cochlear nucleus (DCN) and the ventral cochlear nucleus (VCN) (*Fig. I.5*). As mentioned in the previous section, the tonotopic organisation of the cochlea is maintained in the central auditory system and the cochlear nucleus is no different. The DCN and the VCN process high frequency sounds in their dorsal regions and low frequency sounds in their ventral regions (Langner, 1992). Both structures are also involved in sound localisation. The DCN contributes to localisation of sound in the vertical plane by detecting spectral notches in the acoustic signal (Nelken and Young, 1994, Sutherland et al., 1998b, May, 2000). The DCN neurons decussate and project to the inferior colliculus (IC) and the medial geniculate nucleus (MGN). The VCN localises sound in the horizontal plane via bilateral projections to the medial superior olivary nuclei (MSO) and lateral superior olivary nuclei (LSO) which are involved in processing the inter-aural time difference and the inter-aural intensity difference respectively (Goldberg and Brown, 1969, Tsuchitani, 1997). The VCN also projects to structures such as the contralateral medial nucleus of the trapezoid body (MNTB), the contralateral IC and to the nuclei of the lateral lemniscus (LL). The LL projections

ascend further up the auditory pathway, making inhibitory connections in the IC (Adams, 1979). The IC is a midbrain structure that integrates indirect binaural signals from the MSO, the LSO and the LL (Stotler, 1953, Elverland, 1978, Adams, 1979, Kelly et al., 1998) with direct monaural signals from the DCN (Adams, 1979, Oliver, 1984).

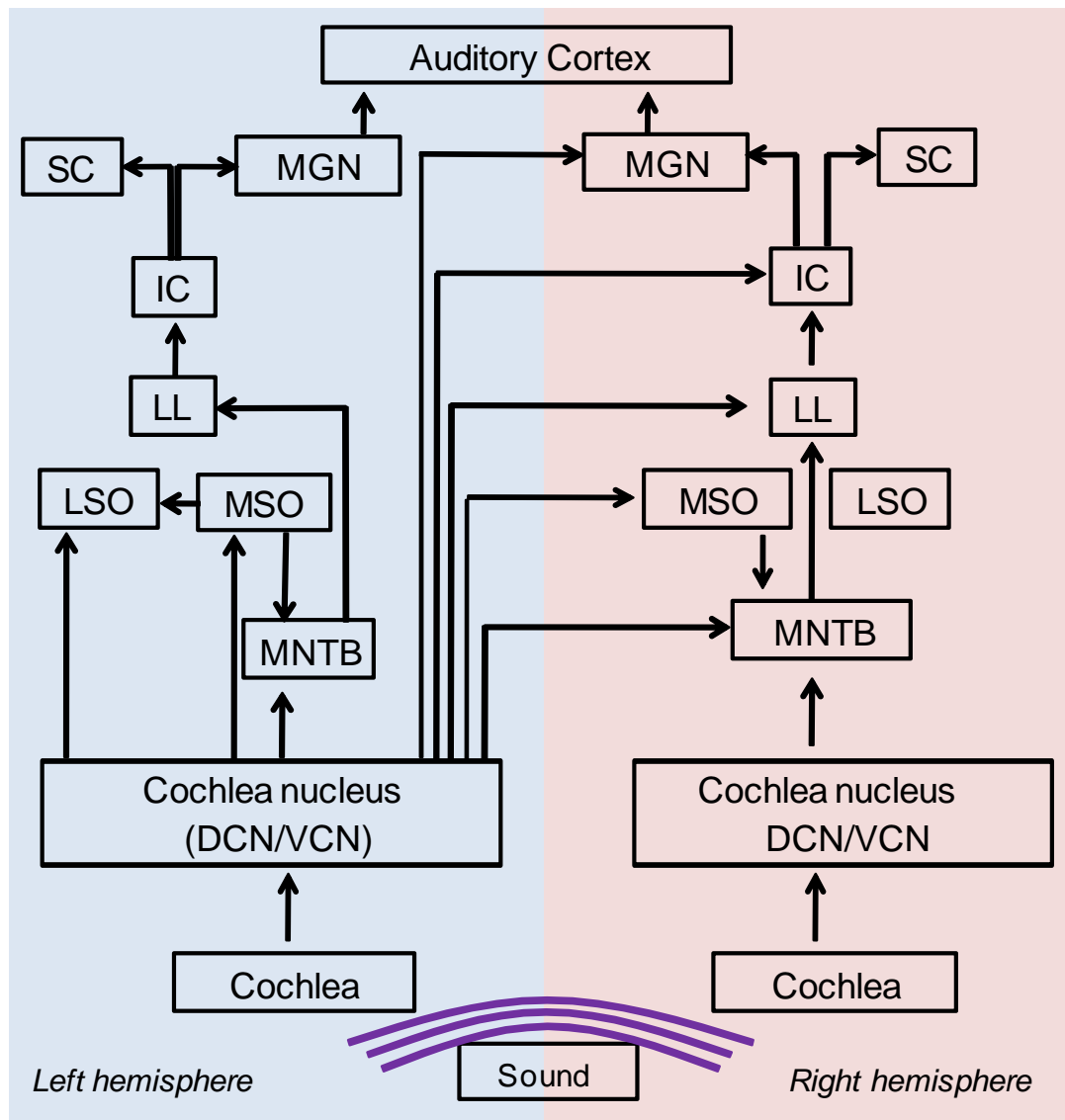


**Figure I.5. The auditory pathway.** Schematic representation of the ascending auditory pathway from the cochlea to the auditory cortex. Contralateral projections have been shown for only the left hand side but these projections are also mirrored by the structures on the right hand side. Abbreviations shown here are defined in the text.

The bulk of IC afferent fibres project to the superior colliculus with a small percentage projecting to the MGN (Oliver and Hall, 1978, Kudo and Niimi, 1980). The MGN then sends final projections to the auditory cortex (AC) located in the Sylvian fissure of the temporal lobe (*Fig. I.5*). The auditory cortex maintains the tonotopic organisation of the auditory system and is surrounded by several structures required for the complex interpretation of sound.

Parallel to the ascending pathway is also a descending pathway which provides auditory feedback modulation to various structures. In particular activity of the OHCs in the cochlea can be negatively modulated by the MSO (Spangler et al., 1987, Puel, 1995) whereas the IHC activity can also be modulated by the LSO (Spangler et al., 1987, Puel, 1995). Feedback modulation of the cochlea activity has been linked to auditory deficits such as tinnitus (Nodar, 1996, Goldstein et al., 2005). In particular, efferent feedback to the cochlea from the olivo-cochlear system can enhance acoustically evoked responses (Kawase and Liberman, 1993) which can translate into an oversensitivity or misrepresentation of sound.

## **I.2. The dorsal cochlear nucleus**

### **I.2.1. Structural organisation of the dorsal cochlear nucleus**

The DCN is subdivided into three layers, namely the molecular, fusiform and deep layer (*Fig.I.6*). The molecular layer is the superficial layer comprising of parallel fibres (unmyelinated axons) projecting from granule cells in the deep layer which carry both auditory (from OHCs i.e. type 'II' AN fibres) and non auditory inputs. Parallel fibres make contact with the apical dendrites of fusiform, cartwheel and stellate cells

(Mugnaini, 1985) in the molecular layer. Stellate cells send inhibitory projections onto cartwheel and fusiform cells (Hackney et al., 1990). Cartwheel cells also send inhibitory projections which are glycinergic in nature onto fusiform cells, giant cells and other cartwheel cells (Golding and Oertel, 1997, Tzounopoulos et al., 2004).

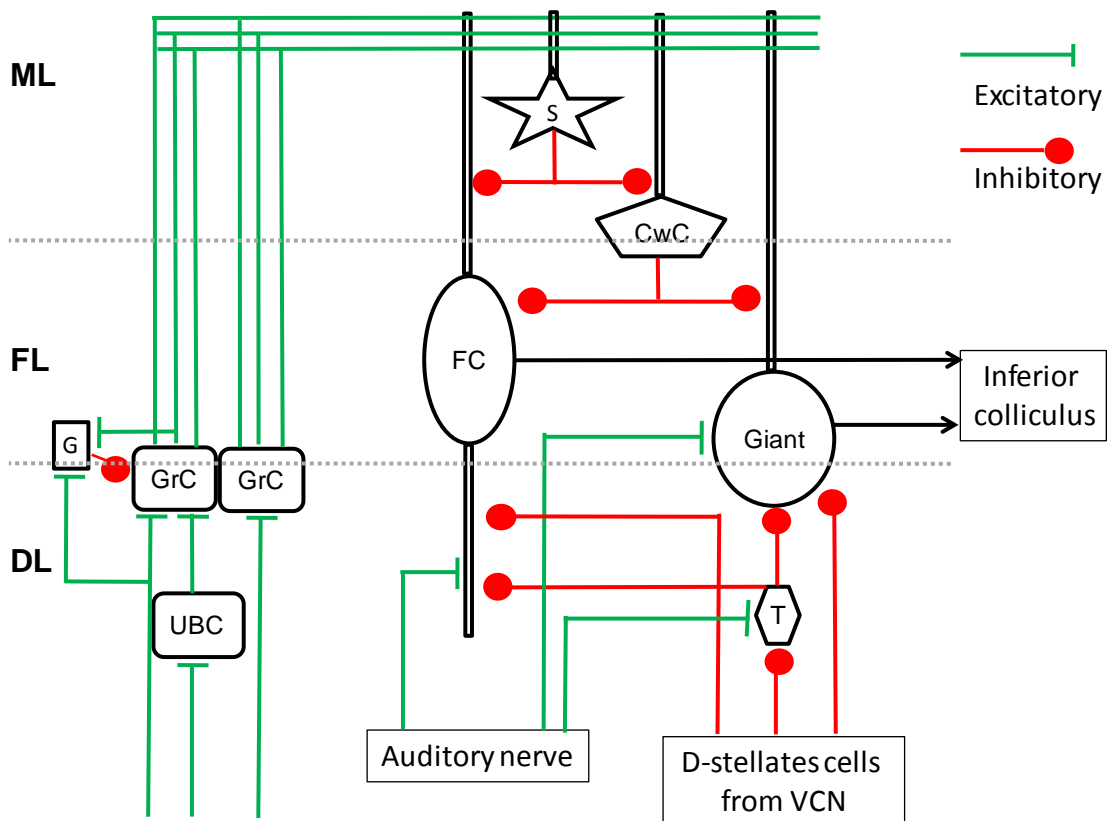


**Figure I.6. Schematic representation of synaptic connections within the dorsal cochlear nucleus.** Fusiform cells (FC) are responsible for the main output of the DCN to the IC. Giant cells (Giant) also form a small proportion of this output. Fusiform cells receive glutamatergic excitatory input from two main sources; parallel fibres projections of granule cells (GrC) which are further excited by unipolar brush cells (UBC) and can be inhibited by Golgi cells (G) in a feedback mechanism and the AN which enters the fusiform cell layer from the deep layer. Fusiform cells receive inhibitory input from stellate (S) and cartwheel cells (CwC) which are also excited by parallel fibres. Cartwheel cells are also inhibited by stellate cells and other cartwheel cells. Fusiform cells receive further inhibition from VCN stellate cells and gabaergic tuberculoventral cells (T).

The fusiform cell layer contains fusiform cells. These are the principal output cells which are bipolar fusiform shaped neurons, having their apical dendrites in the molecular layer and basal dendrites in the deep layer (Osen, 1969, Brawer et al., 1974, Pilati et al., 2008). Fusiform cells integrate multisensory information from parallel fibres in the molecular layer and auditory information from the type 'I' AN fibres (projections from IHCs) in the deep layer (Hackney et al., 1990, Zhang and Oertel, 1994). The fusiform cell layer also contains some giant cells and clusters of granule cell domains which are the most numerous cell types in the cochlear nucleus. They are scattered across the DCN surface but also mark the medial border of the DCN and VCN, separating the two structures (Mugnaini et al., 1980).

The deep layer, which is the last of the three DCN layers, contains giant cells, tuberculoventral cells and granule cell domains (Zhang and Oertel, 1993b, Zhang and Oertel, 1993a). Giant cells receive afferent inputs from the AN and the VCN (Cohen et al., 1972), and project efferent fibres to the IC (Adams and Warr, 1976). Tuberculoventral cells also receive inputs from the AN and the VCN but these send inhibitory GABAergic projections to the fusiform and giant cells (Oertel and Young, 2004). Granule cells previously identified as the source of the parallel fibres are also located in the deep layer alongside Golgi cells (Ferragamo et al., 1998) and unipolar brush cells (Mugnaini et al., 1997).

### **I.2.2. Synaptic integration in the dorsal cochlear nucleus**

Along the auditory pathway, the DCN is considered a major site of auditory and multisensory integration. Inputs from AN onto fusiform, giant and tuberculoventral cells are made up solely of type 'I' AN fibres which maintain the tonotopic organisation

found in the cochlea. Fibres that encode low frequency sounds innervate cells in the ventral region of the DCN whereas fibres encoding high frequency sounds innervate the same cell types in the dorsal region (Rose et al., 1959, Cohen et al., 1972). *In vivo* electrophysiological recordings of DCN neuronal activity in response to single tone stimuli confirmed this tonotopic arrangement and was also used to classify the neurones into five groups (type I to V) based on activity in responses to broadband noise (BBN) and inhibition of activity by single tones (Evans and Nelson, 1973, Davis et al., 1996). Type I neurones exhibited no inhibition whereas type V neurones were predominantly inhibited. Types II, III and IV neurones exhibited various degrees of inhibition by single tone stimuli (Evans and Nelson, 1973). It is thought that a combination of these response types allows the DCN to detect specific spectral cues for sound localisation in the vertical plane such as narrowband sounds and spectral notches (Sutherland et al., 1998a, Sutherland et al., 1998b, May, 2000).

In addition to type II AN fibres, the DCN receives multisensory inputs which originate from various non auditory structures including the spinal trigeminal nucleus, the dorsal column nuclei, the pontine nuclei, the vestibular complex and the Raphe nuclei. The spinal trigeminal nucleus processes sensory information from the head and face (Shore et al., 2000). It is involved in the mediation of pain (Usunoff et al., 1997) as well as non-noxious stimuli such as gentle pressure and jaw movements (Zhou and Shore, 2004). Stimulation of this pathway has been shown capable of modulating the DCN response to acoustic stimuli and it has been suggested that this allows the DCN to suppress internally generated sounds such as chewing and respiration (Shore, 2005, Shore and Zhou, 2006, Zhou and Shore, 2006). The dorsal column nucleus receives information

relative to tactile sensation, proprioception and temperature coming from the head, limbs and trunk. Electrical stimulation of the dorsal column nucleus modulates activity in the DCN and has effects similar to the effects of manual manipulations of the pinna suggesting that the dorsal column nucleus is involved in minute pinna movements to sound which optimize auditory perception (Kanold and Young, 2001). The pontine nuclei principally serve as an intermediate relay structure in the sensory motor pathway (Brodal and Bjaalie, 1992, Schwarz and Thier, 1999). Stimulation of this structure has been shown to elicit both inhibitory and excitatory responses in the DCN, however its role in sound processing remains unknown (Babalian, 2005). The vestibular system processes information in relation to posture, balance and coordination of head and eye movements (Herdman, 1998, Cullen and Roy, 2004). This system which is located in the semicircular canals also responds to acoustic stimulations (Cazals et al., 1983) and sends projections directly or via central vestibular nuclei to the DCN, the cerebellum and the spinal cord (Burian and Gstoettner, 1988, Bukowska, 2002Barker, 2012 #418). Its role in the DCN is unclear but as projections from the vestibular nerve constitute one half of the vestibulo-cochlear nerve (the AN constitutes the other half), it is most likely involved in mediating reflexes in response to sound location (Saunders et al., 1985, Barker et al., 2012). Lastly, the Raphe nucleus which is involved in the regulation of muscle tone and pain perception is located in the brainstem and projects to the forebrain, the spinal cord and other brainstem nuclei including the DCN. Projections from the Raphe nucleus into the DCN have been shown to release serotonin and sound induced serotonin release in the DCN could modulate auditory processing (Cransac et al., 1998).

### **I.3. Deficits related to the auditory system**

The peripheral and central auditory systems are susceptible to damage which manifests itself as hearing disorders, the most common of which are hearing loss and tinnitus. These two conditions can occur simultaneously or independently.

#### **I.3.1. Hearing loss**

Hearing loss describes an inability to perceive sound or a loss of sensitivity to it and be either conductive or sensorineural. Conductive hearing loss is associated with the peripheral auditory system and occurs when there is an inability to effectively conduct sound waves. Sensorineural hearing loss which is the more common of the two is associated with damage of the inner ear (including damage to the hair cells) or central auditory system which could be due to physical head trauma, acoustic overexposure (AOE), ear infections, aging effects, drug reactions or genetic defects (Spoendlin, 1971, Shehata et al., 1991, Weil et al., 1995). Acoustic overexposure is considered the most prevalent cause of hearing loss due to increasing levels of recreational and occupational exposures to loud sounds. Sounds above 85 dB SPL have the potential to induce hearing loss following a prolonged exposure. However louder exposure intensities require less exposure time to damage the auditory system (Yates et al., 1983, Nordmann et al., 2000). This is exemplified in reports of near instant hearing loss following exposure to sounds above 120 dB SPL caused by explosions or gunshots (Abaamrane et al., 2009).

Sound intensity (dB SPL)	Maximum duration (hrs)
< 85	Minimal risk
90	8
92	6
96	2
98	1.5
102	0.5
>105	Extreme risk

**Table I.1. Guidelines of maximum safe exposure times in relation to sound intensity.** The information above outlines daily maximum exposure times advised by the Occupational Safety and Health Administration. Sound intensities below 85 dB SPL are considered of minimal risk whereas working in acoustic environments above 85 dB SPL requires hearing protection to be worn.

The damaging effect of AOE has been related to time and intensity of exposure (Table I.1). One of the earliest changes consistently characterised after AOE is a loss of OHCs (Boettcher et al., 1992) which are more susceptible to damage than IHCs (Jastreboff and Hazell, 1993). The mechanisms underlying hair cell damage have been shown to include increased calcium entry within the cytoplasm of OHCs (Fridberger et al., 1998), changes in the mechanical properties of sensory hair cells (Saunders et al., 1985), increased permeability of the endolymph-perilymph barrier to potassium and sodium ions (Johnstone et al., 1989, Konig et al., 2006) and more recently, there is evidence suggesting that mitogen-activated protein kinases (MAPKs) are involved by playing a role in apoptotic cell death (Tabuchi et al., 2010). Dendritic damage which is observed in spiral ganglion cells following AOE (Spendlin, 1971, Robertson, 1983, Puel et al., 1995) has also been linked to excitotoxic glutamate damage via AMPA and kainate receptors (Puel et al., 1995). In the guinea pig model, an exposure to a loud (130 dB SPL) single tone for 15 minutes was sufficient to induce hair cell degeneration leading to hearing loss (Saunders et al., 1985). A slow but progressive loss of hair cell

innervations by type I and II primary auditory neurones has also been described (Kujawa and Liberman, 2009). All the factors considered above could contribute to raising the hearing threshold and as such decreasing sensitivity to sound (Dallos and Harris, 1978).

### **I.3.2. Tinnitus**

Acoustic overexposure has been shown to generate tinnitus (Kaltenbach et al., 2004) which can be described as the perception of sound in the absence of a corresponding external acoustic stimulus. Tinnitus is often associated with hearing loss (Temmel et al., 1999, Ochi et al., 2003) and the severity has been shown to increase with the degree of hearing loss (Guppy and Coles, 1988). Tinnitus is found to be prevalent among the aging population, war veterans and in countries with increased noise pollution, making tinnitus a major problem of public health (Henry et al., 2005, Belli et al., 2008, Muluk and Oguzturk, 2008, Folmer et al., 2011). The charity organisation 'Action on Hearing Loss', estimates that about 10 % of the UK population suffer from various degrees of tinnitus. Despite tinnitus having an immense impact on the sufferer's quality of life, no effective therapeutic strategy exists because the mechanisms underlying tinnitus are not fully understood (Belli et al., 2008, Muluk and Oguzturk, 2008). Although it is not known for certain whether tinnitus is induced peripherally or centrally, there is a higher correlation between sufferers of sensorineural hearing loss and tinnitus than conductive hearing loss and tinnitus (House and Brackmann, 1981, Savastano, 2008, Hazell, 1990). This suggests that sensorineural hearing loss which is normally associated with damage within central auditory system has greater tinnitus inducing potential than conductive hearing loss

which is associated with deficits of the peripheral auditory system (Eggermont and Roberts, 2004).

Nonetheless, a combination of both dysfunctional IHCs and OHCs representing a peripheral deficit as the cause of tinnitus has been considered. Acoustic overexposure has been shown to trigger IHC dysfunction by increasing the contact between IHC cilia and the tectorial membrane in areas where OHCs are damaged (Canlon, 1987, Nordmann et al., 2000). In addition hair cell damage due to high concentrations of salicylate treatment induces tinnitus in animal models of investigation (Cazals, 2000, Guitton et al., 2003). Furthermore, distortion product otoacoustic emissions (DPOAEs) which measure the functional status of OHCs has been used to show that patients with tinnitus in conjunction with a degree of hearing loss, have lower DPOAE amplitudes when compared to DPOAEs from normal hearing patients (Liu and Fechter, 1996, Satar et al., 2003). Additionally, in a classical study, DPOAEs in tinnitus sufferers were abolished without having any recordable effect on their perception of tinnitus (Penner and Burns, 1987). This suggests that tinnitus perception is unrelated to abnormal hair cell activity in the peripheral system. Furthermore, tinnitus persists after the functional recovery of OHCs or surgical sectioning of the AN (House and Brackmann, 1981). This further suggests that peripheral auditory system deficits alone cannot be responsible for the perception of tinnitus. Therefore it has been hypothesised that the initial deficits leading to tinnitus may occur in the peripheral auditory system and then be consolidated as a memory in the central auditory system (Guitton and Dudai, 2007).

Evidence in favour of a central origin of tinnitus is based on the correlation of DCN hyperexcitability and tinnitus (Kaltenbach and Afman, 2000, Kaltenbach, 2006). A central origin of tinnitus would explain why tinnitus can be perceived as a combination of various sounds and not a single tone, as would be the case if the deficit was localised to an area within the peripheral auditory system (Kaltenbach and Godfrey, 2008). This is because despite the central auditory system having a tonotopic arrangement, sound is re-integrated during processing in the auditory cortex (Schreiner et al., 2000, Wehr and Zador, 2003). In addition changes in the perception of tinnitus can occur over time such as changes in the intensity (Mitchell et al., 1993) and/or changes in the pitch (Penner, 1983). Although OHC deficits could account for changes in sound intensity perception over time, OHC activity is also under modulatory control of feedback mechanisms originating from the central auditory system (Ciuman, 2010). Therefore changes in the intensity and pitch of tinnitus are suggestive of a central origin of tinnitus as perception of all these factors requires a degree of central processing. If tinnitus is indeed generated centrally, the structure responsible would have to integrate auditory and non auditory information because it has been shown that tinnitus perception can be modulated by actions processed by non auditory structures such as mastication, muscle tension and head positioning (Brodal and Bjaalie, 1992, Wright and Bifano, 1997). After AOE, there are several changes that occur within DCN as a result of plasticity, these include a decrease in DCN fusiform cell excitability (Pilati et al., 2012a), differential expression of vesicular glutamate transporters in the DCN (Barker et al., 2012) and an increase in the spontaneous activity of the DCN (Zhang and Kaltenbach, 1998, Kaltenbach et al., 2000). Therefore, the DCN fulfils the requirements previously laid out for a structure involved in tinnitus

perception and has been implicated in the generation of tinnitus, making the DCN a model of investigation.

## **I.4. The dorsal cochlear nucleus and its role in tinnitus**

### **I.4.1. Synaptic plasticity in the central nervous system**

Plasticity is responsible for the ability of synapses to change in response to experience and the underlying mechanisms can be either short or long term. Short term plasticity which enhances transmission includes facilitation occurring on a millisecond timescale and post-tetanic potentiation (PTP) which occurs on a time scale of seconds to minutes (Zucker, 1989). Both these mechanisms are triggered by trains of synaptic stimulations and are expressed presynaptically. These mechanisms are also reliant on the residual calcium at the presynaptic terminal following each action potential (Katz and Miledi, 1968, Zucker and Regehr, 2002). Synapses can also experience a short term depression of activity which normally follows periods of elevated activity. This short term depression is largely due to vesicular depletion as well as inactivation of postsynaptic receptors (Betz, 1970, Miller, 1998, Zucker and Regehr, 2002).

Long term plastic changes include the functional rewiring of circuits alongside morphological changes (Bear et al., 1987, Katz and Shatz, 1996, Feldman, 2009). The most prevalent and studied forms of long term plastic changes are classified based upon their induction and functional consequence. These include long term potentiation (LTP), long term depression (LTD), spike timing dependent plasticity, homeostatic plasticity and metaplasticity (Feldman, 2009). Long term potentiation or depression represents the use dependent enhancement or weakening of a synaptic

connection (Malenka and Bear, 2004). Both LTP and LTD can be expressed either pre- or postsynaptically and have been shown to be mediated by various receptor types including NMDA receptors, metabotropic glutamate receptors (mGluRs) and endocannabinoid receptors (Feldman et al., 1998, Egger et al., 1999, Tzounopoulos, 2008, Feldman, 2009). Together, LTP and LTD are the most studied forms of plasticity due to their role in learning and memory (Sossin, 2008, Schonewille et al., 2011). Spike timing dependent plasticity (STDP) describes a form of plasticity which drives LTP or LTD expression, dependent on the temporal sequence and interval between pre- and postsynaptic spikes (Meliza and Dan, 2006, Jacob et al., 2007). Metaplasticity describes an experience dependent change in the rules that govern synaptic plasticity (Abraham and Bear, 1996). This form of plasticity has been shown in many structures including the visual system where visual deprivation leads to a bias system which supports induction of LTP over LTD (Bienenstock et al., 1982, Clem et al., 2008). Homeostatic plasticity describes a global adjustment of neuronal excitability and synaptic strength to maintain a set level of mean cellular activity (Turrigiano and Nelson, 2004). This form of plasticity is normally triggered by an over- or under-usage of specific synaptic inputs which function as part of a wider network (Yang et al., 2011).

#### **I.4.2. Role of DCN in hearing loss and tinnitus**

In the DCN, both LTP (a prolonged strengthening of the synapse) and LTD (a prolonged weakening of the synapse) can be induced at the synapse of fusiform and cartwheel cells (Fujino and Oertel, 2003, Tzounopoulos, 2008). However this plasticity is restricted to the synapses involving parallel fibres and cannot be induced by AN fibres (Fujino and Oertel, 2003). This is of relevance because plasticity of the parallel fibres

could be essential when integrating multisensory information to allow differentiation between self generated noise from the trigeminal nucleus (e.g. chewing) and acoustic signals generated by the hair cells (Shore, 2005). Plasticity at these synapses could include homeostatic plasticity as a means of compensating for the sensory deprivation experienced during AOE-induced hearing loss (Norena and Farley, 2013). It has previously been reported that during AOE-induced hearing loss, there is a decreased excitability of DCN principal cells (Pilati et al., 2012a). In addition, there is also an increase of the lateral vestibular nuclei connections into the DCN (Barker et al., 2012). This is also associated with increased DCN responses to somatosensory stimulations (Dehmel et al., 2012b) and an increased expression of the vesicular glutamate transporter type 2 (VGLUT2) in relation to the vesicular glutamate transporter type 1 (VGLUT1) in the molecular layer of the DCN (Barker et al., 2012). Cochlear deafferentation also triggers the same differential expression of VGLUT1 and VGLUT2 in the DCN (Zeng et al., 2009) showing that the changes in VGLUT1 and VGLUT2 expression is a consequence of the loss of AN inputs.

In the longer term following AOE, there is a significant increase in the DCN spontaneous activity which has been correlated with the onset of behavioural evidence of tinnitus (Kaltenbach et al., 2000, Kaltenbach, 2006, Zhang and Kaltenbach, 1998). Non auditory structures which exhibit altered activity during tinnitus have been shown to extend projections to the DCN. For example the perception of tinnitus can be modulated by head and neck movement involving the dorsal column nuclei which projects to the DCN (Levine, 1999, Levine et al., 2003). In addition, vagal nerve stimulation which alters activity in the DCN has been shown to permanently alleviate

the behavioural evidence of tinnitus (Engineer et al., 2011). Furthermore trans-electrical nerve stimulation of skin areas close to the ear was shown to increase the somatosensory activation of the DCN which alleviated tinnitus in half of patients tested (Herraiz et al., 2007). Direct electrical stimulation of the DCN surface was also shown to elicit hearing behaviour in otherwise deaf rats (Zhang and Zhang). All this is suggestive of the DCN playing an integral role in the perception of sound and provides evidence of a compensatory response of the multisensory system to deficits which could lead to tinnitus.

As the DCN is the first site of integration along the auditory pathway, plasticity leading to an altered output of the DCN could result in the alteration of synaptic function at all subsequent structures along the auditory pathway, in a bid to restore levels of previous activity (Turrigiano, 1999, Norena, 2011). Indeed plasticity within other auditory structures such as the IC which is also a multisensory site of integration and receives inputs directly from the DCN has been identified (Szczepaniak and Moller, 1996, Vale and Sanes, 2002). A consequence of altered DCN synaptic activity could be the mis-representation of transduced sounds in the central auditory system. The changes induced by AOE are widespread and since structures within the auditory system are integrated with one another, it is highly plausible that deficits within one structure would have a knock-on effect on another structure. This could account for the delayed onset and progressive nature of tinnitus following AOE, as deficits across multiple structures accumulate. In my study I specifically investigate changes in DCN synaptic properties which could account for the switch from decreased excitability during hearing loss (Pilati et al., 2012a) to increased excitability during tinnitus

(Kaltenbach et al., 1998). Early changes within the DCN could underpin all subsequent changes identified in the auditory system and ultimately be responsible for the perception of tinnitus.

## **II. MATERIALS AND METHODS**

## **II.1. Subjects**

Male and female Wistar rats were aged between 16 and 19 days at the time of commencing this study. Rats were initially anaesthetised prior to recording ABRs and subsequently exposed to prolonged periods of loud sound (AOE). A second set of ABRs were recorded 3 to 5 days after the first day of AOE, at which time point *in vitro* electrophysiological recordings were performed. In a separate set of experiments, *in vitro* electrophysiological recordings were performed concurrently with a third set of ABR recordings either 4 weeks or 11 to 13 weeks after the initial AOE. Behavioural gap detection tests were also performed in another set of experiments. Tests commenced when rats were aged 19 to 25 days and run for 12 to 16 weeks. All morphological studies were carried out using rats aged 25 days. All experiments were carried out in accordance with home office regulations as described in the Animals Act (Scientific Procedures) 1986.

## **II. 2. *In vitro* methodology**

### **II.2.1. Cresyl violet staining**

Cresyl violet is a neuronal stain that binds to the acid components of the neuronal cytoplasm such as ribosomes, nuclei and nucleoli (Tureyen et al., 2004). Cresyl violet staining reveals the cytoarchitecture of the brainstem slice and allows identification of the different layers within the DCN (Pilati et al., 2008). Twenty five day old Wistar rats were killed by decapitation and the brain was removed from the head cavity, transferred into tissue tek (Sakura, Tokyo Japan) and frozen using hexane and dry ice. Coronal brainstem slices (20  $\mu$ m thick) were obtained using a cryostat (OTF 5040,

Bright) and mounted on polysine slides. All sections were fixed in a paraformaldehyde solution (5% paraformaldehyde dissolved in phosphate buffer solution – a mixture of  $\text{Na}_2\text{HPO}_4$  and  $\text{NaH}_2\text{PO}_4$ ; pH 7.4) for 15 mins at room temperature. The staining procedure was performed as follows: slides were hydrated in distilled water for 30 mins then placed under agitation in a cresyl violet tank for 5 mins. Slides were then transferred into a distilled water tank for 2 mins to remove excess stain before being dehydrated in a 100% ethanol tank for another 2 mins. The slides were finally placed in xylene for 2 mins before mounting the cover slips using the synthetic resin dibutyl phthalate xylene (DPX). Pictures of the mounted slides were then taken using a Nikon DXM1200F digital camera connected to a Nikon eclipse TE2000-U inverted microscope.

### **II.2.2. Dissection and slicing**

Wistar rats were killed by decapitation as described above, however all rats weighing over 60 g received a lethal overdose of pentobarbitone (sodium 20% w/v, tartrazine 1409 (E102) 0.004% w/v) before decapitation. After decapitation, the brain was removed from the skull and placed with its ventral surface up in a cold low  $\text{Na}^+$  artificial cerebrospinal fluid (aCSF) containing in mM: KCl 2.5,  $\text{NaH}_2\text{PO}_4$  1.2, D-Glucose 10, ascorbic acid 0.5, sucrose 250,  $\text{NaHCO}_3$  26,  $\text{CaCl}_2$  0.1 and  $\text{MgCl}_2$  4, bubbled with 95%  $\text{O}_2$  and 5%  $\text{CO}_2$ , pH 7.4. The low  $\text{Na}^+$  concentration of the solution suppresses neuronal activity while the cold temperature maintains cellular structure (Aghajanian and Rasmussen, 1989). The meninges were removed from the brainstem with forceps and an incision at a 45 degree angle was made to separate the brainstem and cerebellum from the rest of the brain. The brainstem and cerebellum were glued onto the slicing platform (*Fig.II.1*) which was secured in a slicing chamber filled with the low

Na<sup>+</sup> aCSF described above. Coronal brainstem slices (300 μm for extracellular recordings and 180 μm for patch clamp recordings) were obtained using a vibroslicer (Leica VT1000) with a stainless steel blade (Campden Instruments, UK. *Fig. II.1*).

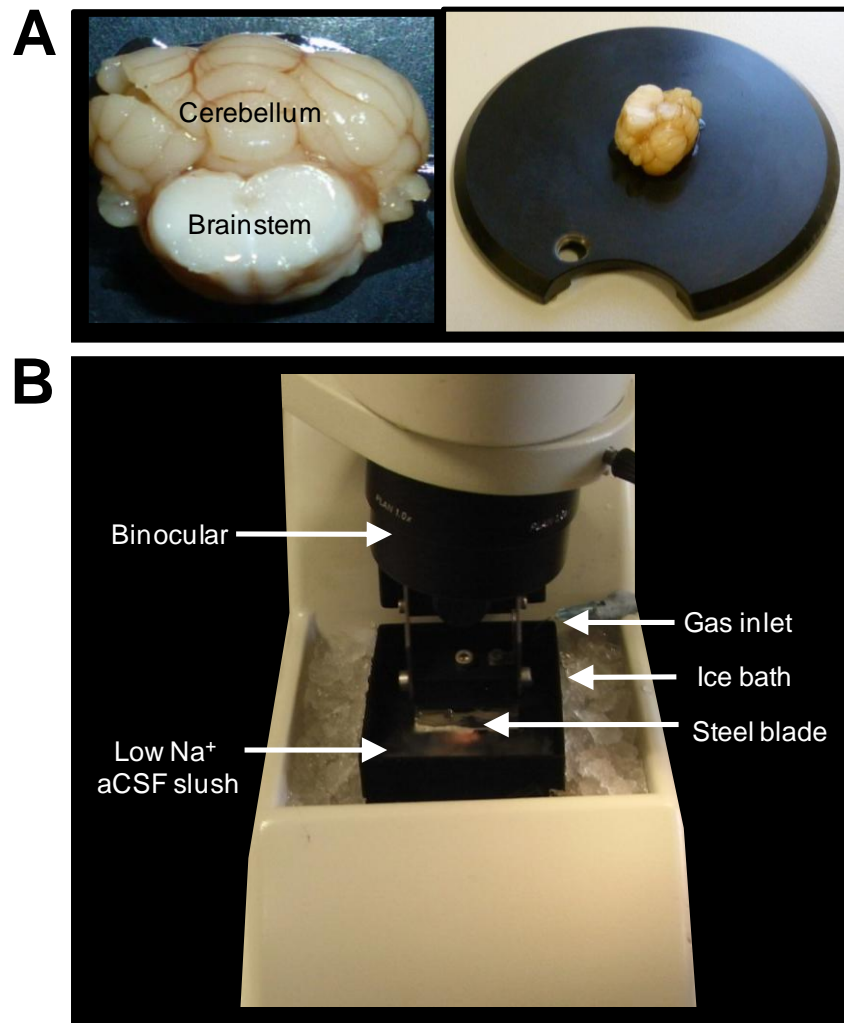


**Figure II.1. The slicing procedure. (A).** Top view of the brainstem and cerebellum (left) dissected from a 25 day old Wistar rat. The tissue is mounted on the slicing platform (right) and secured by glue. **(B)** The mounted brain is submerged into the slicing chamber filled with a low Na<sup>+</sup> aCSF slush solution that is constantly gassed with a mixture of 5 % CO<sub>2</sub> and 95 % O<sub>2</sub>. To further maintain low temperatures, the slicing chamber is held in an ice bath throughout the slicing procedure. A binocular lens located above the chamber helps in identifying the DCN. The stainless steel blade used to cut the slices is also shown.

Slices were transferred into a bubbling chamber with oxygenated normal aCSF containing in mM: NaCl 125, KCl 2.5, NaH<sub>2</sub>PO<sub>4</sub> 1.2, D-glucose 10, ascorbic acid 0.5, Na pyruvate 2, myo-inositol 3, NaHCO<sub>3</sub> 26, CaCl<sub>2</sub> 2 and MgCl<sub>2</sub> 1, bubbled with 95% O<sub>2</sub> and

5% CO<sub>2</sub>, pH 7.4. The bubbling chamber was held in a water bath at 37 °C for an hour then at room temperature for the remainder of the experimental day. Slices used for recording were transferred to the recording chamber of a Zeiss Axiovert upright microscope and were perfused with a normal aCSF as described above with the 1 mM MgCl<sub>2</sub> been replaced with 0.1 mM MgCl<sub>2</sub>. Classical methods pair a presynaptic stimulation with a postsynaptic depolarisation to remove the voltage dependent block of NMDA receptors by magnesium ions (Mayer et al., 1984, Jahr and Stevens, 1987, Danysz and Parsons, 2003). In this study, performing a high frequency stimulation (HFS) protocol may not be able to achieve the same effect of removing the magnesium block. This explains the choice to reduce magnesium concentrations in the extracellular medium to 0.1 mM.

### **II.2.3. Electrophysiological recording setup**

Field potentials were recorded in the fusiform cell layer of the DCN in response to parallel fibre stimulation in the molecular layer. The electrophysiological setup used comprises a patch clamp amplifier (Multiclamp 700A, Axon instruments, USA) connected to an analogue to digital converter (Digidata 1322A). A digitimer stimulation unit connected to the analogue to digital converter was used to directly stimulate the surface of the brain slices via a concentric stimulation electrode. A Cv-7A headstage which contains a voltage follower was used to record field potentials in current clamp mode. The headstage was connected via a silver chloride wire to the recording electrode filled with normal aCSF for field potential recordings or an intracellular solution for patch clamp recordings and housed in an appropriate holder. The headstage was attached to a micromanipulator (Newport, Burleigh) which allowed for

precise positioning of the electrode (*Fig. II.2*). A silver chloride earth electrode also linked the headstage to the perfusion chamber on the stage of the upright microscope (Zeiss, Axioskop). Slices were placed in the perfusion chamber and their location maintained using a custom made harp composed of a platinum wire and nylon filaments. A 4x objective and a charge coupled device (CCD) camera fitted to the microscope were used to enable the visual localisation of the DCN. The microscope was mounted on an X-Y translation table (Mechanical and electronic joint workshop, University of Leicester) which allowed the objective to be positioned around the perfusion chamber (*Fig. II.2*). The microscope and manipulators were surrounded by a homemade Faraday cage and supported by an anti-vibration table (Wentworth Laboratories Ltd). The same setup was used when performing whole cell recordings.

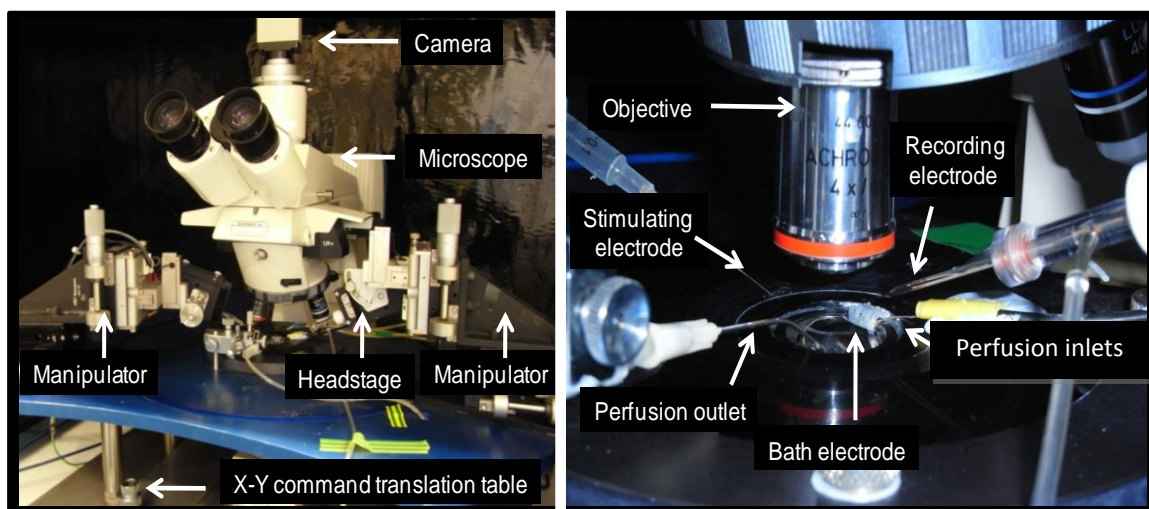


**Figure II.2: Electrophysiological setup.** (A) An upright microscope (Zeiss, Axiovert) with two Burleigh manipulators fixed to its X-Y platform for positioning of recording and stimulating electrodes. A Hamamatsu CCD camera connected to the microscope allows brain slices to be viewed on a monitor for cellular recognition. (B) A closer view of the area surrounding the recording chamber with the various electrodes and the perfusion inlet and outlet lines.

#### **II.2.4. Stimulating and recording electrodes**

Parallel fibres in the DCN molecular layer were stimulated using a concentric bipolar stimulating electrode (FHC Inc, Bowdoinham, ME, USA) connected to a constant voltage isolated stimulator (Digitimer Ltd). The stimulation electrode was attached to a micromanipulator for precise positioning in the DCN molecular layer. Parallel fibres were stimulated with 100  $\mu$ s pulses from 0 to 50 V when using a voltage stimulator and 0 to 2 mA when using a current stimulator with frequencies at 0.3 Hz or 50 Hz. Recording electrodes were pulled from borosilicate glass capillaries (GC150F 7.5, Harvard apparatus, UK) using a two stage puller (PB-10 Narishige, Tokyo, Japan). Final pipette resistance was measured between 4 and 7 M $\Omega$  for all experiments as changes in the pipette resistance can interfere with the measurements of currents

#### **II.2.5. Perfusion of solutions**

Slices in the perfusion chamber were perfused at a rate of 1 ml/min using a peristaltic pump (Gilson). Solutions passed through 5 ml syringes before being transferred to the chamber to avoid the occurrence of bubbles. The incoming perfusion was warmed to 36°C with a Peltier thermostatic controller device with a resulting bath temperature of 34.5°C. Performing experiments in a raised bath temperature rather than at room temperature served to mimic physiological conditions and as such allow the data obtained to be related to *in vivo* conditions. Separate perfusion lines were required to allow the rapid change over of the bath solution without contamination when drug effects were being tested. A zero calcium aCSF solution was also made which was similar in constitution to the normal aCSF except for the 2 mM CaCl<sub>2</sub> and 1 mM MgCl<sub>2</sub> been replaced with 2 mM EGTA and 2 mM MgCl<sub>2</sub>.

## II.2.6. Extracellular field potential recordings

### II. 2.6.1. Analysis of field potentials

Slices in the recording chamber were held in place by a harp and the DCN visualised under an upright microscope. Upon placement of both electrodes (stimulation electrode: molecular layer, recording electrode: fusiform cell layer), the 1 mM Mg<sup>2+</sup> aCSF perfusion solution was exchanged for a 0.1 mM Mg<sup>2+</sup> aCSF. Recordings were carried out at 0.3 Hz to avoid run down of the synaptic response that could result from vesicular depletion (Schneeggenburger et al., 2002). Recording field potentials in response to parallel fibre stimulation resulted in a multiphasic response, in accordance with a previous study performed in the guinea pig (Manis, 1989).

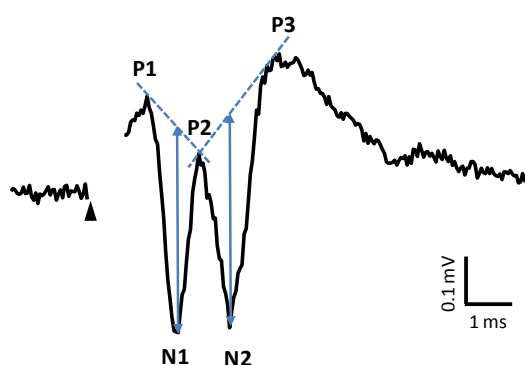


**Figure II.3. Field potential response components.** An average of ten individual traces recorded at 0.3 Hz stimulation. The response consists of an initial triphasic wave (P1-N1-P2), followed by a fast negative (N2) and a slower positive P3. The N1 and N2 amplitudes were measured as indicated by the double arrowed line between the peaks and the baseline indicated by the dotted line.

Each peak in the field potential is identified as a negative or positive deflection. All negative and positive peaks after the artefact of stimulation were numbered sequentially from the first (N1 or P1) through to the last (Fig. II.3). The amplitude of each negative deflection was calculated as the average amplitude of the positive peaks on either side of the baseline minus the amplitude of the negative deflection (Fig. II.3). For example, the N1 amplitude was calculated as shown below:

$$N1 \text{ amplitude} = \frac{(P1 + P2)}{2} - N1$$

An alternative analysis was also performed where the N1 amplitude was calculated as the difference in amplitude from the baseline (pre-artefact of stimulation) to the N1 peak (Appendix 1). This alternate measurement could not be applied to the N2 component because of the wide variety in form of the N2 component between experiments. Indeed, the form of the N2 component has been shown to be sensitive to the position of the recording electrode within the DCN (Manis 1989; See results section 2.2.1 and *Fig. 2.4*). Furthermore, in some experiments, the N2 peak was above the baseline preceding the stimulation artefact. Therefore applying this alternate analysis method would result in negative amplitudes which do not accurately reflect the field potentials recorded.

#### **II.2.6.2. Separation of the pre- and postsynaptic components**

It has previously been shown that the spatial distribution of the field potentials can give an indication of the pre- and postsynaptic components (Manis, 1989). Therefore recordings were performed where the stimulation and recording electrodes were initially placed in the molecular and fusiform cell layer respectively. Once a suitable response was obtained, the stimulation electrode was no longer moved. The microscope view was then switched to the CCD camera and the position of the recording electrode in the DCN fusiform cell layer was noted. Ten traces were captured in this position and the recording electrode was then moved by a distance of 50  $\mu\text{m}$  along the transverse axis to capture another average of ten traces. This was repeated until the position of the recording electrode was in the heart of the molecular layer and a further average of ten traces recorded. Three of the recording electrode positions have been identified in *Fig. II.4*.

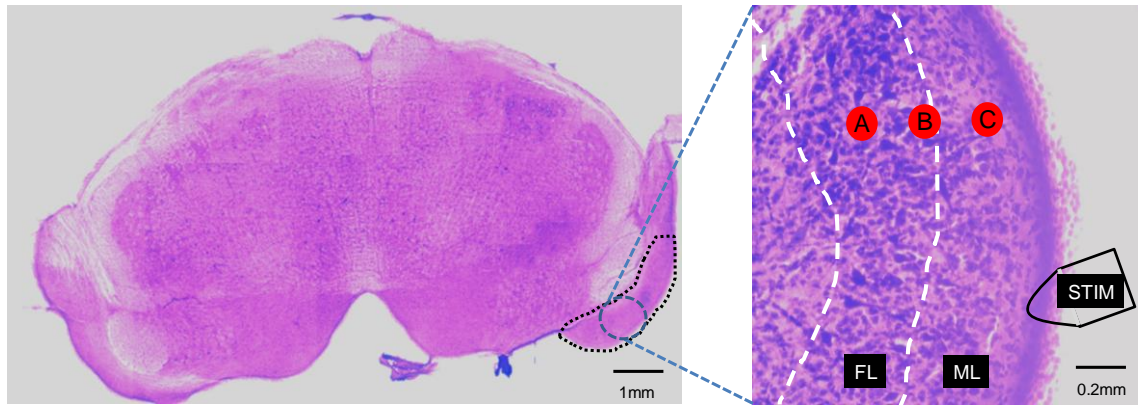


**Figure II. 4: Cresyl violet image showing positioning of stimulating and recording electrodes.** A coronal brainstem slice (left) 300  $\mu\text{m}$  thick with the DCN location indicated (dotted line). A blown up section of the DCN (right) indicates the positioning of the electrodes in relation to each other. The stimulation electrode (STIM) was placed in the molecular layer (ML). The recording electrode was initially placed at position (A) in the fusiform cell layer and then moved along the transverse axis to position (B) and then position (C).

### II.2.6.3. Determination of the conduction velocity

To record the conduction velocity along parallel fibres, both stimulating and recording electrodes were placed in the molecular layer to record presynaptic field potentials (N1) in isolation (Manis, 1989). To record the conduction velocity along the AN, both the stimulating and recording electrode were placed in the deep layer for the same reason. In both cases, the recording electrode was sequentially moved in the longitudinal plane away from the stimulation electrode to allow a longer onset latency of the action potential and to calculate the conduction velocity of the action potential using the formula below:

$$\text{Conduction velocity (m. s}^{-1}\text{)} = \frac{\text{Distance (m)}}{\text{Time (s)}}$$

Where 'Distance' is the distance between the stimulation and recording electrodes in meters (m) and 'Time' is the duration from the artifact of stimulation to the onset of the presynaptic response in seconds (s).

#### II.2.6.4. Stimulus intensity relationships

Preliminary experiments revealed that the minimum voltage intensity to elicit a recordable field potential was between 5 and 10 V. Therefore in this study the minimum intensity of all recordings started from 10 V to maintain uniformity in the data sets. Once a response was established, the stimulation intensity was stepped up in increments of 10 V in order to recruit additional fibres and increase the proportion involved in the evoked response. An average of 10 sweeps was recorded at each stimulation intensity and the intensity eliciting half the maximal amplitude of the N2 response was applied for the remainder of the experiment. The reason for this was not only to avoid neuronal damage which has been shown to occur as a result of over stimulation (Puel, 1995) but also to avoid saturation of the postsynaptic receptors. It is possible that an increase in the response amplitude as a consequence of plasticity could be occluded if recordings are performed at a stimulation intensity which saturates the postsynaptic receptors. The data obtained from recording responses evoked by multiple stimulation intensities was used to plot an input-output graph which was fitted with a linear function ( $y = mx + c$ : where 'y' is the response amplitude, 'm' is the gradient, 'x' is the stimulation intensity and 'c' is the y intercept). Alternatively, the Hill equation was used ( $y = \frac{ax^b}{c^b + x^b}$ ; where 'y' is the response amplitude, 'a' is the maximum of y, 'b' is a free parameter adjusted to obtain an optimal fit, 'c' is the value on the x-axis corresponding to 50% of the y-max and 'x' is the stimulation intensity). From this fitted input-output curve, threshold stimulation was deduced as the minimal stimulation intensity eliciting 5% of the maximum response amplitude (a). Slope was calculated as the linear rising component of the fit

and the maximum response amplitude was the maximum point derived from the Hill equation.

#### **II.2.6.5. Paired pulse facilitation**

Paired pulse stimulations were used to confirm the postsynaptic component of the field potentials. Paired pulse facilitation (PPF) is a phenomenon that is unique to postsynaptic response (Eccles et al., 1967, Manis, 1989) and is explained by a Ca<sup>2+</sup> dependent elevation of transmitter release (Abbott and Regehr, 2004). Residual Ca<sup>2+</sup> that remains in the presynaptic terminal from the calcium influx induced by an initial stimulation primes some vesicle release sites (Katz and Miledi, 1968, Zucker, 1993). A second stimulus arriving shortly after also induces a Ca<sup>2+</sup> influx which causes an increase in the amount of neurotransmitter released and as such a larger response at the postsynaptic terminal (Muller et al., 2008). Paired pulse stimulations at 0.3 Hz were applied with interval gaps ranging from 200 ms to 10 ms with an average of 10 sweeps recorded for each interval gap. The response amplitude evoked by the second stimulus was calculated as a ratio of the response amplitude evoked by the first stimulus.

$$\text{Paired pulse ratio} = \frac{\text{Postsynaptic response evoked by second stimulus}}{\text{Postsynaptic response evoked by first stimulus}}$$

Paired pulse facilitation was described as a significant increase in this ratio.

#### **II.2.6.6. Long term potentiation of field potentials**

The effect of HFS (2 x 50 Hz for 15s with a 1s respite) was used to investigate synaptic plasticity in the DCN (Manis and Molitor, 1996, Fujino and Oertel, 2003). A 10 min stable baseline period in response to 0.3 Hz stimulation at half maximal N2 amplitude was established prior to the HFS. Following the HFS protocol, recordings at 0.3 Hz were

carried out for a further 30 mins or 90 mins to assess the levels of synaptic plasticity. The role of NMDA receptors in DCN synaptic plasticity was also investigated by applying 25  $\mu\text{M}$  D-(-)-2-Amino-5-phosphonopentanoic acid (D-AP5) prior to or 30 mins after the HFS.

#### **II.2.6.7. Pharmacological tests under field potential recordings**

Field potentials were recorded in 0.1 mM  $\text{Mg}^{2+}$  aCSF medium and in zero  $\text{Ca}^{2+}$  aCSF to identify pre- and postsynaptic responses. The effects of blocking excitatory and inhibitory transmission in the DCN were also investigated by carrying out recordings in the presence of 10  $\mu\text{M}$  2,3-dioxo-6-nitro-1,2,3,4-tetrahydrobenzo[f]quinoxaline-7-sulfonamide (NBQX) to block AMPA receptors, 25  $\mu\text{M}$  D-AP5 to block NMDA receptors, 10  $\mu\text{M}$  strychnine to block glycine receptors, 10  $\mu\text{M}$  gabazine to block GABA receptors or 1  $\mu\text{M}$  tetrodotoxin (TTX) to block  $\text{Na}^+$  channels and therefore action potentials. Drugs were made up to 1 mM stock concentration and diluted in 0.1 mM  $\text{Mg}^{2+}$  aCSF on the day of testing to the final concentrations described. Recordings were also performed to test the effects of perfusing a high magnesium (10 mM) extracellular solution. Pharmacological testing required the complete changeover of the perfusion solution for which a 4 to 5 min period was allowed. Upon switching perfusion, recordings lasted 5 to 10 minutes before applying a wash.

### **II.2.7. Whole cell recordings**

#### **II.2.7.1. Whole cell voltage clamp technique**

The whole cell patch clamp (Neher and Sakmann, 1992) requires the formation of a giga-ohm seal between the tip of a glass micropipette and the cell membrane. The pipette is filled with an intracellular solution designed to maintain cell viability upon

'break-in'. This intracellular solution is kept in contact with a silver chloride wire to conduct electrical currents to the patch clamp amplifier. Upon forming a high resistance giga-ohm seal between the pipette tip and the cell membrane, a strong negative pressure or suction is applied to rupture the membrane section under the pipette tip without disrupting the giga-ohm seal or cell viability. This successful 'break-in' into the cell is indicated by a negative shift in the recorded cell membrane potential and a large reduction in the measured resistance. The decreased resistance which is currently recorded will now be due only to the input resistance of the cell and the series resistance of the pipette. When currents flow across the membrane, the series resistance causes an error between the true cell potential and the measured potential. The MultiClamp 700A amplifier used here has an inbuilt system for correcting errors associated with the series resistance. This involves measuring the series resistance and predicting the ensuing error values. The system then adds a proportional voltage signal to correct for the predicted errors which is defined by the user as a percentage of the series resistance (series resistance compensation). In my experiments, I recorded a typical series resistance of 10 to 20 M $\Omega$  which I compensated by 60 to 70%. I used the whole cell recording technique to record ionic currents in voltage clamp mode (Hodgkin and Huxley, 1952) while holding cells at a fixed voltage potential of -70 mV. All electrophysiological data was acquired using the software Clampex 9.2 and analyzed using Clampfit 9.2. Field potentials and whole cell EPSCs were collected via PClamp 9.2 at a sampling rate of 20 kHz and filtered at 6 kHz using an in-built 4-pole Bessel filter. Final graphic representations were performed using Sigmaplot 2000 and Excel 2007.

### **II.2.7.2. Intracellular solutions**

The electrodes were filled with an intracellular solution containing in (mM): Cs-gluconate 130; EGTA 5.4 HEPES 10; MgCl<sub>2</sub> 1; NaCl 2; QX314 2 and adjusted to pH of 7.1-7.3 with CsOH. This solution was used to achieve a chloride equilibrium potential of -90 mV. The use of caesium instead of potassium allowed for reduction of the leak currents underlined by potassium fluxes. This increased the cell viability when recording for prolonged periods in different release probability states. QX314 was added to the intracellular solution to block sodium channels and prevent unwanted unclamped action potentials (Oleskevich et al., 2000). The intracellular medium was filtered using a 0.2 µm filter (Millipore, UK).

### **II.2.7.3. Recording excitatory postsynaptic currents**

Fusiform cell excitatory postsynaptic currents (EPSCs) were evoked by either stimulation of the AN or parallel fibres at intensities between 0.1 to 2 mA. All recordings were performed in the presence of strychnine (20µM), gabazine (10µM) and D-AP5 (25µM) to allow the isolation of EPSCs mediated by AMPA receptors alone. Reported EPSC amplitudes are an average of 5 to 10 individual traces recorded at a stimulation frequency of 0.3 Hz.

### **II.2.7.4. Functional segregation of synaptic pathways**

Fusiform cells receive multisensory inputs via parallel fibres located in the molecular layer and auditory inputs via the AN located in the deep layer (Mugnaini, 1985). Both inputs are theoretically spatially segregated (Osen, 1969, Brawer et al., 1974). However, the cell bodies of the parallel fibres which are the granule cells are also

located in the deep layer. This raises the possibility that placing the stimulation electrode in the deep layer to stimulate the AN may inadvertently stimulate the multisensory inputs. Cross facilitation tests were therefore carried out to confirm the functional segregation of the two pathways (Tzounopoulos et al., 2004). In these tests, two stimulation electrodes were used and the stimulation of the multisensory pathway was preceded by 60 ms with a stimulation of the AN pathway (Fig. II.5).

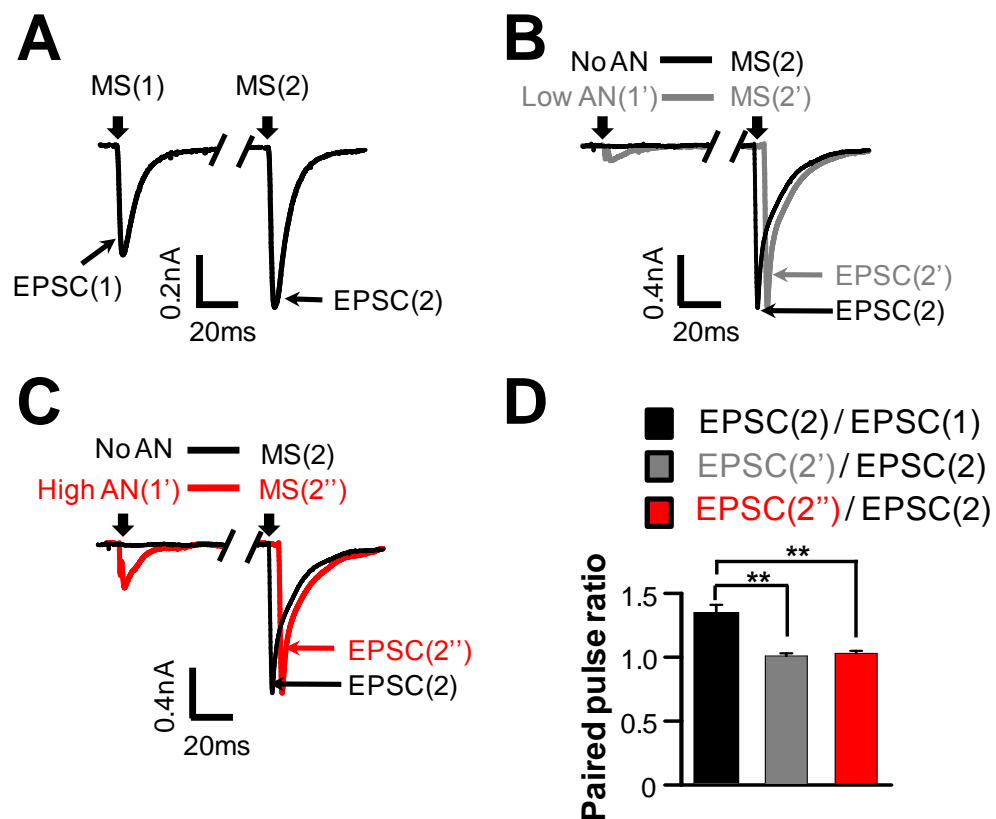


**Figure II.5. Stimulation of the AN fibres specifically activates AN synaptic inputs. (A)** The EPSCs evoked by a paired pulse stimulation of multisensory inputs (MS(1) and MS(2)) at 0.4 mA and 60 ms intervals leads to PPF. **(B)** EPSCs evoked by 0.4 mA stimulation of the MS inputs were preceded 60 ms by either a low (0.4 mA) AN stimulation (EPSC(2')) or no AN stimulation (EPSC(2)). The amplitude of the EPSC evoked by MS input stimulation is unaffected by a preceding low stimulation intensity of the AN. **(C)** Same protocol as **(B)** shows that the amplitude of the EPSC evoked by MS input stimulation is unaffected by a preceding high stimulation intensity (1.6 mA; EPSC(2'')) of the AN. **(D)** Bar charts of PPRs show a significant facilitation only with a paired multisensory pathway stimulation (\*\*  $P < 0.01$ , One way ANOVA on Ranks, Dunnett's test). All traces are averages of ten individual traces. Overlay of EPSCs have been shifted and stimulation artefacts removed for clarity.

Stimulation of the AN pathway was carried out at both high and low intensities because it is known that high intensity stimulations lead to fibre recruitment (Sims and Hartell, 2005). Functional segregation was confirmed if the low or high intensity stimulation of the AN did not affect the EPSC amplitude evoked by stimulation of the parallel fibres 60 ms later. The use of cross facilitation tests led to a total of 5 cells being discarded during this project.

#### **II.2.7.5. Stimulation of synaptic inputs**

Auditory nerve fibres in the deep layer or parallel fibres in the molecular layer were stimulated with a concentric bipolar electrode to evoke recordable EPSCs in fusiform cells. A current stimulator was used in these experiments with a minimal stimulation intensity of 0.1 mA which was increased to a maximal intensity of 2 mA to recruit additional inputs to the cell. Ten traces were averaged together and the EPSC peak amplitude was calculated on the averaged trace. The EPSC amplitude elicited at each stimulation intensity was used to plot an input-output graph which was fitted with a Hill function as previously described. Paired pulse facilitation tests were also performed when recording fusiform cell EPSCs.

#### **II.2.7.6. Quantal analysis**

Quantal analysis was used to calculate the number of functional release sites (N), the quantal size (Q) and the release probability (P) at a synapse. These three parameters are directly linked to the size of the EPSC response by the equation below (Castillo and Katz 1954):

$$\text{Mean EPSC} = N \times P \times Q$$

The technique of variance-mean (VM) analysis also known as multiple probability fluctuation analysis was used to estimate N, P and Q (Clements and Silver, 2000). The technique requires EPSCs to be recorded over a range of extracellular calcium concentrations to alter the probability of release between the ranges of 0 and 1. The mean EPSC amplitude and variance are then calculated over a stable epoch of a minimum of twenty events after wash in of each extracellular solution. The VM relationship can then be fitted with a parabola using the equation

$$y = Ax - Bx^2$$

where y and x are the EPSC variance and mean amplitude respectively, whereas A and B are free parameters adjusted to optimally fit the parabola to the VM plot. The shape of the parabola is closely linked to the three quantal parameters (N, P and Q). The initial slope of the parabola provides an estimate of Q, the degree of curvature estimates P and the size of the parabola is related to N (Clements and Silver, 2000). Upon fitting the data with the parabola function, P and Q can be calculated using the equations below:

$$P = x(B/A)(1+CV^2)$$

$$Q = A/(1+CV^2)$$

Where  $CV^2$  is the square of the coefficient of variation of the EPSC amplitude at a given calcium concentration and calculated as :

$$CV^2 = \left( \frac{\text{Standard deviation}}{\text{Mean}} \right)^2$$

A minimum estimate N can also be calculated using the equation below:

$$N = 1/B$$

The VM analysis was used to calculate quantal parameters because it does not require the assumption that release probability and quantal amplitude are uniformly distributed at all release sites of a given axon (Clements and Silver, 2000). In addition by performing recordings in the presence of D-AP5, gabazine and strychnine, I blocked NMDA, GABA and glycinergic receptors, therefore effectively isolating transmission via AMPA receptors. There are also some limitations to the successful use of this method which were taken into consideration. Firstly, the method requires a constant number of independent release sites to be activated over the course of the experiment to help ensure that both 'Q' and the coefficient of variation of the synaptic response remain unaltered over time (Reid and Clements, 1999). Therefore the stimulation intensity was constant throughout the recording period. The stimulation intensity of 0.4 mA was chosen when studying parallel fibre evoked EPSCs because previous reports from this lab showed that AOE induced deficits at parallel fibre synapses pertaining to the firing rate of cells, persisted at low stimulation intensities and was overcome at high stimulation intensities. When studying AN evoked EPSCs, AOE significantly decreased the EPSC amplitude at 0.2 mA and 2 mA stimulation intensity. Quantal analysis tests were performed at 2 mA stimulation intensity because preliminary experiments showed that upon switching to a low calcium perfusion solution with a 0.2 mA stimulation intensity, there was an unwanted increase in the number of failures which would impede the accurate fitting of a parabola to the VM plot. The second limitation to be considered was that the VM method of quantal analysis requires a minimum number of 20 events per epoch to be collected (Clements and Silver 2000). In line with this, a stable number of 30 to 60 events were collected at each extracellular calcium concentration tested. Lastly, it has been shown that when release probability is

increased closer to 1 due to high extracellular calcium concentrations, the VM relationship becomes skewed and no longer fits a parabola (Oleskevich et al., 2000). Preliminary tests revealed that at extracellular calcium concentrations of 4 to 5 mM, the VM relationship became skewed. For this reason, extracellular calcium concentrations in the range of 0.5 to 3 mM were used. At these concentrations the VM relationship did not deviate from its parabola form so I could confidently use the above equations to derive values for N, P and Q.

### **II.3. *In vivo* methodology**

#### **II.3.1. Anaesthesia and sedation**

Rats were anaesthetised during the recording of auditory brainstem responses (ABRs) and also during the AOE period. The anaesthesia used was a mixture of fentanyl and fluanisone (marketed as Hypnorm; VetaPharma Ltd) and midazolam (marketed as Hypnovel; Roche). Intraperitoneal injections were carried out with a combination of drugs at the following doses: fentanyl (0.15 mg/kg), fluanisone (5 mg/kg) and midazolam (2.5 mg/kg). Fentanyl is a highly potent  $\mu$  opioid agonist with a rapid onset but relatively short duration (Inoue et al., 1994). The side effects of fentanyl include central nervous system and respiratory depression as well as bradycardia (Smydo, 1979, McLoughlin and McQuillan, 1997). Fluanisone, a tranquilizer belonging to the butyrophenone group potentiates the analgesic effect of fentanyl while also antagonising its negative side effects (Inoue et al., 1994). The combination of fentanyl and fluanisone ensures that rats are under anaesthesia for at least 60 minutes. Midazolam is a benzodiazepine which acts as a potent sedative analgesic agent. Midazolam has a rapid onset and a short duration due to its rapid rate of metabolism (Flecknell and

Mitchell, 1984). On its own midazolam does not induce anaesthesia in rodents; however it potentiates the effects of fentanyl (Pieri et al., 1981). A combination of these three drugs produces neuroleptanalgesia with skeletal muscle relaxation in many rodents (Flecknell and Mitchell, 1984). This combination ensured that sedation lasted for about 90 minutes and a 50% top up dose was applied if the rat showed signs of regaining consciousness (e.g. pedal reflex withdrawal). Saline (200  $\mu$ l) was also administered hourly via subcutaneous injection to maintain fluid balance.

### II.3.2. Acoustic overexposure

Acoustic overexposure (AOE) was performed on anaesthetised rats aged between 16 and 19 days in a sound insulated box with a loudspeaker delivering a 14.8 kHz, 110 dB SPL sound for 2 or 3 sessions, of 3 hours across 2 to 3 consecutive days (Fig. II.6).

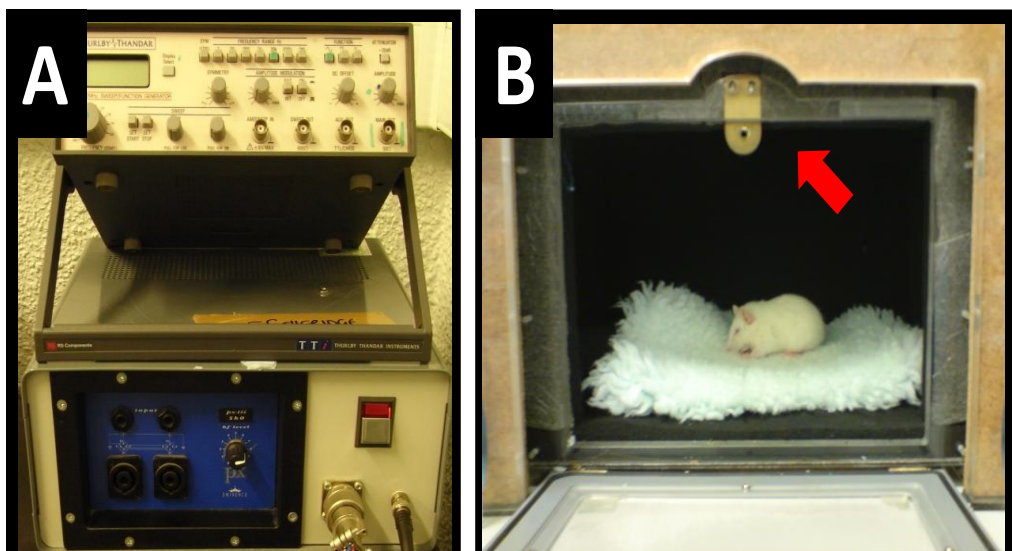


**Figure II.6. Acoustic overexposure setup.** (A) A single tone function generator connected to an amplifier was used to deliver 110 dB SPL, 14.8 kHz tone. (B) The signal was transmitted to a noise insulated enclosure via a loudspeaker (indicated by arrow) located above the anaesthetized rat. Rats were placed on a heating pad to maintain the body temperature.

Although of a longer duration, the intensity of the exposure used falls within the range of intensities utilised by other researchers (Wang et al., 2009; Kujawa and Liberman 2009). The acoustic signal was generated by a TG550 function generator (Thurlby Thandar instruments, UK) linked to loudspeakers via an amplifier (px-iii, Eminence; Fig. II.6). Littermates that were only anaesthetised for the same period as AOE served as controls.

### II.3.3. Auditory brainstem response recordings

#### II.3.3.1. The recording setup

Anaesthetised Wistar rats were placed on a heated pad and exposed to short tone pips (5ms) of varying frequencies (8 to 30 kHz) delivered via an acoustic driver placed directly above the ear of the rat. (Fig. II.7).



**Figure II.7. Placement of the acoustic driver and the recording electrodes.** The acoustic driver (AD) is placed directly above the rat ear and delivered short tone pips of varying frequencies and intensities. The ABR triggered by these tone pips was recorded by three subdermally placed electrodes (a positive (+) and negative (-) electrode in close proximity to the ear and an earth electrode (E) on the rump).

The tone signal was generated by a Thurlby Thunder arbitrary waveform generator (TGA 1230, 300 MHz, Tucker Davis, US) which had a peak to peak amplitude of 20 V corresponding to an intensity of 94 dB SPL. The generator was controlled via the analogue to digital converter (ADC) output of a computer at a stimulus rate of 10 Hz.

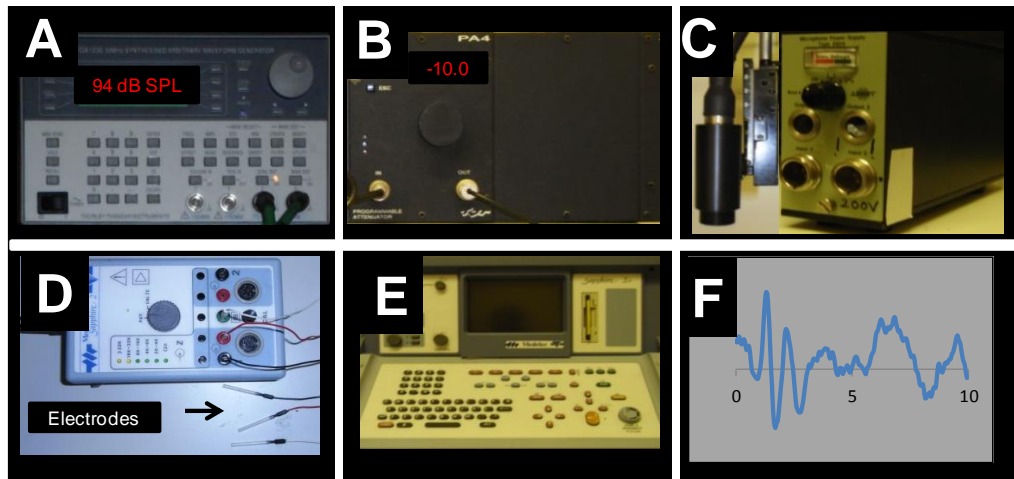


**Figure II.8. Auditory brainstem response recording setup.** A waveform generator (A) produces short tone pips of varying frequencies (8-30 kHz) at 94 dB SPL which can be attenuated in 10 or 3 dB SPL steps (B). Tone pips are delivered to the rat ear via an acoustic driver (C) and the elicited ABR is recorded by three subdermally placed electrodes (D), connected to an amplifier (E). The resulting signal is viewed as an ABR trace via a custom made software (GlaxoSmithKline) (F).

The stimulus signal was fed into two programmable digital attenuators (Tucker Davis technology, USA), the first of which attenuated the signal in 10 dB SPL steps and the second in 3 dB SPL steps before being delivered by a reverse driven battery-operated B&K microphone (B&K 4134) serving as an acoustic driver. The final ABR trace was an average of 100 to 400 responses (depending on signal resolution) recorded by subdermally placed electrodes (Fig. II.7) with an input gain of 20  $\mu\text{V}/\text{div}$  connected to an amplifier (Medelec Sapphier 2A). The amplifier feeds the analogue signal via the ADC input of the ADC sampler at a rate of 16 kHz (Fig. II.8).

### II.3.3.2. Analysis

Auditory brainstem response recordings are a representation of the auditory pathway activity in response to a brief acoustic stimulus such as a single tone frequency (tone pip) or a click (broadband stimulus). The ABR provides an estimation of the hearing threshold or the subject's sensitivity to sound and can be used to identify neurological abnormalities along the auditory pathway (Starr and Achor, 1975). The rat ABR begins

to develop by postnatal day 12, it comprises 2 distinct peaks (peak I and II) by postnatal day 14 and 5 peaks (peak I to V) by postnatal day 36 (Blatchley et al., 1987). At the time of first ABR recordings (P16 - 25), the rat ABR comprised 2 – 4 peaks. However due to their distinct and constant nature, only the presence of peak I and II were used as a measure of the hearing threshold. The ABR peaks are generated by a series of action potentials and postsynaptic potentials ascending the lower portion of the auditory pathway and occurring within 6 ms of onset (Church et al., 1984) (Fig. II.9) . The neurogenerators of the rat ABR have not been determined, however in mice they reflect activity along the AN (peak I), the cochlear nucleus (peak II), the superior olivary complex (peak III) and the LL and/or IC (peak IV) and the auditory cortex (peak V) (Sulkowski, 1988).

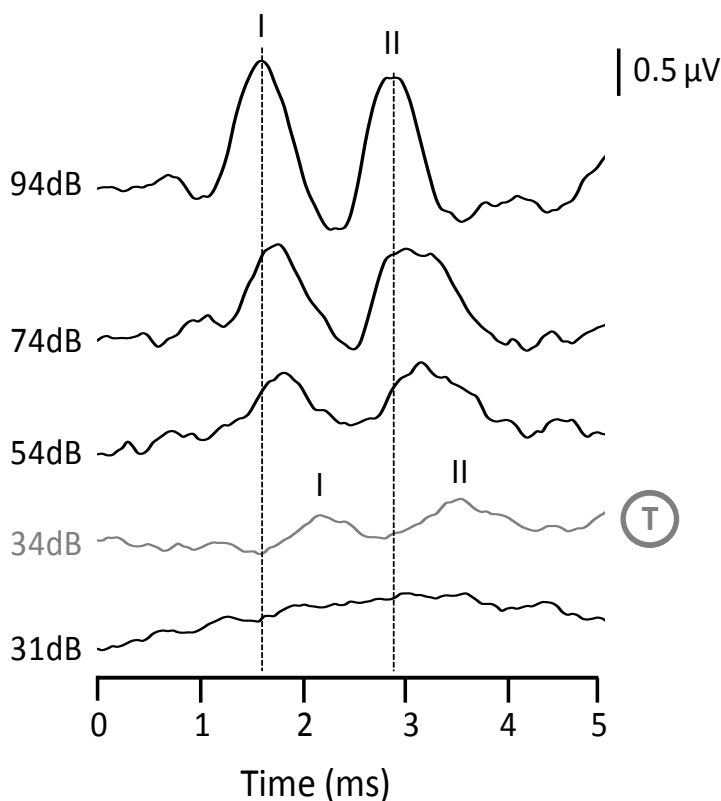


**Figure II.9. Identifying the hearing threshold using ABRs.** The example traces shown were recorded from an anaesthetized Wistar rat (P16) prior to performing an AOE. The ABR recordings were evoked by a 24 kHz single tone frequency at varying intensities (31-94 dB SPL). The dashed lines indicate peak I and II position at 94 dB SPL. The lowest intensity at which peak one (I) and two (II) are detected is defined as the threshold, indicated here by the circled T at 34 dB SPL. Notice that the latency of the peaks increases as the sound intensity decreases.

The ABR recordings were used to assess changes in the hearing threshold induced by AOE and/or administration of specific drugs (memantine: 5mg/g/day or MgCl<sub>2</sub>: 5µl/g/day). In this study the hearing threshold was defined as the minimum sound intensity where ABR peaks 'I' and 'II' can be clearly elicited. A typical example of how this was carried out is shown in *Fig. II.9*. In the short term following AOE, some subjects exhibited a flat ABR trace with no discernible peaks at 94 dB SPL and were therefore assigned a theoretical hearing threshold of 95 dB SPL for the purpose of statistical analysis. To track the changes of the hearing threshold, ABR threshold shifts were calculated as the difference between the hearing thresholds recorded from two separate ABR sessions. Short term threshold shifts were calculated as the hearing threshold recorded on day 3 to 5 (second set of ABRs) minus the hearing threshold recorded on day 0 (first set of ABRs). Long term threshold shifts were calculated as the hearing threshold recorded at the third set of ABRs (either 4 weeks or 13 weeks after first ABRs) minus the hearing threshold recorded at day 0 (first set of ABRs). In addition to the hearing threshold and threshold shifts, parameters such as the peak 'I' amplitude and the latency to peak 'I' were also calculated (*Fig. II.10*). Changes to these parameters between the first, second and third set of ABR recordings were also analysed.

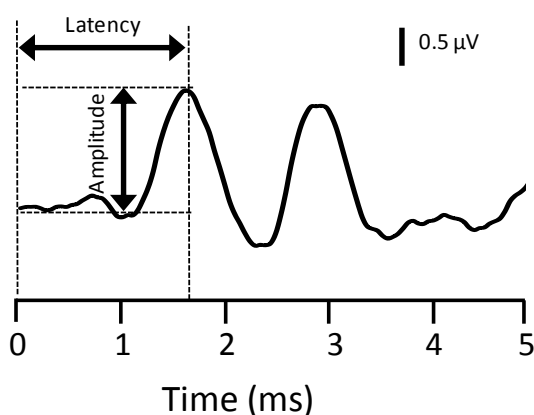


**Figure II.10. Analysis of auditory brainstem responses.** The example trace shown was recorded from an anaesthetised Wistar rat (P16) prior to performing an AOE and elicited by a 24 kHz tone at 94 dB SPL. The peak 'I' latency (ms) and amplitude (µV) are measured as indicated by the arrows.

### **II.3.4. Tinnitus screening via the gap detection method**

Behavioural tests used to screen for tinnitus have always required the training of animals to respond distinctively to the absence or presence of an acoustic stimulus (Bauer et al., 1999, Guitton et al., 2003). These tests require complex behavioural manipulations and months of behavioural training making it difficult to implement. More recently a novel tinnitus screening method which requires no such training has been described (Turner et al., 2006). The technique is based on the modulation of the acoustic startle reflex using background sounds (Koch and Schnitzler, 1997, Braff et al., 1999). The acoustic startle reflex is a contraction of the skeletal and facial muscles in response to an abrupt and intense (> 80 dB SPL) auditory stimulus (Leumann et al., 2001). The force of the reflex is linked to the amplitude of the startle stimulus intensity. The startle reflex can also be attenuated by preceding the startle stimulus with a non-startling stimulus (< 80 dB SPL); this is better described as a pre-pulse inhibition (Hoffman and Donovan, 1994). A variant of this pre-pulse inhibition is to embed a short silent gap into a continuous background tone which precedes the startling stimulus. Rats are capable of detecting silent gaps in a background tone (Ison et al., 1991, Threlkeld et al., 2008) and this can serve as the non-startling stimulus to cause pre-pulse inhibition. The duration of the silent gap used was 50 ms and this has previously been shown capable of attenuating the startle reflex in rats (*Fig. II.11.*)(Turner et al., 2006, Gaese et al., 2009).

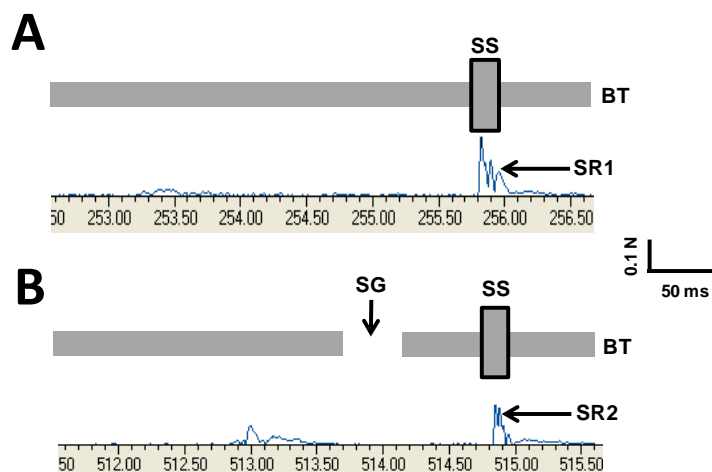


**Figure II.11. Attenuation of the acoustic startle reflex.** Screen shots captured from the StartleFear Panlab system for gap detection. Activity of the rat is recorded in the presence of a 60 dB SPL background tone (BT). **(A)** The startle reflex (SR1) in response to the startle stimulus (SS) is indicated. **(B)** Preceding the startle stimulus (SS) with a 50 ms silent gap (SG) in the background tone (BT) attenuates the amplitude of the startle response (SR2).

Rats with tinnitus are unable to detect the silent gap if the background frequency closely matches the frequency of the perceived tinnitus (Turner et al., 2006, Wang et al., 2009). This provided a basis to use the gap detection tests as a method to screen for rats with tinnitus.

### II.3.5. The gap detection setup

Two different gap detection setups were used in these experiments. The first gap detection setup provided by Panlab industries was later replaced by one which was provided by Kinder Scientific and used to collect data reported in Chapter 3.

#### II.3.5.1. The Panlab gap detection setup

Gap detection tests were first performed using a system acquired from Panlab. Tests were conducted with a broadband or single tone background sound and startle stimuli presented through a speaker placed in the ceiling of a testing chamber located within a noise insulated box. The loudspeakers received computer generated signals delivered via an interface (LE 118-8 start & fear interface, Panlab, Spain). The platform of the test chamber was connected to a transducer (LE 111 load cell coupler, Panlab, Spain) linked

to a computer via the LE 118-8 interface. The transducer gave a measure of motion and force applied to the grid platform on the floor of the enclosure. A homemade Perspex holder (Mechanical and electronic joint workshop, University of Leicester) with holes to allow sound passage was placed onto the grid platform to limit the movement of rats during testing. Sound delivery and recording of the startle response elicited was controlled by the programme StartFear V1.02 (Panlab, Spain).

### II.3.5.2. The Kinder Scientific gap detection setup

As the Panlab system was limited to delivering frequencies up to 10 kHz, experiments were later conducted using a system acquired from Kinder Scientific. Gap detection tests performed with this setup were conducted with background sound which was either a BBN or one of various octave based sounds centred at specific frequencies (8, 10, 12, 16, 20 and 24 kHz)

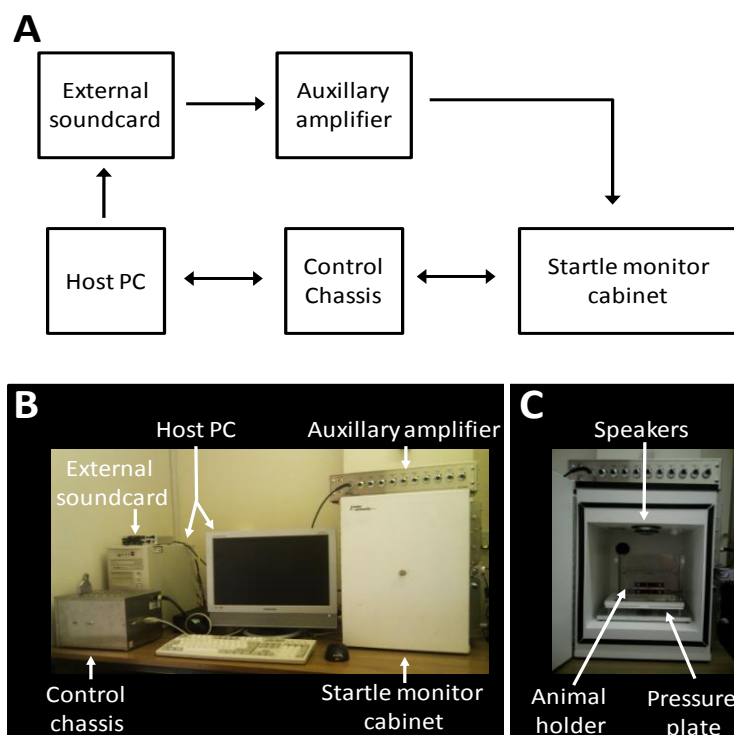


**Figure II.12. Kinder Scientific gap detection setup.** Schematic representation (A) and visual image (B) of connections between components of the setup as described in the text. Tests were carried out in a noise insulated box (C) with a loudspeaker above and a motion sensory plate below. To limit movements, the rat was placed within a holder with holes for sound passage.

The system comprises a startle monitor cabinet connected to the host PC via the control chassis which serves as an interface (*Fig. II.12*). High frequency sounds were generated by an external sound card which is connected via an auxiliary amplifier to loudspeakers located in the ceiling of the cabinet. Rats were kept in a Perspex holder mounted on a pressure plate in a sound insulated box (*Fig. II.12B*). Sound delivery and recording of the startle response was controlled by the programme StartleMonitor (Kinder Scientific). The Perspex holder used in this study had larger holes on all sides to allow better sound passage. Nonetheless it was worthwhile to bear in mind that high frequency sounds will be attenuated to a higher degree compared to lower frequency sounds. This means that errors in behavioural measures of the startle response would be greater for high frequency stimuli compared to low frequency stimuli.

### **II.3.6. Gap detection protocols**

Gap detection tests were carried out in one of multiple background sounds dependent on the gap detection system been used. Specific frequencies were used to screen for tinnitus whereas BBN was used to test for hearing loss. At the time of first gap detection tests, rats were aged between 20 and 25 days old and testing continued for up to 12 weeks. The amplitudes of the background sound and startle stimulus were calibrated to be 60 dB SPL and 110 dB SPL respectively at the level of the rat ear using a B&K 4134 microphone. Each test consisted of 24-trials presented with a 20 to 30 s variable inter-trial interval where only the background sound of choice was played. Each session began with a 2 minute acclimatisation period to the background sound followed by two trials consisting of an abrupt startle eliciting noise burst (BBN, 110 dB SPL, 20 ms duration). The session consisted of 12 startle only trials where no silent

gaps were presented, pseudo-randomly mixed with 12 trials where the silent gap was embedded in the background tone. The silent gaps were 50 ms in duration and began 100 ms before the startle stimulus. This has previously been shown to produce stable levels of gap induced inhibition of the startle reflex in rats (Turner et al., 2006). To obtain a gap detection ratio (GDR) for the purpose of identifying animals with deficits, the amplitude of the startle reflex when the startle stimulus was preceded by a silent gap (G) was divided by the amplitude when there was no preceding silent gap (NG).

$$\text{Gap detection ratio} = \frac{G}{NG}$$

Testing of the startle reflex does not cause a temporary or permanent shift in the hearing threshold, making it possible to use this technique when investigating deficits of the auditory pathway (Turner et al., 2006).

Using the Panlab system, gap detection tests were carried out with either a 10 kHz background sound or a BBN (the system was unable to generate higher frequency tones). Rats were tested once a week for 7 weeks following the first gap detection tests. On the other hand when using the Kinder scientific system, gap detection tests were carried out with a background sound which was either one of the various octave based sounds centred at specific frequencies (8, 10, 12, 16, 20 and 24 kHz) or a BBN. In addition, Wistar rats aged between 19 and 22 days were initially screened for good gap detection in both a BBN and octave based frequency background. Only rats with a GDR below 0.85 in the BBN background were selected and tested again every 3 weeks for up to 12 weeks. This value of 0.85 is higher than the value used by other researchers

because of the under developed auditory system of the young rat which leads to relatively higher GDRs.

## **II.4. Modelling**

A model of a mammalian myelinated axon (McIntyre et al., 2002) was adapted from the database archive of the NEURON simulation environment and was used to estimate the effects of physiological changes in the lamella number, the node length and diameter, the paranode length and diameter, the juxtaparanode length and diameter (McIntyre et al., 2002). The axon was modelled as a multicompartmental double cable, with separate representations of the axolemma and the myelin sheath. Nodes of Ranvier, paranodes and juxtaparanodes segments were included as separate compartments with different geometry and electrical properties. Action potentials were generated at the nodes with modified Hodgkin–Huxley equations that incorporate nonlinear fast  $\text{Na}^+$ , persistent  $\text{Na}^+$ , slow  $\text{K}^+$  conductance, a linear leak conductance, and membrane capacitance. The axolemma and myelin sheath in paranodal and juxtaparanodal segments each have a passive linear conductance in parallel with membrane capacitance. Data from all segments were used to simulate the conduction velocities. The model axons propagated an action potential in response to a supra-threshold, depolarizing current step delivered to the node at one end. Conduction velocity was measured as the distance between the 10<sup>th</sup> and 20<sup>th</sup> nodes, divided by the action potential conduction time between those nodes. All simulations were run in NEURON.

## II.5. Experimental conditions

*In vivo* drug administration to alleviate the deficits induced by AOE was carried with either memantine or magnesium. Subcutaneous memantine (5mg/kg) injections were carried out immediately after each AOE session for three days. After 3 to 5 days the benefits of this drug administration on the shifts in ABR hearing threshold and identified AOE deficits *in vitro* were assessed. Subcutaneous MgCl<sub>2</sub> injections (5 µl/g) were also carried out immediately after each AOE session. In addition some rats had the normal drinking water supplemented with magnesium threonate (604mg/kg/day) which contained 50mg/kg/day elemental magnesium (Scheibe et al., 2001, Abaamrane et al., 2009, Abumaria et al., 2011). The average drinking water was monitored daily and determined to be ~35 ml per day. This allowed the administration of the right daily dose. The following section details the treatments of the various animal groups used in this study.

Unexposed conditions (Un) comprise data from rats unexposed to sound but anaesthetised for the same duration which overexposed rats (AOE) were exposed to sound. During that time, unexposed rats were kept in a recovery enclosure and on a heating pad to help maintain body temperature. In experiments investigating the induction of tinnitus, unexposed rats had ABRs obtained at the time of commencing the study and repeated 3 to 5 days later. The first 3 days following the initial ABR, rats received a daily subcutaneous saline injection (3µl/g). Rats had free access to normal drinking water and diet with a base magnesium content of 0.2%. Gap detection tests were performed every 3 weeks for the next 12 weeks, after which a final ABR was performed at completion of tests. In tests designed to investigate the effects of

specific drugs or compounds, subsets of unexposed rats received subcutaneous injections of memantine (Un-Mem), injections of magnesium chloride (Un-Mg), a high magnesium diet (Un-MgT) or a combination of magnesium chloride injections and the high magnesium diet (Un-MgC). Auditory brainstem responses and gap detection tests were performed similar to the unexposed group. Daily subcutaneous injections were carried out for the first 3 days, after which animals were allowed free access to normal drinking water or drinking water containing magnesium threonate.

Overexposed rats (AOE) had ABRs and gap detection tests performed at similar time points as described for the unexposed group. Immediately following each AOE session, rats received a subcutaneous saline injection and subsequently allowed free access to normal drinking water and diet. Some overexposed rats received memantine injections (AOE-Mem), magnesium chloride injection (AOE-Mg), a high magnesium diet (AOE-MgT) or a combination of magnesium chloride injections and a high magnesium diet (AOE-MgC).

## **II.6. Calibration of acoustic equipment**

The sound intensities emitted by the acoustic driver used to evoke ABR responses were calibrated using a B&K 4134 microphone. The microphone was placed ~0.5 cm away from the acoustic driver which corresponds to the same distance between the rat's ear and the acoustic driver when recording ABRs. The output from the microphone was connected a digital oscilloscope (PicoScope ADC200 sys V6.2) which gave a read out of sound intensity in dB Volt. This value was then converted into dB SPL using the software sound level calibrator (CAL73). The values obtained are detailed in the table below:

Acoustic driver signal		Intensity of sound measured	
kHz	dB	dB V	dB SPL
8	94	-35	83
8	84	-46	72
8	74	-58	60
24	94	-32	86
24	84	-44	74
24	74	-58	60

**Table II.1. Acoustic driver calibration.** Various intensities emitted by the acoustic driver at both low and high frequencies with the respective measure in dB V and dB SPL as recorded by a B&K 4134 microphone.

The sound emitted by the speakers located in the startle box was also calibrated to 60 and 110 dB SPL for all frequencies to be tested. In addition to the sound calibration, the pressure plate in each of the all four startle boxes was calibrated every day before use to record  $\pm 0.004$  N in response to a 1 N force applied by a force generator.

## II.7. Statistical tests

All data sets were tested for normality using the Shapiro-Wilk test. When data groups were normally distributed, the Student's T test was used to establish significant differences between two data sets. A 'paired' or 'unpaired' T test was used when data was compared between the same population or two populations respectively. For tests where the mean of three or more groups were being compared, a one way analysis of variance (ANOVA) was used. Repeated measures (RM) ANOVA tests were also used to identify changes of a specific parameter over time from the same population of data. When a significant difference was detected ( $P < 0.05$ ), Tukey or Student-Newman-Keuls (SNK) post hoc tests were performed. To investigate how GDR

changes over time in relation to treatment group (Un, UnMgC, AOE and AOEMgC) at multiple frequency backgrounds (8 kHz, 12 kHz, 16 kHz, 20 kHz, 24 kHz and BBN) and time points, the linear mixed model (LMM) analysis was used. The LMM determines the mean, variance and covariance between factors. The LMM analysis also takes into account fixed effects which are the treatment variables and random effects which are mainly due to the correlation that occurs from having multiple observations from the same subject in the data set (West, 2009). The LMM analysis was run using a restricted maximum likelihood procedure in SPSS 20. The GDR was selected as the dependent variable, the treatment group as the categorical factor and the time in weeks as the continuous covariate which was analysed using a first order autoregressive covariance structure. The test of fixed effects was performed to identify significant interactions between time and treatment group on GDR at each frequency ( $P < 0.05$ ). Pairwise comparisons and adjustments for multiple comparisons with Bonferroni test ( $P < 0.05$ ) were used to identify differences between groups.

For non-parametric data sets, the Wilcoxon test was used to test for significance following a treatment in the same group. The Mann Whitney test was used to test for significance between two different populations. When testing for significance between three or more populations, the one ANOVA on Ranks test was used instead. When the ANOVA test detected that a difference between the groups ( $P < 0.05$ ), post-hoc tests Student-Newman-Keuls (SNK) or Dunnett's tests were then used to identify which specific groups differed from one another. Significant difference are reported when  $P < 0.05$  (\*) or  $P < 0.01$  (\*\*). In addition a non significance (NS,  $P > 0.05$ ) is also reported. All results shown are presented as a mean  $\pm$  the standard error of mean (SEM).

# **CHAPTER 1**

**Effects of acoustic overexposure  
on action potential propagation and synaptic responses  
evoked by auditory nerve stimulations**

## 1.1. INTRODUCTION: Effects of acoustic overexposure

Acoustic overexposure (AOE) raises the hearing threshold and induces deficits of synaptic transmission along the AN. Following AOE, peak 'I' of the ABR which is indicative of the propagation of action potentials along the AN exhibits significantly lower response amplitudes and delayed latency to onset (Starr and Achor, 1975, Sulkowski, 1988, Ito et al., 2004). In addition, AOE also triggers a reduction in the AN firing rate (Liberman, 1984, Shepherd et al., 2004), degrades the AN tonotopic representation of acoustic stimuli (Miller et al., 1997, Wong et al., 1998), decreases the number of functional myelinated AN fibres (Lin et al., 2011, Pilati et al., 2012a) and promotes demyelination of peripheral AN fibres (Pilati et al., 2012a). Deficits also alter the neuronal activity of cells in DCN (Zhang and Kaltenbach, 1998, Pilati et al., 2012b), the IC (Szczepaniak and Moller, 1996, Ma et al., 2006) and the auditory cortex (Seki and Eggermont, 2003). All the aforementioned deficits could also underlie the subsequent occurrence of tinnitus (Roberts et al., 2010). In this chapter I tested whether AOE affected AN responses to electrical stimulation and whether this influenced the synaptic activity at AN synapse onto fusiform cells in the DCN. I used a combination of *in vivo* and *in vitro* recording techniques to investigate the effects of AOE on the functional properties of the AN. I used ABRs to assess the effect of AOE on the hearing threshold of Wistar rats and also field potential recordings (*in vitro*) to assess deficits to the propagation of action potentials along the AN. Finally, I performed whole cell voltage clamp recordings to quantify changes in synaptic activity at the synapses between the AN and fusiform cells.

## 1.2. RESULTS

### 1.2.1. A typical effect of acoustic overexposure on ABRs

Hearing threshold was assessed by ABRs to measure a subject's sensitivity to single tone frequencies. Changes in a subject's sensitivity to sound were assessed by measuring changes in peak 'I' amplitude, peak 'I' latency, the hearing threshold and the shift in hearing threshold 3 to 5 days after anaesthesia only (unexposed) or the initial AOE (overexposed). An example of ABR recordings obtained at 24 kHz from an unexposed and overexposed animal is shown in *Fig. 1.1*.

In the unexposed subject, the first recording evoked by 24 kHz tones at 94 dB SPL (*Fig 1.1A left*) revealed a peak 'I' amplitude of 1.96  $\mu$ V, the latency to peak 'I' (which is measured as the interval from onset of the ABR response to peak 'I') was 1.6 ms, and the hearing threshold was 31 dB SPL. Four days after the initial recording (*Fig. 1.1B*), the peak 'I' amplitude was 1.84  $\mu$ V, peak 'I' latency was 1.3 ms, the hearing threshold was 38 dB SPL and the calculated shift in hearing threshold was 7 dB SPL (calculated as the 'hearing threshold at second recording' minus 'hearing threshold at first recording'). Analysis of the parameters listed above was repeated for overexposed subjects to determine significant differences induced by the AOE protocol. Between day 0 before AOE and day 4 after AOE, the peak 'I' amplitude decreased from 1.26  $\mu$ V to 0.2  $\mu$ V, the peak 'I' latency increased from 1.4 ms to 2.15 ms and the hearing threshold increased from 34 dB SPL to 81 dB SPL resulting in a calculated threshold shift of 47 dB SPL.

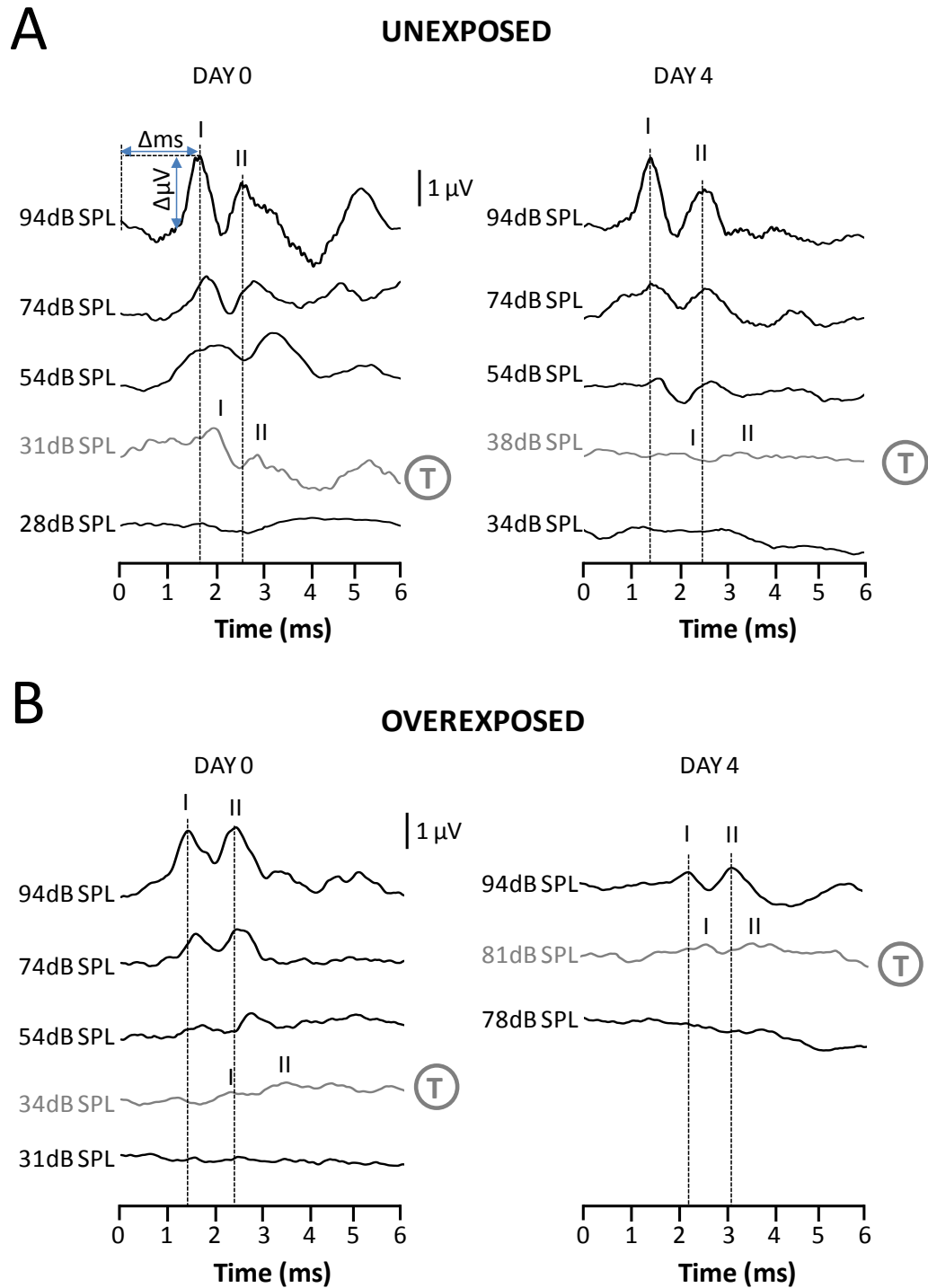


**Figure 1.1. Acoustic overexposure raises the hearing threshold. (A)** An example of ABR recordings obtained from an unexposed rat aged 19 days, on day 0 (left) and day 4 (right) of tests. ABR traces were elicited by short tone pips at 24 kHz and varying intensities (in dB SPL) as indicated. The threshold values are shown as a circled T which was 31 dB SPL on day 0 and 38 dB SPL on day 4. **(B)** Similar recordings obtained from an overexposed rat prior to and following an AOE protocol reveal threshold values of 34 dB SPL on day 0 before AOE and 81 dB SPL on day 4 following AOE.

### 1.2.2. Effect of acoustic overexposure on ABR peak 'I' amplitude

The peak 'I' amplitude was recorded for other rats in both the unexposed and overexposed conditions. In the unexposed condition, there was no significant change in the peak 'I' amplitude between day 0 and day 4 at all frequencies tested (Paired T tests, n = 9). In the overexposed condition, there was also no significant change in the peak 'I' amplitude at 8 kHz (from  $1.82 \pm 0.43 \mu\text{V}$  to  $1.32 \pm 0.22 \mu\text{V}$ ; n = 9, P > 0.05, Paired T test) and at 12 kHz (from  $2.37 \pm 0.4 \mu\text{V}$  to  $1.5 \pm 0.3 \mu\text{V}$ ; n = 9, P > 0.05, Paired T test). However there was a significant decrease in the peak 'I' amplitude at 16 kHz (from  $1.85 \pm 0.21 \mu\text{V}$  to  $0.91 \pm 0.25 \mu\text{V}$ ; n = 9, P < 0.05, Paired T test), 24 kHz (from  $1.51 \pm 0.3 \mu\text{V}$  to  $0.35 \pm 0.12 \mu\text{V}$ ; n = 9, P < 0.01, Paired T test) and 30 kHz (from  $1.28 \pm 0.25 \mu\text{V}$  to  $0.53 \pm 0.14 \mu\text{V}$ ; n = 9, P < 0.05, Paired T test). A bar chart summarising all the changes in peak 'I' amplitude is shown in *Fig. 1.2*.

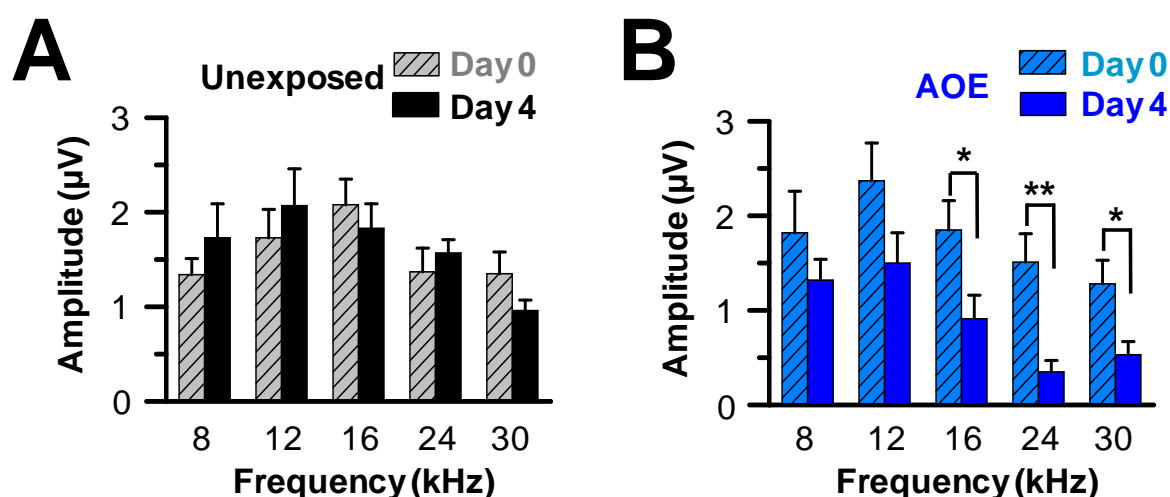


**Figure 1.2. Acoustic overexposure decreases the peak I amplitude at specific frequencies. (A)** In the unexposed condition (n = 9) there is no change in the 'peak I' amplitude 3-5 days after first ABR recordings. **(B)** Following AOE (n = 9) there is a significant decrease in the peak 'I' amplitude at all frequencies tested above the frequency of the AOE protocol which was 15 kHz (\*P < 0.05, \*\*P < 0.01, Paired T tests. 8kHz: P=0.3; 12kHz: P=0.09; 16kHz: P=0.03; 24kHz: P=0.002; 30kHz: P=0.01).

### 1.2.3. Effects of acoustic overexposure on ABR peak 'I' latency

Between day '0' and day '4', unexposed rats exhibited a decrease in the peak 'I' latency at all frequencies tested ( $n = 9$ ,  $P < 0.05$ , Paired T tests, Fig. 3.3). Conversely, 3 to 5 days following AOE, there were changes to the peak 'I' latency which were not uniform across all frequencies. Indeed, the latency decreased at 8 kHz (from  $1.59 \pm 0.03$  ms to  $1.47 \pm 0.05$  ms;  $n = 9$ ,  $P < 0.05$ , Paired T test), but was unchanged at 12 kHz (from  $1.52 \pm 0.03$  ms to  $1.57 \pm 0.06$  ms;  $n = 9$ ,  $P > 0.05$ , Paired T test,) and also at 30 kHz (from  $1.34 \pm 0.05$  ms to  $1.44 \pm 0.07$  ms;  $n = 9$ ,  $P > 0.05$ , Paired T test,). However, the latency increased at 16 kHz (from  $1.52 \pm 0.04$  ms to  $1.85 \pm 0.11$  ms;  $n = 9$ ,  $P < 0.05$ , Paired T test) and 24 kHz (from  $1.4 \pm 0.4$  ms to  $1.77 \pm 0.13$  ms;  $n = 9$ ,  $P < 0.05$ , Paired T test).

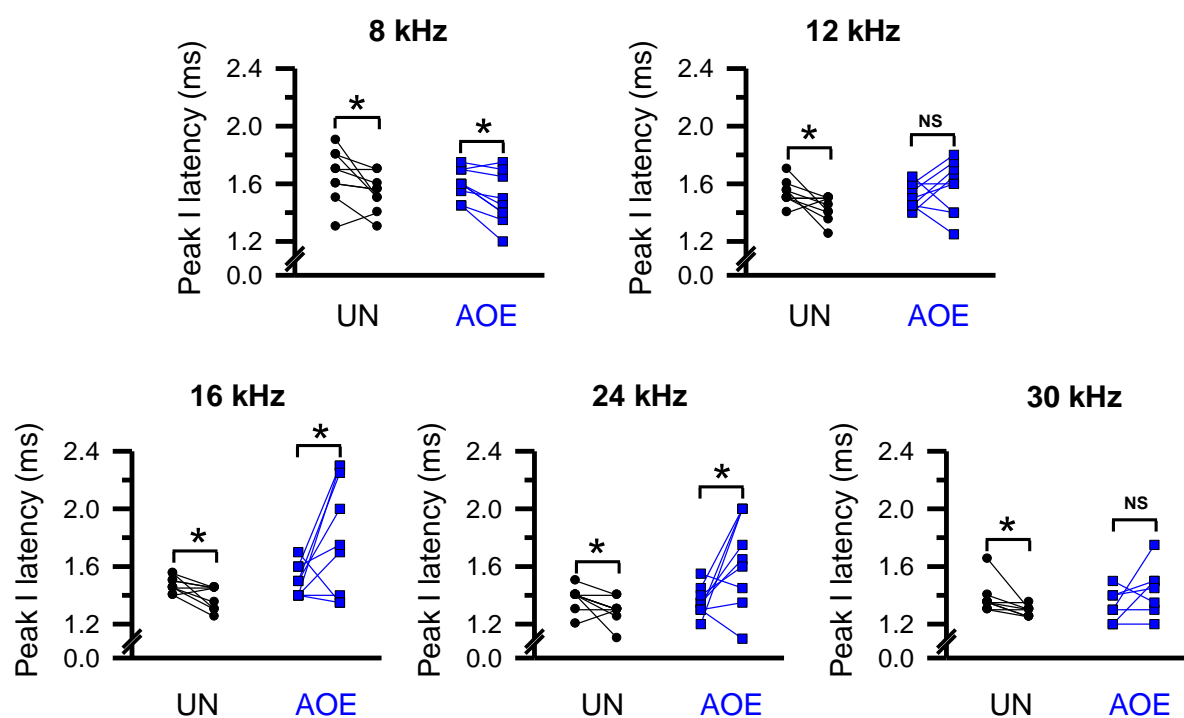


**Figure 1.3. Acoustic overexposure (AOE) increases the latency to peak I.** In the unexposed condition (black circles,  $n=9$ ) there is a decrease in the latency to peak 'I' 3 to 5 days after first ABR recordings. However following AOE (blue squares,  $n = 9$ ), latencies are decreased at 8 kHz, increased at 16 and 24 kHz whereas they remain unchanged at 12 and 30 kHz. Each point plotted represents data collected from one animal. Points on the left represent control values before Un or AOE treatment on day 0 whereas points on the right represent values collected 3 to 5 days after treatments associated with each group. \*  $P < 0.05$ , NS:  $P > 0.05$ , Paired T tests.

### 1.2.4. Effects of acoustic overexposure on hearing thresholds

Unexposed subjects serving as controls exhibited no significant change in the hearing threshold for all frequencies tested (*Table 1.1*; Paired T tests). However following AOE, changes in hearing thresholds were observed at frequencies of 12 kHz and above (*Fig. 1.1B*; *Tab 1.1*). These results were in accordance with previous publications showing that an increase in the hearing threshold occurs at frequencies close to the frequency of the AOE (Spendlin, 1971).

Group	Frequency	Threshold at day 0 (dB SPL)	Threshold at day 3-5 (dB SPL)	P value (Paired T test)
Unexposed (n = 6)	8 kHz	49 ± 8	50 ± 6	0.651
	12 kHz	45 ± 8	41 ± 7	0.93
	16 kHz	42 ± 7	44 ± 6	0.916
	24 kHz	42 ± 5	39 ± 4	0.224
	30 kHz	44 ± 5	46 ± 5	0.856
AOE (n = 9)	8 kHz	41 ± 4	43 ± 6	0.449
	12 kHz	32 ± 3	52 ± 5	0.003(**)
	16 kHz	37 ± 4	80 ± 4	8 × 10 <sup>-8</sup> (**)
	24 kHz	36 ± 4	91 ± 2	2.6 × 10 <sup>-6</sup> (**)
	30 kHz	37 ± 4	90 ± 2	7.6 × 10 <sup>-7</sup> (**)

**Table 1.1. Average hearing thresholds.** Hearing thresholds (dB SPL) are shown for both unexposed and overexposed rats at five frequencies tested. A significant difference between the means has been identified between day 0 and day 3 to 5 (\*\*  $P < 0.01$ , Paired T tests).

The differences between the hearing thresholds at the time of first ABRs and 3 to 5 days later in both the unexposed and AOE conditions were calculated as a threshold shift. In the unexposed condition (n = 6), these values were -2 ± 3 dB SPL at 8 kHz, -4 ± 5 dB SPL at 12 kHz, 0 ± 3 dB SPL at 16 kHz, -4 ± 3 dB SPL at 24 kHz and -1 ± 3 dB SPL at 30 kHz. After AOE (n = 9) threshold shifts were 2 ± 3 dB SPL at 8 kHz, 20 ± 6 dB SPL at 12 kHz, 43 ± 3 dB SPL at 16 kHz, 54 ± 5 dB SPL at 24 kHz and 53 ± 4 dB SPL at 30 kHz. Threshold shifts calculated after AOE were significantly higher than the values

reported for the unexposed condition at 12, 16, 24 and 30 kHz (Fig. 3.4;  $P < 0.05$ , Unpaired T tests).

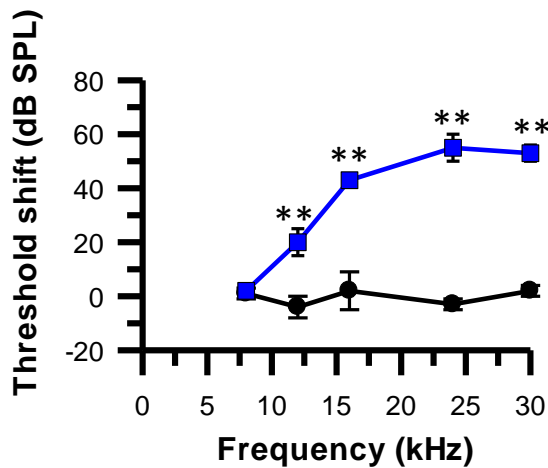


**Figure 1.4. Effects of acoustic overexposure on hearing threshold shifts.** Mean threshold shifts  $\pm$  SEM (dB SPL) measured from 16 rats (Control: black,  $n=6$ , AOE: blue,  $n=9$ ) at various frequencies. The increase in hearing threshold was significant at frequencies of 12 kHz and above (\*\*  $P < 0.01$ , Unpaired T tests). There was no significant difference in the hearing threshold shifts calculated at 8 kHz ( $P > 0.05$ , Unpaired T tests).

In summary, the AOE protocol used in this study at 15 kHz raises the hearing threshold at frequencies of 12 kHz and above.

### 1.2.5. Effects on auditory nerve compound action potentials

It has previously been reported that cochlear damage induced by acoustic trauma or an ototoxic drug is capable of triggering a plethora of AN deficits such as a decrease in the compound action potential (CAP) amplitude (Wang and Dallos, 1972, Salvi et al., 1980, Salvi et al., 2000), demyelination of the peripheral AN fibres (Pilati et al., 2012a) and more recently, unpublished data obtained by Matt Barker in this lab indicated that AOE can also induce demyelination of the central AN fibres. The next question was therefore to confirm deficits related to the AN such as changes in the action potential conduction velocity in my model of acoustic trauma. In the unexposed conditions, stimulating the AN at 40 V evoked a presynaptic volley (or CAP) with a mean amplitude of  $0.4 \pm 0.08$  mV ( $n = 6$ ). Following AOE ( $n = 7$ ), the amplitude was significantly lower at  $0.12 \pm 0.03$  mV (Fig. 3.5;  $P < 0.05$ , Unpaired T tests).

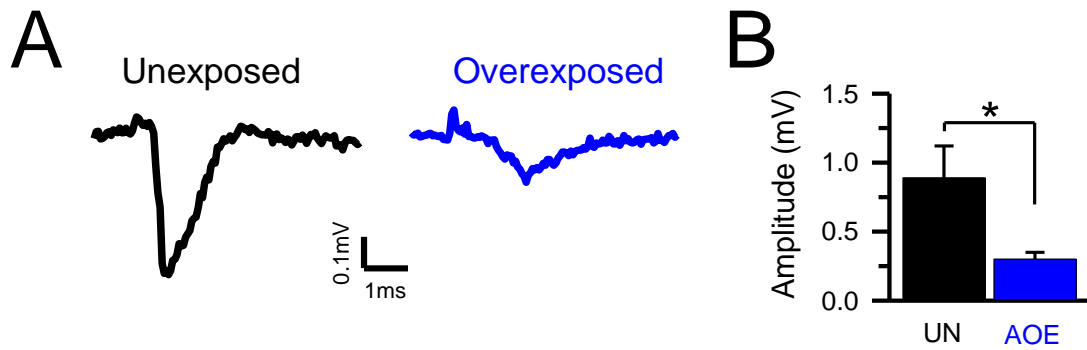


**Figure 1.5. Acoustic overexposure decreases the size of AN (pre-synaptic) field potentials.** (A) Average of 10 AN field potentials evoked at a 40 V stimulation intensity in both the unexposed (left) and overexposed (right) conditions. (B) Bar chart showing a significantly lower field potential peak amplitude in the overexposed (AOE) condition (UN: n=6; AOE: n=7; \*  $P < 0.05$ , Unpaired T test).

The effect of AOE on the conduction properties of the AN CAP was also assessed. As before, the AN was stimulated at an intensity of 40 V in both conditions and the evoked CAP were recorded at multiple positions along the length of the AN section in coronal brainstem slices. In the unexposed condition, CAPs were recorded at varying intervals between the stimulation and recording electrode ranging from 1 to 1.8 mm. Recordings at shorter interval gaps could not be obtained due to a merging of the CAP with the stimulation artefact. Interestingly, after AOE, CAPs could never be recorded at intervals exceeding 1 to 1.2 mm. (Fig. 1.6). At intervals exceeding this distance, the CAP could not be distinguished from the background noise.

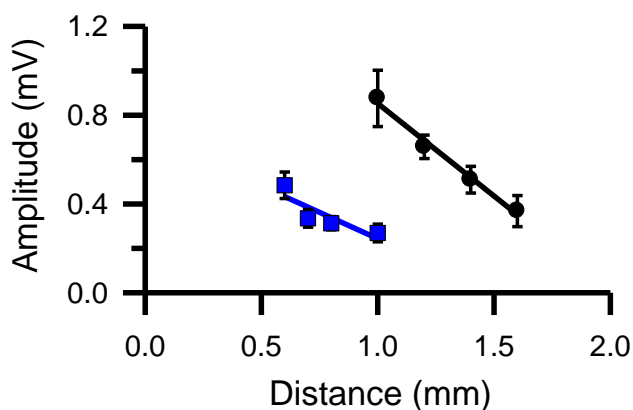


**Figure 1.6. Acoustic overexposure decreases the length for which AN fields potentials can be recorded.** The CAP amplitude was plotted against the interval between stimulation and recording electrode. The AN CAPs can be recorded between 1 and 1.8 mm intervals in the unexposed condition (black; n = 7) and between 0.5 and 1 mm intervals in the overexposed condition (blue; n = 7).

In addition a lower conduction velocity of  $0.79 \pm 0.03 \text{ ms}^{-1}$  ( $n = 7$ ) was recorded after AOE, in comparison to a conduction velocity of  $3.2 \pm 0.01 \text{ m.s}^{-1}$  ( $n = 7$ ) in the unexposed condition (Fig. 1.7;  $P < 0.05$ , Unpaired T test).

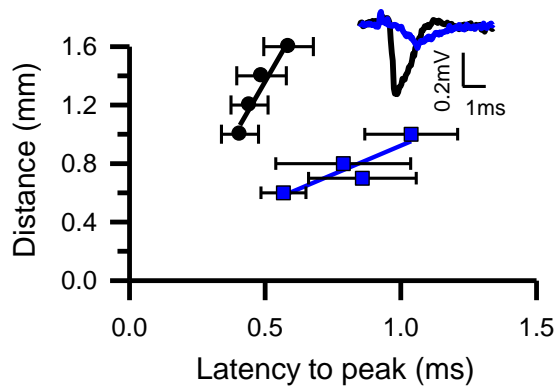


**Figure 1.7. Acoustic overexposure decreases the conduction velocity of action potentials recorded along a segment of the AN (Un: black circles,  $CV = 3.2 \text{ m.s}^{-1}$ ,  $n = 7$ ; AOE: blue squares,  $CV = 0.8 \text{ m.s}^{-1}$ ,  $n = 7$ ;  $P < 0.05$ , Unpaired T test). Insert shows examples of CAPs evoked a distance of 1 mm by 40 V AN stimulation in unexposed (black) and overexposed (blue) conditions.**

Previous experiments carried out in this lab made available morphological data detailing changes in the myelin structure and axonal domains of the AN following AOE (APPENDIX 1). I took advantage of this data and using a modelling program based on modified Hodgkin–Huxley equations, run in NEURON 7.2 (see section II.4). The conduction velocity was calculated by using morphological data in Appendix 2 and modelling the action potential propagation through nodes 0 to 5 considering an unchanged intermodal length of  $200 \mu\text{m}$ . The action potential latency obtained at those two distances allowed a conduction velocity of  $11.1 \text{ m.s}^{-1}$  and  $7.1 \text{ m.s}^{-1}$  to be determined for the unexposed and overexposed conditions respectively. This corresponded to a 35 % reduction in conduction velocity after AOE. Subsequently, individual domains of the axon were altered in the modelling program to identify how each parameter contributes to the conduction velocity. By altering individual parameters, I was able to identify that the decrease in conduction velocity was largely due to a decrease in myelin thickness or lamella number, an increase in node length and an increase in paranode diameter (Fig. 1.8).

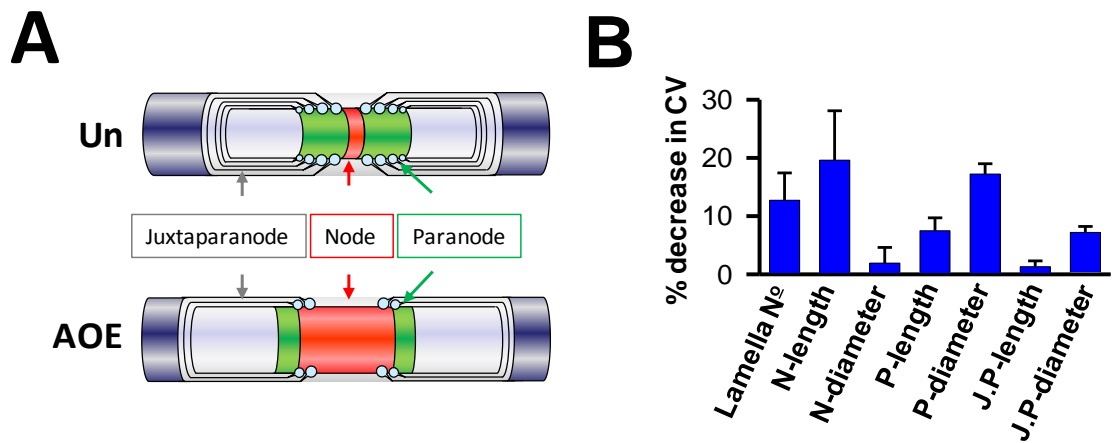


**Figure 1.8. Multiple AN morphological deficits contribute towards a decreased conduction velocity.** (A) Schematic representation of the morphological changes to the axonal domains induced by AOE (unexposed: above; overexposed: below). (B) Modelling shows how alterations in each axonal domain after AOE contribute towards the overall decreased conduction velocity along the AN.

### 1.2.6. Effects on fusiform cell excitatory postsynaptic currents

Having shown in the previous section that AOE affects the action potential properties of the AN, I proceeded to investigate the effects on AN evoked EPSCs in fusiform cells. Auditory nerve evoked EPSCs were recorded at various stimulation intensities ranging from 0.2 to 2 mA in both the unexposed and overexposed condition (Fig. 1.9A).

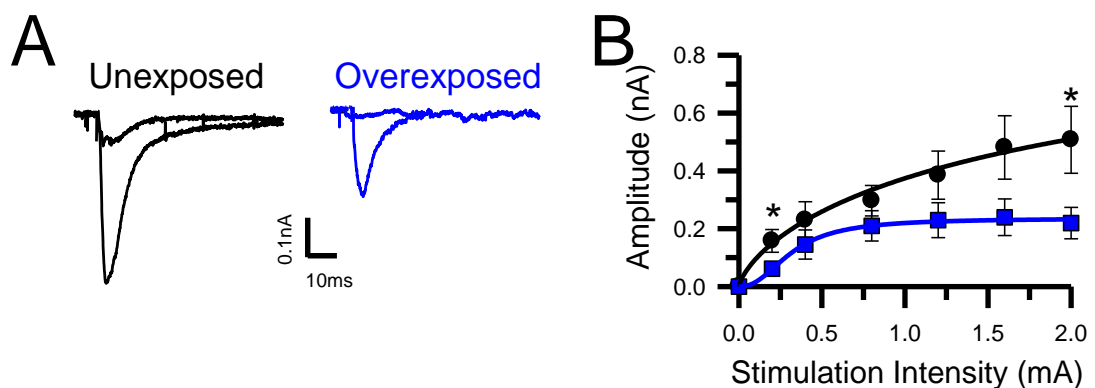


**Figure 1.9. Acoustic overexposure decreases AN evoked EPSCs in fusiform cells.** (A) Average of ten EPSCs in fusiform cells evoked at minimal (0.2mA) and maximal (2mA) intensities in both conditions. (B) Relationship between stimulation intensities and EPSC amplitudes fitted with a Hill Function in the unexposed (black circles, n=6) and overexposed conditions (blue squares, n=8). EPSC amplitudes at minimal and maximal stimulation intensities are significantly lower following AOE when compared to the unexposed condition (Unpaired T tests; \*  $P < 0.05$ ).

In the unexposed condition, 0.1 mA stimulations always elicited an EPSC response with a mean amplitude of  $0.08 \pm 0.02$  nA (n=6). However after AOE, 0.1 mA stimulations failed to evoke an EPSC in 25% of cells tested and stimulations at 0.2 mA were required to evoke EPSCs in all cells. Therefore I compared the amplitude of evoked EPSCs in both the unexposed and AOE conditions at a stimulation intensity of 0.2 mA and found that cells responded with an EPSC amplitude of  $0.16 \pm 0.04$  nA (n = 6) in the unexposed condition and a lower amplitude of  $0.06 \pm 0.01$  nA after AOE (n=8;  $P < 0.05$ , Unpaired T test). The maximum EPSC amplitude evoked at 2 mA stimulation was also significantly lower after AOE (Unexposed:  $0.51 \pm 0.12$  nA; Overexposed:  $0.22 \pm 0.05$  nA;  $P < 0.05$ , Unpaired T test). There was no significant difference in the EPSC amplitudes evoked at stimulation intensities between 0.4 – 1.6 mA ( $P > 0.05$  Unpaired T test).

### **1.2.7. Effects of acoustic overexposure on presynaptic release**

It is accepted that synaptic alterations which decrease release probability can simultaneously increase the PPR (Schulz, 1997, Oleskevich and Walmsley, 2002). A likely mechanism behind the decrease in EPSC amplitude shown above could be a decrease in the synaptic release probability, as such I tested for significant differences in the PPR between the unexposed and overexposed conditions. I performed paired pulse tests with a pulse interval of 60 ms which falls within the range where facilitation has been reported in the cerebellum and at DCN parallel fibre synapses (Tzounopoulos et al., 2004, Sims and Hartell, 2005). At this interval, PPF was absent in both conditions (*Fig.1.10*; Unexposed:  $1.06 \pm 0.09$ , n = 6; AOE:  $1.12 \pm 0.03$ , n = 6). This lack of facilitation suggested that a decrease in release probability was not responsible for the overall decrease in EPSC amplitude witnessed after AOE.

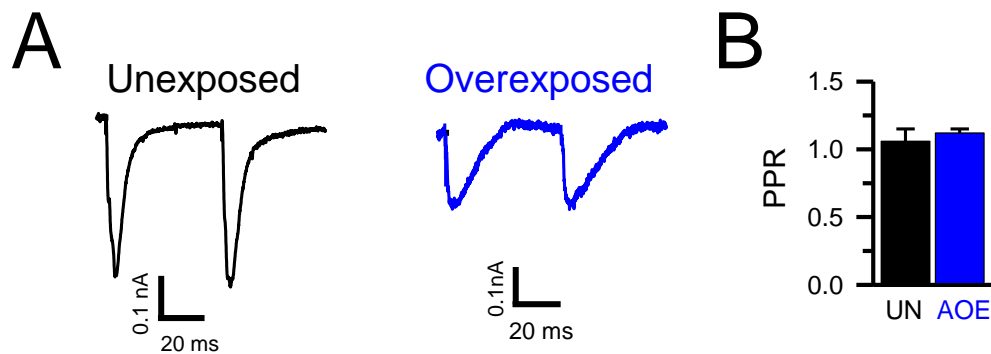


**Figure 1.10. Lack of paired pulse facilitation at AN synapses.** (A) Average of ten traces obtained when paired pulse tests were carried out at 60 ms intervals in both the unexposed (left) and overexposed (right) conditions. (B) Bar charts representing the PPR as shown in (A) for both the unexposed (UN: black bar,  $n = 6$ ) and overexposed (AOE: blue bar,  $n = 6$ ) conditions. There was no difference between the PPR values ( $P > 0.05$ , Unpaired T test).

However AN synapses have been described as been non plastic in nature (Oertel, 2004), therefore to assess the mechanism behind the decrease in EPSC amplitude, I used the VM method of quantal analysis to deduce the N, P and Q values in both the unexposed (Fig. 1.11A&C) and overexposed (Fig.1.11B&C) conditions. Experimentally decreasing the release probability (by decreasing extracellular calcium concentration) led to a decrease in the EPSC amplitude whereas an increase in the release probability (by increasing extracellular calcium concentration) increased the EPSC amplitude (Fig 1.11A left and 1.11B left). This pattern of change in EPSC amplitudes in relation to release probability was the same in both the unexposed and overexposed conditions. In the unexposed condition ( $n = 6$ ), N, P and Q values were  $186 \pm 47$ ,  $0.37 \pm 0.07$  and  $4.3 \pm 1.04$  pA respectively. In the overexposed condition, N, P and Q values were  $83 \pm 20$ ,  $0.44 \pm 0.06$  and  $2.8 \pm 0.4$  pA respectively ( $n = 7$ ). There was a significantly lower number of release sites in the overexposed condition ( $P < 0.05$ , Unpaired T test; Fig. 3.11C); however release probability and quantal size remained unaffected. In conclusion, 3 to 5 days following AOE there was a decrease in the amplitude of AN

evoked EPSCs in DCN fusiform cells which was linked to a decrease in the number of release sites at the synapse.

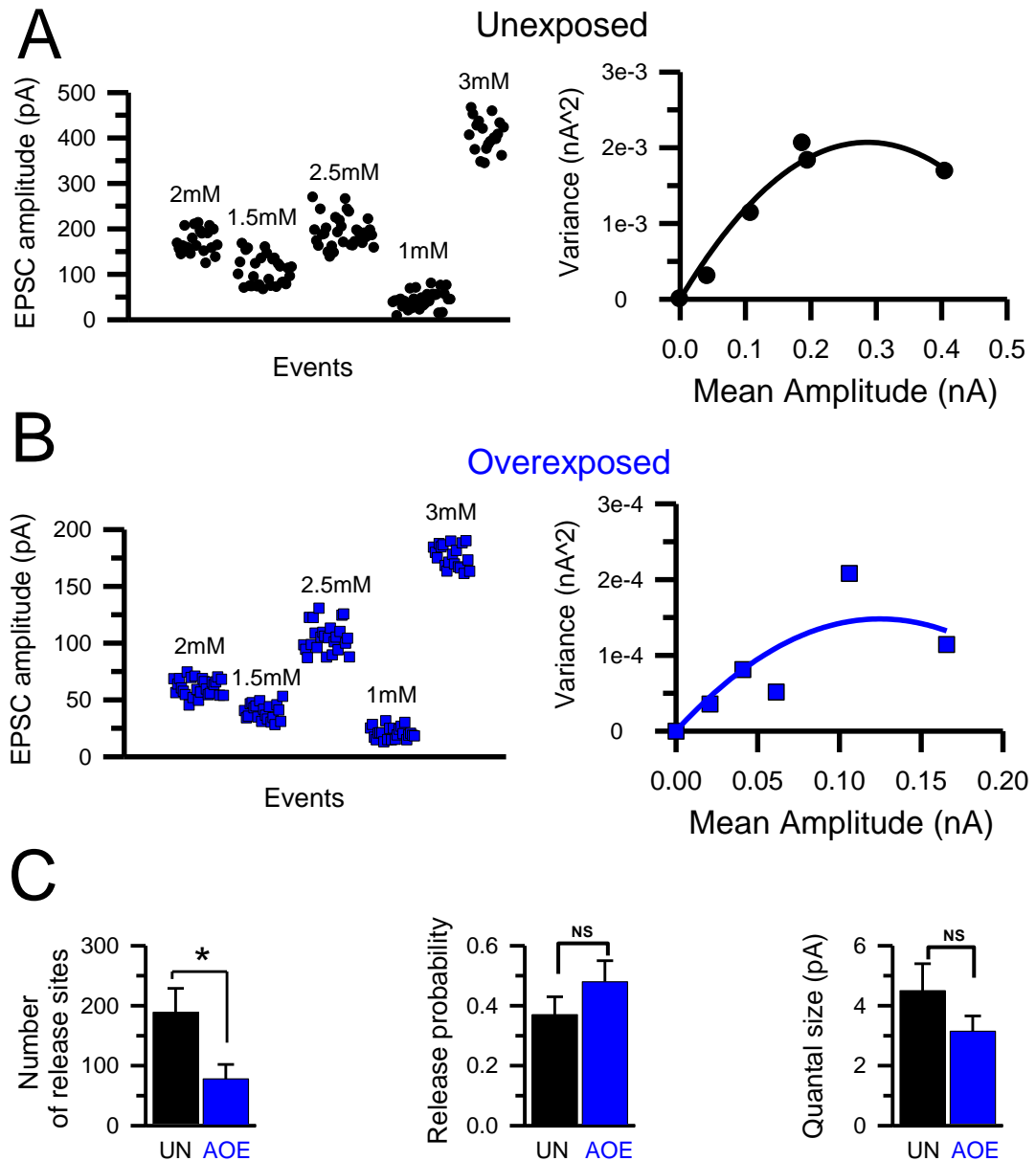


**Figure 1.11. Acoustic overexposure decreases the number of release sites at AN synapses.** Amplitude of AN evoked EPSCs in fusiform cells of slices from unexposed (**A:left**) and overexposed (**B:left**) rats at the various calcium concentrations indicated. Variance-mean graph fitted with a parabola function to calculate  $N$ ,  $P$  and  $Q$  in both the unexposed (**A:right**) and overexposed (**B:right**) conditions. (**C**) Bar charts showing the mean  $\pm$  SEM values obtained for  $N$ ,  $P$ ,  $Q$  in both unexposed (UN) (black,  $n = 6$ ) and overexposed (AOE, blue,  $n = 7$ ) conditions. VM analysis reveal a significant decrease in the number of release sites at AN-fusiform cell synapses following AOE (\*  $P < 0.05$ , Unpaired T test). There was no significant difference between the calculated 'P' or 'Q' values (NS).

## **1.3. DISCUSSION**

### **1.3.1. Characteristics of ABR properties in the unexposed condition**

In this project, ABRs were first recorded between P 16 and P 19 and subsequently repeated 3 to 5 days afterwards. The ABR can be evoked in rats as early as P 12 with characteristics developing until P 36 (Blatchley et al., 1987). Although the properties of the ABR reach a steady level by P 36, peaks 'I' and 'II' were well developed by the time point at which I tested ABRs, i.e. between P 16 and P 24 days (Blatchley et al., 1987). Therefore I was able to confidently use peak 'I' to assess the hearing thresholds. At time of first ABR recordings (prior to allocation into the unexposed or overexposed group), Wistar rats had ABR thresholds between 30 and 40 dB SPL at all frequencies tested. These thresholds are closely related to the ABR hearing threshold of Wistar rats reported in other studies (Church et al., 2007, Zheng et al., 2012). It has been reported that prior to P 16, rats respond preferentially less to high frequency stimulus and after this age, there is a reduction in the peak 'I' amplitude elicited by 8 kHz tones (Blatchley et al., 1987). I did not find this in my model of investigation, at the time of first ABR recordings, there was no significant difference in the hearing thresholds recorded at all frequencies.

### **1.3.2. Changes in auditory brainstem response properties**

Results presented here show a shift in the hearing thresholds 3 to 5 days after AOE. Past research has shown that the ABR is temperature sensitive and a fall in temperature results in significantly higher ABR thresholds (Brown et al., 1983, Rossi and Britt, 1984). This could lead to false threshold shifts being calculated when ABRs were performed on different days. Therefore in this project all rats were kept on a

heated pad during ABR testing to help minimise the drop in body temperature due to anaesthesia. This safety measure allowed changes in the body temperature to be excluded when considering factors that led to elevated ABR thresholds following AOE.

Following AOE at 15 kHz, the ABR threshold was significantly elevated at four frequencies tested (12, 16, 24 and 30 kHz), providing evidence of poor auditory acuity at these frequencies. At 24 and 30 kHz the hearing threshold was above 94 dB SPL in 50 to 60 % of the rats exposed. This suggests that the greatest shift in the hearing threshold occurred at these frequencies. This conclusion is supported by previous studies showing that the maximal effect of AOE occurs between half an octave and one octave above the frequency of overexposure (Salvi et al., 1980, Brozoski et al., 2002). This is attributed to the optimal vibration point of the cochlear basilar membrane being maximally amplified at frequencies half an octave above their incoming rate (Puel et al., 1988). Nonetheless, there was also a significant increase of about 20 dB SPL in the hearing threshold at 12 kHz, which is below the frequency of AOE. This threshold shift was less than the hearing threshold shifts of about 40 dB SPL calculated at the other frequencies. Similar results have been reported in the literature where a tonal AOE has induced threshold shifts at frequencies both above and below that of insult (Gourevitch et al., 2009, Browne et al., 2012, Yang et al., 2012). In addition it has also been shown that following cochlear damage by AOE, axonal degeneration in the cochlear nucleus is greatest in frequency regions lower than the site of cochlear damage (Kim et al., 1997, Morest et al., 1998).

Results in the unexposed condition show a developmental shift in the peak 'I' latency, 3 to 5 days after commencing tests. Normal developmental processes such as axonal

growth and further myelination of axons in the central nervous system could account for the decrease in peak 'I' latency, as further myelination will increase the conduction velocity (Morell et al., 1972, Blatchley et al., 1987). Changes in the peak 'I' latencies after AOE were found to be frequency specific. A decreased peak 1 latency was observed at 8 kHz. As thresholds were unaffected at this frequency, this could be due to the aforementioned developmental processes (Morell et al., 1972, Blatchley et al., 1987). By contrast, at 16 and 24 kHz, hearing thresholds and peak 'I' latencies were increased. From *Fig1.3* it can be seen that 2 rats exhibited no change or a decreased peak I latency at 16 kHz and 24 kHz. Therefore, it is possible that individuals possess various levels of resilience to AOE induced deficits to auditory processing. An increase in the hearing threshold alongside an increase in peak I latency can be attributed to changes such as a loss of OHCs (Liberman et al., 2002), demyelination (El-Badry et al., 2007) and/or a reduction in the number of myelinated AN fibres (Pilati et al., 2012a). Interestingly, although there was a significant increase in the hearing threshold at both 12 and 30 kHz, there was no change in the peak 'I' latency. Concerning the lack of a latency shift at 12 kHz, limited latency shifts have been reported when the threshold shift induced by the acoustic trauma was below 40 dB SPL (Boettcher et al., 1993, Sohmer et al., 1991). The threshold shift reported at 12 kHz in this study was about 20 dB SPL and this could explain why there was no latency shift at 12 kHz. However, contrary to this finding, human studies report a prolonged latency even when the threshold shift was below 40 dB SPL (Rosenhamer et al., 1981, Janczewski et al., 1988, Markand, 1994). Another reason for the lack of a latency shift even with a reported threshold shift at 12 and 30 kHz could be that changes in hearing threshold and peak latency can be dissociated (Donaldson and Ruth, 1996, Gourevitch et al., 2009). This

dissociation could be due to the type of threshold shift which has occurred, whether it is a temporary or a permanent threshold shift. These two types of threshold shifts have been shown to be mediated by different mechanisms (Nordmann et al., 2000, Yang et al., 2011, Yang et al., 2012). Temporary shifts in the hearing threshold were associated with a buckling of the pillar bodies whereas permanent shifts in the hearing threshold correlate with permanent hair cell damage and loss of hair cells (Nordmann et al., 2000). Furthermore the induction of temporary or permanent threshold shifts is not only dependent on the intensity and duration of the AOE protocol but also marred by inter-animal variability (Cody and Robertson, 1983, Maison and Liberman, 2000).

### **1.3.3. Effect of AOE on the compound action potentials**

Over the years there has been an increased amount of research to further our understanding of AN responses to both acoustic and electrical stimulus. This has been driven by the need for cochlear implants to help treat all manner of auditory system deficits. In line with this, recording of AN activity has been carried out in multiple species both *in vivo* (Shepherd and Javel, 1997, Noguchi et al., 1999, Brown and Patuzzi, 2010) and *in vitro* (Babalian et al., 2003, Buran et al., 2010). *In vivo* studies investigating AN activity utilise techniques such as electrocochleography, magnetic resonance imaging and DPOAEs (Kaga et al., 1996, Polak et al., 2004, Poma et al., 2008, Buran et al., 2010). These techniques are preferable as information gained can be easily translated and applied to human studies. *In vitro* AN recordings include both single fibre (van den Honert and Stypulkowski, 1984) and CAP recordings (Salvi et al., 2000). These allow stable recordings in a controlled environment with the possibility to manipulate the composition of the perfusion solution. Over the years, a combination

of both *in vivo* and *in vitro* techniques have been able to yield results showing that cochlea damage (either by AOE or ototoxic drugs) results in a reduction of the AN CAP (Salvi et al., 2000), increases the jitter of action potential timing (Kim et al., 2013) and promotes asynchronous firing of the AN fibres (Zeng et al., 2005). In my model of acoustic trauma, AOE induced three distinct deficits in the properties of the AN all of which can be considered a consequence of AN demyelination or a reduction in the number of AN myelinated fibres. The deficits reported in this study were (i) a decrease in AN CAP amplitude, (ii) a decrease in effective CAP propagation distance and (iii) a decrease in the CAP conduction velocity along the AN.

Electrically evoked population field potentials depend on the synchronous firing of a large population of neurones. Therefore a decrease in AN field potential amplitude could be attributed to a desynchronisation of the neuronal firing caused by demyelination (Bostock et al., 1983). The raised hearing threshold and the decrease in the ABR peak 'I' amplitude after AOE predicts a decreased drive of AN inputs into the DCN which was confirmed by the decrease in CAP amplitudes. Furthermore, decreased CAP amplitude could also be due to a decreased number of myelinated AN fibres (Pilati et al., 2012a) and demyelination of the peripheral AN (Pilati et al., 2012a) which have all been shown to be a consequence of AOE.

Another consequence of demyelination is an increase in membrane time constants (Bostock et al., 1983) and decreased membrane resistance (Cragg and Thomas, 1964) which could in turn promote conduction blocks and be responsible for the decrease in the effective CAP propagation distance (Bostock et al., 1983). In addition the exposure and redistribution of juxtapanodal potassium channels can contribute to the loss of

axonal conduction (Wang et al., 1993; Rhodes et al., 1997; Polak and Peles 2003). This could explain why following AOE, CAPs could not be recorded when distances exceeded 1 to 1.2 mm. Alternatively, loss of myelin after AOE could promote the desynchronisation of CAPs which will also contribute to the decreased CAP amplitudes reported and cause recordings to be lost in the noise of the background signal. Desynchronisation of the evoked CAPs would also increase variability in the spike timing which would be especially evident at longer intervals between the stimulation and recording electrodes. Therefore the lack of recordable CAPs at longer distances following AOE may not be evidence of conduction block but rather of asynchronous activity which is magnified at longer distances due to deficits in the conduction velocity (Javel and Shepherd, 2000, Javel and Viemeister, 2000, Manschot et al., 2003, Kim et al., 2013). This suggests that the modelling program to simulate AN action potentials as a support for the physiological findings was incomplete, because modelling single fibre action potentials following AOE could not reproduce the supposed conduction block reported at distances exceeding 1 to 1.2 mm. Indeed the model did not take into account AOE induced deficits affecting the expression and distribution of ionic channels at the node (England et al., 1990, Vabnick et al., 1997). In addition, morphological data on the internode length was unavailable and this value (200  $\mu\text{m}$ ) had to be inferred from other nerves. Although incomplete, the modelling data supports the physiological data to reach the conclusion that AOE induces a decrease in AN conduction velocity. The functional consequence of which is a decreased AN input to the DCN.

Experiments showed that myelin was altered after AOE. This has been shown by other studies reporting a decreased number of myelinated nerve fibres in subjects with sensorineural hearing loss (Spoendlin and Schrott, 1989). Under normal physiological conditions myelinated fibres with a rapid conduction velocity display action potentials with a short refractory period and typically have nodes with 1  $\mu\text{m}$  in length (Rydmark, 1981, Imennov and Rubinstein, 2009). Demyelination has been reported to decrease the length of the internodes (Lasiene et al., 2008) and also change the expression pattern of both voltage gated sodium and potassium channels leading to deficits in the action potential propagation (England et al., 1990, Vabnick et al., 1997). The conduction velocity of myelinated AN fibres has previously been reported in the range of 6 to 14  $\text{ms}^{-1}$  (Poma et al., 2008, Imennov and Rubinstein, 2009). However, in this study a slower conduction velocity of 3.2  $\text{ms}^{-1}$  was recorded in the unexposed condition. The reason for this discrepancy could be due to other studies being performed *in vivo* or recording activity along fewer nerve fibres when performed *in vitro* (Poma et al., 2008, Imennov and Rubinstein, 2009). Recording single fibre activity will avoid certain variabilities and factors which could affect conclusions reached when recording CAPs. Such factors include the number of fibres recruited to the CAP response, the firing threshold of individual fibres recruited and the dissipation of the CAP response with distance as single fibres branch out or synchronisation of fibres is lost. Fibre damage occurring during the slicing procedure and performing recordings at room temperature rather than physiological temperature could also contribute to a slower conduction velocity being recorded. However the AN conduction velocity following AOE was also recorded under the same conditions, therefore even if the conduction velocities recorded are lower than physiological values, it still remains that

AOE significantly reduces the AN conduction velocity. It can also be argued that the slower AN conduction velocity recorded after AOE might arise entirely from the difference in appearance of the compound action potential. However this is unlikely, due to the fact that the all other evidence points to AOE triggering a deficit in action potential propagation. These lines of evidence include the increased ABR peak I latency, auditory nerve demyelination and the modelled decrease in conduction velocity.

#### **1.3.4. Is hearing loss linked to deficits identified in the DCN?**

Fusiform cells receive multisensory inputs via parallel fibres located in the molecular layer and auditory inputs via the AN located in the deep layer (Mugnaini, 1985). Both inputs are spatially segregated as parallel fibres project onto fusiform cell apical dendrites and the AN inputs project onto fusiform cell basal dendrites (Osen, 1969, Brawer et al., 1974). However, stimulations of the AN can inadvertently also stimulate cell bodies of the parallel fibres which are the granule cells (Mugnaini, 1985, Zhang and Oertel, 1994). Cross facilitation tests as previously described (see section II.2.7.4.) were therefore carried out to confirm the functional segregation of the two pathways. Data were discarded when cross facilitation was observed and this allowed for only pure AN evoked EPSCs to be collected.

The identification of fusiform cells was based on previously published criteria describing the cell morphology, location in the DCN and resting membrane potential (Pilati et al., 2008, Pilati et al., 2012a). In the unexposed condition, increasing stimulus intensity up to 2 mA resulted in a graded increase in the evoked EPSC amplitude without a plateau at the maximal stimulation intensity. This confirms the recruitment

of AN fibres with increasing stimulus intensity (Magee, 2000, Phillips, 1987) and suggests that the maximal EPSC response is evoked at stimulation intensities higher than 2 mA. This will explain why the response amplitudes do not plateau. Paired pulse tests showed that AN synapses onto fusiform cells do not exhibit PPF, this is in line with our current understanding of the non-plastic nature of the AN synapse onto fusiform cells. (Fujino and Oertel, 2003, Oertel and Young, 2004). Subsequently, the VM method of quantal analysis revealed that AOE induced a decrease in the number of functional release sites. Auditory nerve stimulations during my experiment were carried out using a concentric bipolar electrode which stimulates an area of AN fibres whereas other researchers using the VM method of quantal analysis, performed tests with single fibre evoked EPSCs in their cells of interest (Oleskevich and Walmsley, 2002). However this does not affect the reliability of the results because the VM method can be applied to multi fibre synaptic inputs (Clements and Silver, 2000). The decrease in the number of release sites identified can be linked to other morphological changes such as a decrease in synaptic vesicle density which have been identified at the calyx of Held following ototoxic drug induced deafness (Ryugo et al., 2010).

Previous work performed in this lab reported that AOE reduced the number of myelinated AN fibres resulting in smaller AN evoked EPSPs in fusiform cells (Pilati et al., 2012a). In this study I performed voltage clamp recording of fusiform cells and obtained further evidence to support this finding. Following AOE, AN evoked EPSCs in fusiform cells exhibited smaller response amplitudes at threshold (0.2 mA) and maximal (2 mA) stimulation intensity in comparison to cells from unexposed rats. The advantage of performing these tests in voltage clamp mode is that I am able to limit

the indirect activation of unwanted voltage dependent conductances. Another benefit is that the fundamental parameters that determine the size of an EPSC could be separated and analysed using the VM method of quantal analysis (Del Castillo and Katz, 1954, Clements and Silver, 2000). This method was used to identify a decrease in the number of AN release sites onto a given fusiform cell. This data can be interpreted in light of previous results indicating that AOE decreases the number of myelinated AN fibres (Pilati et al., 2012a). Therefore it can be concluded that after AOE, there is a reduction in the number of fibres that are recruited at a given stimulation intensity. This in turn leads to a reduction in the number of activated terminals that synapse onto a given fusiform cell, thereby reducing the number of functional release sites that contribute to the EPSC subsequently evoked in a fusiform cell. Without corresponding morphological and structural analysis, it will be inaccurate to conclude that the reported decrease in the number of functional release sites represents either a decrease in the total number of synaptic projections onto a given fusiform cell or a decrease in the number of release site at a given synaptic terminal.

Changes in the PPR are a good indicator of release probability modulations; however there was an identical lack of PPF in both conditions which is typical of non-plastic nature of the AN synapse (Tzounopoulos et al., 2004). It is not fully understood why AN evoked EPSCs in fusiform cells do not exhibit PPF whereas parallel fibre evoked EPSCs do exhibit PPF. One reason could be if AN synapses had an intrinsically higher release probability as synapses with high release probability do not exhibit PPF (Zucker, 1993, Dobrunz and Stevens, 1997, Oleskevich et al., 2000). However my results show that AN synapses onto fusiform cells have a release probability between 0.4 and 0.6 which falls

within what has previously been described as a mid-range (Clements and Silver, 2000) and synapses with a release probability within this range have been shown capable of PPF (Oleskevich and Walmsley, 2002, Sims and Hartell, 2005). Another reason could be the expression of specific synaptic proteins at the AN synapse which prevent the expression of PPF. This hypothesis is strengthened by the fact that AN synapses onto fusiform cells do not undergo modulation of plasticity (Fujino and Oertel, 2003). This could have a functional significance, for example, isoforms of the vesicular glutamate transporter (VGluT1 and VGluT2) are differentially expressed between somatosensory and AN inputs into the DCN. The AN synapses specifically express VGluT1 whereas somatosensory inputs via the parallel fibre synapses expresses VGluT2 (Zhou et al., 2007, Zeng et al., 2009). A functional consequence is that AN synapses exhibit a faster recycling rate helping to maintain spike timing intervals and the information encoded within (Blaesse et al., 2005). In addition to PPF being dependent on the residual calcium from a previous stimulation (Katz and Miledi, 1968), it has also been postulated that saturation of intracellular local calcium buffers could also contribute to PPF (Klingauf and Neher, 1997). Therefore differential expression of intracellular calcium buffering proteins could affect how quickly these proteins are saturated and modulate the expression of PPF. All the aforementioned factors could contribute to the non-plastic nature of the AN. However the precise mechanism remains a matter of speculation. It has been postulated that the non-plastic nature of the AN is key to maintaining the timing of action potentials which is essential to convey specific aspects of the acoustic environment (Trussell, 1999).

### **1.3.5. Is tinnitus linked to auditory nerve action potential deficits?**

Acoustic overexposure triggering hearing loss has been shown to increase spontaneous activity within the DCN which correlates with behavioural evidence of tinnitus (Kaltenbach et al., 1998, Kaltenbach and Afman, 2000, Brozoski et al., 2002). The correlation between DCN hyperactivity and tinnitus persists even after recovery from hearing loss (Brozoski et al., 2002) suggesting that the decrease in AN activity during hearing loss triggers long lasting plastic adjustments in the DCN which could underlie the perception of tinnitus (Norena and Eggermont, 2003, Kaltenbach et al., 2004, Lanting et al., 2009). Indeed it has been shown that a loss of synaptic inputs from the AN to the DCN triggers changes in the expression of protein kinase C at the synaptic terminal which has been linked to modulation of neuronal activity (Garcia et al., 2000). Another link between AN deficits and tinnitus has been shown in experiments using ototoxic drugs which specifically target and degrade myelin (Cazals, 2000, Yang et al., 2007). In other studies, demyelination of AN fibres has been proposed to be one of the underlying deficits leading to auditory neuropathy, a condition that manifests as a deficit in temporal processing and auditory perception despite intact hair cells (Starr et al., 1996, El-Badry et al., 2007). Interestingly enough, some of principal features of auditory neuropathy such as impaired speech discrimination are also present in tinnitus patients (Flor et al., 2004, Norena, 2011). This further enforces the relation between AN deficits and tinnitus.

One of the proposed mechanisms underlying tinnitus is homeostatic plasticity which is a regulation of cellular excitability to restore mean neuronal activity across a network following a period of overuse or deprivation (Turrigiano and Nelson, 2004, Kuba et al.,

2010). Homeostatic plasticity within the auditory network will therefore be triggered by hearing loss and reduction in AN inputs (“deprivation”). Neurons become hyperactive in an effort to counteract the decreased activity and restore normal mean levels of firing activity (see Chapter 2 for a more detailed discussion on plasticity). In conclusion, AN deficits reduce the amount of excitatory inputs into the DCN upsetting the balance of excitation and inhibition of fusiform cells. This change in neuronal activity of the DCN could trigger a series of plasticity-like mechanisms which culminate in the perception of tinnitus. Such possible changes would be driven by homeostatic plasticity and have been shown to include the down regulation of inhibitory synapses (Yang et al., 2011) and increased membrane excitability and spontaneous firing rate at the axonal initial segment (Kuba et al., 2010).

## 1.4. CONCLUSION

In summary, the lower number of release sites reported in the overexposed condition ties in with other findings reported here and also with results from previous studies.

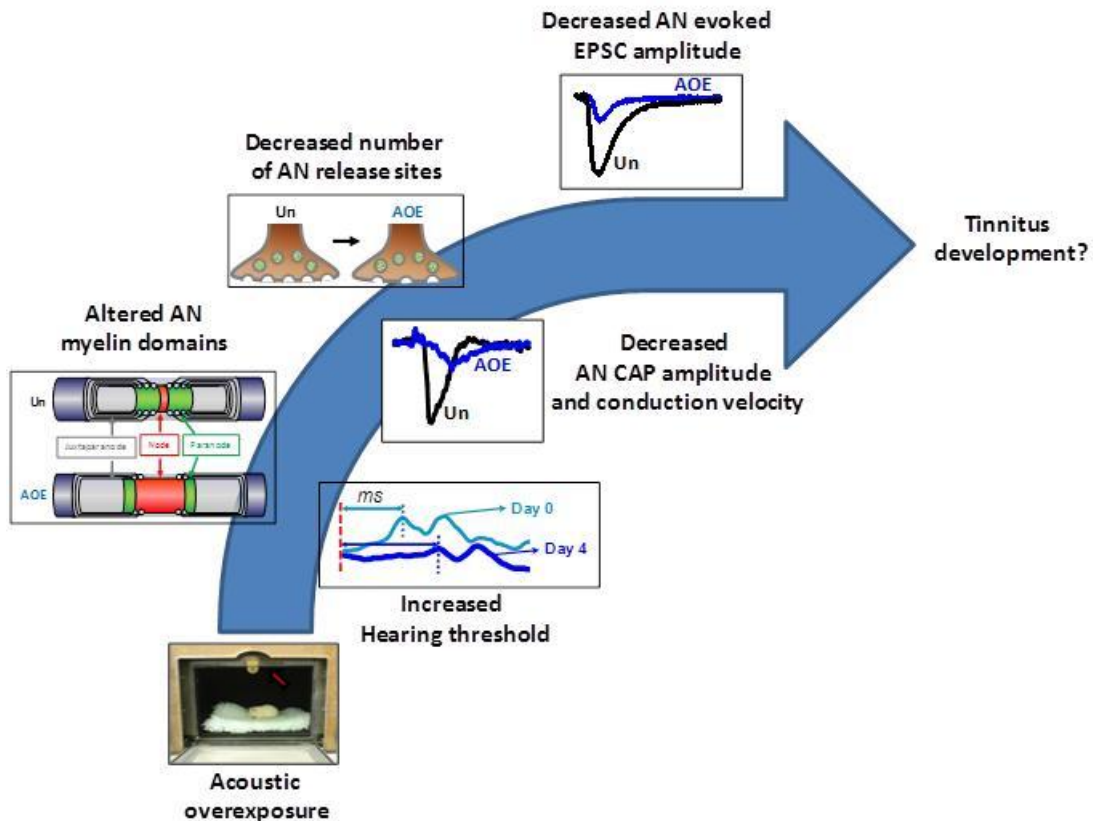


**Figure 1.12. Summary of AOE induced deficits along the auditory nerve.** A schematic representation summarising the functional and morphological changes in the auditory pathway following AOE. Immediately after AOE, there is an increase in the hearing threshold. Excitotoxic damage caused by the AOE alters the myelin domains leading to a decreased CAP amplitude and conduction velocity. Inefficient action potential propagation results in less functional release sites contributing to an evoked response and as such a smaller evoked EPSC amplitude in the DCN. These changes could eventually lead to the perception of tinnitus.

Altogether these findings indicate that in the short term (3 to 5 days) following AOE, an increase in the hearing threshold is accompanied by a decrease in myelinated AN fibres which is likely to be a consequence of demyelination rather than an overall decrease in the number of AN fibres (Appendix 1). The consequences of demyelination include a slower conduction velocity and decreased AN CAP amplitude. This in turn limits fibre recruitment, decreasing the number of functional release sites which

contribute to an evoked EPSC and resulting in smaller EPSC amplitudes (*Fig. 1.12*). The decrease in AN input to the DCN has been linked to plasticity of the somatosensory inputs, DCN hyperexcitability and the eventual development of tinnitus (Kaltenbach and Afman, 2000, Shore et al., 2008, Norena, 2011, Norena and Farley, 2013).

# **CHAPTER 2**

**Effects of acoustic overexposure  
on synaptic responses evoked  
by multisensory input stimulations**

## 2.1. INTRODUCTION

Multisensory inputs into the DCN (parallel fibres) project onto most identified DCN cell types (e.g. fusiform cells, cartwheel cells, stellate cells and giant cells) (Mugnaini, 1985) and the evoked synaptic responses have been shown to exhibit various forms of synaptic plasticity including long term potentiation (LTP), long term depression (LTD) and paired pulse facilitation (PPF) (Fujino and Oertel, 2003, Tzounopoulos et al., 2004, Tzounopoulos, 2008). This plasticity can also be modulated by the application of endogenous ligands within the DCN (Tzounopoulos et al., 2007). In addition it has previously been shown that the direction of plasticity (LTP or LTD) at these synapses is dependent on the timing intervals between the co-activation of pre- and postsynaptic signalling mechanisms (Tzounopoulos et al., 2007). However it remains unknown if this modulation of synaptic plasticity can be achieved by *in vivo* experiences such as AOE. I investigated the effect of AOE on the synaptic properties and plasticity of the multisensory (parallel fibre) inputs into the DCN. I identified changes to the mechanisms governing the induction of LTP by stimulating the multisensory inputs and using field potential recordings of the fusiform cell layer to assess network activity in addition to whole cell recordings of fusiform cells to assess single cell activity. This approach allowed me to investigate the effects of AOE on synaptic activity and plasticity of the responses across the fusiform cell layer of the DCN. I also used the VM analysis of EPSCs recorded in the fusiform cells to specifically investigate the effects on the presynaptic release mechanisms. Finally pharmacological tests were performed to abolish the phenotype associated with AOE rats and restore responses associated with the normal unexposed rats.

## 2.2. RESULTS

### 2.2.1. Characterisation of field potentials

First, there was the need to characterise the properties of extracellular field potential recordings in the fusiform cell layer of the DCN. Recording field potentials in the rat

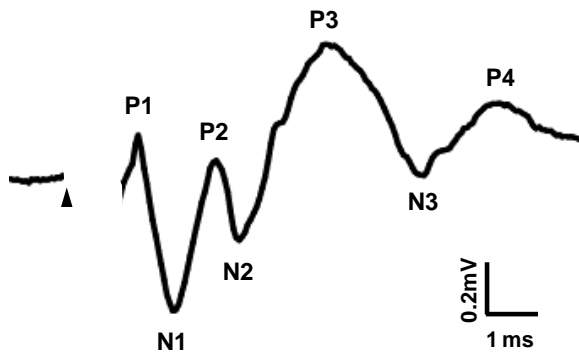


**Figure 2.1: Identification of field potential response components.** The sample trace shown is an average of ten individual traces recorded at 0.3 Hz stimulation. The response consists of an initial triphasic wave (P1-N1-P2), followed by a fast negative (N2) and a slower P3. Subsequent N3 and P4 components were not always present. The time of stimulation is indicated by the arrowhead. The stimulation artefact has been removed for clarity.

DCN fusiform cell layer in response to molecular layer parallel fibre stimulation resulted in a multiphasic response (Fig. 2.1). This is in accordance with a study carried out in the DCN of the guinea pig (Manis, 1989). Each peak of the field potential is identified as a negative or positive deflection. All negative and positive peaks after the stimulation artefact are numbered sequentially from the first (N1 or P1) through to the last (Fig. 2.1).

I first characterised the presynaptic and postsynaptic components of the response (Fig. 2.2 & 2.3). As extracellular calcium is required to induce the release of neurotransmitters at the parallel fibre synapse (Katz and Miledi, 1968, Kataoka and Ohmori, 1994), the initial experiment was to record field potentials when calcium was absent from the extracellular medium (0 mM  $[Ca^{2+}]_e$ ). After 5 to 10 minutes perfusion with a 0 mM  $[Ca^{2+}]_e$  solution, the initial triphasic wave (P1-N1-P2) remained unaffected whereas all subsequent waves were abolished (Fig. 2.2). This confirmed that all responses following the initial P1-N1-P2 component were postsynaptic in nature.

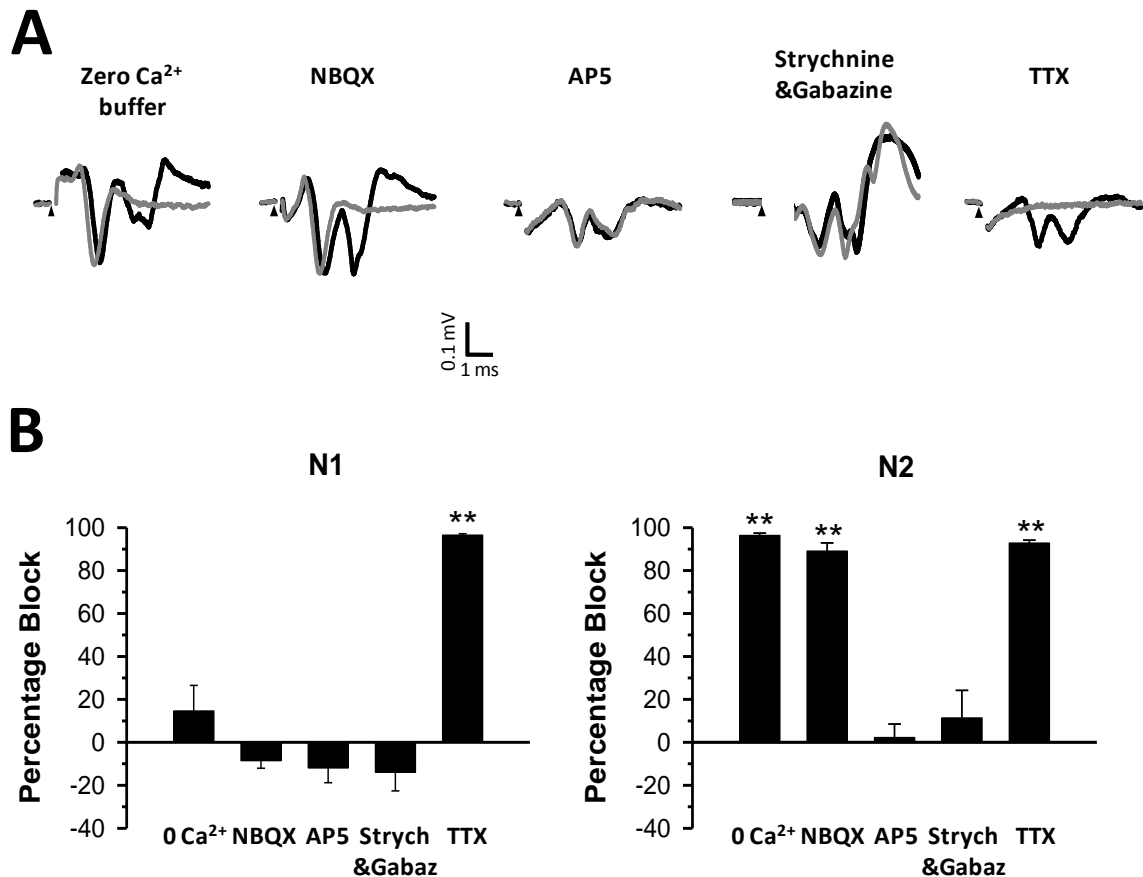


**Figure 2.2: Separating field potentials into pre- and postsynaptic components. (A)** Field potentials recorded in normal 0.1 mM Mg<sup>2+</sup> aCSF (black) and in test conditions (grey). Changing the perfusion to a zero Ca<sup>2+</sup> solution or adding 10 μM NBQX did not affect N1 but completely blocked N2. Addition of 25 μM AP5 or 10 μM strychnine had no significant effect on either the N1 or N2 amplitudes. Recording in the presence of 1 μM TTX abolished the presynaptic action potential volley (N1) and the post-synaptic response this would have elicited (N2). **(B)** Bar chart showing the effects of each pharmacological test on both N1 (left) and N2 (right) components. The N1 component was completely blocked by TTX (n = 6; P < 0.01) and the N2 component was completely blocked by 0 mM Ca<sup>2+</sup> (n = 7), NBQX (n = 7) or TTX (n = 6; P < 0.01). Strychnine and gabazine had no significant effect on either N1 or N2 (n = 5; N1: P = 0.35, N2: P = 0.1; Paired T tests).

To identify which receptors mediated the postsynaptic response, I used D-AP5 and NBQX to block NMDA and AMPA receptors respectively. Applying 25 μM D-AP5 affected neither N1 nor N2 components. However in some preparations, D-AP5 perfusion blocked a slow and delayed component of the response (Fig. 2.3). The slow and delayed nature of this current which has been labelled P4 is in line with the functional properties of NMDA receptors at synapses (Clarke and Johnson, 2006) and has also been described in other preparations (Manis, 1989). Perfusing 10 μM NBQX

resulted in the block of the N2 component and subsequent response components whereas the N1 component remained unaffected (*Fig 2.2*). This suggests that the bulk of the postsynaptic N2 response was mediated via AMPA receptors. The inhibitory cartwheel cells are also excited by parallel fibres and project onto the DCN fusiform cells (Oertel and Young, 2004). Therefore I used the glycine receptor antagonist strychnine (10  $\mu$ M) and the GABA receptor antagonist gabazine (20  $\mu$ M) to investigate their contribution to the field potentials. Application of these drugs did not affect the overall amplitude of either N1 ( $-14 \pm 8.6 \%$ ,  $n = 5$ ;  $P = 0.35$  Paired T test) or N2 ( $5.11 \pm 12.8 \%$ ,  $n = 5$ ,  $P = 0.1$ ; Paired T test; *Fig. 2.2*). However it did make the responses less smooth, suggestive of a loss of inhibition (*Fig 2.2*) Lastly the propagation of action potentials was blocked by using a sodium channel blocker (1  $\mu$ M TTX) which also abolished all components (*Fig. 2.2*).

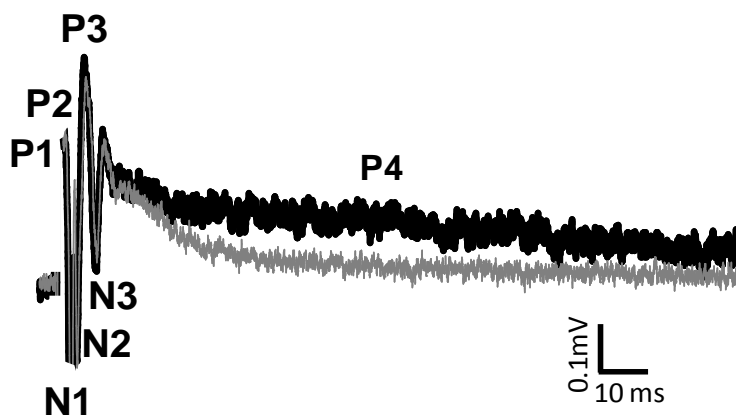


**Figure 2.3: D-AP5 blocks a delayed response.** The trace shows an average field potential response of ten sweeps on an extended timescale. Perfusion of AP5 blocked a slow outward P4 component (thin grey trace), therefore the NMDA receptors are responsible for this delayed current.

A final test was carried out to confirm that N1 was the presynaptic action potential volley (see section II.2.6.2). The stimulation electrode was kept in the same location across the parallel fibres and the recording electrode was placed at three different positions (*Fig. 2.4; A, B & C*) along the transverse axis of the DCN surface. Different

amplitudes were recorded for both the N1 and the N2 components at these positions (Fig. 2.4).

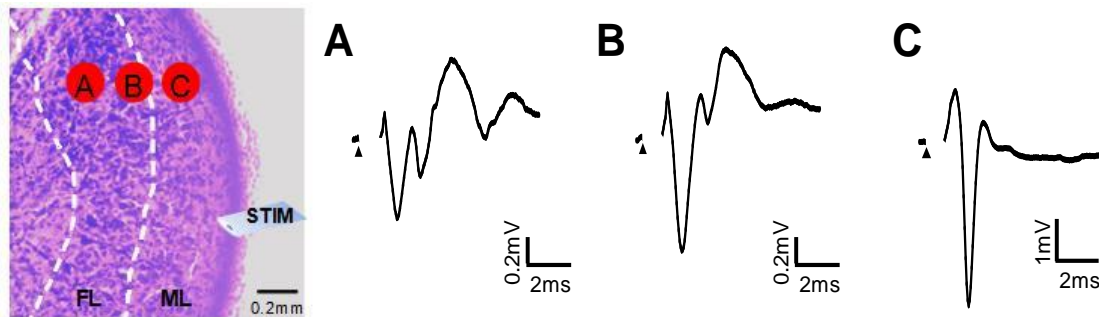


**Figure 2.4. Recordings from differential positions along the transverse axis of the DCN.** The image in the left panel shows a cresyl violet stained image of the DCN and the position of the stimulation (SE) and recording electrode along the DCN surface when each trace was recorded (circled A-C). Field potentials were recorded from three locations, (A): in the fusiform cell layer (FL); (B): between the fusiform and molecular layer (ML); and (C): in the ML. Note that in the ML only N1 is recorded, consistent with the location of the presynaptic parallel fibres.

In the example shown above, the N1 amplitude increased from 0.8 mV when recording in the fusiform cell layer (Fig. 2.4A) to 5 mV when recording in the molecular layer (Fig. 2.4C). This is in accordance with the properties of action potentials which are larger in amplitude when recorded closer to the site of stimulation (Manis, 1989, Jackson and Zhang, 1995). Having shown that action potentials could solely be recorded along the parallel fibres (Fig. 2.4C), I proceeded to record the conduction velocity of the action potential along these fibres (Fig. 2.5). Parallel fibre conduction velocity could be calculated as  $0.34 \text{ m.s}^{-1}$  and this was similar to a previous study reporting a conduction velocity of  $0.30 \text{ m.s}^{-1}$  along DCN unmyelinated parallel fibres (Manis, 1989).

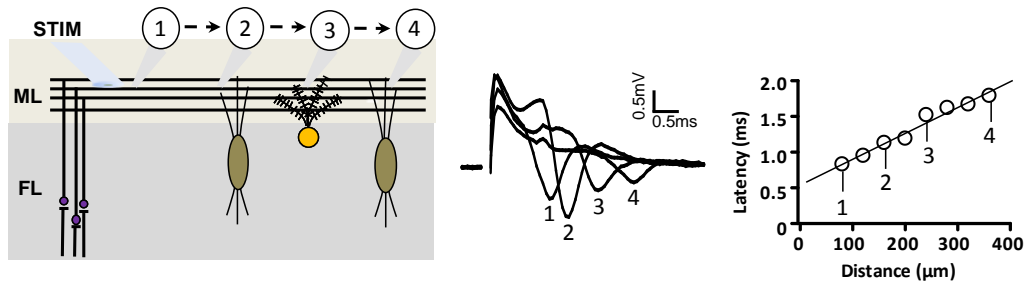


**Figure 2.5. Selective recording of the presynaptic volley allows the conduction velocity of the parallel fibres to be measured.** *Left:* Schematic representation of the recording configuration where the position of the recording electrode is moved longitudinally (shown here from 1 to 4) along the molecular layer (ML) while the position of the stimulating electrode (STIM) is left unchanged. *Middle:* Only presynaptic field potentials are recorded in this condition with N1 peaks revealing a latency increase with increasing distance between the recording and the stimulation electrodes. *Right:* Latency to the N1 peak is plotted against the distance between the recording and the stimulation electrode and fitted with a linear regression ( $r^2 = 0.971$ ).

### 2.2.2. Effect of acoustic overexposure on evoked field potentials and paired pulse facilitation

Parallel fibres were stimulated at a rate of 0.3 Hz with a stimulation intensity which was increased from 0 V to a maximum of 50 V in order to recruit additional fibres and to establish an input-output relationship. In the unexposed condition, minimum stimulation intensity to elicit a recordable field potential response for both N1 and N2 were consistently found to be between 5 V to 10 V. The N1 and N2 amplitudes evoked at 10 V stimulation intensity were  $0.24 \pm 0.03$  mV ( $n=11$ ) and  $0.18 \pm 0.04$  mV ( $n=11$ ) respectively. The N1 amplitude increased continuously with increasing stimulation intensity in contrast to the N2 amplitude which levelled out, amplitudes that were  $0.42 \pm 0.05$  mV ( $n=11$ ) and  $0.5 \pm 0.05$  mV ( $n=11$ ) at 30 and 50 V stimulation respectively (Fig. 2.6). In the overexposed condition ( $n = 9$ ), the N1 and N2 amplitudes were similar to the unexposed condition at both 10 V (N1:  $0.24 \pm 0.03$  mV; N2:  $0.16 \pm 0.03$  mV) and 50 V stimulation intensity (N1:  $1.1 \pm 0.14$  mV; N2:  $0.46 \pm 0.08$  mV). After AOE, the N1 amplitude was also continually increased with increasing stimulation intensity and the

N2 amplitude also levelled out with recorded amplitudes of  $0.41 \pm 0.08$  mV ( $n=9$ ) and  $0.46 \pm 0.08$  mV ( $n=9$ ) at 30 and 50 V respectively (Fig. 2.6). This shows that AOE did not change the basic characteristics of the action potentials along the parallel fibres (N1) or of the evoked postsynaptic response (N2).

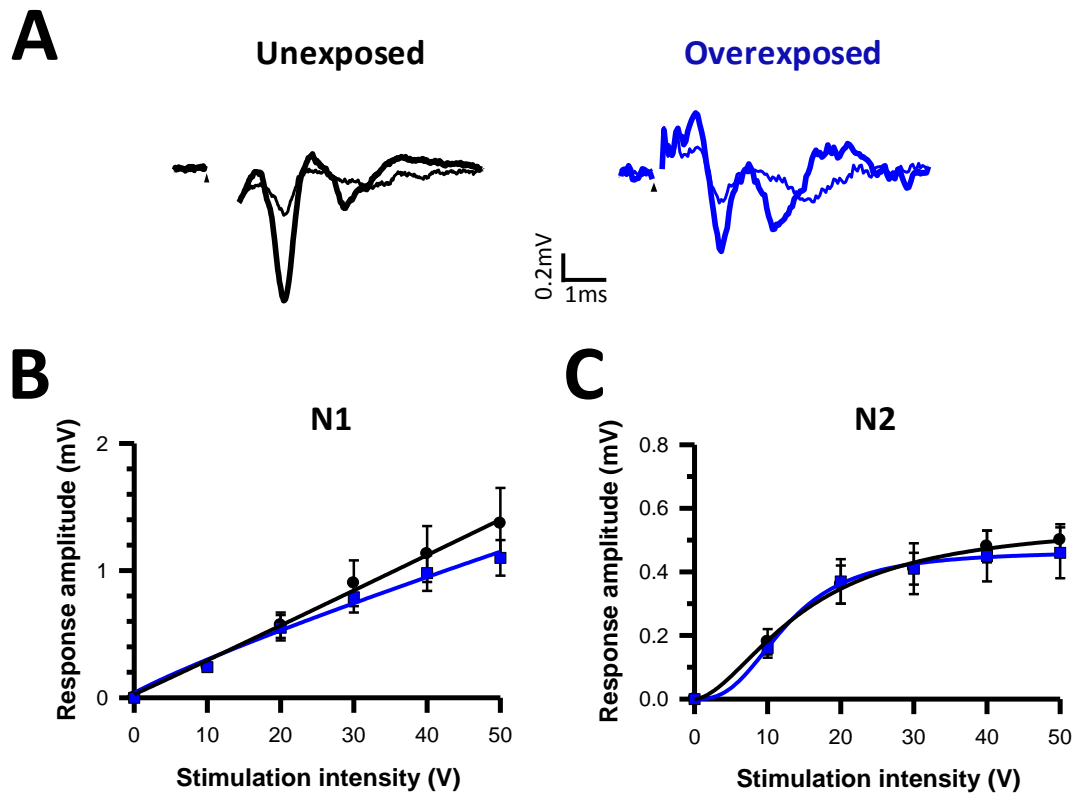


**Figure 2.6.** Effect of stimulation intensity on the pre- and postsynaptic field potentials (A) Average of ten sample traces showing the N1 and N2 responses at minimum (thin traces) and maximum (thick traces) stimulation intensities as recorded in both the unexposed (left) and overexposed (right) conditions. Characteristics of N1 (B) and N2 (C) were unchanged. Data show mean amplitudes recorded in response to graded stimulation intensities in both the unexposed (black circles,  $n=11$ ) and overexposed (blue squares,  $n=9$ ) condition. The N1 input-output relationship has been fitted with a straight line whereas the N2 input-output relationship has been fitted with a Hill function.

However, the continual increase of the N1 amplitude with increasing stimulation intensity in both conditions suggests that fibres can still be recruited at stimulations exceeding 50 V. Tests with a supra-50 V stimulation were not performed therefore an alternative method of analysing the N1 amplitude was implemented. Using this

method, similar results were obtained as detailed in appendix 1. Furthermore there was still no significant difference in fibre recruitment between the unexposed and overexposed conditions.

Paired pulse tests were also performed at intensities that evoked a half maximal response of the N2 amplitude at varying intervals between 10 to 300 ms (*Fig. 2.7*)

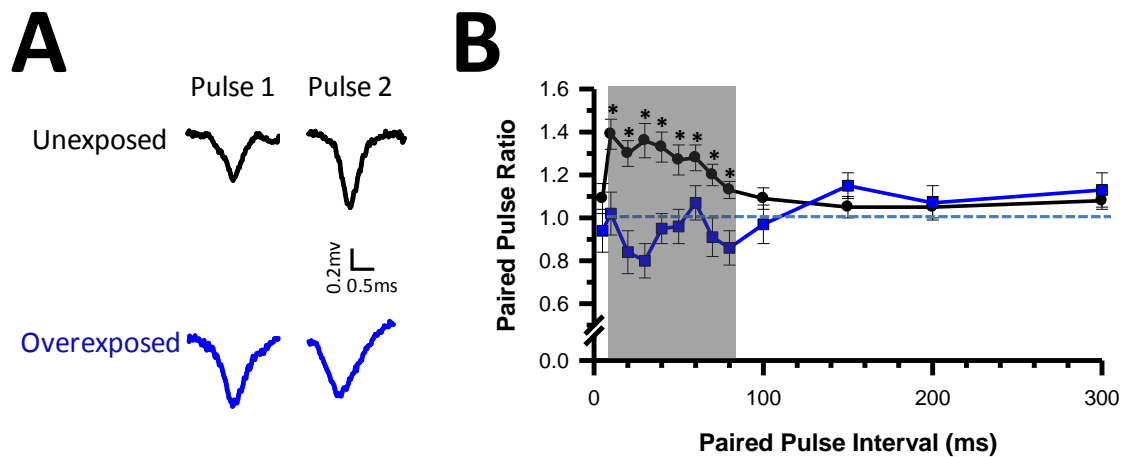


**Figure 2.7. Acoustic overexposure abolishes paired pulse facilitation of postsynaptic responses evoked by parallel fibre stimulation.. (A)** Average of ten N2 traces obtained in response to a paired pulse stimulation with a 50 ms interval gap in both the unexposed (above) and the overexposed condition (below). The N1 amplitude has been omitted for clarity. **(B)** Graph summarising the paired pulse ratio at various paired pulse intervals. The range of intervals within which PPF was recorded in the unexposed condition ( $n = 9$ ) is highlighted and significance has been indicated ( $* P < 0.05$ , Paired T tests). There was no recordable PPF in the overexposed condition ( $n = 8$ ).

In the unexposed condition, the postsynaptic N2 component exhibited a significant PPF ranging from  $1.39 \pm 0.07$  to  $1.1 \pm 0.04$  at intervals between 20-80 ms (*Fig. 2.7*). In the overexposed condition however, PPF was absent at all intervals tested (*Fig. 2.7*). Previous researchers have linked a lack of PPF to a high release probability at synapses investigated (Schulz, 1997, Oleskevich et al., 2000). This suggests that the lack of PPF after AOE could be due to a coinciding increase in release probability.

### 2.2.3. Effect of acoustic overexposure on long term synaptic plasticity

Plasticity within the DCN was observed by recording changes in the amplitudes of field potentials in the fusiform cell layer following HFS of parallel fibres in the molecular layer. Stimulus intensity was first set to generate half the maximal N2 response at 0.3 Hz frequency and a 10 minute period of stable N1 and N2 responses was established (*Fig. 2.8*). High frequency stimulation (2 x 15 s 50 Hz stimulation with a 1s interval) was then carried out and recordings proceeded for a further 30 minutes at 0.3 Hz. Values were normalised to the average of the last 5 minute period before HFS and plotted against time (*Fig. 2.8*). Immediately following HFS in the unexposed condition, neither the normalised N1 nor the N2 amplitude was significantly changed (N1:  $1.05 \pm 0.09$ ,  $P > 0.05$ ; N2:  $0.89 \pm 0.09$ ,  $P > 0.05$ ;  $n=16$ ; Wilcoxon tests, *Fig. 2.8, Appendix 2*). However after a few minutes, both the N1 and N2 component exhibited a steady increase in amplitude and after 30 minutes, the normalised amplitudes of both components were significantly increased to  $1.17 \pm 0.05$  ( $P < 0.01$ , Wilcoxon test) and  $1.39 \pm 0.09$  ( $P < 0.01$ , Wilcoxon test) respectively (*Fig. 2.8*). This was considered a long term potentiation (LTP) due to the increase in amplitude persisting after 30 minutes and in some instances up to 90 minutes (data not shown) (Bliss and Lomo, 1970, Nicoll and Malenka, 1999, Fujino and Oertel, 2003). Similar HFS protocols were also performed following AOE. In the overexposed condition ( $n = 20$ ), there was no significant change in either the N1 ( $1.02 \pm 0.04$ ;  $P > 0.05$ , Wilcoxon tests) or the N2 ( $0.96 \pm 0.06$ ;  $P > 0.05$ , Wilcoxon Test) normalised amplitudes 30 minutes after the HFS (*Fig. 2.8*).

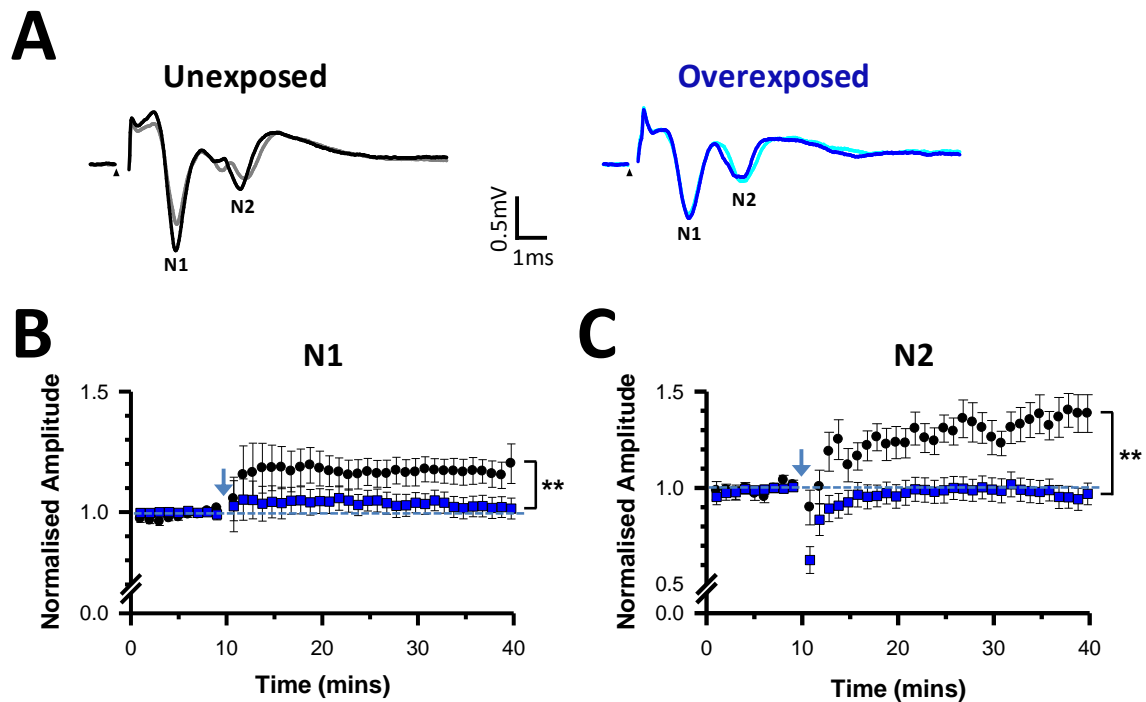


**Figure 2.8. Acoustic overexposure abolishes LTP induction by HFS.** (A) Examples of averaged field potential responses recorded before (grey and cyan) and 30 minutes after (black and blue) HFS in both the unexposed (left) and overexposed (right) condition. Graph showing amplitudes of the N1 (B) and the N2 components (C) normalised to the average of the last 5 minutes of baseline recording and plotted against time in both conditions (unexposed, black circles,  $n=16$ ; overexposed, blue squares,  $n=20$ ). The time of HFS is indicated by the arrow. Thirty minutes after HFS, both the N1 and N2 amplitudes recorded in the unexposed condition were significantly higher than that recorded in the overexposed condition (\*\*  $P < 0.05$ , Mann Whitney test).

Comparing the changes in normalised amplitude (N1 and N2) in both conditions revealed a significantly higher amplitude in the unexposed condition over the overexposed condition (N1:  $P < 0.01$ ; N2:  $P < 0.01$ , ANOVA on Ranks, Dunns test). This leads to the conclusion that AOE inhibits the induction of LTP by HFS.

#### 2.2.4. Mechanisms underlying long term potentiation

As previously described, N1 represents the presynaptic volley which triggers neurotransmitter release and evokes the subsequent N2 postsynaptic response. Thirty minutes after HFS in the unexposed condition, both the N1 and N2 amplitudes were significantly increased. However the possibility remains that the increase in the N2

amplitude is simply a result of the increased presynaptic volley (N1). To exclude this possibility, the N2 amplitude elicited at a given stimulation intensity (10 – 50 V) was plotted against the corresponding N1 amplitude and the relationship was fitted with a Hill function. This relationship was then used to predict the N2 amplitude which will correspond to the potentiated N1 amplitude recorded after the HFS (Fig. 2.9A).

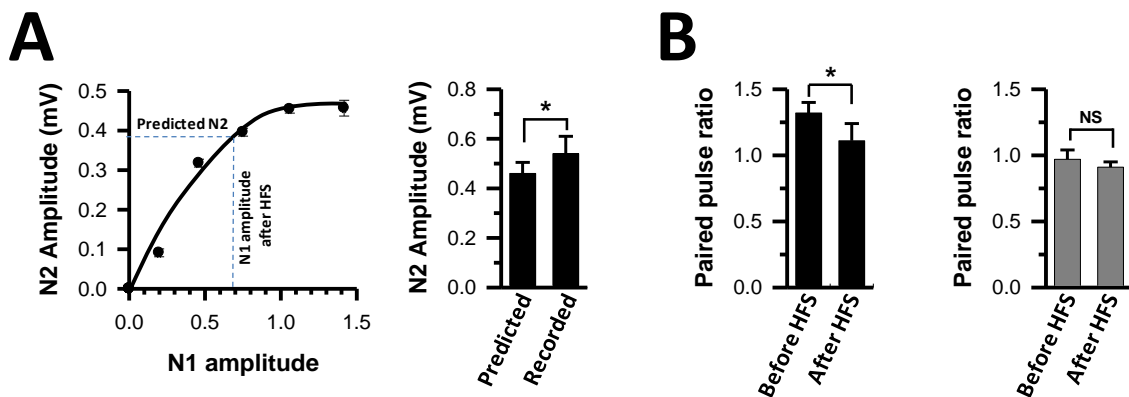


**Figure 2.9** Long term potentiation is accompanied by a decrease in the paired pulse ratio of the postsynaptic N2 response. **(A:left)** Plotting N2 amplitude against N1 amplitude allowed the fitting of a Hill function between the two responses. The predicted N2 amplitude evoked by the potentiated N1 amplitude alone is indicated with the dotted line. **(A:right)** Bar charts revealed that the N2 amplitude recorded after HFS was significantly higher than the amplitude predicted by the fit ( $P < 0.05$ , Unpaired T test;  $n = 16$ ). **(B)** Upon LTP induction, PPF was significantly decreased in the unexposed conditions (**Left**; Paired T tests,  $P < 0.05$ ). The lack of PPF in the overexposed condition persisted after HFS (**right**).

The predicted N2 amplitude ( $0.46 \pm 0.05$  mV,  $n=16$ ) was significantly lower than the N2 amplitude recorded after HFS ( $0.54 \pm 0.07$  mV,  $n=16$ ,  $P < 0.05$ , Unpaired T test), suggesting that the potentiated N2 amplitude was unlikely to be due only to the increased presynaptic volley (N1). Previous studies have shown that changes in release probability can be inversely related to changes in the PPF (Oleskevich et al., 2000). Therefore the significant reduction of the PPR in the unexposed condition from  $1.35 \pm 0.08$  ( $n = 9$ ) to  $1.09 \pm 0.07$  ( $n = 9$ ;  $P < 0.05$ , Wilcoxon tests) suggests that the potentiation of the N2 amplitude was due to an increase in release probability (Fig. 2.9B). To further investigate this, input-output relationships were determined before

and during LTP in a subset of experiments. This helped identify the range of stimulation intensities where the N2 amplitude remained significantly elevated after LTP induction. At low to moderate stimulation intensities (10 – 30 V), N2 amplitudes recorded during LTP were higher than that recorded before HFS (*Fig. 2.10*,  $P < 0.05$ , Paired T tests), indicative of increased release probability. At higher stimulation intensities (40 & 50 V), there was no difference between the N2 amplitudes recorded (*Fig. 2.10*;  $P > 0.05$ , Paired T test), indicative of postsynaptic receptor saturation.

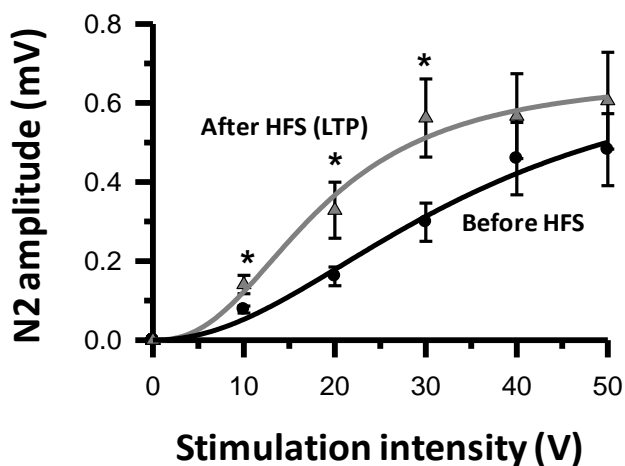


**Figure 2.10. LTP is evoked at submaximal stimulation intensities.** During LTP the N2 amplitude was significantly increased from  $0.08 \pm 0.01$  mV to  $0.14 \pm 0.02$  mV at 10 V;  $0.16 \pm 0.02$  mV to  $0.33 \pm 0.07$  mV at 20 V; and  $0.30 \pm 0.05$  mV to  $0.56 \pm 0.1$  mV at 30 V ( $n = 6$ , Paired T test,  $P < 0.05$ ). There was no significant increase at 40 and 50 V ( $P = 0.46$  and  $0.44$  respectively, Paired T tests).

I next tested whether LTP could be further potentiated after the initial induction protocol by performing three HFS protocols at 30 minute intervals. In the unexposed condition ( $n = 7$ ) the first HFS induced LTP as the normalised N2 amplitude increased by  $25 \pm 4$  % ( $P < 0.05$ , Wilcoxon test). However, the N2 amplitude could not be further potentiated, with normalised amplitudes varying by  $6 \pm 3$  % ( $n=7$ ) and  $13 \pm 7$  % ( $n=7$ ) following the second and third HFS protocols respectively (*Fig.2.11*).

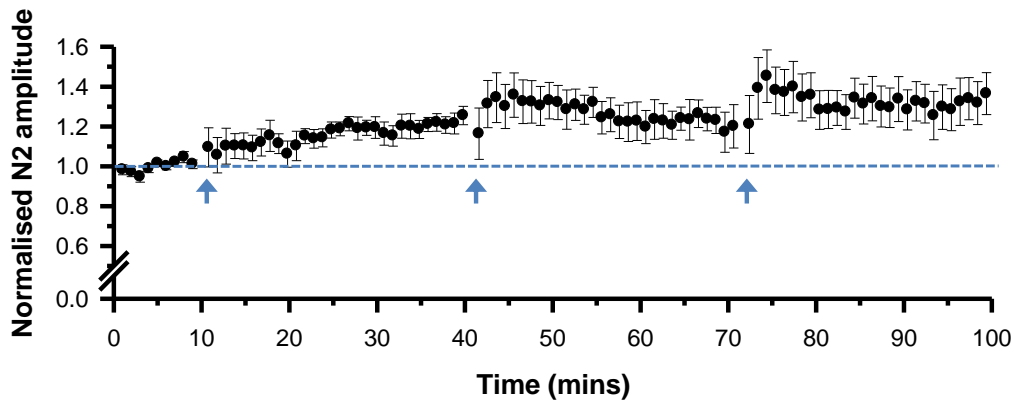


**Figure 2.11. Multiple high frequency stimulations do not induce further potentiation in the unexposed condition.** The normalised change in N2 post synaptic field potential amplitudes as induced by multiple HFS (indicated by arrows). The first HFS induces LTP ( $1.25 \pm 0.04$ ,  $n=7$ ;  $P < 0.05$ ; Wilcoxon test). Subsequent HFS at 30 minute intervals did not induce any further significant changes in the size of the postsynaptic field potential (Wilcoxon tests).

I next investigated the receptors mediating LTP in my model, by performing tests using both the AMPA receptor antagonist, NBQX ( $10 \mu\text{M}$ ), and the NMDA receptor antagonist, D-AP5 ( $25 \mu\text{M}$ ). Addition of NBQX during LTP completely abolished the N2 response (Fig. 2.12), in a manner similar to that which was witnessed when NBQX was added prior to the HFS (Fig. 2.3).

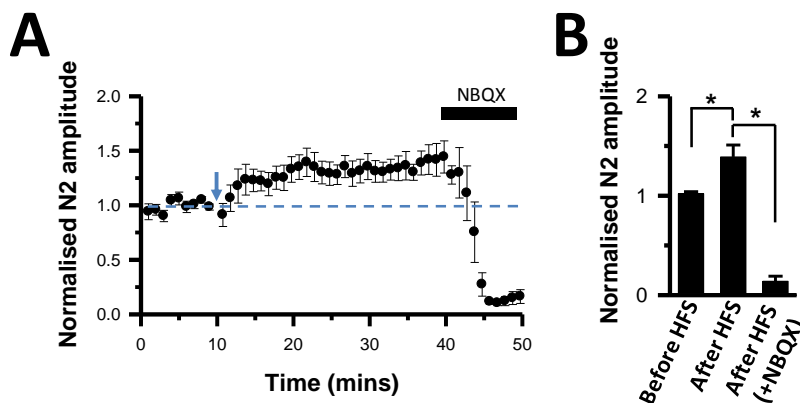


**Figure 2.12: Effect of NBQX on the long term potentiation of postsynaptic field potentials in the unexposed condition.** (A) NBQX ( $10 \mu\text{M}$ ) addition 30 minutes after LTP induced by HFS (indicated by arrow) completely abolished the postsynaptic field potential (N2) response. (B) Bar chartss show a significant increase in the N2 amplitude 30 minutes following HFS and the complete abolishment of the N2 response upon addition of NBQX (right). (One way ANOVA on Ranks; SNK tests,  $P < 0.05$ ;  $n = 8$ ).

Despite this finding suggesting that the N2 response after HFS was expressed solely via AMPA receptors, addition of D-AP5 (25  $\mu\text{M}$ ) had an unexpected effect as it abolished the LTP and returned the normalised N2 amplitude to baseline levels recorded prior to the HFS (from  $1.46 \pm 0.19$  to  $0.94 \pm 0.18$ ;  $n = 9$ ; Wilcoxon test,  $P < 0.05$ ; Fig. 2.13A). The decrease in amplitude induced by D-AP5 addition also increased the PPR from  $1.18 \pm 0.07$  to  $1.67 \pm 0.19$  ( $n = 9$ ;  $P < 0.05$ , Wilcoxon test; Fig. 2.13B). This increase in the PPR suggests that D-AP5 addition after HFS had a presynaptic effect of decreasing the release probability.

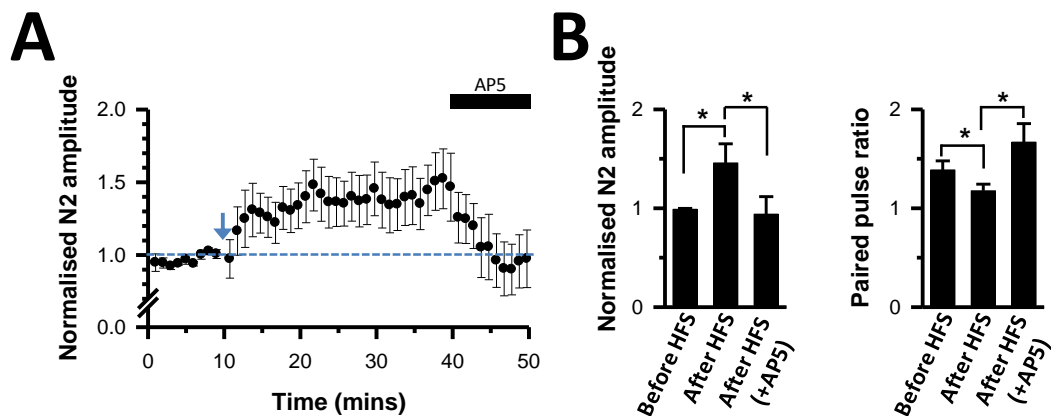


**Figure 2.13. Addition of D-AP5 abolishes the LTP induced by high frequency stimulation.** (A) The amplitude of LTP induced by the HFS (arrow) was reversed by the addition of D-AP5 (25  $\mu\text{M}$ ) 30 minutes after the HFS (Left;  $n=8$ ). (B) Bar chartss show that the LTP (left) was also associated with a significant decrease in paired pulse ratio (right). D-AP5 addition reversed the LTP and decreased the paired pulse ratio. (\*  $P < 0.05$ , One way ANOVA on Ranks, SNK tests).

As D-AP5 addition had an effect on the maintenance of LTP, I next investigated its effect on the induction of LTP. Perfusing D-AP5 prior to the HFS did not have a significant effect on the normalised N2 amplitude (from  $1.00 \pm 0.05$  to  $1.02 \pm 0.02$ ;  $n=8$ ;  $P > 0.05$ , Wilcoxon test, Fig. 2.14). Subsequently performing HFS in the presence of D-AP5 led to a significant LTP (from  $1.02 \pm 0.02$  to  $1.52 \pm 0.2$ ;  $n=8$ ;  $P < 0.05$ , Wilcoxon test, Fig. 2.14), which was also accompanied by a significant reduction in the PPR (from  $1.71 \pm 0.27$  to  $1.1 \pm 0.04$ ;  $n = 6$ ;  $P < 0.05$ ; Wilcoxon test, Fig. 2.14A).

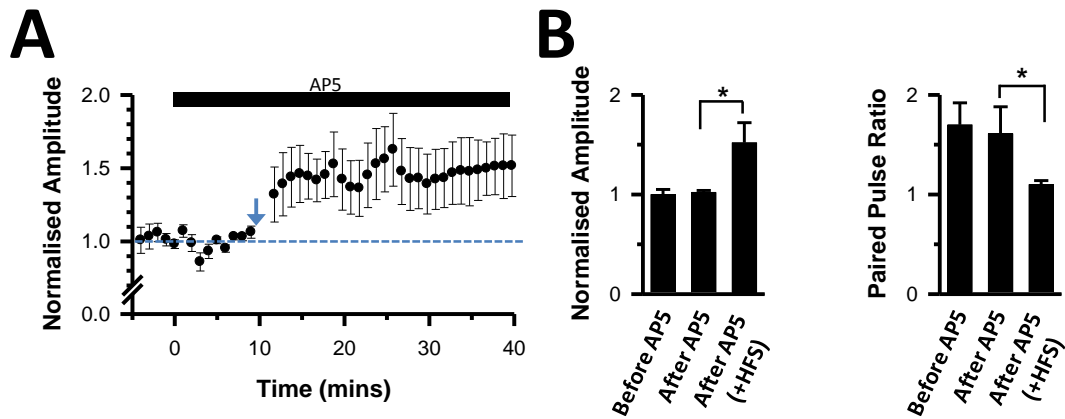


**Figure 2.14. Induction of LTP by high frequency stimulation is independent of NMDA receptor activation.** (A) Performing HFS in the presence of D-AP5 did not affect the induction of LTP ( $n = 8$ ). (B) Bar charts confirm that LTP (left) was still associated with a significant decrease in the PPR (right) ( $P < 0.05$ , One way ANOVA on Ranks, Dunnett's test,  $n = 6$ ).

This reduction in the PPR was similar to that witnessed with LTP induction in the absence of D-AP5. Showing that LTP was maintained via the action of NMDA receptors and the inhibition of NMDA receptors inhibited LTP via a decreased release probability.

### 2.2.5. Mechanism underlying a lack of LTP after exposure to loud sound

I next investigated the effect of D-AP5 on N2 amplitudes following AOE. Similar to the unexposed condition, addition of D-AP5 30 minutes after HFS led to a decrease of the normalised N2 amplitude (from  $1.11 \pm 0.09$  to  $0.46 \pm 0.14$ ;  $n = 7$ ) while also increasing the PPR from  $1.06 \pm 0.06$  to  $1.39 \pm 0.07$  ( $n = 7$ ; Fig. 2.15B).

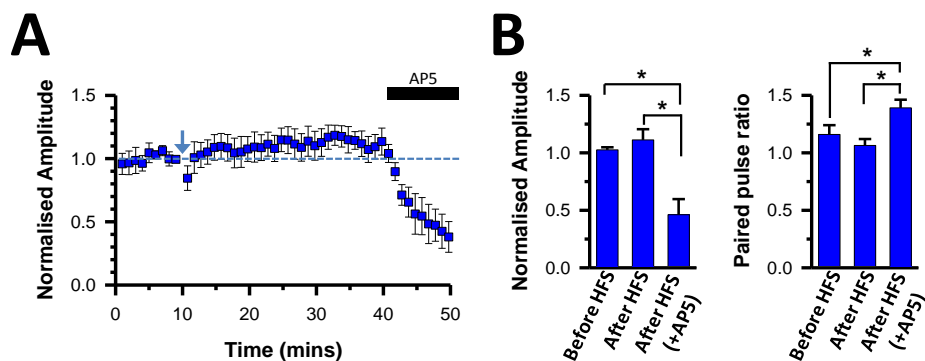


**Figure 2.15. Addition of D-AP5 after HFS restores paired pulse facilitation in the overexposed condition.** (A) D-AP5 ( $25 \mu\text{M}$ ) addition 30 minutes after HFS reduced the amplitude of the post-synaptic (N2) response below pre-HFS baseline levels. (B) This significant decrease in amplitude (left:  $P < 0.05$ , One way ANOVA on Ranks, SNK tests,  $n = 14$ ) was accompanied by a significant increase in the PPR (right: One way ANOVA on Ranks; SNK test  $P < 0.05$ ,  $n = 7$ ).

Increasing the extracellular magnesium concentration from 0.1 mM to 10 mM, was used as an alternative means of blocking NMDA receptors (Coan and Collingridge, 1985, Petrenko et al., 2003). Indeed, perfusing 10 mM  $Mg^{2+}$  after the HFS significantly decreased the normalised N2 amplitude ( $P < 0.05$ , Wilcoxon test,  $n = 5$ , Fig. 2.16). Attempts to confirm that the decrease in N2 amplitude was due to a decrease in release probability using paired pulse tests proved futile. This was because whereas the first stimulation in the paired pulse evoked a near zero N2 amplitude which could not be discerned from the baseline, the second stimulation in the paired pulse elicited a recordable N2 amplitude.

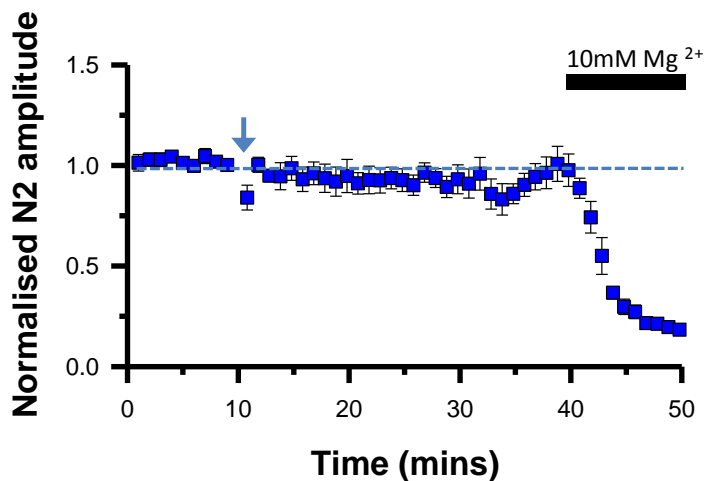


**Figure 2.16.** Perfusing 10 mM  $Mg^{2+}$  30 minutes after HFS reduces the normalised N2 amplitude after acoustic overexposure from  $0.96 \pm 0.07$  to  $0.22 \pm 0.02$  (Mann Whitney Test,  $P < 0.05$ ;  $n = 5$ ).

Based on the fact that D-AP5 addition 30 minutes after HFS reversed one of the deficits induced by AOE (i.e. lack of PPF), I performed a second HFS protocol during this state of decreased release probability in an attempt to reverse the second deficit and induce LTP. However performing the second HFS did not induce LTP and the normalised N2 amplitude remained unchanged: from  $0.57 \pm 0.07$  to  $0.56 \pm 0.05$  when measured before and after the second HFS protocol respectively ( $n = 7$ ; Fig. 2.17).

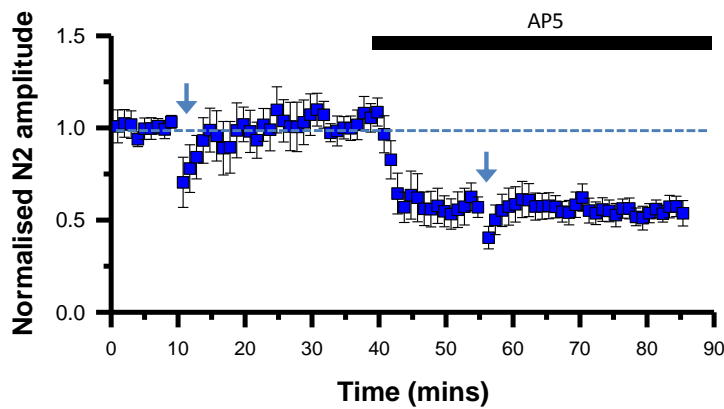


**Figure 2.17. Multiple HFS do not alter the N2 response in the overexposed condition.** The first HFS was performed in the absence of D-AP5 and the second in the presence of D-AP5. D-AP5 decreases the release probability but does not promote LTP ( $n = 7$ ; Wilcoxon Test,  $P = 0.83$ ).

Although the first of the HFS protocol did not induce any recordable changes in the N2 amplitude or release probability, this did not exclude the fact that other synaptic changes might have occurred. Therefore I repeated the tests in slices which had not undergone a previous HFS. Similar to the unexposed condition, perfusing D-AP5 prior to the HFS protocol did not alter the normalised N2 amplitude (from  $1.06 \pm 0.07$  to  $1.02 \pm 0.01$ ;  $n = 14$ ; Fig. 4.18) nor the PPR (from  $1.17 \pm 0.07$  to  $1.26 \pm 0.06$ ;  $n = 7$ ; Fig. 4.18).

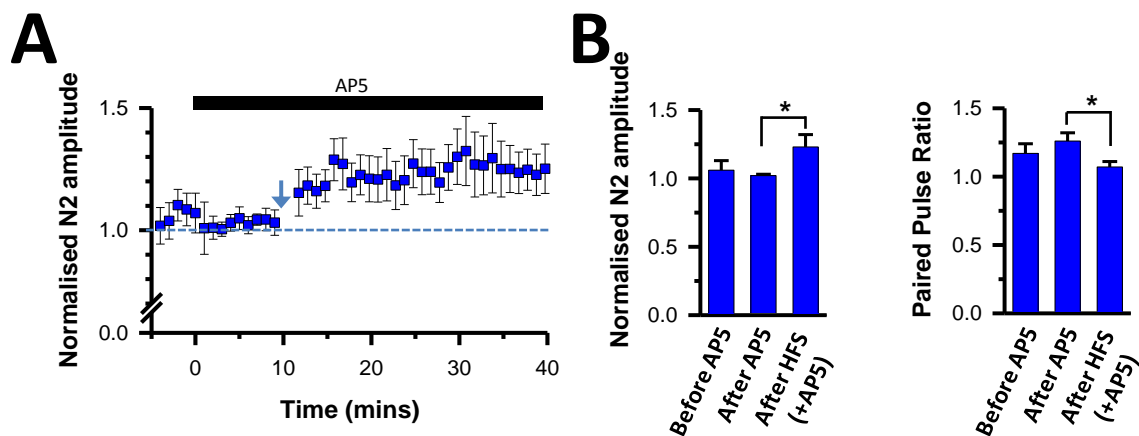


**Figure 2.18. Addition of D-AP5 leads to the induction of LTP by high frequency stimulation in the overexposed condition.** (A) Performing HFS in the presence of D-AP5 promoted the induction of LTP in the overexposed condition ( $n = 14$ ). (B) Bar charts show that LTP (Mann Whitney tests,  $P < 0.05$ ,  $n = 14$ ) was associated with a significant decrease in the PPR (Mann Whitney tests  $P < 0.05$ ;  $n = 7$ ).

However, subsequently performing HFS in the presence of D-AP5 promoted the induction of LTP (from  $1.02 \pm 0.01$  to  $1.23 \pm 0.09$ ;  $n = 14$ ;  $P < 0.05$ , Wilcoxon test) alongside a decrease in the PPR (from  $1.26 \pm 0.06$  to  $1.07 \pm 0.04$ ;  $n = 7$ ;  $P < 0.05$ , Wilcoxon test, *Fig. 2.18B:right*). This indicates that blocking NMDA receptors by the addition of D-AP5 was capable of reversing the synaptic deficits induced by AOE and promoted the induction of LTP.

### **2.2.6. Modulation of release probability in the dorsal cochlear nucleus**

To further test whether the lack of PPF and LTP induction after AOE were due to an increased release probability, the synaptic release probability was altered by changing the extracellular calcium concentration prior to the HFS. In the unexposed condition, increasing the extracellular calcium concentration from 2 mM to 3 mM prior to HFS increased the N2 amplitude from  $0.4 \pm 0.09$  mV to  $0.46 \pm 0.09$  mV ( $n = 6$ ;  $P < 0.05$ , Paired T test) and significantly decreased the PPR from  $1.33 \pm 0.12$  to  $0.92 \pm 0.07$  ( $n=5$ ; Paired T test,  $P < 0.05$ ; *Fig. 2.19A*). This increase in N2 amplitude and decrease in PPR provided evidence in accordance with an increase in release probability. I next investigated the effect of HFS in this state of increased release probability. In the unexposed condition, performing HFS in 3 mM  $\text{Ca}^{2+}$  did not induce LTP ( $0.96 \pm 0.07$ ;  $n=7$ ; Wilcoxon test,  $P = 0.51$ ; *Fig.2.19B*), suggesting that LTP induction by HFS in the unexposed condition was abolished when the synapses had a high release probability.

In the overexposed condition decreasing the extracellular calcium concentration (from 2 mM to 1 mM) significantly decreased the N2 amplitude (from  $0.4 \pm 0.06$  mV to  $0.21 \pm 0.03$  mV;  $n=11$ ; Paired T test,  $P < 0.05$ ) while also increasing the PPR (from  $0.97 \pm 0.07$  to  $2.45 \pm 0.29$ ;  $n = 5$ ;  $P < 0.05$ , Paired T test; *Fig. 2.19C*). These changes in the N2

amplitude and PPR were in accordance with a decrease in release probability. Performing HFS in this state of decreased release probability induced LTP as the normalised N2 amplitude increased from  $1.01 \pm 0.01$  to  $1.27 \pm 0.09$  ( $P < 0.05$ , Wilcoxon tests,  $n=11$ ; Fig. 2.19D).

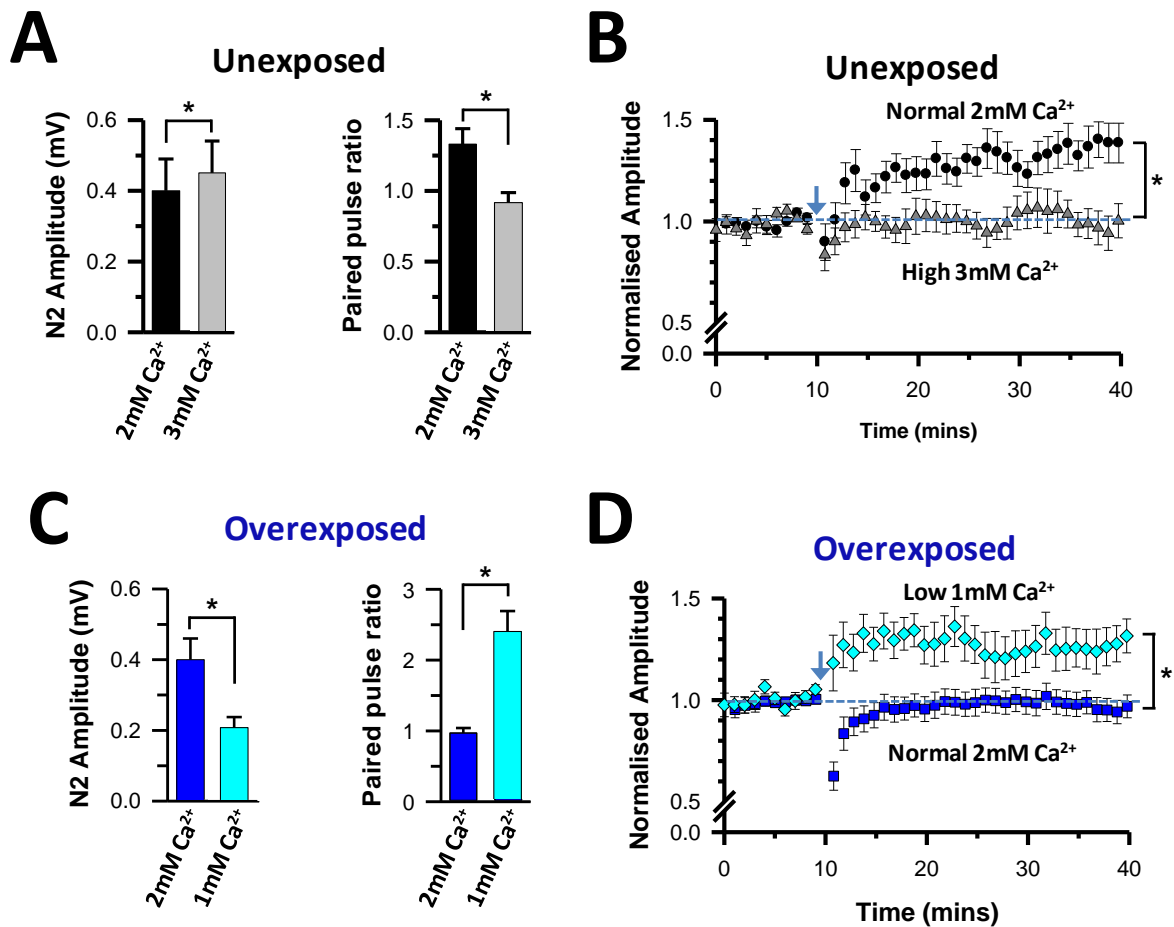


**Figure 2.19. Altering the release probability reverses the absence of LTP after AOE. (A,B)** In the unexposed conditions, increasing extracellular  $Ca^{2+}$  increased the basal amplitude of N2 evoked at 0.3 Hz stimulations ( $P < 0.05$ , Paired T test,  $n = 6$ ) and decreased the PPR (A,  $P < 0.05$ , Wilcoxon test,  $n = 7$ ). It also abolished the LTP (B,  $P < 0.05$ , Mann Whitney test,  $n = 7$ ). (C,D) Decreasing the extracellular  $Ca^{2+}$  concentration after AOE decreased the basal amplitude of N2 evoked at 0.3 Hz stimulations ( $P < 0.05$ , Paired T test,  $n = 11$ ) and increased the PPR (C,  $P < 0.05$ , Wilcoxon test,  $n = 5$ ). It also restored the LTP otherwise absent after AOE (D). (D;  $n=11$ ; Mann Whitney test,  $P < 0.05$ ).

Altogether this leads to the conclusion that the lack of LTP induction after AOE can be attributed to an increased release probability and experimentally decreasing the release probability can reverse this AOE phenotype.

### 2.2.7. Quantal analysis of evoked excitatory postsynaptic currents

Whole cell recordings of fusiform cells were performed to confirm the effects of AOE on the release probability. Parallel fibres were stimulated at a rate of 0.3 Hz with increasing stimulation intensity to facilitate parallel fibre recruitment. Results presented in *Fig. 2.20.* show that AOE did not affect the threshold, slope or maximum response of the input-output relationship obtained from the evoked EPSCs.

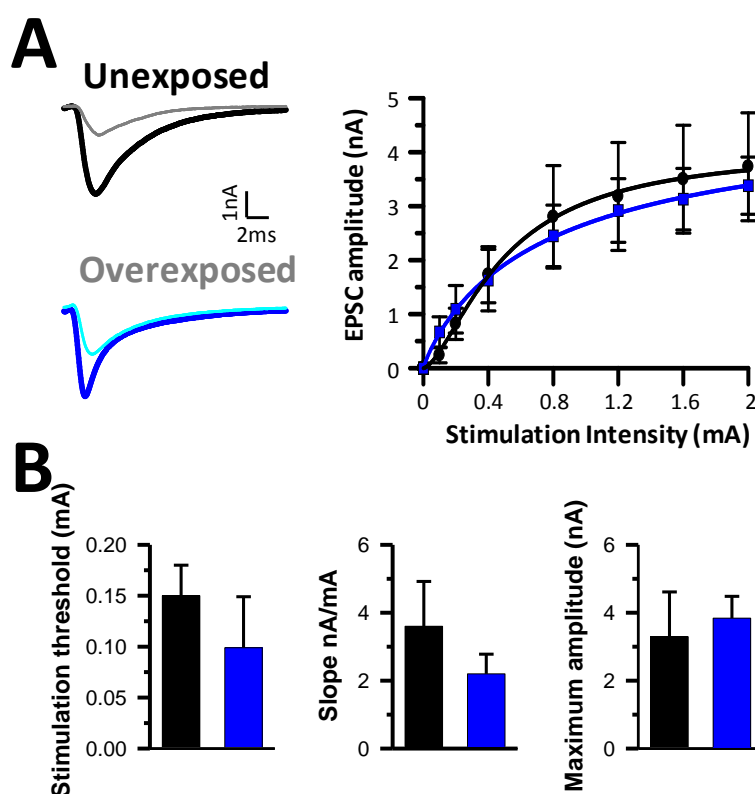


**Figure 2.20. Input-output relationships are unaffected by AOE.** (A:left) Average of ten EPSC traces evoked by parallel fibre stimulations at 0.4mA (cyan and grey) and 1.6mA (black and blue) in slices from an unexposed and overexposed rat. **Right:** Input-output relationships of the EPSCs evoked at various current stimulation intensities and fitted with a Hill function in the unexposed (black squares;  $n=7$ ) and overexposed (blue circles;  $n=6$ ) conditions. (B) Bar chart plotting the stimulation threshold (left), slope (centre) and maximal response (right).

My previous results obtained while performing field potential recordings have shown an absence of PPF following AOE. This suggests that AOE induced a deficit of synaptic transmission at the presynaptic level. However field potential recordings are limited due to the contribution of multiple cell types to the response. To further investigate the mechanisms underlying the modulation of PPF, I performed the same paired pulse tests while recording EPSCs from identified fusiform cells within the fusiform cell layer of the DCN. In unexposed conditions, paired pulse stimulation of the parallel fibres

elicited a significant PPF of  $1.35 \pm 0.06$  ( $n = 9$ ; Paired T test,  $P < 0.01$ ; Fig. 2.21A). However, similar results were found following AOE where paired parallel fibre stimulations induced a significant PPF of  $1.30 \pm 0.4$  ( $n = 7$ ;  $P < 0.01$ , Paired T tests; Fig. 2.21B). There was no significant difference between the PPR in the unexposed and the overexposed condition ( $P > 0.05$ ; Mann Whitney test).

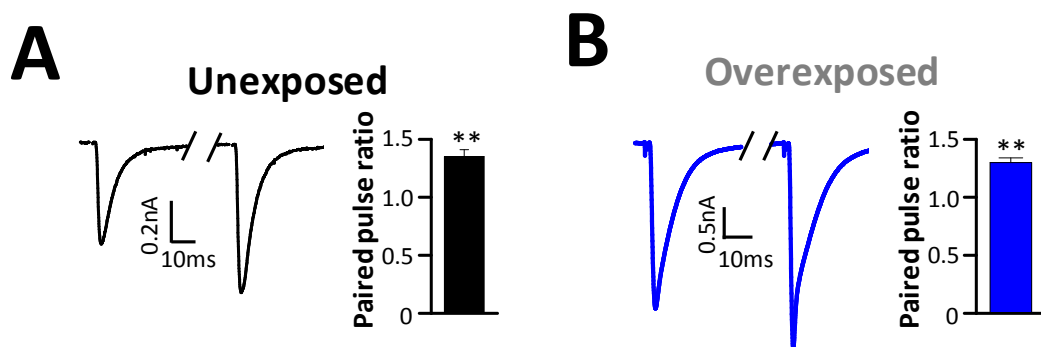


**Figure 2.21. Paired pulse facilitation of EPSCs evoked by parallel fibre stimulations in unexposed and overexposed conditions.** Sample traces are an average of ten individual traces evoked by paired pulse stimulation at 60 ms intervals in the unexposed (A;  $n = 9$ ) and the overexposed (B;  $n = 7$ ) condition. Bar charts representing reveal a significant PPF in both conditions ( $P < 0.01$ ; Paired T test).

The VM analysis (see section II.2.7.6.) was next used to measure the number of release sites, the release probability and the quantal size (Clements and Silver, 2000). The AMPA receptor mediated EPSCs were recorded by performing tests in presence of strychnine, gabazine and D-AP5. Two protocols were used, the first protocol aimed at confirming the higher release probability after AOE. In this protocol VM analysis was performed on EPSCs recorded in basal conditions. My previous experiments have shown that NMDA receptors were not involved in mediating the basal postsynaptic response, however blocking NMDA receptors after HFS abolished the LTP (unexposed) or decreased the postsynaptic response below the basal level (AOE). Therefore the second protocol was aimed at showing that blocking NMDA receptors (after HFS) decreased the release probability. In this protocol the presence or absence of LTP (in

Un and AOE conditions respectively) was first assessed by field potential recordings. Fifteen minutes after the HFS, D-AP5 was added to the perfusion already containing strychnine and gabazine. The VM analysis was then performed on the EPSCs recorded.

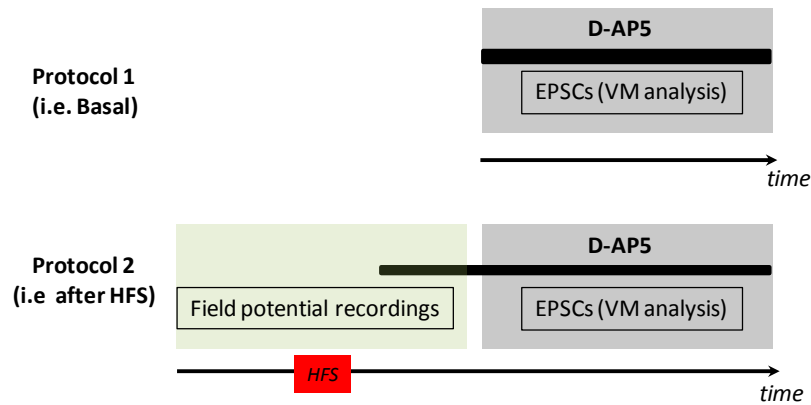


**Figure 2.22. Schematic representation of the two recording protocols used to measure the release probability.** Protocol 1 referred to as 'basal' will allow the normal quantal parameters of the synapse to be recorded. Protocol 2 referred to as 'after HFS' will give an indication of how D-AP5 addition after HFS alters the quantal parameters. Changes in extracellular calcium concentrations for the quantal analysis were performed while performing whole cell recordings.

Using protocol one, there was no significant difference in the number of release sites (Un:  $365 \pm 78$ ,  $n = 9$ ; AOE:  $258 \pm 89$ ,  $n = 9$ ;  $P > 0.05$ , Unpaired T test) or the quantal size (Un:  $2.6 \pm 0.4$  pA,  $n = 9$ ; AOE:  $2.1 \pm 0.4$  pA,  $n = 9$ ;  $P > 0.05$ , Unpaired T test) between the two conditions (Fig.2.23). However the release probability in the overexposed condition was significantly higher than that recorded in the unexposed condition (Un:  $0.43 \pm 0.07$ ,  $n = 9$ ; AOE:  $0.64 \pm 0.04$ ,  $n = 9$ ;  $P < 0.05$ , Unpaired T test; Fig. 2.23). As the mean EPSC amplitude is equal to the product of N, P and Q, (Del Castillo and Katz, 1954), the increase in release probability in the overexposed group should therefore result in a significant increase in the mean EPSC amplitude; however this was not the case (Fig. 2.20). I therefore tested whether the apparent absence of effect on the amplitude was due to a simultaneous decrease of 'N' and 'Q', which would

compensate for the increased release probability. Although neither 'N' nor 'Q' were significantly decreased after AOE (Fig. 2.23), the product of 'N' and 'Q' was significantly lower in the overexposed condition and as such could account for the lack of altered EPSC amplitude after AOE (Unexposed:  $NQ = 740 \pm 128$ ,  $n = 9$ ; AOE:  $NQ = 387 \pm 80$ ,  $n = 9$ ;  $P < 0.05$ , Unpaired T test).

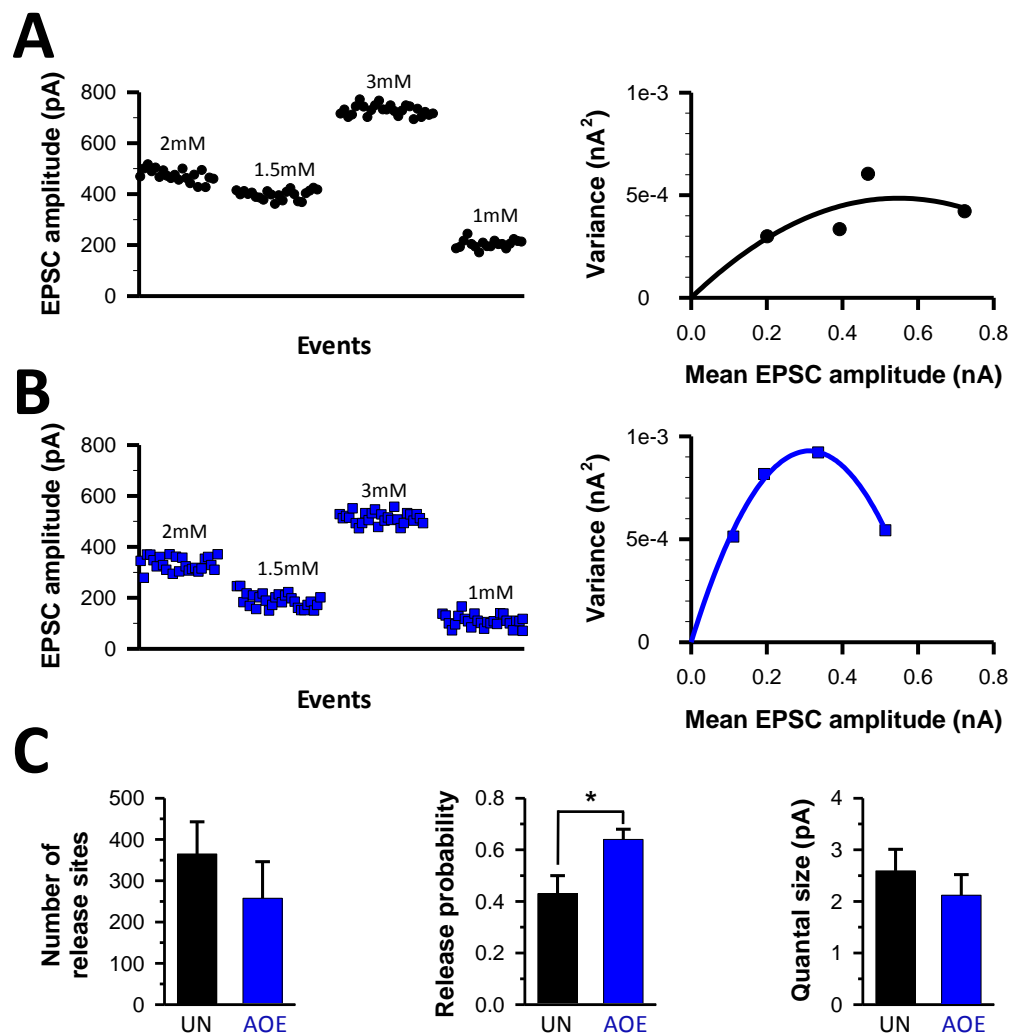


**Figure 2.23. Acoustic overexposure leads to an increased presynaptic release probability.** (A) Scatter plots show the amplitudes and variation of EPSC amplitudes in various extracellular  $Ca^{2+}$  concentrations obtained from a fusiform cell in both the unexposed (A:left) and overexposed (B:left) condition. The corresponding variance ( $nA^2$ ) was plotted against the mean EPSC amplitude (Unexposed: A:right; Overexposed: B:right) and fitted with a parabola function allowing the synaptic parameters to be deduced. (C) Bar charts showing the average number of release sites (N: left), the release probability (P: centre) and the quantal size (Q: right) in the unexposed (Black bars;  $n = 9$ ) and the overexposed (blue bars;  $n = 9$ ) conditions. Release probability is significantly higher in the overexposed condition ( $P < 0.05$ , Unpaired T test).

The VM analysis was repeated using protocol 2 to test whether D-AP5 addition after HFS reduced the N2 amplitude by decreasing the release probability (Fig. 2.24).

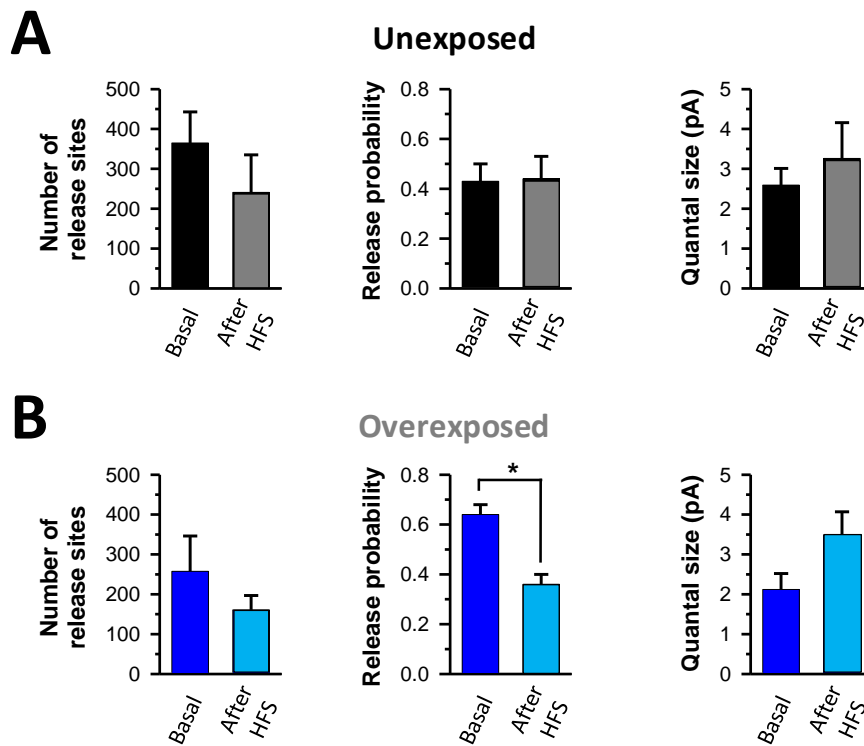


**Figure 2.24: D-AP5 addition after HFS decreases the synaptic release probability. (A)** In the unexposed condition, similar parameters were measured with either protocol (Basal: 'N' = 365 ± 78, 'P' = 0.43 ± 0.07, 'Q' = 2.6 ± 0.4 pA. After HFS: 'N' = 241 ± 94, 'P' = 0.44 ± 0.09, 'Q' = 3.26 ± 0.9 pA. **(B)** In the overexposed condition, 'N' and 'Q' were similar between when assessed with protocol 1 or 2 (Basal: 'N' = 258 ± 89, 'Q' = 2.1 ± 0.4 pA; After HFS: 'N' = 161 ± 36, 'Q' = 3.49 ± 0.6 pA). However 'P' was significantly lower in protocol 2 (Basal: 'P' = 0.64 ± 0.04. After HFS: 'P' = 0.36 ± 0.04; P < 0.05, Unpaired T test).

the unexposed condition, perfusing with D-AP5 15 minutes after the HFS revealed a release probability of  $0.44 \pm 0.09$  (n=5) which was equal to the release probability deduced from protocol 1 ( $P > 0.05$ , Unpaired T test; Fig. 2.23). This is consistent with the D-AP5 abolishing LTP and returning the N2 amplitude to pre-HFS baseline. In the AOE condition, perfusing D-AP5 after HFS also led to a decreased release probability as witnessed in the unexposed condition. However in contrast to the unexposed condition, the release probability deduced from protocol 2 ( $0.36 \pm 0.04$ ) was lower than that deduced from protocol 1 ( $0.64 \pm 0.04$ ; n =10;  $P < 0.05$ , Unpaired T test).

In conclusion these results show that after AOE, a high release probability is required in the DCN to maintain equal amplitudes of postsynaptic responses witnessed in the unexposed condition. This increase in release probability prevents HFS from inducing LTP. Following the HFS, NMDA receptor activity is required to maintain a high release probability at the synaptic terminal as D-AP5 addition reduced the N2 amplitude by reducing the release probability. Therefore AOE induces a form of metaplasticity in the DCN which alters the synaptic response to subsequent plasticity inducing stimulation.

## 2.3. DISCUSSION

### 2.3.1. Interpretation of field potential recordings

Field potential recordings make a good method to address the questions posed in this study by investigating network activity in the fusiform cell layer of the DCN. Field potentials evoked in the DCN by parallel fibre stimulations have previously been characterised in the guinea pig (Manis, 1989). Nonetheless it was essential to characterise these potentials in my model of investigation due to possible inter-species differences which if unaccounted for, could lead to the false interpretations of data. Previous studies have described the role of inhibitory synapses in the DCN particularly from cartwheel cell connections (Hackney et al., 1990, Golding and Oertel, 1997). In this study, although addition of strychnine and gabazine did not significantly alter the amplitude of the field potential responses, in some cases it altered the smoothness of the responses in a manner suggestive of a loss of inhibition.. Nonetheless all tests were performed in the presence of strychnine and gabazine to confidently exclude any contribution of the inhibitory synapses to the field potentials recordings before or after plasticity induction.

As in the guinea pig, the initial triphasic wave of the field potential was a presynaptic compound action potential that was unaffected by removal of external calcium but abolished by TTX (Manis, 1989). In addition the conduction velocity could be calculated along the axis where parallel fibres have been morphologically identified (Mugnaini, 1985, Manis, 1989). This conduction velocity of  $0.3 \text{ m.s}^{-1}$  was similar to previously reported values for the unmyelinated parallel fibres and far slower than the values recorded for myelinated fibres such as the AN (Poma et al., 2008, Imennov and

Rubinstein, 2009). All subsequent responses to the N1 were postsynaptic in nature based on the calcium dependence, the mediation by AMPA receptors and the expression of PPF. The initial negative deflection of the postsynaptic component (N2), was due to the population spike of cells in the fusiform cell layer. The ensuing P3 component was attributed to slow EPSCs in cells with dendrites spanning the molecular layer and the fusiform cell layer, principally the fusiform cells (Manis, 1989). Previous studies have shown that the size of the N2 and the P3 deflections was determined by the number of cells, the synchrony of cellular responses and the size of overall postsynaptic response to transmitter release (Manis, 1989, Manis and Molitor, 1996). It is for this reason that the P3 component was taken into account when calculating the amplitude of the postsynaptic response.

### **2.3.2. Plasticity in the dorsal cochlear nucleus**

The mechanisms underlying LTP remains a subject of wide research due to its proposed role in learning and memory (Stent, 1973, Zajaczkowski et al., 1997, Feldman, 2009). Over the years, the induction and maintenance of LTP has been linked to both pre- and postsynaptic mechanisms. Presynaptic mechanisms of LTP involve an increase in quantal content (Kullmann and Nicoll, 1992) and release probability (Buonomano, 1999, Malenka and Nicoll, 1999). Experimental evidence for these conclusions was based upon a decreased number of synaptic failures and an increased glutamate overflow during LTP (Palmer et al., 2004, Feldman, 2009). However, proponents of a postsynaptic mechanism of LTP highlight the phosphorylation and rapid AMPA receptor trafficking to the postsynaptic membrane (Malinow and Malenka, 2002), recruitment of extrasynaptic receptors (Oh et al., 2006) and the

turning on of silent synapses during LTP as mediators of a postsynaptic mechanism of LTP (Nicoll and Malenka, 1999, Kullmann, 2003). Silent synapses are of particular interest because these are synapses where a postsynaptic response cannot be elicited in response to a presynaptic stimulation (Kullmann, 1994, Voronin and Cherubini, 2004). Silent synapses can in principle be silent through pre- or postsynaptic mechanisms. Presynaptic mechanisms that define silent synapses include a low release probability or a low concentration of glutamate release which is insufficient to produce a detectable quantal response (Choi et al., 2000, Voronin and Cherubini, 2004, Lee and Dong, 2011). Whereas postsynaptic mechanisms that result in silent synapses prevent channels at the postsynaptic terminal from passing a current without a prior depolarisation of the membrane. (Kerchner and Nicoll, 2008). Such synapses are therefore thought to express the functional response of NMDA receptors and not AMPA receptors (Isaac et al., 1995, Liao et al., 1995). Considering the evidence for both pre- and postsynaptic mechanisms underlying the expression of LTP and the action of endocannabinoids as a retrograde signalling mechanism, it is also possible that both pre- and postsynaptic mechanism are involved in the DCN LTP (Tzounopoulos et al., 2007). In support of this, a unified model of LTP in the hippocampus combining both pre- and postsynaptic mechanisms has recently been proposed, based on the proximity of synapses to the area of altered synaptic activity (Lisman and Raghavachari, 2006).

In the DCN, LTP of fusiform and cartwheel cells is well documented (Fujino and Oertel, 2003, Tzounopoulos et al., 2007). The LTP of fusiform and cartwheel cells can be induced using a pairing protocol comprising presynaptic parallel fibre stimulation and

postsynaptic depolarisation of the cell. This LTP was dependent on the action of NMDARs or mGluRs in fusiform cells and GABA receptors in cartwheel cells (Fujino and Oertel, 2003). However in both cell types, LTP was dependent on the postsynaptic rise of intracellular calcium mediated by calcium release from intracellular stores (Fujino and Oertel, 2003). This indicates that LTP can be mediated by multiple receptor types in the DCN and has a postsynaptic site of induction. Nonetheless studies did not proceed to identify the site of LTP expression or maintenance. These questions were answered by others who showed that similar pairing protocols induced a postsynaptic LTP in fusiform and cartwheel cells which was dependent on the rise in intracellular calcium leading to the activation of CaMKII and phosphorylation of AMPARs (Tzounopoulos et al., 2007, Zhao and Tzounopoulos, 2011). The studies also identified a postsynaptically induced LTD mechanism which was expressed presynaptically by the retrograde transmission of endocannabinoids acting via CB1 receptors to reduce release probability (Zhao et al., 2009, Zhao and Tzounopoulos, 2011). The LTP and LTD were expressed concomitantly and the direction of plasticity was dependent on the combined size of the LTP or LTD.

It has been reported in other brain structures that the plasticity induction protocol can determine the mechanism by which plasticity is expressed (Kleschevnikov et al., 1997) and HFS in the cerebellum and hippocampus results in a presynaptic form of LTP (Larkman and Jack, 1995, Salin et al., 1996, Kleschevnikov et al., 1997). Furthermore PTP of DCN field potentials induced by tetanic stimulation of parallel fibres, was found to be mediated by a temporary presynaptic increase in release probability (Manis, 1989). In this study I have identified LTP expression as a presynaptic increase of release

probability. This conclusion was based on a lack of LTP induction in the unexposed condition when HFS was performed in a state of high release probability in addition to a decreased PPF during LTP which could be reversed when LTP was also reversed. My findings do not necessarily contradict the current literature, which shows fusiform and cartwheel cell LTP to be a postsynaptic mechanism, as the LTP induction protocol used here was based on a HFS protocol rather than a pairing protocol. Therefore the different protocols of LTP induction could result in different mechanisms of LTP expression.

As previously mentioned, a paired protocol induced LTP which was mediated by GABA receptors in cartwheel cells whereas LTP in fusiform cells was mediated by NMDARs and mGluRs (Fujino and Oertel, 2003). In my model, all recordings were performed in the presence of gabazine, which excludes any possible contribution of GABA receptors to the induced LTP. Considering that I show LTP induction to be independent of NMDARs, it is possible that mGluRs could mediate the induction of LTP although this was not tested as part of my study. Nonetheless I showed that the expression and maintenance of LTP was dependent on the continued activity of NMDA receptors. This suggests that LTP in the DCN comprises of an induction phase and a maintenance phase (Reymann and Frey, 2007, Vickers et al., 2005). This further suggests that the induction phase is NMDA receptor independent and comprises a fast trigger mechanism via unidentified receptors leading to what appears to an early onset of increase in the N2 amplitude after HFS. The maintenance phase is likely to consist of slower mechanisms mediated by NMDA receptor activation. Furthermore, the maintenance phase mechanisms are likely to shut-down the 'induction phase'

mechanisms. This could explain why the induction of LTP persists in the presence of NMDA receptor antagonist while its maintenance is blocked by perfusing the NMDA receptor antagonist thirty minutes after HFS. Further tests to identify when LTP expression completely switches from the 'induction phase' mechanism to the 'maintenance phase' mechanism will require the perfusion of an NMDA receptor antagonist at earlier time points after HFS (e.g. 5 mins, 10 mins, 15 mins and 20 mins).

The proposed NMDA receptors that maintain the increased release probability which underlie LTP in my model could be localised presynaptically and have a direct effect on release probability or postsynaptically and have an effect on release probability via a retrograde mechanism. In the DCN, the action of postsynaptic NMDA receptors activating the retrograde signalling of the endocannabinoid system has been shown to mediate LTD rather than LTP (Zhao and Tzounopoulos, 2011), indicating that a retrograde signalling mechanism does exist in the DCN. However further tests will be required to identify if the pathway can also mediate LTP expression. An alternative mechanism for postsynaptic NMDA receptors activating a retrograde signalling mechanism could be the presence of presynaptic NMDA receptors which have been identified in the DCN (Petralia et al., 1996, Tzounopoulos et al., 2007, Zhao and Tzounopoulos, 2011). Presynaptic NMDARs have also been identified in other structures where their action mediates synaptic plasticity (Madara and Levine, 2008, Rodriguez-Moreno et al., 2010) particularly in cortical and hippocampal pyramidal neurones where the activity of brain-derived neurotrophic factor via presynaptic NMDA receptors increased the release probability (Madara and Levine, 2008).

In addition to the postsynaptic response potentiation, the presynaptic N1 component also potentiated following the HFS. This was unexpected as LTP is mostly described as a mechanism amplifying postsynaptic response amplitudes. Nonetheless, potentiation of the presynaptic action potential could be a viable means of increasing the postsynaptic response as demonstrated by the input-output relationship, i.e. increasing stimulus intensity increased both the N1 and N2 components. However, in this study LTP of the postsynaptic component was confirmed as independent of the potentiation of the presynaptic action potential (*Fig. 2.9*). The increase in the N1 amplitude is most likely a consequence of increased fibre recruitment. Potentiation of the N1 response could be achieved by a decreased threshold of presynaptic fibres via mechanisms such as altered biophysical properties of the axonal channels (Colbert and Pan, 2002) activity of calcium activated chloride channels (Frings et al., 2000).

### **2.3.3. Effects of acoustic overexposure on synaptic properties**

The effects of AOE on parallel fibre evoked activity and short term plasticity in the DCN was investigated by recording field potentials and fusiform cell EPSCs. Quantal analysis of fusiform cell EPSCs reported that AOE increased the release probability at the parallel fibre synapses. Such an increase could represent a mechanism of homeostatic plasticity compensating for the loss of AN inputs (Pilati et al., 2012b). This increase in release probability could also account for the increase in mini EPSC frequency in the DCN which has previously been reported after AOE (Rich et al., 2010, Yang et al., 2011). It also correlates with an increased expression of VGluT2 over VGluT1 after AOE, as VGluT2 dominant synapses generally express higher release probabilities (Fremeau et al., 2004, Zeng et al., 2009). Interestingly, although the release probability was

increased, the size of the field potentials or fusiform cell EPSC was unchanged. This could be attributed to a decreased excitability of fusiform cells after AOE (Pilati et al., 2012a). Therefore a larger release of neurotransmitters will be required to achieve the same postsynaptic response as witnessed in the unexposed conditions. Alternatively the unaltered size of field potentials and fusiform cell EPSCs after AOE could be due to a significant decrease in the product of the other two parameters which determine the EPSC amplitude, i.e. the number of release sites (N) and the quantal size (Q). It will be of interest to identify whether the increase in 'P' is a compensatory mechanism in response to the combined decrease of 'N' and 'Q' or whether the combined decrease in 'N' and 'Q' is rather in response to the increase in 'P'. It is likely that during the AOE protocol, there is a period of intense and continuous activation of the auditory system which can be likened to an *in vitro* tetanic stimulation. Considering that PTP in the DCN has been shown to increase the release probability (Manis and Molitor, 1996), it is likely that following the AOE protocol, the release probability will be first to change which could then trigger all subsequent changes in the DCN synaptic properties. A decrease in 'N' can be attributed to a decreased number of synaptic inputs following AOE whereas a decrease in 'Q' can be attributed to the altered phosphorylation state of postsynaptic AMPARs which will ultimately lead to a decreased postsynaptic response to glutamate release (Malinow and Malenka, 2002).

Nonetheless it was unexpected that AOE did not have a significant effect on evoked synaptic activity in response to graded stimulus intensities. It has previously been shown that 3 to 5 days following AOE when hearing loss persisted, there is a reduction of the excitatory postsynaptic potentials (EPSPs) evoked by parallel fibre stimulations

(Pilati et al., 2012a). Although I obtained contradictory data it is worth mentioning that previous data were obtained while recording fusiform cell EPSPs in current clamp mode at room temperature whereas the fusiform cell data I report here was obtained in voltage clamp mode at a raised bath temperature of 32°C. Recordings in voltage clamp mode offer an advantage over current clamp mode as they allow a direct measurement of ionic currents independently of voltage fluctuations that could activate voltage gated ion channels. In my experiments, cells were held at a potential of -70 mV and at this potential, only channels that contribute to the resting membrane potential are active. Therefore I can exclude the action of voltage gated ion channels which are activated at more depolarising potentials. The same claim cannot be made for the previous experiments performed in current clamp mode. Indeed, AOE triggering noise induced hearing loss has been shown to alter currents such as Kv3.1 currents in the DCN and Kv2.2 currents in the central medial olivocochlear system (Pilati et al., 2012b, Tong et al., 2013). Furthermore there is a wide array of potassium channels which are expressed in the DCN and the effects of AOE on the currents mediated by these channels are yet to be investigated (Friedland et al., 2007).

The second variable between the two sets of experiments is the difference in bath temperature. Cellular activity can be increased by increasing temperature, therefore it is possible that performing the experiments at physiological temperature might have increased the release of transmitters thereby shadowing any deficits effect previously observed (Pilati et al., 2012a). This previous study also described that after AOE, the decrease in fusiform cell firing frequency following multisensory input stimulation could be overcome with increased stimulation intensity (Pilati et al., 2012a). Increased

bath temperature can increase activity similar to increasing stimulation intensity and as such could account for the absence of AOE-induced deficits in the input-output relationship. Nonetheless it would be expected that responses in the unexposed and overexposed conditions would increase equally with raised temperature and as such maintain the difference in response amplitudes recorded at room temperature in current clamp mode. It is likely that recordings in current clamp and voltage clamp mode account for the differences observed in previous studies (Pilati et al., 2012a).

Paired pulse facilitation is the increase in the postsynaptic potential in response to a pair of closely timed stimuli (Qian and Delaney, 1997, Varela et al., 1997) and has been described in many other brain structures including the hippocampus and the cerebellum (Mennerick and Zorumski, 1995, Zucker and Regehr, 2002, Sims and Hartell, 2005). In the unexposed conditions, PPF was recorded in the DCN at paired pulse intervals between 20 to 100 ms using field potentials and between 20 to 80 ms using whole cell recordings. When recording field potentials, PPF was absent following AOE suggesting an increased release probability. This is also consistent with an increased response to somatosensory inputs in the DCN following AOE (Shore et al., 2008, Zeng et al., 2009). It has been shown that experimentally increasing synaptic release probability can occlude the occurrence of PPF (Oleskevich et al., 2000). Indeed increasing the extracellular calcium concentration in the unexposed condition not only increased postsynaptic responses amplitudes but also significantly decreased the PPR. The opposite also held true as after AOE, decreasing the extracellular calcium concentration decreased postsynaptic response amplitudes alongside a significant increase in the PPR leading to facilitation. This provided evidence that the lack of PPF

of the field potentials in the overexposed condition was indeed due to an increased release probability triggered by the AOE protocol. Nonetheless, despite the lack of facilitation while recording field potentials, whole cell recordings of fusiform cells showed that PPF could be elicited at paired pulse intervals similar to the unexposed condition. This suggests that the increased release probability at parallel fibre synapses onto fusiform cells was insufficient to occlude and prevent PPF. In addition, it is unknown if the release probability was also increased at parallel fibre synapses onto other cell types in the DCN and if PPF was occluded at these synapses. Indeed, changes to synaptic properties have been shown to be both cell and input specific. In particular, plasticity and PPF have been shown to depend on the initial strength of the synapse. Synapses with a low release probability potentiate in response to a tetanic stimulation whereas synapses with a higher release probability depress (Hardingham et al., 2007). This can also be applied to synapses in the DCN as it has been shown that the same plasticity induction protocol that leads to potentiation at fusiform cell synapses leads to a depression at cartwheel cell synapses (Tzounopoulos et al., 2004, Tzounopoulos, 2008). This could suggest that parallel fibre synapses onto cartwheel cells have higher release probabilities than parallel fibre synapses onto fusiform cells. Although it is possible that after AOE, a lack of PPF in cartwheel cells and other DCN cell types was responsible for the overall lack of PPF of field potentials, this cannot be confirmed without performing whole cell recordings of individual cell types in the DCN. It is generally accepted that synapses with low release probabilities exhibit PPF and any manipulation of the release probability inversely correlates with changes in the PPR (Schulz, 1997, Thomson, 2000). However this is not always the case as reported in

the cerebellum (Dittman and Regehr, 1998) and the absence of positive correlation between PPF and release probability could also occur for specific cell types in the DCN. For example in the brainstem of congenitally deaf mice the release probability can be decreased without a significant change in the PPR (Oleskevich and Walmsley, 2002). Another mechanism for the proposed increase in release probability not translating into an absence of PPF could be that the release probability was simply not increased sufficiently for PPF to be abolished. Altogether, the higher release probability quantified by the VM analysis of EPSCs after AOE suggests that there is indeed an increased release probability after AOE.

#### **2.3.4. Effects of acoustic overexposure on induction of plasticity**

Previous work carried out in this lab reported that AOE decreases the excitability of fusiform cells in the early stages following the onset of hearing loss (Pilati et al., 2012a). This preceded the increase in excitability of DCN cells reported at later stages after AOE (Zhang and Kaltenbach, 1998). Studies performed as part of this project aimed to establish changes in synaptic properties which could be responsible for the hyperexcitability observed at later stages after AOE. Following AOE, an increase in release probability at DCN multisensory synapses was linked to an absence of LTP at those synapses, probably due to the inability of those synapses to be further potentiated. The increase in release probability reported here is supported by the enhancement of multisensory inputs to the cochlear nucleus which has previously been shown to occur following AOE (Shore et al., 2008, Zeng et al., 2009). Furthermore, homeostatic plastic mechanisms to sustain cortical excitability have also been reported in the auditory cortex following hearing loss (Kotak et al., 2007),

confirming that AOE is capable of inducing long term plastic adjustments at multiple levels of the auditory pathway. However, this study is the first to report metaplastic changes after AOE, altering the synaptic response to a plasticity inducing stimulus and preventing the induction of LTP. The absence of LTP and the lack of PPF after AOE could also be reversed by decreasing the extracellular calcium concentration or blocking the NMDA receptors to effectively reduce the release probability.

In both the unexposed and overexposed conditions, blocking NMDARs with D-AP5 did not affect responses prior to HFS. However, D-AP5 perfusion after the HFS protocol decreased the release probability and as such the amplitude of the postsynaptic N2 component. In the unexposed condition, HFS led to an increase in release probability which was mediated by the continuous action of NMDA receptors. Blocking these receptors reduced the release probability and as such abolished LTP, returning the postsynaptic response to its initial pre-HFS amplitude. After AOE, the high release probability led to an absence of LTP which could have been mediated by the continuous activation of NMDA receptors. The pathway by which AOE increased the release probability and the pathway by which HFS induces LTP, are likely to overlap because blocking NMDA receptors by D-AP5 was still capable of decreasing the release probability. In addition, high extracellular magnesium concentration which blocks NMDA receptors (Coan and Collingridge, 1985, Petrenko et al., 2003) had a similar effect as D-AP5 when perfused after the HFS.

Although D-AP5 addition prior to the HFS did not reduce the release probability, performing HFS in the presence of D-AP5 promoted the induction of LTP. I have previously established that a low release probability is a prerequisite for LTP induction

by HFS. This suggests that the release probability could have transiently decreased during the 30 second period of HFS and as such facilitating the induction of LTP. An alternative explanation could be that performing HFS in the presence of D-AP5 triggered an increase in release probability (and therefore LTP) via an NMDA receptor independent pathway. Indeed this would explain why in the unexposed condition, LTP induction by HFS persisted even in the presence of D-AP5. Long term potentiation in the DCN could therefore be induced via an NMDA receptor independent pathway and maintained via an NMDA receptor dependent pathway. Indeed, previous studies have shown that LTP in DCN fusiform cells was dependent on either the activation of NMDA receptors or mGluRs, whereas the LTP observed in cartwheel cells was independent of either pathway (Fujino and Oertel 2003). However it is still unclear how one specific pathway is selected over the other. One possibility could be linked to the subset of parallel fibres which are stimulated. The little overlap of parallel fibre projections (Roberts and Trussell, 2010) could therefore allow for an input specific plasticity. Indeed, input specificity has been described in cartwheel cells where it has been suggested that feedforward or lateral inhibition of cartwheel cells to their postsynaptic targets was dependent on the set of parallel fibres activated by a particular sensory stimulus (Roberts and Trussell, 2010).

### **2.3.5. Role of NMDA receptors in hearing loss and tinnitus**

As discussed in the previous chapter, AOE triggers an increase in the hearing threshold which is principally due to deficits in both the IHCs and OHCs and the AN structural and functional properties (Cody and Robertson, 1983, Liberman and Dodds, 1987, Shepherd et al., 2004). The deficits identified in this chapter at the parallel fibre

synapses did not alter the overall evoked synaptic activity at these synapses. However these deficits did alter the synaptic properties related to plasticity, suggesting that changes in the DCN at this time point do not contribute to the hearing loss previously discussed. In regards to synaptic properties, acoustic overexposure is known to trigger a myriad of deficits in synaptic processing along the auditory pathway. Such changes include a decrease of synaptic efficacy at spiral ganglion boutons (Kujawa and Liberman, 2009, Norena, 2011), an increased excitability in the AC and IC (Ma et al., 2006, Eggermont, 2008) and a decreased release probability in the VCN (Wang and Manis, 2005). In the DCN particularly, AOE also reduced the membrane resistance of granule cells which are the parallel fibre cell bodies and reduced excitability of the fusiform cells in the short term following AOE (Pilati et al., 2012a), increased the excitability of cells in the fusiform cell layer in the long term following AOE (Zhang and Kaltenbach, 1998), introduced burst firing of fusiform cells (Pilati et al., 2012b), increased NO production which in turn increased the phosphorylation of Kv3.1 subunits to decrease channel activity (Song et al., 2005, Brown and Kaczmarek, 2011), increased the representation of somatosensory inputs into the DCN (Shore et al., 2008, Dehmel et al., 2012b) and increased VGluT2 expression at parallel fibre synapses (Shore et al., 2008, Dehmel et al., 2012b). All the deficits listed above point towards both structural and functional plasticity induced by AOE. Reducing the release probability could potentially reverse all these AOE-induced deficits identified in the DCN. Perfusing slices with D-AP5 or a high magnesium extracellular solution also had similar effects on the release probability. These findings support a previously identified role of NMDA receptors in mediating deficits induced by AOE. Blocking cochlear NMDA receptors or administration of memantine (a clinically approved NMDA receptor

antagonist) have been shown to prevent or reduce tinnitus induced by acoustic trauma (Guitton and Dudai, 2007, Zeng et al., 2009). This suggests that long lasting deficits induced by AOE are mediated by NMDA receptor activation. Furthermore, salicylate which induces tinnitus in animal models has been shown to increase the open probability of some ligand gated ion channels including NMDA receptors (Miller et al., 1992, Casado and Ascher, 1998). Cochlear injections of NMDA receptor antagonists also prevented or reduced the perception of tinnitus induced by salicylate (Guitton et al., 2003, Puel and Guitton, 2007).

## 2.4. CONCLUSION

In addition to previously reported findings of AOE modulating the excitability of fusiform cells, I have shown that AOE induced metaplastic changes in the DCN translated as an inhibition of LTP induction due to elevation of the release probability at parallel fibre synapses onto fusiform cells. I have also shown that decreasing the release probability *in vitro* was capable of reversing all the deficits identified. A single mechanism underlying AOE induced deficits at such an early stage (and within a structure involved in early sound integration), is pivotal to understanding AOE induced deficits leading to tinnitus. The work reported here could serve as a foundation to reverse AOE-induced deficits which have been identified in other auditory structures and at other time points. Plastic adjustments in the DCN following AOE could represent an intermediate state between the decrease in DCN excitability and DCN hyperexcitability associated with the onset of tinnitus. Based on this, my next chapter will investigate *in vivo* therapeutic interventions which could be used as therapeutical treatments against noise induced tinnitus.

# **CHAPTER 3**

**Modulation of synaptic activity  
in the dorsal cochlear nucleus:  
a biomarker for tinnitus?**

### 3.1. INTRODUCTION

Over the last two decades, many researchers have carried out studies which have improved our current understanding of the mechanisms underlying noise induced hearing loss and tinnitus. These studies have identified the functional loss of inputs from the hair cells to be a key factor in mediating noise induced hearing loss (Doetsch, 1998, Norena et al., 2002). This peripheral damage can promote plastic changes in various central auditory processing structures which have been proposed to underlie the perception of tinnitus (Salvi et al., 2000, Guitton, 2012). Action of NMDA receptors are heavily implicated in both hearing loss and tinnitus (Guitton and Dudai, 2007, Abaamrane et al., 2009, Zheng et al., 2012). This line of investigation was bolstered by findings showing that elevating blood and perilymph magnesium concentrations attenuates noise induced hearing loss (Abaamrane et al., 2009). Furthermore blocking cochlear NMDA receptors with an NR2B specific antagonist (within a short time window after AOE) reduced the number of subjects that later exhibited behavioural evidence of tinnitus (Guitton and Dudai, 2007). Other studies have also shown that pharmacological interventions which target the action of NMDA receptors in both human and animal models can alleviate tinnitus with various degrees of success (Guitton et al., 2003, Guitton and Dudai, 2007, Darlington and Smith, 2007, Wu et al., 2011, Zheng et al., 2012).

Therefore in this chapter, I investigated the effects of either memantine injections (a clinically approved NMDA receptor antagonist) or elevating *in vivo* magnesium concentrations ( $MgCl_2$  injections and/or magnesium threonate dissolved in drinking water) on hearing loss and tinnitus triggered by AOE.

## 3.2. RESULTS

### 3.2.1. Effects of memantine and MgCl<sub>2</sub> injections in unexposed rats

My previous results showed that the perfusion of D-AP5 allowed the induction of LTP after AOE. I next checked whether blocking NMDA receptors *in vivo* allowed deficits specific to hearing loss (threshold shifts) or to tinnitus (gap detection) to be alleviated. I first tested memantine which is a clinically approved NMDA receptor antagonist used as a treatment against mild to moderate Alzheimer's diseases (Parsons et al., 2007). Memantine has previously been shown to alleviate tinnitus (Zheng et al., 2012), however the results are inconsistent and a consensus is yet to be reached (Lobarinas et al., 2006, Zheng et al., 2012). I also used MgCl<sub>2</sub> injections as it has been shown that magnesium is capable of blocking NMDA receptors (Nowak et al., 1984, Danysz and Parsons, 2003) and it is protective against the effects of acoustic trauma (Abaamrane et al., 2009). To clarify the effect of each compound in control conditions, twenty one day old unexposed rats were split into three groups with the first group receiving a daily injection of memantine for three consecutive days (Un-Mem), the second group receiving a daily injection of MgCl<sub>2</sub> instead (Un-Mg) while the third group received saline only injections at similar time periods (Un).

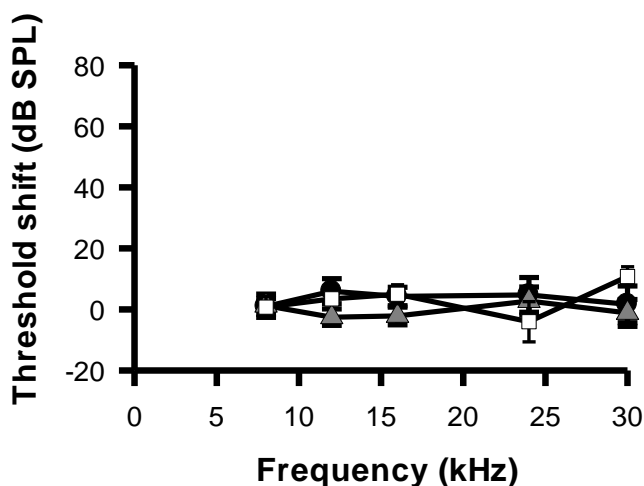


**Figure 3.1.** *In vivo* memantine or Mg<sup>2+</sup> administration leaves the hearing threshold in unexposed animals unaffected. There was no shift when hearing threshold was measured between day 0 and day 4, for the Un group (black circles; n = 6), the Un-Mem group (grey triangles; n = 5) and the Un-Mg group (white squares; n = 8) at all frequencies tested. (One way ANOVA on Ranks).

Auditory brainstem response recordings before treatments revealed that hearing thresholds were all between 20 and 30 dB SPL for frequencies between 8 and 30 kHz (Table 3.1) and that those thresholds were unaffected after memantine or magnesium administration. Consequently threshold shifts after 3 days were nonexistent and similarly unchanged at all frequencies tested in all three sub-groups (Fig. 3.1).

Tone pip Frequency	Hearing threshold (dB SPL)								
	Un (n = 6)			Un-Mem (n = 5)			Un-Mg (n = 8)		
	Day 0	Day 4	T test	Day 0	Day 4	T test	Day 0	Day 4	T test
8 kHz	35 ± 3	37 ± 3	NS	38 ± 3	39 ± 2	NS	31 ± 2	32 ± 2	NS
12 kHz	28 ± 4	31 ± 3	NS	27 ± 3	30 ± 1	NS	28 ± 3	25 ± 2	NS
16 kHz	27 ± 2	31 ± 2	NS	26 ± 4	31 ± 4	NS	34 ± 2	32 ± 2	NS
24 kHz	26 ± 3	30 ± 4	NS	36 ± 9	32 ± 5	NS	32 ± 4	35 ± 3	NS
30 kHz	32 ± 3	34 ± 4	NS	36 ± 5	47 ± 8	NS	34 ± 4	33 ± 3	NS

**Table 3.1. Absence of memantine or magnesium injections effects on hearing thresholds of unexposed rats.** Three day consecutive daily injection of saline (Un: n = 6), memantine (Un-Mem: n = 5) or MgCl<sub>2</sub> (Un-Mg: n = 8) did not significantly alter the hearing thresholds at all frequencies tested. (NS: non-significant, Paired T tests between day 0 and day 4).

*In vitro* electrophysiological recordings revealed that the amplitude of postsynaptic field potential responses (N2) elicited by parallel fibre stimulation in the DCN was identical between the groups (Fig. 3.2A). The minimal stimulation intensity to elicit a response (stimulation threshold), the slope and the maximal response of the postsynaptic N2 component was 2.2±0.2 V, 0.02 ± 0.006 mV/V and 0.69 ± 0.16 mV respectively (n = 4-6) for the unexposed group without drug treatment (Un) (Fig. 3.2B). Similar values were obtained in the Un-Mem group (stimulation threshold: 3.58 ± 1.09 V; slope: 0.025 ± 0.004 mV/V; maximum amplitude: 0.78 ± 0.12; n = 5, Fig. 3.2B) and the Un-Mg group (stimulation threshold: 4.16 ± 2.4 V; slope: 0.05 ± 0.02 mV/V; maximum: 0.85 ± 0.2; n = 4- 5, Fig. 3.2B). Although one way ANOVA tests revealed no significant difference in the values recorded between the groups, there appears to be

larger error bar values in the Un-Mg group suggesting an increased variation in recordings.

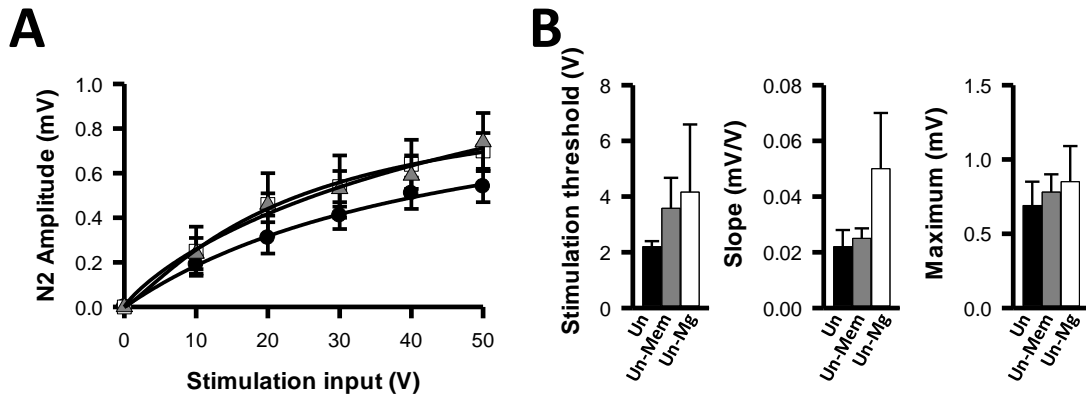


**Figure 3.2.** The input-output relationship in the DCN of unexposed animals is unaltered by memantine or magnesium injections. (A) Input-output relationship of the N2 field potential amplitude elicited by various stimulation intensities (black circles;  $n=6$ ), Un-Mem (grey triangles;  $n=5$ ) and the Un-Mg (white squares;  $n=5$ ) groups. (B) Data points were fitted with a Hill function. Bar charts showing that the stimulation thresholds, the slope of the fitted data and the maximal responses were unaffected by the treatments ( $n=4-6$ ). ( $P > 0.05$ , One way ANOVA).

The next step comprised testing the effects of memantine and magnesium injections on the potentiation of the N2 component after HFS. As previously reported, HFS elicited an LTP in the unexposed group and this was true for all the unexposed conditions, irrespective of the treatment. The N2 amplitude elicited at half maximal stimulation intensity was increased by  $26 \pm 8\%$  (Un,  $n = 6$ ),  $25 \pm 9\%$  (Un-Mem  $n = 5$ ) and  $59 \pm 2\%$  (Un-Mg  $n=6$ ) (Fig. 3.3).

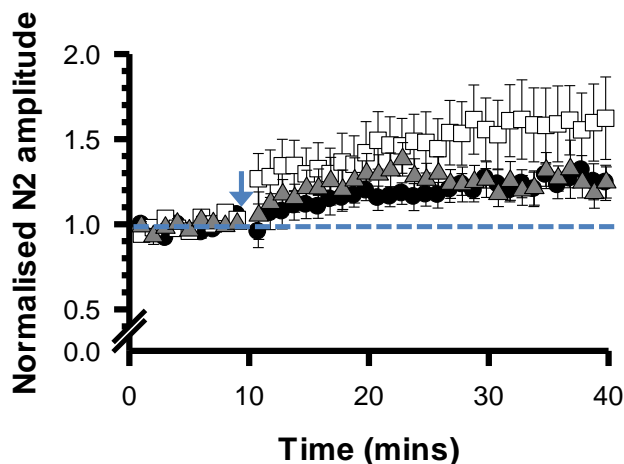


**Figure 3.3.** Induction of LTP by HFS persists following in vivo memantine or magnesium injections. In all conditions, HFS (arrow) induced a significant LTP after 30 mins. There was no significant difference between the LTP induced in the Un group (Black circles;  $n = 6$ ), the Un-Mem group (grey triangles;  $n = 5$ ) and the Un-Mg groups (white squares;  $n = 6$ ). ( $P > 0.05$ , One way ANOVA).

In summary the *in vivo* administration of memantine or  $Mg^{2+}$  had no effect on the hearing threshold or on the synaptic activity and plasticity in the DCN.

### 3.2.2. Effect of memantine injections following exposure to loud sound

I next investigated the effects of memantine injections on rats that had been acoustically overexposed. Saline (AOE) or memantine (AOE-Mem) was injected into two sub groups of rats immediately following each day of the AOE protocol.

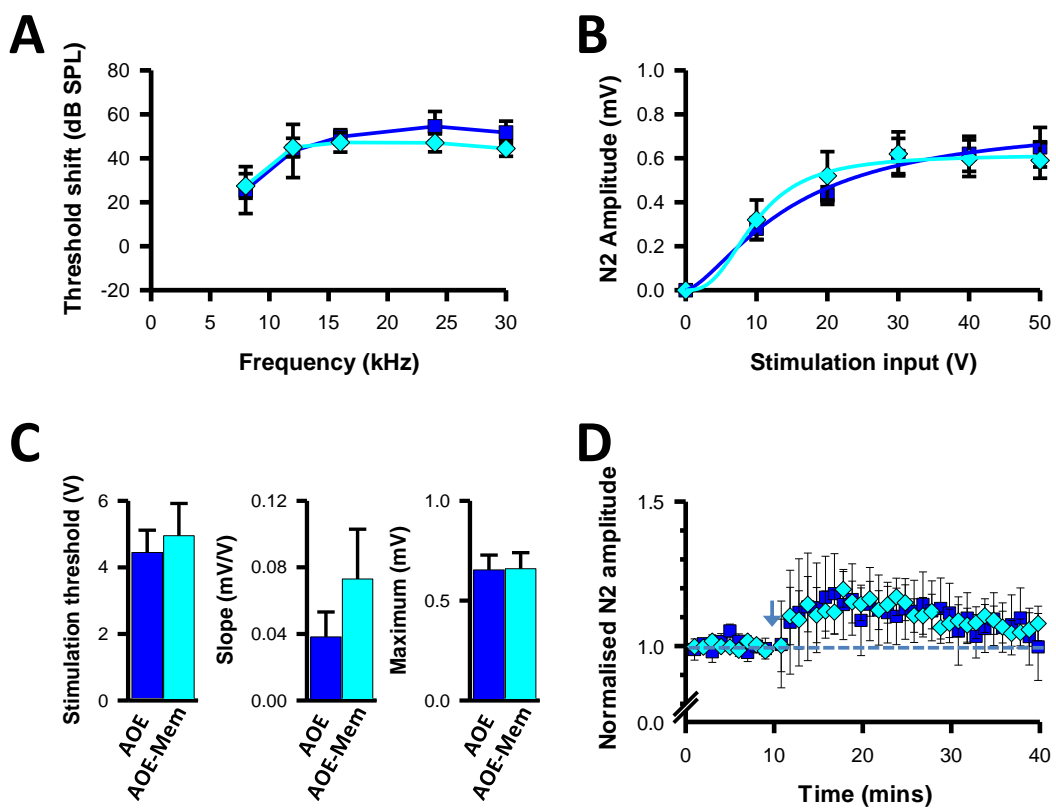


**Figure 3.4. Hearing threshold shifts and absence of LTP in the DCN after AOE persists following administration of memantine.** (A) Hearing thresholds shifts 3 to 5 days after AOE at frequencies from 8 to 30 kHz (blue, n=6) persist following administration of memantine (cyan n=7). (B) Input-output relationships elicited by parallel fibre stimulations are similar for both the AOE group (blue squares, n = 5) and AOE-Mem group (cyan diamonds, n = 9). Data points were fitted with a Hill function. (C) The stimulation thresholds, the slope and the maximal N2 amplitude were unaffected by memantine. ( $P > 0.05$ ; Unpaired T test). (D) High frequency stimulations (arrow) failed to induce LTP in both conditions (measured 30 minutes after the HFS). The dashed line represents the amplitude normalised to 1. AOE: blue, n=5; AOE-Mem: cyan, n=9.

Memantine administration did not prevent the hearing loss as indicated by large threshold shifts in both conditions measured 3 to 5 days after initial exposure and

treatment (*Fig 3.4A*). The size of the postsynaptic N2 amplitude and the parameters of the input-output relationship were also unaffected by memantine injections (*Fig 3.4B-C*). Lastly, the absence of LTP after AOE was still observed after memantine was injected in rats having been exposed to AOE, with normalised N2 amplitudes measured thirty minutes after the HFS protocol of  $1.05 \pm 0.1$  ( $n = 5$ ) and  $1.06 \pm 0.05$  ( $n = 9$ ) in the AOE and AOE-Mem group respectively (*Fig. 3.4D*; Unpaired T tests). Interestingly, the N2 amplitude appears to be increased within the first fifteen minutes after HFS in comparison to the amplitudes reported in Chapter 2 (*Fig. 2.8, 2.15, 2.16, 2.17, 2.19*).

### **3.2.3. Effects of MgCl<sub>2</sub> injections following exposure to loud sound**

Daily injections of magnesium have been reported to be protective in a different model of acoustic trauma (Abaamrane et al., 2009), therefore I next investigated the effects of daily subcutaneous injections of MgCl<sub>2</sub> for 3 to 5 days after AOE. One group of rats received MgCl<sub>2</sub> injections immediately following each 3 hr AOE session (AOE-Mg, corresponding to a total of 3 day injections) whereas the other group received a control saline injection (AOE). The MgCl<sub>2</sub> injections did not prevent AOE induced threshold shifts at high frequencies measured 3 to 5 days after the initial AOE and MgCl<sub>2</sub> injection (frequencies above 16 kHz; *Fig 3.5A*). However injections of MgCl<sub>2</sub> reduced the threshold shift measured at low frequencies (below 16 kHz) particularly at 16 kHz (AOE:  $51.3 \pm 3.6$  dB SPL,  $n = 8$ ; and AOE-Mg:  $33 \pm 3.6$  dB SPL,  $n=8$ ;  $P < 0.05$ , Unpaired T test; *Fig. 3.5A*). Similarly to the conditions reported above whereby the *in vitro* effects of memantine were tested, the size of the postsynaptic N2 amplitude and the input-output relationship were unaffected by MgCl<sub>2</sub> injections (*Fig 3.5B-C*).

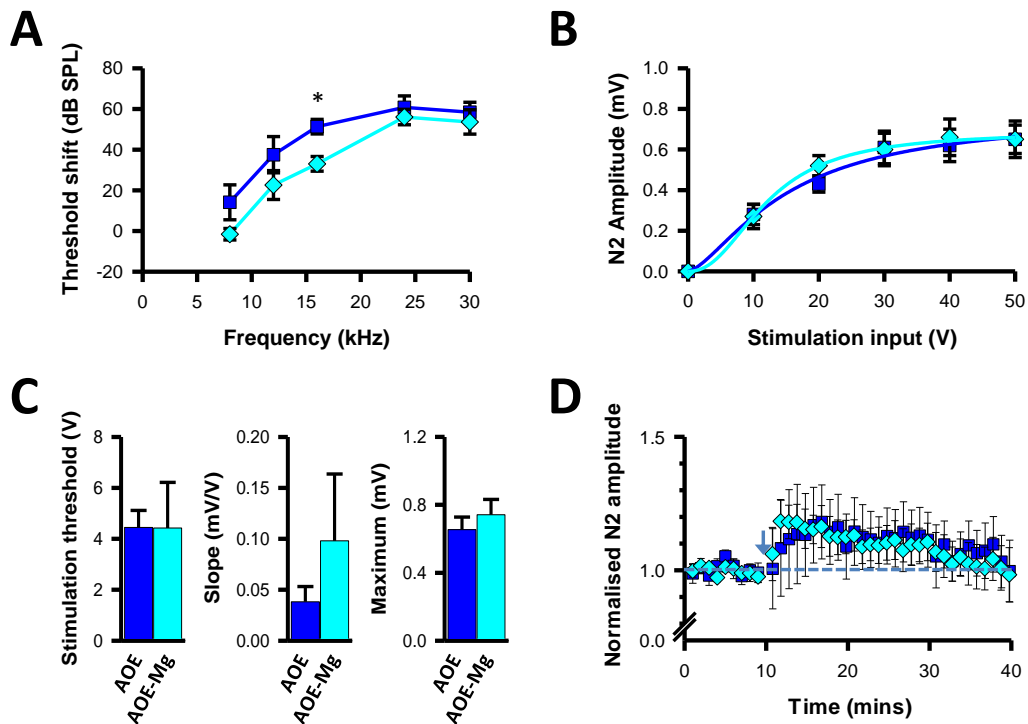


**Figure 3.5. Partial protection against hearing loss and absence of LTP following  $Mg^{2+}$  injections.** (A)  $Mg^{2+}$  injections significantly decreased the threshold shift induced by AOE at 16 kHz (cyan,  $n = 8$ ,  $P < 0.05$ , Unpaired T test). (B) Input-output relationships are similar for both AOE (blue squares,  $n = 5$ ) and AOE-Mg groups (cyan diamonds,  $n = 6$ ). Data are fitted with a Hill function. (C) The stimulation thresholds, the slope and the maximal N2 amplitude were unaffected by  $MgCl_2$ . ( $P > 0.05$ ; Unpaired T test). (D) High frequency stimulation (arrow) failed to induce LTP in both conditions (measured 30 minutes after the HFS;  $P > 0.05$ , Wilcoxon test). The dashed line represents the amplitude normalised to 1. AOE: blue,  $n=5$ ; AOE-Mg: cyan,  $n=6$ .

Furthermore, LTP remained absent in the AOE-Mg group. Thirty minutes after the HFS protocol, normalised N2 amplitudes were  $1.05 \pm 0.1$  ( $n = 5$ ) and  $1.01 \pm 0.1$  ( $n=6$ ) in the AOE and AOE-Mg group respectively (Fig. 3.5D).

### 3.2.4. Effects of magnesium threonate diet

I next investigated the effects of chronic oral supplementation of magnesium threonate which has been shown to achieve high levels of magnesium in the brain after 4 weeks and also capable of altering plasticity in the amygdala (Abumaria et al., 2011). Unexposed and overexposed rats were maintained on a high magnesium threonate diet (Un-MgT and AOE-MgT respectively) for four weeks after which the hearing threshold, synaptic activity and plasticity in the DCN were investigated. Other

unexposed controls (Un) and overexposed rats (AOE) were maintained on a normal diet for the same duration. I first tested the effects of magnesium threonate in rats unexposed to loud sound (Un-MgT). Performing ABR recordings before the four week diet revealed that hearing thresholds were all between 20 and 40 dB SPL for frequencies between 8 and 30 kHz and that these thresholds were unaffected after 28 days on the diet (Table 3.2).

	Hearing threshold (db SPL)					
Tone pip Frequency	Un (n = 6)			Un-MgT (n = 6)		
	Day 0	Day 28	T test	Day 0	Day 28	T test
8 kHz	36 ± 3	34 ± 3	NS	33 ± 2	30 ± 2	NS
12 kHz	25 ± 2	32 ± 4	NS	29 ± 3	26 ± 1	NS
16 kHz	27 ± 2	36 ± 5	NS	33 ± 3	36 ± 2	NS
24 kHz	25 ± 3	31 ± 2	NS	37 ± 4	26 ± 2	NS
30 kHz	32 ± 4	32 ± 2	NS	38 ± 4	31 ± 2	NS

**Table 3.2. The high magnesium diet leaves hearing thresholds of unexposed animals unaffected.** Four weeks of being on a normal diet (Un: n = 6) or high magnesium diet (Un-MgT: n = 6) left the hearing thresholds unaltered at all frequencies tested. (NS: non significant Paired T tests between day 0 and week 4).

The amplitude of the postsynaptic N2 component, the stimulation threshold, slope and maximum response were also unaffected by the high magnesium diet (*Fig 3.6B-C*). In addition, HFS induced similar levels of LTP in both conditions with normalised N2 amplitude of  $1.18 \pm 0.12$ , (n = 8) in the Un group and  $1.18 \pm 0.05$  (n= 8) in the Un-MgT 30 minutes after HFS (Mann Whitney Test, *Fig3.6D*). Interestingly, although non-significant, LTP amplitudes appear lower compared to the LTP amplitudes reported in previous sections (Chapter 2). This apparent difference could be due to differences in age as the animals used in this group were four weeks older than the animals used in Chapter 2.

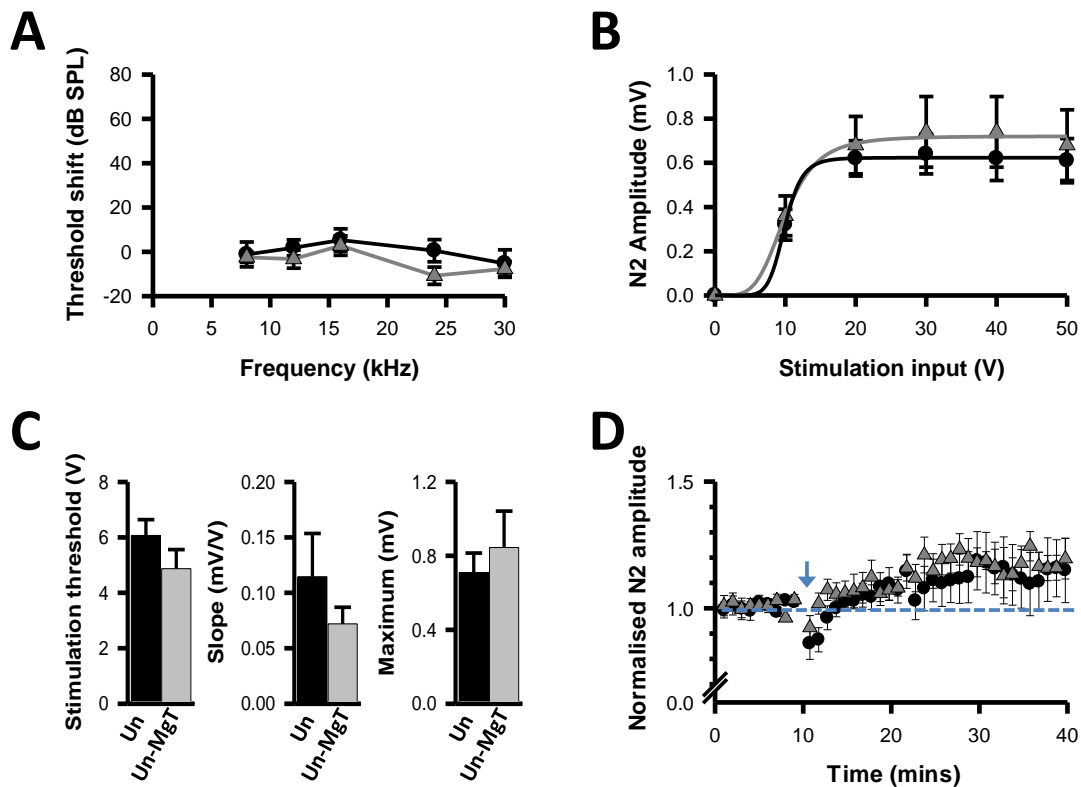


**Figure 3.6. Absence of *in vivo* and *in vitro* effects following a high  $Mg^{2+}$  diet in unexposed rats.** **A.** High  $Mg^{2+}$  diet produces no shifts in hearing threshold between day 0 and day 28 (Un:black circles,  $n = 6$ ; Un-MgT: grey triangles;  $n = 6$ ) at all frequencies tested ( $P > 0.05$ , Paired T test) **(B)** Input-output relationships are similar for both unexposed group (black circles,  $n = 7$ ) and Un-MgT group (grey triangles,  $n = 8$ ). **(C)** The stimulation threshold, the slope and the maximal N2 amplitude are unaffected by the  $Mg^{2+}$  diet. ( $P > 0.05$ ; Unpaired T test). **(D)** High frequency stimulations (arrow) significantly increased the normalised N2 amplitude measured 30 minutes after the HFS (LTP:  $P < 0.05$ , Wilcoxon test). The dashed line represents the amplitude normalised to 1. Un: black circles,  $n = 8$ ; Un-MgT: grey triangles,  $n = 8$ .

Similar tests were repeated 4 weeks after the AOE procedure in rats that were maintained on a normal diet (AOE) or high  $Mg^{2+}$  diet (AOE-MgT). Four weeks after the initial AOE, the high  $Mg^{2+}$  diet did not prevent threshold shifts after AOE and this was valid at all frequencies tested (Fig 3.7A). Similar to the conditions reported above whereby the *in vitro* effects of memantine and  $MgCl_2$  injections were tested, the size of the postsynaptic N2 amplitude, the threshold stimulation, slope and maximum response were unaffected by MgT (Fig 3.7B-C). In contrast to the absence of LTP still observed after memantine or magnesium injections, LTP in the DCN could be induced by HFS of the multisensory inputs in rats belonging to the AOE-MgT group. Thirty

minutes after the HFS protocol, normalised N2 amplitudes were  $1.06 \pm 0.07$  ( $n = 6$ ,  $P=0.41$ ) and  $1.33 \pm 0.10$  ( $n = 12$ ,  $P<0.05$ , Wilcoxon test; Fig. 3.7D) in the AOE and AOE-MgT group respectively (Fig. 3.7D).

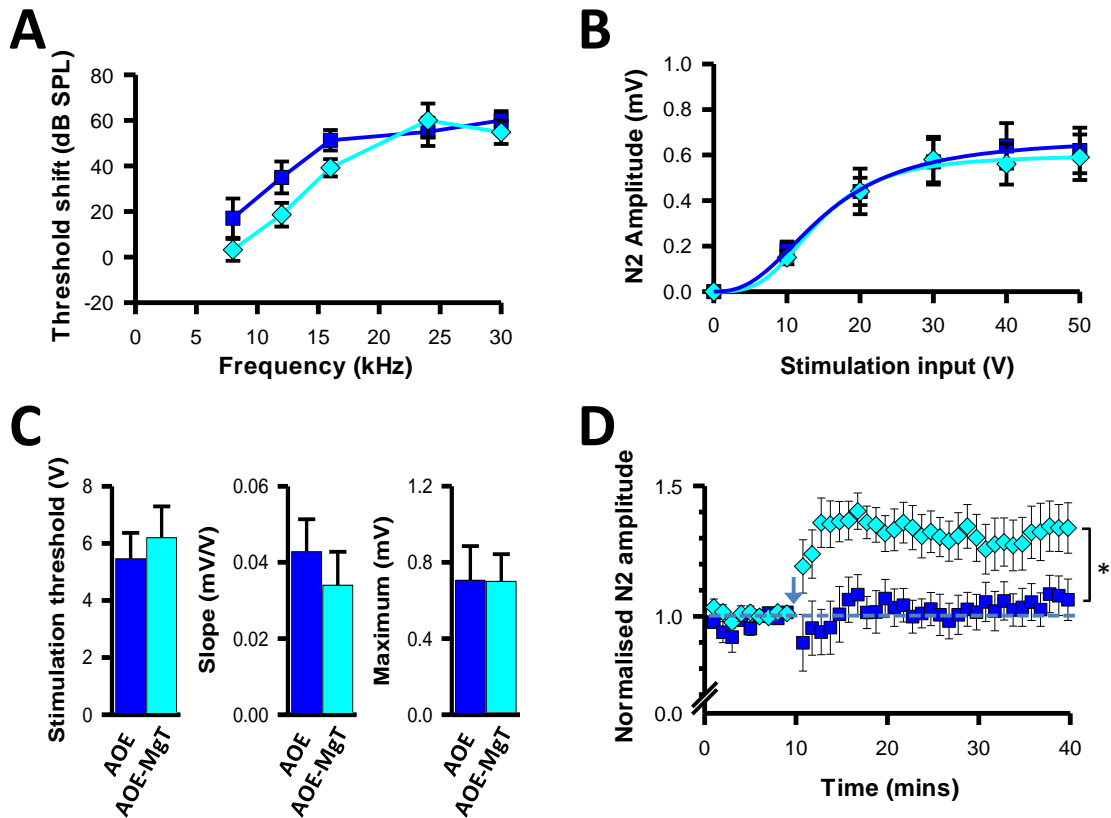


**Figure 3.7. The high MgT diet promotes induction of LTP in the DCN following AOE. (A)** Similar shifts in hearing thresholds were recorded in both the AOE ( $n=8$ ) and the AOE-MgT ( $n=8$ ) at all frequencies tested 4 weeks after the exposure protocol ( $P>0.05$ , Mann Whitney Test). **(B)** Input-output relationships are also similar for both the AOE (blue squares,  $n = 7$ ) and the AOE-MgT group (cyan diamonds,  $n = 9$ ). **(C)** The stimulation thresholds, slope and the maximal N2 amplitude represented calculated from the transfer functions fit (Hill equation) were similarly unaffected by the  $Mg^{2+}$  diet. ( $P>0.05$ ; Unpaired T test). **(D)** High frequency stimulation (arrow) fails to induce LTP in the AOE group ( $n=6$ ) whereas the LTP could be measured in the AOE-MgT group ( $P < 0.05$ , Wilcoxon test,  $n = 12$ ). The dashed line represents the amplitude normalised to 1 (\*  $P < 0.05$ , Mann Whitney test).

In summary, short term subcutaneous  $Mg^{2+}$  injections partially protects against AOE-induced hearing loss without altering central deficits in the synaptic properties within the DCN. In contrast, a long term  $Mg^{2+}$  diet to elevate brain magnesium (Abumaria et al., 2011), could not protect against AOE-induced hearing loss but prevented central deficits in the DCN synaptic properties and promoted the induction of LTP by HFS.

### 3.2.5. Effects of combined delivery of magnesium

The last step comprised of investigating the *in vivo* effects of combining 3 to 5 days of MgCl<sub>2</sub> injections with a long term MgT diet (MgC). *In vivo* tests included performing ABR recordings before (day 0), 4 days (day 4) and 90 days (day 90) after the AOE protocol. Gap detection tests were also performed as an indicator of tinnitus before the AOE protocol (week 0) and repeated every 3 weeks for up to 12 weeks, as noise induced tinnitus generally develops after 2 months following AOE (Kaltenbach, 2011, Engineer et al., 2011). Thirty three rats were used for these tests and split into four groups (Un: n = 7; Un-MgC: n = 6; AOE: n = 10; AOE-MgC: n = 10).

#### 3.2.5.1. Effects on hearing thresholds

Hearing thresholds rather than hearing threshold shifts are referred to here to enable reference to raw hearing thresholds recorded at day 0, day 4 and day 90. Hearing thresholds were first measured in the unexposed (Un) and Un-MgC groups (Fig. 3.8A).

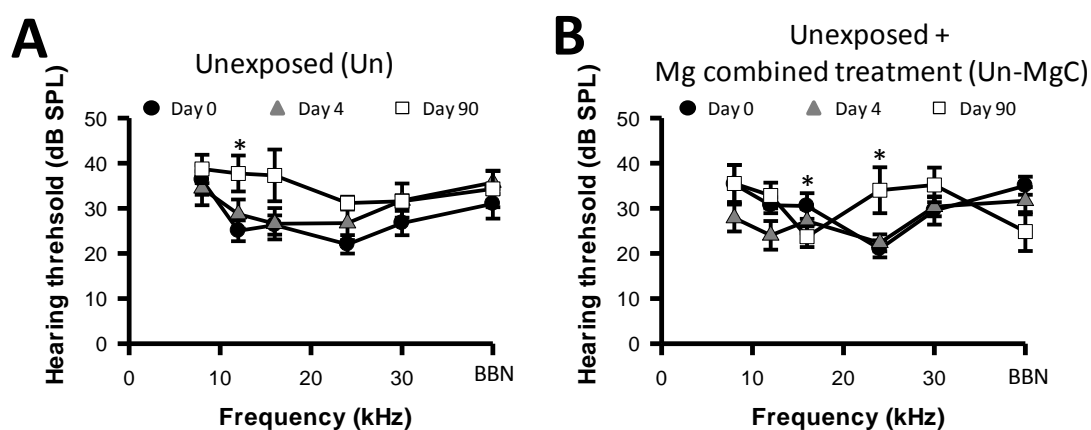


**Figure 3.8. Effects of combined magnesium delivery on hearing thresholds of unexposed rats.** (A) In the unexposed condition (n = 7), similar hearing thresholds were observed across time at all frequencies except at 12 kHz where the hearing thresholds were elevated at day 90 (B) With combined Mg<sup>2+</sup> treatment (Un-MgC, n = 6), similar hearing thresholds were observed across time at all frequencies except at 24 kHz where the hearing threshold was elevated and at 16 kHz where the hearing threshold was decreased at day 90. BBN: broadband noise (\* P < 0.05, RM ANOVA, SNK tests).

Hearing thresholds in the Un groups were found to be unaffected between day 0 and day 90 at 8 kHz, 16 kHz, 30 kHz and BBN (One way ANOVA tests). However at 12 kHz and 24 kHz, hearing thresholds were increased from  $25 \pm 2$  dB SPL (day 0) to  $37.7 \pm 4$  dB SPL (day 90) and from  $22 \pm 2$  dB SPL (day 0) to  $31.1 \pm 1.4$  at 24 kHz (day 90) respectively ( $n = 7$ ;  $P < 0.05$ , One way ANOVA, SNK tests). Hearing thresholds in the Un-MgC group were also unaffected between day 0 and day 90 at 8 kHz, 12 kHz, 16 kHz, 30 kHz and BBN. However in contrast to the Un group, hearing thresholds were increased at only 24 kHz from  $21 \pm 2$  dB SPL (day 0) to  $34 \pm 5$  dB SPL ( $n = 6$ ;  $P < 0.05$ , One way ANOVA, SNK tests; *Fig. 3.8B*). Increased hearing thresholds overtime is compatible with presbycusis observed in aging animals (Derin et al., 2004, Chen et al., 2012). Following on from this, hearing thresholds were also measured in rats exposed to loud sound (AOE and AOE-MgC; *Fig. 3.9*). As previously reported (*Fig. 3.5A*), AOE-induced shifts in hearing thresholds were less pronounced at 16 kHz in rats that received only  $MgCl_2$  injections. This was also the case when a combined delivery of magnesium was performed after AOE. Four days after AOE, rats in the AOE-MgC group exhibited lower ABR thresholds at 16 kHz, ( $73 \pm 5$  dB SPL,  $n=10$ ) compared to hearing thresholds measured in the AOE group at the same time point ( $87 \pm 1$  dB SPL  $n=10$ , *Fig. 3.9*,  $P < 0.05$ , Unpaired T tests).

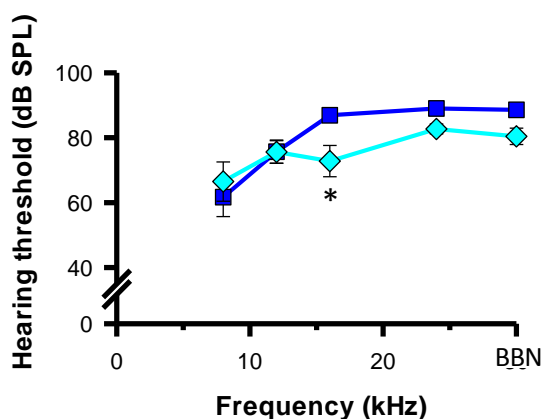


**Figure 3.9. Effects of combined magnesium delivery on hearing thresholds four days following acoustic overexposure.** Combined magnesium treatment (injections + diet) partially protect against the hearing deficits at 16 kHz (AOE: Blue,  $n = 10$ ; AOE-MgC: Cyan,  $n = 10$ ). \*  $P < 0.05$ , Unpaired T test.

In addition to the hearing thresholds recorded before the AOE protocol (day 0) and at day 4, recordings were also performed at day 90 after AOE (Fig. 3.10). Auditory brainstem response thresholds measured on day 90 in AOE group showed a partial recovery from  $87 \pm 1$  dB SPL (day 4 after AOE) to  $63 \pm 6$  dB SPL ( $n = 10$ ,  $P < 0.05$ , One way ANOVA, SNK tests, Fig 3.10A) at 16 kHz and from  $70 \pm 5$  dB SPL (day 4 after AOE) to  $55 \pm 4$  dB SPL by for BBN ( $P < 0.05$ , One way ANOVA, SNK tests Fig. 3.10A). In the AOE-MgC group, a partial recovery of the hearing thresholds was only observed for the BBN ( $n = 10$ ; Fig. 3.10B).

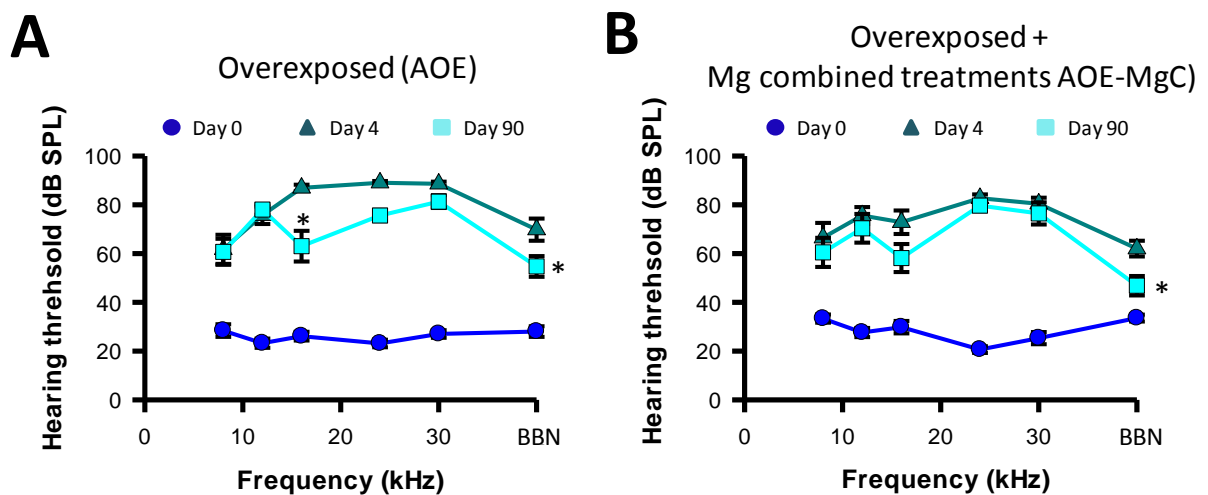


**Figure 3.10. Effects of combined magnesium treatment on hearing thresholds of rats at multiple time following acoustic overexposure.** Hearing thresholds at day 0, day 4, and day 90 were recorded in both the AOE ( $n = 10$ ) (A) and AOE-MgC ( $n = 10$ ) (B) groups. A partial recovery observed at day 90 at specific frequencies is denoted by \* ( $P < 0.05$ , One way ANOVA test SNK tests). Note that hearing thresholds measured 4 days after AOE were lower at 16 kHz in the AOE-MgC group.

Despite this, hearing thresholds measured at 16 kHz on day 90 were similar between the AOE and the AOE-MgC groups ( $P > 0.05$ , Unpaired T test).

### 3.2.5.2. Effects on gap detection

Prior to the experimental procedure, thirty three rats were selected based on their ability to detect silent gaps within a BBN background. Rats were then randomly assigned to groups to undergo the associated experimental procedure and gap detection tests were repeated every three weeks for the next twelve weeks, at multiple frequency backgrounds including BBN. Initial GDRs for BBN within the unexposed groups (Un and Un-MgC) were  $0.77 \pm 0.04$  ( $n = 7$ ) and  $0.81 \pm 0.04$  ( $n = 6$ ) respectively.

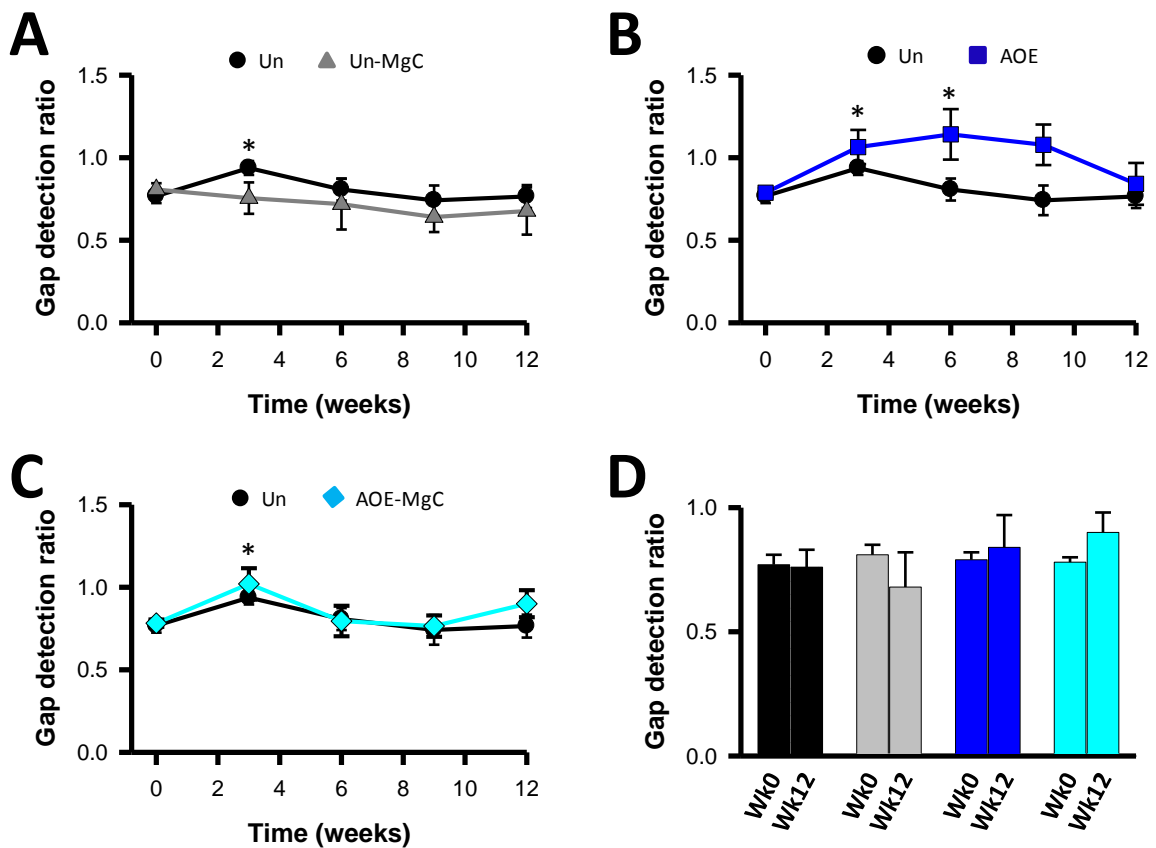


**Figure 3.11. Effects of combined magnesium delivery on the gap detection within a BBN background.** (A) Un-MgC rats did not exhibit an increased GDR at week 3 as witnessed in the Un group. (B) Increase of the GDR values at 3 weeks after AOE (reflecting an absence of gap detection) and recovery of the gap ratios at week 12. (C) Un and AOE-MgC increase of the GDR at weeks 3 post AOE and recovery of the GDR at week 6 through to week 12 (\*  $P < 0.05$  RM ANOVA on Ranks, SNK tests). (D) Similar GDRs for BBN between week 0 and 12 indicate that the recovery after AOE has been achieved by week 12. (Un: black,  $n = 7$ , Un-MgC: grey,  $n = 6$ ; AOE: blue,  $n = 10$ ; AOE-MgC: Cyan,  $n = 10$ ; Wilcoxon tests). Note that day 0 is the time before AOE for both groups.

Gap detection ratios in the Un group increased to  $0.94 \pm 0.04$  at week 3 ( $P < 0.05$ , RM ANOVA on Ranks, SNK tests; *Fig. 3.11A*) to then regain their initial values by week 12. There was no significant difference between the GDRs recorded at week 0 ( $0.77 \pm 0.04$ ) and week 12 ( $0.76 \pm 0.07$ ;  $P > 0.05$ , Wilcoxon tests; *Fig. 3.11D*). By contrast, GDRs in the Un-MgC remained unchanged at all time points including week 12 ( $0.67 \pm 0.14$ ; RM ANOVA on Ranks, SNK tests, *Fig. 3.11D*). Similar initial GDRs were obtained at week 0 for the BBN background from rats that were subsequently overexposed (AOE: $0.79 \pm 0.03$ ,  $n = 10$  and AOE-MgC: $0.78 \pm 0.02$ ,  $n = 10$ ,  $P > 0.05$ , Mann Whitney test). The GDR was significantly increased when measured 3 weeks after AOE in both the AOE ( $1.06 \pm 0.1$ ) and AOE-MgC group ( $1.02 \pm 0.09$ ,  $P < 0.05$ , RM ANOVA on Ranks, SNK tests; *Fig. 3.11B*). However by week 6, GDRs in the AOE-MgC group had recovered ( $0.79 \pm 0.09$ ; *Fig. 3.11C*, RM ANOVA on Ranks, SNK tests) in contrast to GDRs in the AOE group which remained elevated ( $1.14 \pm 0.15$ ; *Fig. 3.11C*, RM ANOVA on Ranks, SNK tests). By week 12, GDRs in both groups had recovered (*Fig. 3.11D*, RM ANOVA on Ranks, SNK tests) and were equal to GDRs measured prior to the AOE procedure ( $P > 0.05$ , Wilcoxon tests; *Fig. 3.11D*). As all GDRs in a BBN background recovered by week 12, tests were performed to identify changes in the GDR between week 0 and week 12 when silent gaps were imbedded in frequency specific backgrounds. Gap detection ratios for specific frequencies were first measured in the unexposed groups (Un and Un-MgC) and were shown to decrease between the two time points for frequencies tested between 8 to 24 kHz in both the Un and the Un-MgC groups ( $P < 0.05$ , Wilcoxon test; *Fig. 3.12*). None of these changes were detected for the AOE or the AOE-MgC groups ( $P > 0.05$ , Wilcoxon test; *Fig. 3.12*).

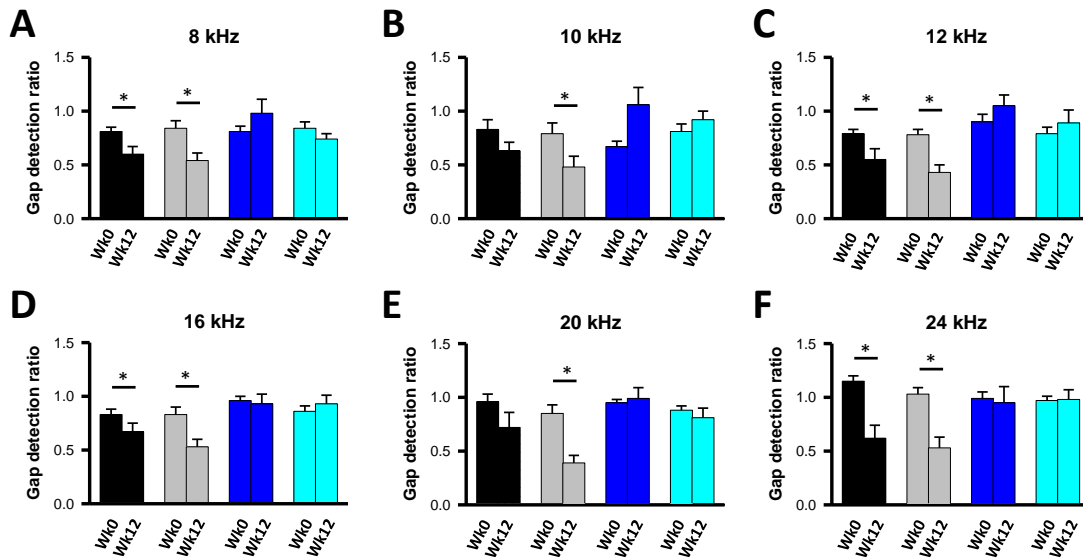


**Figure 3.12. Changes in GDRs overtime in all conditions and at various frequencies.** Between week 0 and week 12, a decreased GDR was exhibited in the Un and Un-MgC group at 8 kHz (A), in the Un-MgC group at 10 kHz (B), in the Un and Un-MgC groups at 12 kHz (C), in both groups at 16 kHz (D), in the Un-MgC group at 20 kHz (E) and in both the Un and Un-MgC groups at 24 kHz (F). ( $P < 0.05$ , Wilcoxon tests). There were no changes in the AOE and AOE-MgC GDRs between the two time points. Un: Black,  $n=7$ ; Un-MgC: Grey,  $n=6$ ; AOE: Blue,  $n=10$ ; AOE-MgC: Cyan,  $n=10$ .

However, when the GDR at week 12 was compared between all four groups, the GDR from the AOE group ( $n = 10$ ) was significantly higher at 12, 16 and 20 kHz whereas GDRs in the AOE-MgC group ( $n = 10$ ) were elevated at 16 and 24 kHz (One way ANOVA on Ranks; Fig. 3.13). The limited effects of MgC on the GDR deficits could be due to the fact that AOE induces tinnitus (i.e. GDR deficits) in about half of the rats exposed to loud sound (Turner et al., 2006, Wang et al., 2009). As such performing statistical tests with an averaged data set could mask any benefits conveyed by chronic magnesium supplementation. Therefore, a significant difference between startle amplitudes in presence and absence of the silent gap was tested for with each animal (Lobarinas et al., 2013). Significant differences between startle amplitudes were indicative of the rat's ability to discern the silent gaps imbedded in background sounds of specific frequencies (green squares indicating the absence of deficit, Fig. 3.14).

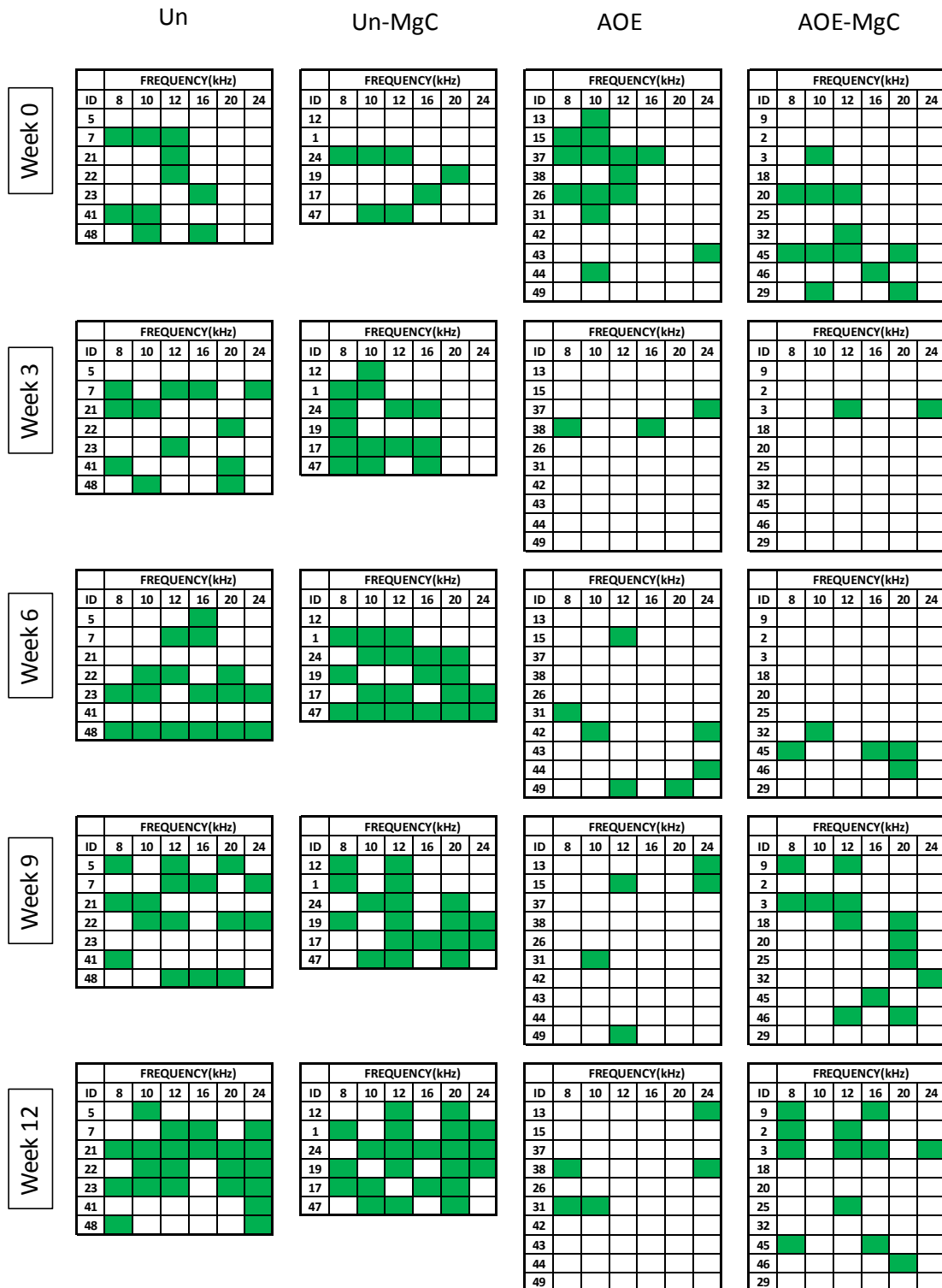


**Figure 3.14. Gap detection abilities and deficits expressed over time at various frequencies for each animal.** Each animal tested is identified by a number (ID) in the left hand column of every table. Green filled cells represent a significant GDR ( $P < 0.05$  Unpaired T test,) indicating that the animal was capable of detecting the silent gap whereas empty cells represent an inability to detect the silent gap. AOE was performed immediately after week 0.

It can be seen from *Fig. 3.14* that rats unexposed to sound (Un and Un-MgT group) exhibited a trend towards better gap detection with age. This is also represented in *Fig. 3.15* showing the average percentage of gap detection per animal as a function of time. A significant increase in the gap detection was achieved in the Un-MgC group from week 0 to week 12 ( $P < 0.05$ , RM ANOVA on Ranks, SNK test).

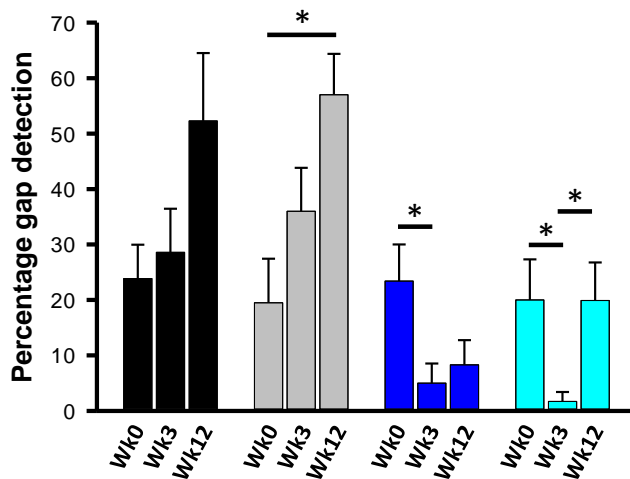


**Figure 3.15. Percentage of gap detection expressed over time per treatment group.** The percentages calculated for all frequencies (8, 10, 12, 16, 20 and 24 kHz) was deduced from the green filled cells represented in *Fig. 3.16*. (Un:black,  $n=7$ ; Un-MgC:grey,  $n=6$ ; AOE:blue,  $n=10$ ; AOE-MgC:cyan,  $n=10$ .  $*P < 0.05$  RM ANOVA on Ranks, SNK test). Note the increase of the gap detection over time in the Un-MgC condition, the decrease of the percentage of gap detection 3 weeks after AOE, in both AOE and AOE-MgC groups and the recovery of the gap detection deficit at week 12 in the AOE-MgC group only.

Acoustic overexposure performed shortly after week 0 decreased the ability of rats to detect the gaps (represented as a decreased percentage of gap detection per rat at week 3 in *Fig. 3.15*). This was true for both AOE and AOE-MgC groups ( $P < 0.05$ , RM ANOVA on Ranks, SNK tests). Decreased gap detection percentages were still observed at week 12 in the AOE group (represented as an absence of difference between week 3 and week 12). However, AOE rats that were treated with MgC had recovered their ability to detect gaps by week 12 (demonstrated as a percentage increase of the gap detection between week 3 and week 12, *Fig. 3.15*). Also by week 12, whereas all 10 rats in the AOE group exhibited a gap detection deficit at 12 and 16 kHz, 3 out of 10 rats in the AOE-MgC group did not exhibit such deficits (*Fig. 3.14*).

This further enforced the notion that animals in the AOEMgC group exhibited less behavioural evidence of tinnitus compared to animals in the AOE group. At this juncture, I then used the linear mixed model (LMM) analysis as an alternative to RM ANOVA. The LMM is considered an appropriate alternative when conducting a longitudinal study because it adjusts for the autocorrelation that is present when collecting data from the same subjects over a given time period while also allowing tests for complex interactions between multiple independent variables and the measured dependent variable (see section II.7). The LMM analysis revealed that the relationship between time (week 0 and week 12) and GDR at 8 kHz, 10 kHz and 20 kHz varied depending on the treatment group (*Table 3.4*;  $P < 0.05$ , LMM tests of fixed effects).

GDR 8kHz	Numerator df	Denominator df	F	Sig.
Intercept	1	18.890	757.337	.000
Group	3	18.897	.322	.809
Time	1	26.646	2.040	.165
Group * Time	3	26.635	5.331	.005

GDR 16kHz	Numerator df	Denominator df	F	Sig.
Intercept	1	1.401	846.227	.006
Group	3	32.169	1.415	.256
Time	1	11.014	3.408	.092
Group * Time	3	11.058	3.170	.067

GDR 10kHz	Numerator df	Denominator df	F	Sig.
Intercept	1	1.296	475.841	.013
Group	3		1.914	
Time	1	13.783	.003	.958
Group * Time	3	13.788	3.405	.048

GDR 20kHz	Numerator df	Denominator df	F	Sig.
Intercept	1	33.362	1082.086	.000
Group	3	33.382	.843	.480
Time	1	32.091	9.009	.005
Group * Time	3	32.087	5.648	.003

GDR 12kHz	Numerator df	Denominator df	F	Sig.
Intercept	1	.218	621.268	.367
Group	3		.743	
Time	1	.735	1.855	.457
Group * Time	3		4.527	

GDR 24kHz	Numerator df	Denominator df	F	Sig.
Intercept	1	.117	1739.109	.527
Group	3		3.420	
Time	1	3.847	12.193	.027
Group * Time	3	3.853	3.068	.158

**Figure 3.16.** Table summarising the effect of treatments on gap detection tests using LMM. Type III tests of fixed effects show a significant interaction (green filled cells,  $P < 0.05$ ) between treatment conditions (i.e. group) and time on the changes in GDR between week 0 and week 12 at specific frequencies.

Having identified the frequencies where interactions between group and time significantly correlated with changes in the GDR, I repeated the LMM analysis between the AOE and AOEMgC groups alone to test whether MgC treatment resulted in better GDRs. Tests reveal a significant difference between the AOE and AOEMgC groups at 8 kHz and 20 kHz (*Fig. 3.16*;  $P < 0.05$ , LMM pairwise comparison). In summary these data show that combined delivery of magnesium shortly after the AOE protocol and for a period of 3 months was able to decrease the gap detection deficits at select frequencies (8 kHz and 20 kHz).

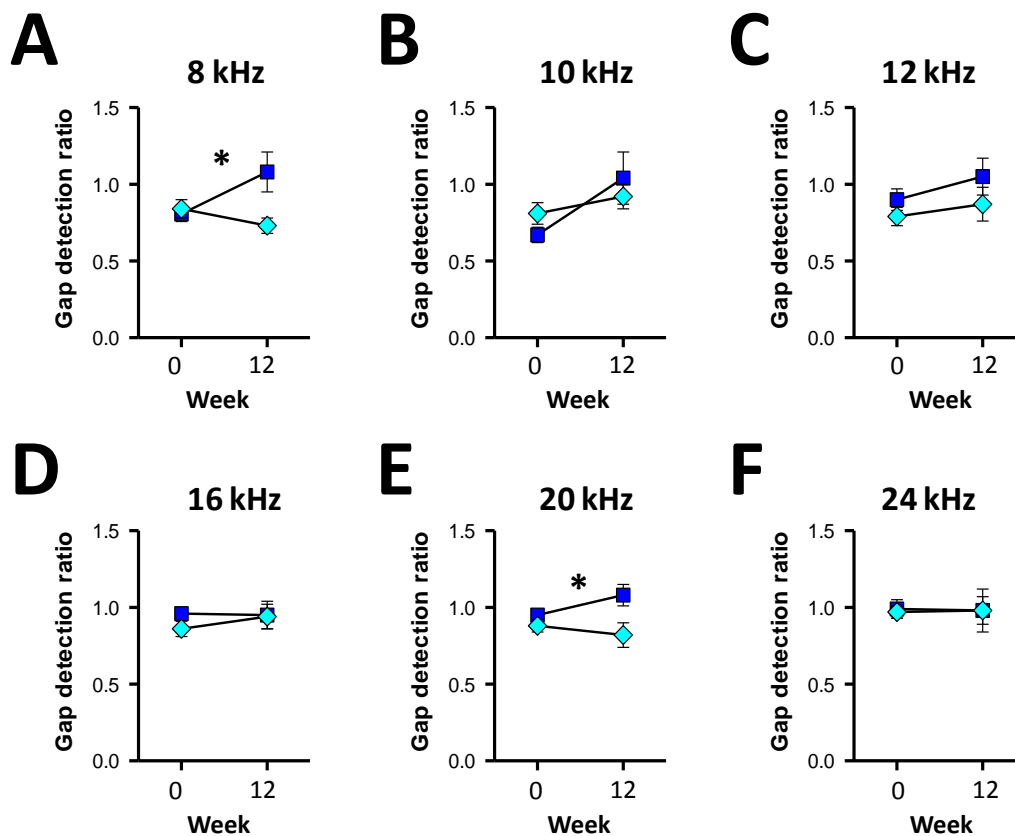


**Figure 3.17. Reduced gap detection deficits in AOEMgC rats.** Graphs show the relationship between GDRs recorded at week 0 before AOE and 12 weeks after AOE at frequencies between 8 – 24 kHz (A-F) in both the AOE (blue squares,  $n = 10$ ) and AOEMgC (cyan diamonds,  $n = 10$ ) groups. There is a significant difference between the AOE and AOEMgC populations at 8 kHz and 20 kHz ( $P < 0.05$ , LMM analysis, Pairwise comparison)

Lastly, it was important to show that differences in GDR between the two groups were not due to varying degree of hearing loss. Auditory brainstem responses recorded at week 12 (Fig. 3.10) show that there is no difference in the hearing thresholds between the groups at 8 kHz ( $P < 0.05$ , Mann Whitey test) and at frequencies adjacent to 20 kHz (i.e. 16 and 24 kHz;  $P < 0.05$ , Mann Whitney test). In addition, the ability or inability to detect gaps was uncorrelated with hearing threshold (Fig. 3.18).

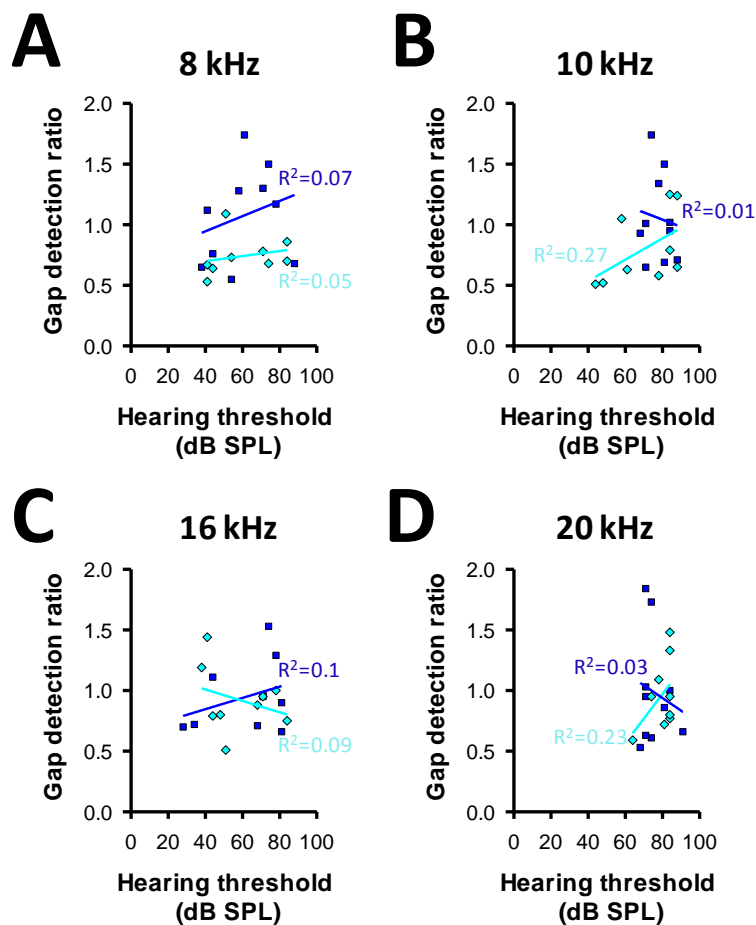


**Figure 3.18. Lack of correlation between hearing threshold and GDR.** Graphs show a lack of correlation between hearing threshold and GDR in both the AOE (blue squares) and AOEMgC groups (cyan diamonds) at 8 kHz (A), 10 kHz (B), 16 kHz (C) and 24 kHz (D).  $R^2$  values are shown on each graph.

In summary the inability to detect gaps at 12 weeks following AOE was not due to hearing loss and the protective effect of magnesium against AOE induced gap detection deficits was not due to the recovery from AOE induced hearing loss.

### **3.3. DISCUSSION**

#### **3.3.1. Gap detection deficits as a means to quantify tinnitus**

The earliest behavioural tests described for identifying animals with tinnitus were based on a conditional lick suppression method (Jastreboff et al., 1988). Animals were conditioned to elicit freezing behaviour during a silent period in a background noise. Following an AOE protocol, animals with tinnitus failed to elicit a freezing behaviour during silent periods. However, tinnitus perception has been linked to the amygdala which also mediates the freezing behaviour and as such could introduce errors in interpreting of freezing behaviour as a result of tinnitus perception (De Ridder et al., 2006, Moller, 2007). Therefore future conditioning tests required animals to elicit an active behaviour in response to sound or silence. Such elicited behaviour have included jumping onto a pole (Guitton et al., 2003), accessing a reward (Ruttiger et al., 2003) and decisions when navigating a T-maze platform (Guitton and Dudai 2007). These new methods were considered an improvement on the first described method. The method of gap detection used in this study is based on the acoustic startle reflex instead. This method was chosen because it is easier to implement and does not require months of training (Turner et al., 2006). This made it a suitable method to use in this study because the young age at which testing begun would not allow for months of behavioural training. The method is not without its flaws as there are some restrictions and variations in how the data can be obtained and interpreted. Firstly the sequence of presenting trials where a startle stimulus was preceded or not by a silent gap must be pseudo randomly generated so the animal does not learn the sequence of presentations. In addition a variable inter-trial interval must be used so the animal does not anticipate the next startle stimulus based on timing intervals. The gap

detection tests at each frequency lasted 10 to 12 mins dependent on the inter-trial intervals. Running multiple frequencies raises the chances of an animal losing attention and failing to respond to the startle stimulus regardless of a preceding silent gap or no silent gap. Other researchers have worked around this problem by reducing the inter-trial intervals (Turner et al., 2012). However this also raises the chances of the animal predicting the timing intervals between startle stimuli due to shorter intervals.

### **3.3.2. Age related changes to hearing loss and gap detection**

Gap detection tests are classically used to investigate age related changes in temporal processing which follows a bell curve, i.e. during development, animals' exhibit better temporal acuity and gap detection which then deteriorates in old age at the onset of presbycusis (Mendelson and Ricketts, 2001, Friedman et al., 2004). Unexposed rats (Un and Un-MgC) exhibited an age dependent decrease in the GDR which was evident at multiple frequency backgrounds between week 0 when rats were aged about 21 days and week 12. This developmental increase in gap detection has previously been shown (Friedman et al., 2004) and is an indication of the continuous development of the auditory system between the time points at which tests were performed (Rubel and Fritsch, 2002, Friedman et al., 2004). In addition, performing the final set of ABR recordings at week 12 revealed that unexposed rats exhibit minor age dependent increases in the hearing threshold at specific frequencies. These findings suggest an age related hearing loss (presbycusis) which triggers auditory system dysfunction in multiple central structures along the auditory pathway, including the DCN where the maximum discharge rate of fusiform cells is increased (Banay-Schwartz et al., 1989) and in the IC and AC where temporal processing is lost (Shaddock Palombi et al., 2001,

Mendelson and Ricketts, 2001). All these deficits are believed to stem from a loss of peripheral inputs due to deafferentation and the irreplaceable loss of hair cells which typically leads to an increase in the hearing thresholds (Frisina, 2001, Caspary et al., 2008, Kujawa and Liberman, 2009). In addition, a decreased inhibitory transmission could trigger homeostatic plastic adjustments across the auditory system (Caspary et al., 2008) leading to further loss in the temporal processing which could manifest itself as gap detection deficits (Willott et al., 1991, Strouse et al., 1998, Ison and Allen, 2003). However, presbycusis in Wistar rats is normally studied when animals are aged 24 months and over (Derin et al., 2004, Chen et al., 2012) suggesting that the rats used in this study (aged 4 months) were far too young to have presbycusis. Furthermore, the fact that not all rats exhibited significant gap detection should not be linked to presbycusis as it is more likely a result of commonly reported false negatives in gap detection (Turner et al., 2006, Engineer et al., 2011). The apparent trend of rats in the Un-MgC group to exhibit better GDRs than rats in the Un group could be due to MgC accelerating the age dependent improvements in gap detection (Friedman et al., 2004). Previous studies have reported that the NMDA receptor NR2A/NR2B subunit expression ratio increases with development (Molnar et al., 2002, Hogsden and Dringenberg, 2009, Cui et al., 2009). The NR2B subunits are also known to mediate prolonged synaptic responses which could restrict the rapid temporal processing required for efficient gap detection (Sun et al., 2011, Zorumski and Izumi, 2012). The reduced action of NMDA receptors containing the NR2B subunit in the Un-MgC rats could therefore be responsible for the increased temporal processing which allows better gap detection (Zorumski and Izumi, 2012).

### **3.3.3. Induction of hearing loss and gap detection deficits**

Acoustic overexposure is followed by an immediate increase in the hearing threshold, the degree of which has been shown to be dependent on the intensity and duration of the AOE protocol used (Nordmann et al., 2000). These factors in addition to the type of exposure (i.e. unilateral or bilateral) also contribute towards determining whether the AOE induces a permanent or temporary threshold shift (Nordmann et al., 2000). In my model, 3 to 5 days following AOE, rats exhibited a significantly elevated hearing threshold at multiple frequencies and 90 days later there was only a partial recovery at 16 kHz and in response to BBN. This suggests a more permanent shift in the hearing threshold at the other frequencies tested. A higher degree of recovery from hearing loss has previously been reported in this lab when the AOE protocol was carried out over 2 rather than 3 days as performed here (Pilati et al., 2012a). This supports our current understanding that duration of the AOE protocol contributes towards triggering a temporary or permanent hearing threshold shift. It is therefore possible that performing the AOE protocol over 3 days induced damage associated to permanent shifts in the hearing threshold such as OHC stereocilia damage (Slepecky et al., 1982), loss of OHCs (Liberman and Beil, 1979) and/or fusion of IHC stereocilia (Mulroy and Curley, 1982).

In addition to shifts in the hearing thresholds, all overexposed rats exhibited decreased startle reflex amplitudes and gap detection deficits in at multiple frequencies tested. Gap detection deficits represent the inability to detect short periods of silent gaps imbedded in a background sound. In mature animals with a fully developed temporal processing, gap detection deficits are used as a tool to identify animals with tinnitus

due to a masking of the silent gap by the inherent tinnitus perception (Zeng et al., 2005, Turner et al., 2006, Wang et al., 2009, Dehmel et al., 2012a, Turner et al., 2012). In this study, a gap detection deficit was initially described as having a GDR above 0.85. The arbitrary value chosen for this study was higher than values previously used by other researchers (Turner et al., 2006) because my study began when rats were still of a young age (P 21) and yet to develop the full complement of temporal processing necessary for better gap detection (Friedman et al., 2004). Such developmental changes include the refinement of excitatory responses (Chang et al., 2005), maturation of inhibitory neurotransmission (Kotak et al., 2008, Dornn et al., 2010) and a decrease in NR2B subunits expression which is associated with high levels of plasticity (Cui et al., 2009, Hogsden and Dringenberg, 2009, Sun et al., 2011). This presented difficulties when interpreting data measured after AOE because GDRs obtained before AOE were not representative of a fully developed animal. It is for this reason that significant gap detection by individual rats at week 12 of tests was also identified. This was measured as a significant difference in the startle reflex amplitude elicited when the startle stimulus was preceded or not preceded by a silent gap. Taking this approach helped identify rats with intact temporal processing at specific frequencies independently of development or of the arbitrary gap detection value initially used to screen rats. It was also used as a measure to highlight the therapeutic benefits of MgC against the development of tinnitus.

In addition to tinnitus, AOE can also trigger hearing loss and hyperacusis (over sensitivity to sound) (Nelson and Chen, 2004). There was a need to differentiate these deficits when using the gap detection tests because previous studies have performed

gap detection tests when animals had recovered from hearing to ensure that animals could perceive the background tone within which the silent gap would be embedded (Turner et al., 2006, Wang et al., 2009, Engineer et al., 2011, Dehmel et al., 2012a). In my study, rats exhibited permanent threshold shifts, however the recovery of ABR responses to BBN stimulus suggests animals maintained some hearing ability across multiple frequencies. In addition there was no correlation between gap detection deficits and ABR thresholds at specific frequencies. Interestingly some rats with ABR thresholds above 60 dB SPL exhibited significant gap detection ability. This lends support to previous reports showing that sound stimulation which did not elicit any recordable ABR peaks could still elicit activity in the auditory cortex related to sound processing such as gap detection (Engineer et al., 2011). Altogether this suggests that gap detection deficits were not a result of hearing loss. Another factor which could prevent the direct interpretation of gap detection deficits as tinnitus is hyperacusis. The startle reflex amplitude is directly correlated to the amplitude of the startle stimulus, therefore when the startle stimulus is presented with no gap, animals with hyperacusis will startle with higher amplitudes compared to animals without hyperacusis (Engineer et al., 2011, Eggermont, 2013). By comparing the startle response amplitudes between the unexposed and overexposed groups, I was able to confirm that none of the overexposed rats suffered from hyperacusis (Appendix 3). On the contrary, overexposed rats exhibited lower startle response amplitudes, in accordance with previous reports (Engineer et al., 2011, Eggermont, 2013). Overexposed animals will exhibit lower startle response amplitudes because the startle stimulus will be perceived as of lower intensity (Lobarinas et al., 2013). Although this could present a problem in the data collection and analysis, the sensitivity of the

platform on which the animals were tested ensured that startle reflexes of low amplitude could still be recorded and comparisons made to identify effects of silent gap presentation on the subsequently evoked startle reflex. In addition, the short time window (250 ms) after the startle stimulus during which motion within the enclosure was recorded, maximised the chances of recording motion elicited by the startle stimulus (i.e. the startle reflex) and not random motions.

#### **3.3.4. *In vitro* markers of tinnitus**

Acoustic overexposure induced deficits were identified both *in vivo* and *in vitro* as part of this study. *In vivo* markers included an increase in the hearing threshold and gap detection deficits. *In vitro* markers included an increase in the release probability of DCN multisensory inputs, a decrease in the AN conduction velocity and a decreased number of AN release sites onto fusiform cells in the DCN. In an attempt to identify *in vivo* methods of reversing these *in vitro* deficits, emphasis was placed on the multisensory pathway because of its plastic nature. Short term Mg<sup>2+</sup> injections reduced the AOE-induced deficits to the hearing threshold but had no effect on the central deficits which were principally due to an increase in release probability. On the other hand, a 4 week MgT diet had no effect on the AOE-induced deficits to the hearing threshold but reversed the lack of LTP induction in the DCN attributed to an increased release probability. This suggests that a 4 week MgT diet was capable of preventing the AOE-induced increase in release probability at DCN synapses. In line with the tinnitus induction model of a peripheral deficit which is consolidated centrally (Guitton and Dudai, 2007, Norena and Farley, 2013), a combined approach presented the best chance to reduce the behavioural manifestations of tinnitus. The combined

magnesium treatment (short term  $Mg^{2+}$  injections and long term MgT supplements) was shown capable of reducing the increase in hearing threshold and the behavioural evidence of tinnitus, supporting previous reports that long term administration of magnesium after AOE attenuated hearing loss (Abaamrane et al., 2009). The exact mechanisms by which magnesium conveys this protection is unknown due to its multiple effects. In particular, magnesium acting as a calcium antagonist could limit excessive calcium release leading to excitotoxic or ischaemic damage (Haupt and Scheibe, 2002). Magnesium also associates with reactive oxygen species which are implicated in mediating hair cell death following AOE (Henderson et al., 2006). Another important mechanism by which magnesium acts is by blocking NMDA receptors (Nowak et al., 1984, Dubray et al., 1997, Yi et al., 2013). Interestingly blocking NMDA receptors using the NMDA receptor antagonist MK-801 protects against AOE induced hearing loss (Chen et al., 2001) similar to the protective effects achieved by magnesium (Abaamrane et al., 2009). In addition, blocking NR2B subunits of NMDA receptors in the cochlea prevents the behavioural manifestations of tinnitus induced by AOE (Guitton and Dudai, 2007). A previous study has shown that elevating brain magnesium with MgT also acted via the NR2B subunit of NMDA receptors (Abumaria et al., 2011). However, the effect of magnesium promoting plasticity was specific to the prefrontal cortex despite elevated levels also in the lateral amygdale, suggesting variations in the response of specific brain regions to elevated magnesium (Abumaria et al., 2011). It is unknown whether the combined use of  $MgCl_2$  injections and magnesium threonate diet also elevated the concentration of magnesium within the DCN or other auditory structures as tests to directly measure this were not performed in this study. However, in conjunction with other reports mentioned above, the

effects of the combined magnesium treatment used here could be via a reduction in NMDA receptor mediated activity.

Despite what appears to be a central effect of the magnesium threonate diet, it cannot be ignored that the tinnitus amelioration is simply a consequence of the otoprotective effect of the  $\text{MgCl}_2$  injections which forms part of the MgC treatment. Indeed, blockade of cochlear NMDA receptors during a brief time window has been shown to have otoprotective as well as tinnitus ameliorative effects (Guitton and Dudai, 2007). However the lack of correlation between the hearing threshold and GDR in my model suggests dissociation between hearing threshold and tinnitus development. Furthermore, the otoprotective effects of MgC was evident at 16 kHz only whereas the tinnitus ameliorative effects was evident at 8 kHz and 20 kHz. Further studies to differentiate the degree of hearing loss from tinnitus development will require gap detection tests to be performed on AOE animals that received either  $\text{MgCl}_2$  injections or MgT diet rather than the combined MgC treatment.

### 3.4. CONCLUSION

The first two chapters of this study identified *in vitro* markers representing AOE-induced deficits and *in vitro* methods of reversing these identified deficits. Particularly AOE was shown to increase the release probability at DCN parallel fibre synapse which prevented the induction of LTP. *In vitro* manipulations that reduced the release probability were shown capable of reversing this deficit. The work reported in this chapter has also identified *in vivo* interventions capable of promoting the induction of LTP *in vitro* most likely via the same mechanism previously identified i.e. reversing the increase in release probability induced by AOE. These interventions were also shown capable of reducing the behavioural evidence of tinnitus measured as gap detection deficits. In conclusion, this study has provided an *in vitro* marker of tinnitus which sheds light on the mechanisms of synaptic plasticity which precede the onset of tinnitus. It has also provided treatment possibilities involving compounds which decrease release probability to alleviate the tinnitus perception.

# DISCUSSION

Many studies have implicated the DCN as a possible source of the tinnitus generating signal and throughout this study I have provided evidence which lends support to this. I have shown that 3 to 5 days after AOE when there is hearing loss, there is also a decreased AN CAP, a decreased AN action potential conduction velocity and finally a decreased number of release sites at AN synapse onto fusiform cells. A decreased CAP and conduction velocity can be linked to deficits in the AN fibre recruitment, temporal acuity and fusiform cell firing rate which has previously been shown as a consequence of AOE (Salvi et al., 2000, Pilati et al., 2012a). Most importantly, the decrease in the number of release sites could represent the period of sensory deprivation which has been proposed to trigger all other subsequent changes in the DCN, the IC and the AC associated with tinnitus (Norena, 2011). Sensory deprivation has been shown to trigger an increase in both the stimulus driven and spontaneous activity in the VCN (Sumner et al., 2005, Cai et al., 2009), the DCN (Brozoski et al., 2002, Kaltenbach et al., 2005), the IC (Salvi et al., 1990, Ma et al., 2006) and the AC (Eggermont, 2008, Norena et al., 2010). In each of these structures, the increase in spontaneous activity occurs at different time points after AOE. Spontaneous activity increases after a few hours in the AC (Norena and Eggermont, 2003), after 2 to 5 days in the DCN (Kaltenbach et al., 2000) and up to a week in the IC (Ma et al., 2006). Sensory deprivation has also been shown to trigger structural plasticity in the form of cortical map reorganisation (Norena and Eggermont, 2005) and homeostatic plasticity in the form of synaptic scaling of various structures along the auditory pathway including the DCN (Oleskevich and Walmsley, 2002, Caspary et al., 2008, Whiting et al., 2009). In the visual system, sensory deprivation can trigger metaplasticity which is dependent on the modulation of the NR2A/NR2B composition ratio of NMDA receptors (Quinlan et al., 1999, Philpot

et al., 2003). This is the first study to show that in the auditory system, a sensory deprivation like phenomenon (i.e. hearing loss) also triggers metaplasticity in the DCN. The decrease in AN inputs reported here could lead to an increase in the release probability at the multisensory parallel fibre inputs which in turn dictates the induction or lack thereof of LTP. The increase in release probability also reported here could also represent the underlying mechanism behind the increase in DCN responses to trigeminal stimulation (Shore et al., 2008, Zeng et al., 2009) and the somatosensory enhancement of sound evoked responses in animals with tinnitus (Dehmel et al., 2012b). As the DCN is the first site of integration between auditory and non-auditory inputs, an increase in the release probability at the multisensory inputs could also be interpreted in light of homeostatic plasticity. That is to say, an increase in the activity of non-auditory inputs compensating for the decrease in auditory inputs to maintain mean neural activity of the DCN around a set level. This enhancement of cross modal interactions in the DCN could also account for types of tinnitus which can be induced or manipulated by head or neck movements (Levine et al., 2003). My results also support the previously suggested role of NMDA receptors in mediating the effects of AOE leading to tinnitus (Guitton and Dudai, 2007, Zheng et al., 2012). The increase of release probability which resulted in a lack of LTP induction could be reversed when LTP induction was performed in the presence of D-AP5 or when rats received a combined treatment of MgCl<sub>2</sub> injections and an elevated magnesium diet prior to commencing *in vitro* studies. Moreover, rats that received this combined treatment recovered faster from AOE-induced hearing loss at specific frequencies in addition to fewer rats developing behavioural evidence of tinnitus. Based on previously available reports and the evidence gathered in this study, AOE could damage the hair cells and

alter AN myelin domains leading to a decrease in sound evoked activity in the DCN and sensory deprivation (Salvi et al., 2000, Nordmann et al., 2000, El-Badry et al., 2007). Over the next 3 - 5 days the release probability at multisensory parallel fibres increased, possibly to compensate for the decrease in AN inputs (homeostatic plasticity). This increase in release probability also shifted the LTP induction threshold preventing HFS from inducing LTP (metaplasticity). Over the following weeks, continuous action of NMDA receptors could facilitate the prolonged calcium influx required to consolidate the altered neural activity. Tinnitus could therefore arise as a consequence of the compensatory mechanisms for the loss of AN inputs and the amplification of spared inputs/non-auditory signals. Mechanisms to treat tinnitus should therefore be aimed at limiting the initial excitotoxic damage which leads to the sensory deprivation (Guitton and Dudai, 2007) or limiting the homeostatic plasticity and metaplasticity which subsequently alters the neuronal firing patterns along the auditory pathway (as reported here).

My research has provided new insights into the AOE induced deficits that occur when there is hearing loss and a decrease in DCN fusiform cell excitability. Due to the plastic nature of the deficits identified, these deficits could possibly underlie the subsequent increase in DCN excitability which has been correlated with tinnitus. In addition, the use of the MgC treatment suggests that the continuous action of NMDA receptors is required to mediate the deficits in plasticity induction and the subsequent development of tinnitus which was evidenced by a decreased number of rats developing tinnitus once placed on the MgC diet.

Currently there are other models of tinnitus which reverse altered neural activity in a bid to identify therapeutic treatments that could be used to treat tinnitus. For example regular auditory frequency discrimination tests designed to induce cortical map reorganisation in human subjects was shown to reduce the severity of tinnitus (Flor et al., 2004). The tests assume that neurons that generate tinnitus at a specific frequency can be recruited to the network of neurons responsible for frequency discrimination at neighbouring frequencies of the tinnitus perception and by doing so, inhibit tinnitus perception by reducing the number of neurons responsible for the tinnitus signal (Recanzone et al., 1993, Flor et al., 2004). Electrical stimulation of the DCN surface has also been shown to decrease the perception of tinnitus with various degrees of success (Herraiz et al., 2007). In addition, ablation of the DCN has been shown to reduce hyperactivity in the contralateral IC which is also a correlate of tinnitus (Manzoor et al., 2012). However this finding serves more to highlight the pivotal role of the DCN in tinnitus development as DCN ablation may present a different set of complications in relation to retrieving positional information from auditory signals. Other studies take an alternate approach and investigate the use of drugs as a means of treating tinnitus. For example, the use of memantine has been shown to reduce chronic tinnitus in rats 2 months after AOE (16 kHz, 110 dB SPL, 1h) (Zheng et al., 2012). However other studies into salicylate induced tinnitus (Lobarinas et al., 2006) and human clinical trials (Figueiredo et al., 2008) report contradictory results. More importantly these results highlight the need for drug induced tinnitus and AOE induced tinnitus to be studied separately as the underlying mechanisms differ (Eggermont and Roberts, 2004, Kaltenbach, 2006, Roberts et al., 2010). Blocking NMDA receptor activity remains an attractive model as has been shown here in this study and in a previous report where

it was shown that blocking cochlear NMDA receptors within a short time window after AOE can reduce the onset of tinnitus (Guitton and Dudai, 2007). Another study reported hyperactivity in the fusiform cells of hamsters which correlated with tinnitus and could be suppressed by application of the cholinergic agonist; carbachol onto the DCN surface (Manzoor et al., 2013). Interestingly in another model where behavioural evidence of tinnitus was recorded in rats 4 to 11 weeks after AOE, vagus nerve stimulation (which is cholinergic in nature at DCN synapses) was capable of alleviating tinnitus perception (Engineer et al., 2011). Although the mechanism by which this effect is mediated remains unknown, this finding provides support that enhancing cholinergic inputs in the DCN could present a drug useful target.

In addition to the *in vivo* models described above there are also *in vitro* models that mimic the hyperactivity identified in the AC (Wu et al., 2011). It has been proposed that making use of these *in vitro* models will allow the rapid screening of current clinically approved drugs which could have the added benefit of alleviating tinnitus perception (Wu et al., 2011). Some of the potential drugs which have been tested include linopiridine which is a potassium channel blocker, pregabalin which is a calcium channel antagonist and gabapentin which is a GABA analogue (Wu et al., 2011). However the effective dosage at which these drugs convey benefits against tinnitus also triggers unwanted side effects (Darlington and Smith, 2007).

Despite these findings, some questions remain unanswered which could potentially consolidate the work done in this study and further advance the understanding of tinnitus development. Firstly it will be of interest to perform imaging studies to identify any changes in the NMDA receptor subtypes or expression following AOE. Indeed the

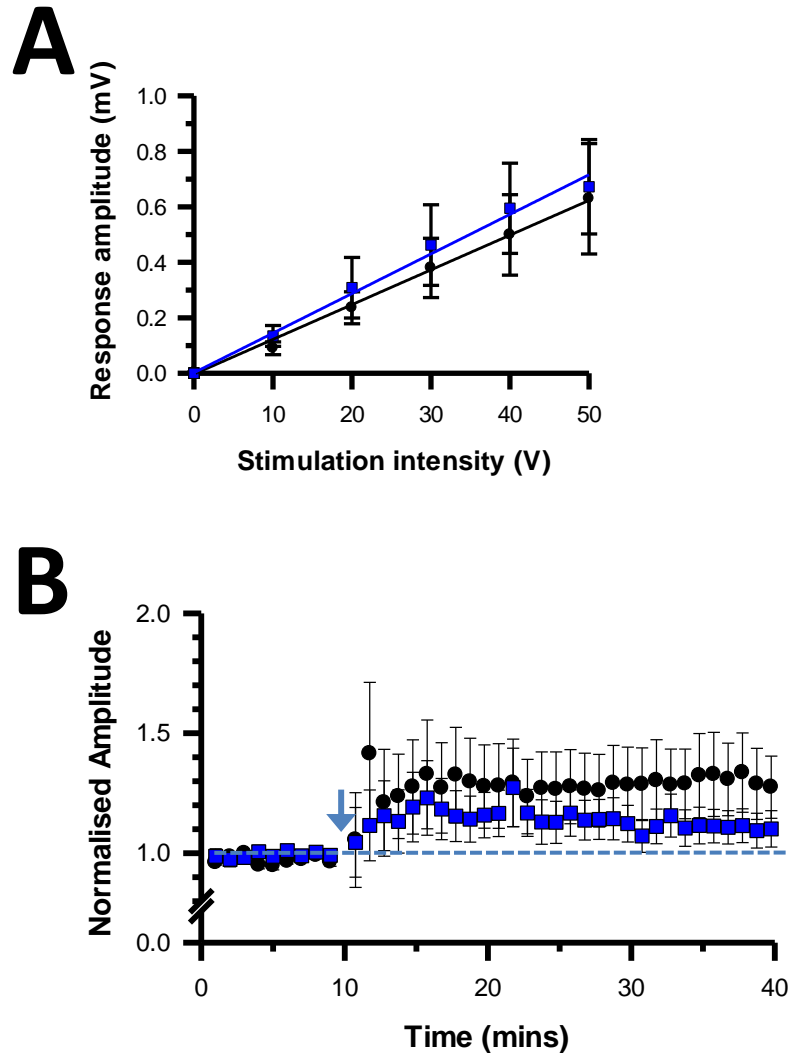
NR2B subtype is highly expressed during development and promotes plasticity in multiple brain structures (Sun et al., 2011, Zorumski and Izumi, 2012). A differential expression in this receptor subtype could therefore mediate metaplastic changes identified here. It will also be of interest to investigate the state of the DCN synapses in overexposed rats that exhibited behavioural evidence of tinnitus and rats that were placed on the MgC diet. Whole cell recordings of EPSCs or cell attached recordings could provide insight into the rates of spontaneous activity from which information about release probability could be deduced.

Lastly it will be of interest to expand the current model of investigation. Rather than performing experiments using juvenile rats, AOE could be performed in adult rats instead. This will allow better GDRs to be recorded prior to the AOE and will help exclude the development of the auditory system when interpreting results.

In conclusion, the findings presented in this thesis represent a step in the direction of identifying changes that occur following AOE-induced hearing loss leading to tinnitus. This makes it essential for the research into early synaptic changes in the DCN to be carried on beyond the scope covered in this project.

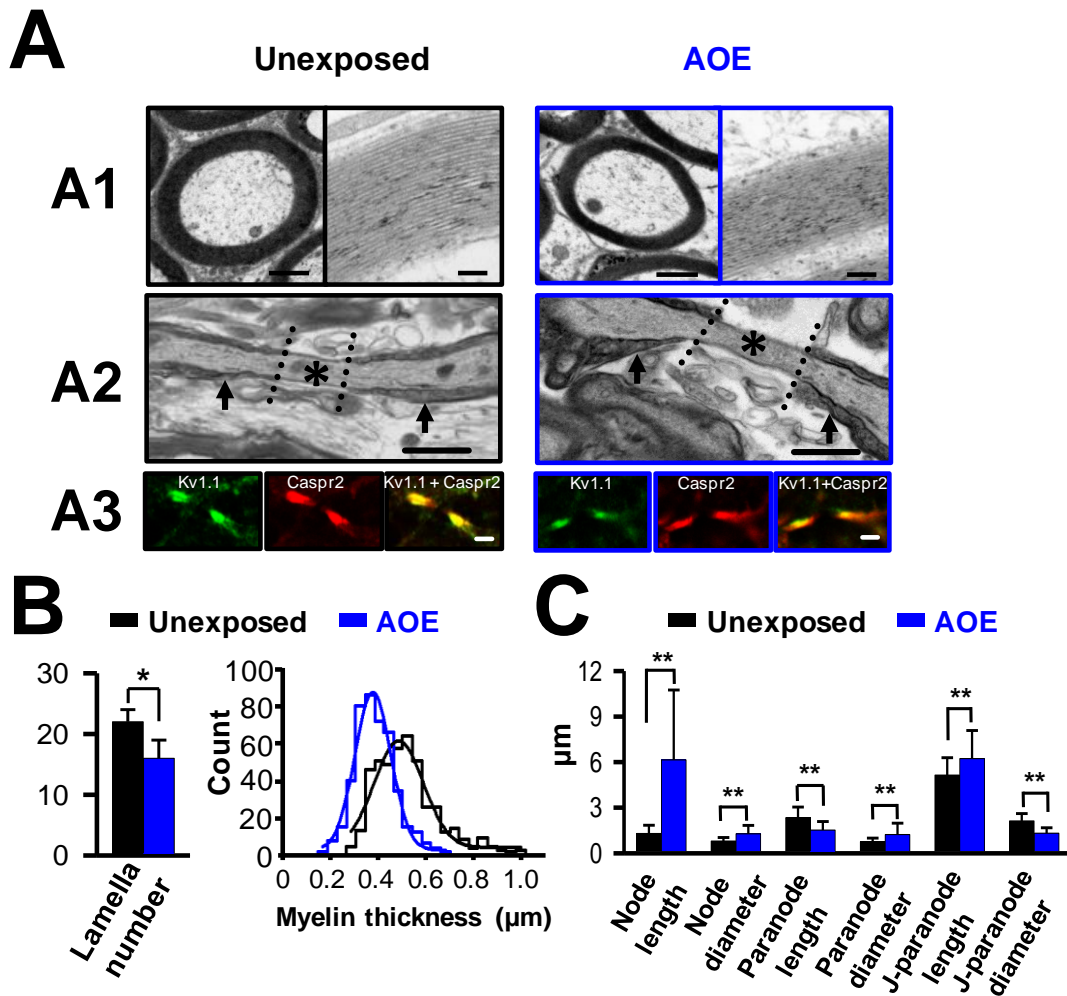
## APPENDICES

### Appendix 1.

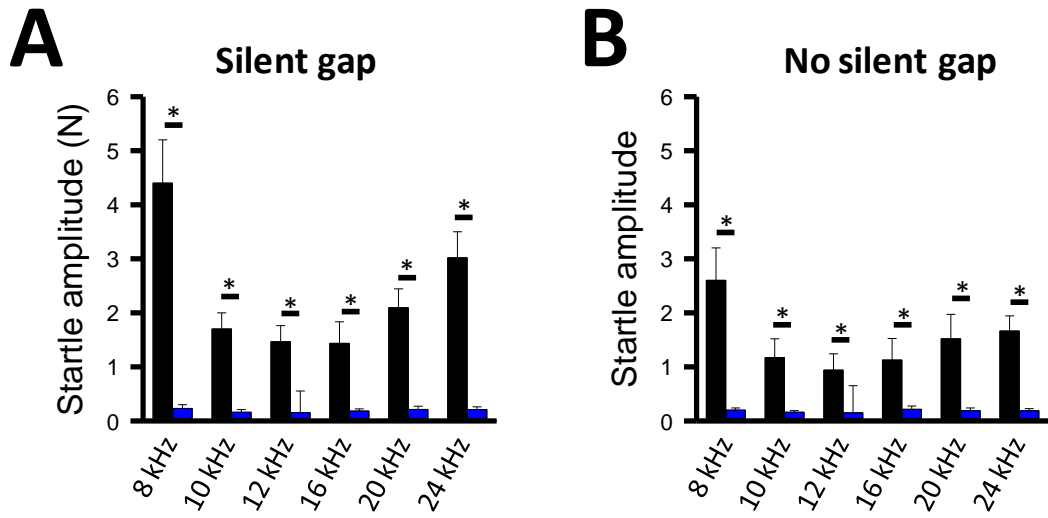


**Alternative measurements for the N1 amplitude (A)** The N1 amplitude was measured from the baseline pre-artefact of stimulation to the peak of the N1 deflection. Mean amplitudes recorded in response to graded stimulation intensities in both the unexposed (black circles,  $n=11$ ) and overexposed (blue squares,  $n=9$ ) condition. **(B)** The effect of HFS on N1 amplitudes was determined by measuring the N1 amplitude using the alternative method described. Graph showing N1 amplitudes normalised to the average of the last 5 minutes of baseline recording and plotted against time in both conditions (unexposed, black circles,  $n=16$ ; overexposed, blue squares,  $n=20$ ). The time of HFS is indicated by the arrow. Thirty minutes after HFS, the N1 amplitudes recorded in the unexposed condition was potentiated ( $P < 0.05$ , Wilcoxon test) whereas that recorded in the overexposed condition remained unchanged.

Appendix 2.



**Effects of acoustic overexposure on auditory nerve morphology.** (A) Electron microscopy showing that AOE decreases the myelin thickness (A1), elongates the node of Ranvier (A2 asterisks between the dotted lines) and increases the diameter of the paranodes (A2, arrows). (A3) Double immunolabelling of Kv1.1 (green) and Caspr2 (red) show an elongation and a decreased width of the juxtaparanodes after AOE. Scale bar (A1) left: 1  $\mu\text{m}$ , (A1) right: 100nm; (2): 1  $\mu\text{m}$ , (A3) 2  $\mu\text{m}$ . (B) AOE decreases the myelin lamella number (left) and the Gaussian distribution of myelin thickness is shifted to the left (right) ( $n = 450$  axons from 18 sections (3 rats, 3 litters) each, unpaired  $t$  test  $P = 1.1e^{-62}$ ,  $t(898)=18.1$ ). (C) Summary histograms showing the properties of the nodes, the paranodes and the juxtaparanodes in unexposed and AOE rats (\*\*  $P < 0.01$ , Unpaired  $T$  tests). Courtesy of Matt Barker.



**Attenuation of the startle reflex amplitude following acoustic overexposure.** Amplitude of the startle reflex elicited by animals (Unexposed: black,  $n = 7$ ; AOE: blue,  $n = 10$ ) 12 weeks after testing began. The startle stimulus was a 20 ms 110 dB SPL BBN sound presented in a background sound of the various frequencies indicated. A silent gap **(A)** or no silent gap **(B)** preceded the startle stimulus. (\*  $P < 0.05$ , Unpaired T test)

## REFERENCES

- ABAAMRANE, L., RAFFIN, F., GAL, M., AVAN, P. & SENDOWSKI, I. 2009. Long-term administration of magnesium after acoustic trauma caused by gunshot noise in guinea pigs. *Hear Res*, 247, 137-45.
- ABBOTT, L. F. & REGEHR, W. G. 2004. Synaptic computation. *Nature*, 431, 796-803.
- ABRAHAM, W. C. & BEAR, M. F. 1996. Metaplasticity: the plasticity of synaptic plasticity. *Trends Neurosci*, 19, 126-30.
- ABUMARIA, N., YIN, B., ZHANG, L., LI, X. Y., CHEN, T., DESCALZI, G., ZHAO, L., AHN, M., LUO, L., RAN, C., ZHUO, M. & LIU, G. 2011. Effects of elevation of brain magnesium on fear conditioning, fear extinction, and synaptic plasticity in the infralimbic prefrontal cortex and lateral amygdala. *J Neurosci*, 31, 14871-81.
- ADAMS, J. C. 1979. Ascending projections to the inferior colliculus. *J Comp Neurol*, 183, 519-38.
- ADAMS, J. C. & WARR, W. B. 1976. Origins of axons in the cat's acoustic striae determined by injection of horseradish peroxidase into severed tracts. *J Comp Neurol*, 170, 107-21.
- AGHAJANIAN, G. K. & RASMUSSEN, K. 1989. Intracellular studies in the facial nucleus illustrating a simple new method for obtaining viable motoneurons in adult rat brain slices. *Synapse*, 3, 331-8.
- BABALIAN, A. L. 2005. Synaptic influences of pontine nuclei on cochlear nucleus cells. *Exp Brain Res*, 167, 451-7.
- BABALIAN, A. L., RYUGO, D. K. & ROUILLER, E. M. 2003. Discharge properties of identified cochlear nucleus neurons and auditory nerve fibers in response to repetitive electrical stimulation of the auditory nerve. *Exp Brain Res*, 153, 452-60.
- BANAY-SCHWARTZ, M., LAJTHA, A. & PALKOVITS, M. 1989. Changes with aging in the levels of amino acids in rat CNS structural elements. I. Glutamate and related amino acids. *Neurochem Res*, 14, 555-62.
- BARKER, M., SOLINSKI, H. J., HASHIMOTO, H., TAGOE, T., PILATI, N. & HAMANN, M. 2012. Acoustic overexposure increases the expression of VGLUT-2 mediated projections from the lateral vestibular nucleus to the dorsal cochlear nucleus. *PLoS One*, 7, e35955.
- BAUER, C. A., BROZOSKI, T. J., ROJAS, R., BOLEY, J. & WYDER, M. 1999. Behavioral model of chronic tinnitus in rats. *Otolaryngol Head Neck Surg*, 121, 457-62.
- BEAR, M. F., COOPER, L. N. & EBNER, F. F. 1987. A physiological basis for a theory of synapse modification. *Science*, 237, 42-8.
- BELLI, S., BELLI, H., BAHCEBASI, T., OZCETIN, A., ALPAY, E. & ERTEM, U. 2008. Assessment of psychopathological aspects and psychiatric comorbidities in patients affected by tinnitus. *Eur Arch Otorhinolaryngol*, 265, 279-85.

- BERGLUND, A. M. & RYUGO, D. K. 1987. Hair cell innervation by spiral ganglion neurons in the mouse. *J Comp Neurol*, 255, 560-70.
- BETZ, W. J. 1970. Depression of transmitter release at the neuromuscular junction of the frog. *J Physiol*, 206, 629-44.
- BIENENSTOCK, E. L., COOPER, L. N. & MUNRO, P. W. 1982. Theory for the development of neuron selectivity: orientation specificity and binocular interaction in visual cortex. *J Neurosci*, 2, 32-48.
- BLAESSE, P., EHRHARDT, S., FRIAUF, E. & NOTHWANG, H. G. 2005. Developmental pattern of three vesicular glutamate transporters in the rat superior olivary complex. *Cell Tissue Res*, 320, 33-50.
- BLATCHLEY, B. J., COOPER, W. A. & COLEMAN, J. R. 1987. Development of auditory brainstem response to tone pip stimuli in the rat. *Brain Res*, 429, 75-84.
- BLISS, T. V. & LOMO, T. 1970. Plasticity in a monosynaptic cortical pathway. *J Physiol*, 207, 61P.
- BOETTCHER, F. A., MILLS, J. H., NORTON, B. L. & SCHMIEDT, R. A. 1993. Age-related changes in auditory evoked potentials of gerbils. II. Response latencies. *Hear Res*, 71, 146-56.
- BOETTCHER, F. A., SPONGR, V. P. & SALVI, R. J. 1992. Physiological and histological changes associated with the reduction in threshold shift during interrupted noise exposure. *Hear Res*, 62, 217-36.
- BOSTOCK, H., SEARS, T. A. & SHERRATT, R. M. 1983. The spatial distribution of excitability and membrane current in normal and demyelinated mammalian nerve fibres. *J Physiol*, 341, 41-58.
- BRAFF, D. L., SWERDLOW, N. R. & GEYER, M. A. 1999. Symptom correlates of prepulse inhibition deficits in male schizophrenic patients. *Am J Psychiatry*, 156, 596-602.
- BRAWER, J. R., MOREST, D. K. & KANE, E. C. 1974. The neuronal architecture of the cochlear nucleus of the cat. *J Comp Neurol*, 155, 251-300.
- BRODAL, P. & BJAALIE, J. G. 1992. Organization of the pontine nuclei. *Neurosci Res*, 13, 83-118.
- BROWN, D. J. & PATUZZI, R. B. 2010. Evidence that the compound action potential (CAP) from the auditory nerve is a stationary potential generated across dura mater. *Hear Res*, 267, 12-26.
- BROWN, M. C. 1987. Morphology of labeled efferent fibers in the guinea pig cochlea. *J Comp Neurol*, 260, 605-18.
- BROWN, M. C., SMITH, D. I. & NUTTALL, A. L. 1983. The temperature dependency of neural and hair cell responses evoked by high frequencies. *J Acoust Soc Am*, 73, 1662-70.
- BROWN, M. R. & KACZMAREK, L. K. 2011. Potassium channel modulation and auditory processing. *Hear Res*, 279, 32-42.
- BROWNE, C. J., MORLEY, J. W. & PARSONS, C. H. 2012. Tracking the expression of excitatory and inhibitory neurotransmission-related proteins and

- neuroplasticity markers after noise induced hearing loss. *PloS one*, 7, e33272.
- BROZOSKI, T. J., BAUER, C. A. & CASPARY, D. M. 2002. Elevated fusiform cell activity in the dorsal cochlear nucleus of chinchillas with psychophysical evidence of tinnitus. *J Neurosci*, 22, 2383-90.
- BUKOWSKA, D. 2002. Morphological evidence for secondary vestibular afferent connections to the dorsal cochlear nucleus in the rabbit. *Cells Tissues Organs*, 170, 61-8.
- BUONOMANO, D. V. 1999. Distinct functional types of associative long-term potentiation in neocortical and hippocampal pyramidal neurons. *J Neurosci*, 19, 6748-54.
- BURAN, B. N., STRENZKE, N., NEEF, A., GUNDELFINGER, E. D., MOSER, T. & LIBERMAN, M. C. 2010. Onset coding is degraded in auditory nerve fibers from mutant mice lacking synaptic ribbons. *J Neurosci*, 30, 7587-97.
- BURIAN, M. & GSTOETTNER, W. 1988. Projection of primary vestibular afferent fibres to the cochlear nucleus in the guinea pig. *Neurosci Lett*, 84, 13-7.
- CAI, S., MA, W. L. & YOUNG, E. D. 2009. Encoding intensity in ventral cochlear nucleus following acoustic trauma: implications for loudness recruitment. *J Assoc Res Otolaryngol*, 10, 5-22.
- CANLON, B. 1987. Acoustic overstimulation alters the morphology of the tectorial membrane. *Hear Res*, 30, 127-34.
- CASADO, M. & ASCHER, P. 1998. Opposite modulation of NMDA receptors by lysophospholipids and arachidonic acid: common features with mechanosensitivity. *J Physiol*, 513 ( Pt 2), 317-30.
- CASPARY, D. M., LING, L., TURNER, J. G. & HUGHES, L. F. 2008. Inhibitory neurotransmission, plasticity and aging in the mammalian central auditory system. *J Exp Biol*, 211, 1781-91.
- CAZALS, Y. 2000. Auditory sensori-neural alterations induced by salicylate. *Prog Neurobiol*, 62, 583-631.
- CAZALS, Y., ARAN, J. M., ERRE, J. P., GUILHAUME, A. & AUROUSSEAU, C. 1983. Vestibular acoustic reception in the guinea pig: a saccular function? *Acta Otolaryngol*, 95, 211-7.
- CHANG, E. F., BAO, S., IMAIZUMI, K., SCHREINER, C. E. & MERZENICH, M. M. 2005. Development of spectral and temporal response selectivity in the auditory cortex. *Proc Natl Acad Sci U S A*, 102, 16460-5.
- CHEN, G. D., KONG, J., REINHARD, K. & FECHTER, L. D. 2001. NMDA receptor blockage protects against permanent noise-induced hearing loss but not its potentiation by carbon monoxide. *Hear Res*, 154, 108-15.
- CHEN, S. Q., CAI, Q., SHEN, Y. Y., WANG, P. J., TENG, G. J., ZHANG, W. & ZANG, F. C. 2012. Age-related changes in brain metabolites and cognitive function in APP/PS1 transgenic mice. *Behav Brain Res*, 235, 1-6.

- CHOI, S., KLINGAUF, J. & TSIEN, R. W. 2000. Postfusional regulation of cleft glutamate concentration during LTP at 'silent synapses'. *Nat Neurosci*, 3, 330-6.
- CHURCH, M. W., JEN, K. L., STAFFERTON, T., HOTRA, J. W. & ADAMS, B. R. 2007. Reduced auditory acuity in rat pups from excess and deficient omega-3 fatty acid consumption by the mother. *Neurotoxicol Teratol*, 29, 203-10.
- CHURCH, M. W., WILLIAMS, H. L. & HOLLOWAY, J. A. 1984. Brain-stem auditory evoked potentials in the rat: effects of gender, stimulus characteristics and ethanol sedation. *Electroencephalogr Clin Neurophysiol*, 59, 328-39.
- CIUMAN, R. R. 2010. The efferent system or olivocochlear function bundle - fine regulator and protector of hearing perception. *Int J Biomed Sci*, 6, 276-88.
- CLARKE, R. J. & JOHNSON, J. W. 2006. NMDA receptor NR2 subunit dependence of the slow component of magnesium unblock. *J Neurosci*, 26, 5825-34.
- CLEM, R. L., CELIKEL, T. & BARTH, A. L. 2008. Ongoing in vivo experience triggers synaptic metaplasticity in the neocortex. *Science*, 319, 101-4.
- CLEMENTS, J. D. & SILVER, R. A. 2000. Unveiling synaptic plasticity: a new graphical and analytical approach. *Trends Neurosci*, 23, 105-13.
- COAN, E. J. & COLLINGRIDGE, G. L. 1985. Magnesium ions block an N-methyl-D-aspartate receptor-mediated component of synaptic transmission in rat hippocampus. *Neurosci Lett*, 53, 21-6.
- CODY, A. R. & ROBERTSON, D. 1983. Variability of noise-induced damage in the guinea pig cochlea: electrophysiological and morphological correlates after strictly controlled exposures. *Hear Res*, 9, 55-70.
- COHEN, L. B., KEYNES, R. D. & LANDOWNE, D. 1972. Changes in light scattering that accompany the action potential in squid giant axons: potential-dependent components. *J Physiol*, 224, 701-25.
- COLBERT, C. M. & PAN, E. 2002. Ion channel properties underlying axonal action potential initiation in pyramidal neurons. *Nat Neurosci*, 5, 533-8.
- CRAGG, B. G. & THOMAS, P. K. 1964. The Conduction Velocity of Regenerated Peripheral Nerve Fibres. *J Physiol*, 171, 164-75.
- CRANSAC, H., COTTET-EMARD, J. M., HELLSTROM, S. & PEYRIN, L. 1998. Specific sound-induced noradrenergic and serotonergic activation in central auditory structures. *Hear Res*, 118, 151-6.
- CUI, Y., ZHANG, J., CAI, R. & SUN, X. 2009. Early auditory experience-induced composition/ratio changes of N-methyl-D-aspartate receptor subunit expression and effects of D-2-amino-5-phosphonovaleric acid chronic blockade in rat auditory cortex. *J Neurosci Res*, 87, 1123-34.
- CULLEN, K. E. & ROY, J. E. 2004. Signal processing in the vestibular system during active versus passive head movements. *J Neurophysiol*, 91, 1919-33.
- DALLOS, P. & HARRIS, D. 1978. Properties of auditory nerve responses in absence of outer hair cells. *J Neurophysiol*, 41, 365-83.

- DANYSZ, W. & PARSONS, C. G. 2003. The NMDA receptor antagonist memantine as a symptomatological and neuroprotective treatment for Alzheimer's disease: preclinical evidence. *Int J Geriatr Psychiatry*, 18, S23-32.
- DARLINGTON, C. L. & SMITH, P. F. 2007. Drug treatments for tinnitus. *Prog Brain Res*, 166, 249-62.
- DAVIS, K. A., MILLER, R. L. & YOUNG, E. D. 1996. Effects of somatosensory and parallel-fiber stimulation on neurons in dorsal cochlear nucleus. *J Neurophysiol*, 76, 3012-24.
- DE RIDDER, D., FRANSEN, H., FRANCOIS, O., SUNAERT, S., KOVACS, S. & VAN DE HEYNING, P. 2006. Amygdalohippocampal involvement in tinnitus and auditory memory. *Acta Otolaryngol Suppl*, 50-3.
- DEHMEL, S., EISINGER, D. & SHORE, S. E. 2012a. Gap prepulse inhibition and auditory brainstem-evoked potentials as objective measures for tinnitus in guinea pigs. *Front Syst Neurosci*, 6, 42.
- DEHMEL, S., PRADHAN, S., KOEHLER, S., BLEDSOE, S. & SHORE, S. 2012b. Noise overexposure alters long-term somatosensory-auditory processing in the dorsal cochlear nucleus--possible basis for tinnitus-related hyperactivity? *J Neurosci*, 32, 1660-71.
- DEL CASTILLO, J. & KATZ, B. 1954. Quantal components of the end-plate potential. *J Physiol*, 124, 560-73.
- DERIN, A., AGIRDIR, B., DERIN, N., DINC, O., GUNEY, K., OZCAGLAR, H. & KILINCARSLAN, S. 2004. The effects of L-carnitine on presbycusis in the rat model. *Clin Otolaryngol Allied Sci*, 29, 238-41.
- DITTMAN, J. S. & REGEHR, W. G. 1998. Calcium dependence and recovery kinetics of presynaptic depression at the climbing fiber to Purkinje cell synapse. *J Neurosci*, 18, 6147-62.
- DOBRUNZ, L. E. & STEVENS, C. F. 1997. Heterogeneity of release probability, facilitation, and depletion at central synapses. *Neuron*, 18, 995-1008.
- DOETSCH, G. S. 1998. Perceptual significance of somatosensory cortical reorganization following peripheral denervation. *Neuroreport*, 9, R29-35.
- DONALDSON, G. S. & RUTH, R. A. 1996. Derived-band auditory brain-stem response estimates of traveling wave velocity in humans: II. Subjects with noise-induced hearing loss and Meniere's disease. *J Speech Hear Res*, 39, 534-45.
- DORRN, A. L., YUAN, K., BARKER, A. J., SCHREINER, C. E. & FROEMKE, R. C. 2010. Developmental sensory experience balances cortical excitation and inhibition. *Nature*, 465, 932-6.
- DUBRAY, C., ALLOUI, A., BARDIN, L., ROCK, E., MAZUR, A., RAYSSIGUIER, Y., ESCHALIER, A. & LAVARENNE, J. 1997. Magnesium deficiency induces an hyperalgesia reversed by the NMDA receptor antagonist MK801. *Neuroreport*, 8, 1383-6.

- ECCLES, J. C., SASAKI, K. & STRATA, P. 1967. Interpretation of the potential fields generated in the cerebellar cortex by a mossy fibre volley. *Exp Brain Res*, 3, 58-80.
- ECHTELER, S. M. 1992. Developmental segregation in the afferent projections to mammalian auditory hair cells. *Proc Natl Acad Sci U S A*, 89, 6324-7.
- EGGER, V., FELDMAYER, D. & SAKMANN, B. 1999. Coincidence detection and changes of synaptic efficacy in spiny stellate neurons in rat barrel cortex. *Nat Neurosci*, 2, 1098-105.
- EGGERMONT, J. J. 2008. Role of auditory cortex in noise- and drug-induced tinnitus. *Am J Audiol*, 17, S162-9.
- EGGERMONT, J. J. 2013. Hearing loss, hyperacusis, or tinnitus: what is modeled in animal research? *Hear Res*, 295, 140-9.
- EGGERMONT, J. J. & ROBERTS, L. E. 2004. The neuroscience of tinnitus. *Trends Neurosci*, 27, 676-82.
- EL-BADRY, M. M., DING, D. L., MCFADDEN, S. L. & EDDINS, A. C. 2007. Physiological effects of auditory nerve myelinopathy in chinchillas. *Eur J Neurosci*, 25, 1437-46.
- ELVERLAND, H. H. 1978. Ascending and intrinsic projections of the superior olivary complex in the cat. *Exp Brain Res*, 32, 117-34.
- ENGINEER, N. D., RILEY, J. R., SEALE, J. D., VRANA, W. A., SHETAKE, J. A., SUDANAGUNTA, S. P., BORLAND, M. S. & KILGARD, M. P. 2011. Reversing pathological neural activity using targeted plasticity. *Nature*, 470, 101-4.
- ENGLAND, J. D., GAMBONI, F., LEVINSON, S. R. & FINGER, T. E. 1990. Changed distribution of sodium channels along demyelinated axons. *Proc Natl Acad Sci U S A*, 87, 6777-80.
- EVANS, E. F. & NELSON, P. G. 1973. The responses of single neurones in the cochlear nucleus of the cat as a function of their location and the anaesthetic state. *Exp Brain Res*, 17, 402-27.
- FARRIS, H. E., LEBLANC, C. L., GOSWAMI, J. & RICCI, A. J. 2004. Probing the pore of the auditory hair cell mechanotransducer channel in turtle. *J Physiol*, 558, 769-92.
- FELDMAN, D. E. 2009. Synaptic mechanisms for plasticity in neocortex. *Annu Rev Neurosci*, 32, 33-55.
- FELDMAN, D. E., NICOLL, R. A., MALENKA, R. C. & ISAAC, J. T. 1998. Long-term depression at thalamocortical synapses in developing rat somatosensory cortex. *Neuron*, 21, 347-57.
- FERRAGAMO, M. J., GOLDING, N. L. & OERTEL, D. 1998. Synaptic inputs to stellate cells in the ventral cochlear nucleus. *J Neurophysiol*, 79, 51-63.
- FETTIPLACE, R. & HACKNEY, C. M. 2006. The sensory and motor roles of auditory hair cells. *Nat Rev Neurosci*, 7, 19-29.
- FIGUEIREDO, R. R., LANGGUTH, B., MELLO DE OLIVEIRA, P. & APARECIDA DE AZEVEDO, A. 2008. Tinnitus treatment with memantine. *Otolaryngol Head Neck Surg*, 138, 492-6.

- FLECKNELL, P. A. & MITCHELL, M. 1984. Midazolam and fentanyl-fluanisone: assessment of anaesthetic effects in laboratory rodents and rabbits. *Lab Anim*, 18, 143-6.
- FLOR, H., HOFFMANN, D., STRUVE, M. & DIESCH, E. 2004. Auditory discrimination training for the treatment of tinnitus. *Appl Psychophysiol Biofeedback*, 29, 113-20.
- FOLMER, R. L., MCMILLAN, G. P., AUSTIN, D. F. & HENRY, J. A. 2011. Audiometric thresholds and prevalence of tinnitus among male veterans in the United States: data from the National Health and Nutrition Examination Survey, 1999-2006. *J Rehabil Res Dev*, 48, 503-16.
- FREMEAU, R. T., JR., KAM, K., QURESHI, T., JOHNSON, J., COPENHAGEN, D. R., STORM-MATHISEN, J., CHAUDHRY, F. A., NICOLL, R. A. & EDWARDS, R. H. 2004. Vesicular glutamate transporters 1 and 2 target to functionally distinct synaptic release sites. *Science*, 304, 1815-9.
- FRIDBERGER, A., FLOCK, A., ULFENDAHL, M. & FLOCK, B. 1998. Acoustic overstimulation increases outer hair cell Ca<sup>2+</sup> concentrations and causes dynamic contractions of the hearing organ. *Proc Natl Acad Sci U S A*, 95, 7127-32.
- FRIEDLAND, D. R., EERNISSE, R. & POPPER, P. 2007. Potassium channel gene expression in the rat cochlear nucleus. *Hear Res*, 228, 31-43.
- FRIEDMAN, J. T., PEIFFER, A. M., CLARK, M. G., BENASICH, A. A. & FITCH, R. H. 2004. Age and experience-related improvements in gap detection in the rat. *Brain Res Dev Brain Res*, 152, 83-91.
- FRINGS, S., REUTER, D. & KLEENE, S. J. 2000. Neuronal Ca<sup>2+</sup>-activated Cl<sup>-</sup> channels--homing in on an elusive channel species. *Prog Neurobiol*, 60, 247-89.
- FRISINA, R. D. 2001. Subcortical neural coding mechanisms for auditory temporal processing. *Hear Res*, 158, 1-27.
- FUJINO, K. & OERTEL, D. 2003. Bidirectional synaptic plasticity in the cerebellum-like mammalian dorsal cochlear nucleus. *Proceedings of the National Academy of Sciences of the United States of America*, 100, 265-270.
- GAESE, B. H., NOWOTNY, M. & PILZ, P. K. 2009. Acoustic startle and prepulse inhibition in the Mongolian gerbil. *Physiology & Behavior*, 98, 460-466.
- GARCIA, M. M., EDWARD, R., BRENNAN, G. B. & HARLAN, R. E. 2000. Deafferentation-induced changes in protein kinase C expression in the rat cochlear nucleus. *Hear Res*, 147, 113-24.
- GOLDBERG, J. M. & BROWN, P. B. 1969. Response of binaural neurons of dog superior olivary complex to dichotic tonal stimuli: some physiological mechanisms of sound localization. *J Neurophysiol*, 32, 613-36.
- GOLDING, N. L. & OERTEL, D. 1997. Physiological identification of the targets of cartwheel cells in the dorsal cochlear nucleus. *J Neurophysiol*, 78, 248-60.

- GOLDSTEIN, B. A., LENHARDT, M. L. & SHULMAN, A. 2005. Tinnitus improvement with ultra-high-frequency vibration therapy. *Int Tinnitus J*, 11, 14-22.
- GOUREVITCH, B., DOISY, T., AVILLAC, M. & EDELINE, J. M. 2009. Follow-up of latency and threshold shifts of auditory brainstem responses after single and interrupted acoustic trauma in guinea pig. *Brain Res*, 1304, 66-79.
- GUITTON, M. J. 2012. Tinnitus: pathology of synaptic plasticity at the cellular and system levels. *Front Syst Neurosci*, 6, 12.
- GUITTON, M. J., CASTON, J., RUEL, J., JOHNSON, R. M., PUJOL, R. & PUEL, J. L. 2003. Salicylate induces tinnitus through activation of cochlear NMDA receptors. *The Journal of neuroscience : the official journal of the Society for Neuroscience*, 23, 3944-3952.
- GUITTON, M. J. & DUDAI, Y. 2007. Blockade of cochlear NMDA receptors prevents long-term tinnitus during a brief consolidation window after acoustic trauma. *Neural plasticity*, 2007, 80904.
- GUPPY, A. & COLES, R. B. 1988. Acoustical and neural aspects of hearing in the Australian gleaning bats, *Macroderma gigas* and *Nyctophilus gouldi*. *J Comp Physiol A*, 162, 653-68.
- HACKNEY, C. M., OSEN, K. K. & KOLSTON, J. 1990. Anatomy of the cochlear nuclear complex of guinea pig. *Anat Embryol (Berl)*, 182, 123-49.
- HARDINGHAM, N. R., HARDINGHAM, G. E., FOX, K. D. & JACK, J. J. 2007. Presynaptic efficacy directs normalization of synaptic strength in layer 2/3 rat neocortex after paired activity. *J Neurophysiol*, 97, 2965-75.
- HAUPT, H. & SCHEIBE, F. 2002. Preventive magnesium supplement protects the inner ear against noise-induced impairment of blood flow and oxygenation in the guinea pig. *Magnes Res*, 15, 17-25.
- HAZELL, J. 1990. Tinnitus and disability with ageing: adaptation and management. *Acta Otolaryngol Suppl*, 476, 202-8.
- HENDERSON, D., BIELEFELD, E. C., HARRIS, K. C. & HU, B. H. 2006. The role of oxidative stress in noise-induced hearing loss. *Ear Hear*, 27, 1-19.
- HENRY, J. A., DENNIS, K. C. & SCHECHTER, M. A. 2005. General review of tinnitus: prevalence, mechanisms, effects, and management. *J Speech Lang Hear Res*, 48, 1204-35.
- HERDMAN, S. J. 1998. Role of vestibular adaptation in vestibular rehabilitation. *Otolaryngol Head Neck Surg*, 119, 49-54.
- HERRAIZ, C., TOLEDANO, A. & DIGES, I. 2007. Trans-electrical nerve stimulation (TENS) for somatic tinnitus. *Prog Brain Res*, 166, 389-94.
- HODGKIN, A. L. & HUXLEY, A. F. 1952. Propagation of electrical signals along giant nerve fibers. *Proc R Soc Lond B Biol Sci*, 140, 177-83.
- HOFFMAN, D. C. & DONOVAN, H. 1994. D1 and D2 dopamine receptor antagonists reverse prepulse inhibition deficits in an animal model of schizophrenia. *Psychopharmacology (Berl)*, 115, 447-53.

- HOGSDEN, J. L. & DRINGENBERG, H. C. 2009. Decline of long-term potentiation (LTP) in the rat auditory cortex in vivo during postnatal life: involvement of NR2B subunits. *Brain Res*, 1283, 25-33.
- HOUSE, J. W. & BRACKMANN, D. E. 1981. Tinnitus: surgical treatment. *Ciba Found Symp*, 85, 204-16.
- HUDSPETH, A. J. 1989. Mechanoelectrical transduction by hair cells of the bullfrog's sacculus. *Prog Brain Res*, 80, 129-35; discussion 127-8.
- IMENNOV, N. S. & RUBINSTEIN, J. T. 2009. Stochastic population model for electrical stimulation of the auditory nerve. *IEEE Trans Biomed Eng*, 56, 2493-501.
- INOUE, T., CHANDLER, S. H. & GOLDBERG, L. J. 1994. Neuropharmacological mechanisms underlying rhythmical discharge in trigeminal interneurons during fictive mastication. *J Neurophysiol*, 71, 2061-73.
- ISAAC, J. T., NICOLL, R. A. & MALENKA, R. C. 1995. Evidence for silent synapses: implications for the expression of LTP. *Neuron*, 15, 427-34.
- ISON, J. R. & ALLEN, P. 2003. A diminished rate of "physiological decay" at noise offset contributes to age-related changes in temporal acuity in the CBA mouse model of presbycusis. *J Acoust Soc Am*, 114, 522-8.
- ISON, J. R., O'CONNOR, K., BOWEN, G. P. & BOCIRNEA, A. 1991. Temporal resolution of gaps in noise by the rat is lost with functional decortication. *Behav Neurosci*, 105, 33-40.
- ITO, T., TOKURIKI, M., SHIBAMORI, Y., SAITO, T. & NOJYO, Y. 2004. Cochlear nerve demyelination causes prolongation of wave I latency in ABR of the myelin deficient (md) rat. *Hear Res*, 191, 119-24.
- JACKSON, M. B. & ZHANG, S. J. 1995. Action potential propagation and propagation block by GABA in rat posterior pituitary nerve terminals. *J Physiol*, 483 ( Pt 3), 597-611.
- JACOB, V., BRASIER, D. J., ERCHOVA, I., FELDMAN, D. & SHULZ, D. E. 2007. Spike timing-dependent synaptic depression in the in vivo barrel cortex of the rat. *J Neurosci*, 27, 1271-84.
- JAHN, C. E. & STEVENS, C. F. 1987. Glutamate activates multiple single channel conductances in hippocampal neurons. *Nature*, 325, 522-5.
- JANCZEWSKI, G., KOCHANEK, K., DAWIDOWICZ, J., DOBRZYNSKI, P. & CHECINSKI, P. 1988. [Evaluation of the effect of auditory fatigue on the human ear by auditory brain stem responses (ABR). I. Effect of auditory fatigue on temporary threshold shifts of ABR]. *Med Pr*, 39, 108-14.
- JASTREBOFF, P. J., BRENNAN, J. F., COLEMAN, J. K. & SASAKI, C. T. 1988. Phantom auditory sensation in rats: an animal model for tinnitus. *Behav Neurosci*, 102, 811-22.
- JASTREBOFF, P. J. & HAZELL, J. W. 1993. A neurophysiological approach to tinnitus: clinical implications. *Br J Audiol*, 27, 7-17.

- JAVEL, E. & SHEPHERD, R. K. 2000. Electrical stimulation of the auditory nerve. III. Response initiation sites and temporal fine structure. *Hear Res*, 140, 45-76.
- JAVEL, E. & VIEMEISTER, N. F. 2000. Stochastic properties of cat auditory nerve responses to electric and acoustic stimuli and application to intensity discrimination. *J Acoust Soc Am*, 107, 908-21.
- JOHNSTONE, B. M., PATUZZI, R., SYKA, J. & SYKOVA, E. 1989. Stimulus-related potassium changes in the organ of Corti of guinea-pig. *J Physiol*, 408, 77-92.
- KAGA, K., NAKAMURA, M., SHINOGAMI, M., TSUZUKU, T., YAMADA, K. & SHINDO, M. 1996. Auditory nerve disease of both ears revealed by auditory brainstem responses, electrocochleography and otoacoustic emissions. *Scand Audiol*, 25, 233-8.
- KALTENBACH, J. A. 2006. Summary of evidence pointing to a role of the dorsal cochlear nucleus in the etiology of tinnitus. *Acta Otolaryngol Suppl*, 20-6.
- KALTENBACH, J. A. 2011. Tinnitus: Models and mechanisms. *Hear Res*, 276, 52-60.
- KALTENBACH, J. A. & AFMAN, C. E. 2000. Hyperactivity in the dorsal cochlear nucleus after intense sound exposure and its resemblance to tone-evoked activity: a physiological model for tinnitus. *Hear Res*, 140, 165-72.
- KALTENBACH, J. A. & GODFREY, D. A. 2008. Dorsal cochlear nucleus hyperactivity and tinnitus: are they related? *Am J Audiol*, 17, S148-61.
- KALTENBACH, J. A., GODFREY, D. A., NEUMANN, J. B., MCCASLIN, D. L., AFMAN, C. E. & ZHANG, J. 1998. Changes in spontaneous neural activity in the dorsal cochlear nucleus following exposure to intense sound: relation to threshold shift. *Hearing research*, 124, 78-84.
- KALTENBACH, J. A., ZACHAREK, M. A., ZHANG, J. & FREDERICK, S. 2004. Activity in the dorsal cochlear nucleus of hamsters previously tested for tinnitus following intense tone exposure. *Neurosci Lett*, 355, 121-5.
- KALTENBACH, J. A., ZHANG, J. & AFMAN, C. E. 2000. Plasticity of spontaneous neural activity in the dorsal cochlear nucleus after intense sound exposure. *Hearing research*, 147, 282-292.
- KALTENBACH, J. A., ZHANG, J. & FINLAYSON, P. 2005. Tinnitus as a plastic phenomenon and its possible neural underpinnings in the dorsal cochlear nucleus. *Hear Res*, 206, 200-26.
- KANOLD, P. O. & YOUNG, E. D. 2001. Proprioceptive information from the pinna provides somatosensory input to cat dorsal cochlear nucleus. *J Neurosci*, 21, 7848-58.
- KATAOKA, Y. & OHMORI, H. 1994. Activation of glutamate receptors in response to membrane depolarization of hair cells isolated from chick cochlea. *J Physiol*, 477 ( Pt 3), 403-14.
- KATZ, B. & MILEDI, R. 1968. The role of calcium in neuromuscular facilitation. *J Physiol*, 195, 481-92.

- KATZ, L. C. & SHATZ, C. J. 1996. Synaptic activity and the construction of cortical circuits. *Science*, 274, 1133-8.
- KAWASE, T. & LIBERMAN, M. C. 1993. Antimasking effects of the olivocochlear reflex. I. Enhancement of compound action potentials to masked tones. *J Neurophysiol*, 70, 2519-32.
- KELLY, J. B., LISCUM, A., VAN ADEL, B. & ITO, M. 1998. Projections from the superior olive and lateral lemniscus to tonotopic regions of the rat's inferior colliculus. *Hear Res*, 116, 43-54.
- KERCHNER, G. A. & NICOLL, R. A. 2008. Silent synapses and the emergence of a postsynaptic mechanism for LTP. *Nat Rev Neurosci*, 9, 813-25.
- KIM, J., MOREST, D. K. & BOHNE, B. A. 1997. Degeneration of axons in the brainstem of the chinchilla after auditory overstimulation. *Hear Res*, 103, 169-91.
- KIM, J. H., RENDEN, R. & VON GERSDORFF, H. 2013. Dysmyelination of Auditory Afferent Axons Increases the Jitter of Action Potential Timing during High-Frequency Firing. *J Neurosci*, 33, 9402-7.
- KLESCHEVNIKOV, A. M., SOKOLOV, M. V., KUHNT, U., DAWE, G. S., STEPHENSON, J. D. & VORONIN, L. L. 1997. Changes in paired-pulse facilitation correlate with induction of long-term potentiation in area CA1 of rat hippocampal slices. *Neuroscience*, 76, 829-43.
- KLINGAUF, J. & NEHER, E. 1997. Modeling buffered Ca<sup>2+</sup> diffusion near the membrane: implications for secretion in neuroendocrine cells. *Biophys J*, 72, 674-90.
- KOCH, M. & SCHNITZLER, H. U. 1997. The acoustic startle response in rats--circuits mediating evocation, inhibition and potentiation. *Behav Brain Res*, 89, 35-49.
- KONIG, O., SCHAETTE, R., KEMPTER, R. & GROSS, M. 2006. Course of hearing loss and occurrence of tinnitus. *Hear Res*, 221, 59-64.
- KOTAK, V. C., BREITHAUPT, A. D. & SANES, D. H. 2007. Developmental hearing loss eliminates long-term potentiation in the auditory cortex. *Proc Natl Acad Sci U S A*, 104, 3550-5.
- KOTAK, V. C., TAKESIAN, A. E. & SANES, D. H. 2008. Hearing loss prevents the maturation of GABAergic transmission in the auditory cortex. *Cereb Cortex*, 18, 2098-108.
- KUBA, H., OICHI, Y. & OHMORI, H. 2010. Presynaptic activity regulates Na<sup>(+)</sup> channel distribution at the axon initial segment. *Nature*, 465, 1075-8.
- KUDO, M. & NIIMI, K. 1980. Ascending projections of the inferior colliculus in the cat: an autoradiographic study. *J Comp Neurol*, 191, 545-56.
- KUJAWA, S. G. & LIBERMAN, M. C. 2009. Adding insult to injury: cochlear nerve degeneration after "temporary" noise-induced hearing loss. *The Journal of neuroscience : the official journal of the Society for Neuroscience*, 29, 14077-14085.

- KULLMANN, D. M. 1994. Amplitude fluctuations of dual-component EPSCs in hippocampal pyramidal cells: implications for long-term potentiation. *Neuron*, 12, 1111-20.
- KULLMANN, D. M. 2003. Silent synapses: what are they telling us about long-term potentiation? *Philos Trans R Soc Lond B Biol Sci*, 358, 727-33.
- KULLMANN, D. M. & NICOLL, R. A. 1992. Long-term potentiation is associated with increases in quantal content and quantal amplitude. *Nature*, 357, 240-4.
- KURIYAMA, H., ALBIN, R. L. & ALTSCHULER, R. A. 1993. Expression of NMDA-receptor mRNA in the rat cochlea. *Hear Res*, 69, 215-20.
- LANGNER, G. 1992. Periodicity coding in the auditory system. *Hear Res*, 60, 115-42.
- LANTING, C. P., DE KLEINE, E. & VAN DIJK, P. 2009. Neural activity underlying tinnitus generation: results from PET and fMRI. *Hear Res*, 255, 1-13.
- LARKMAN, A. U. & JACK, J. J. 1995. Synaptic plasticity: hippocampal LTP. *Curr Opin Neurobiol*, 5, 324-34.
- LASIENE, J., SHUPE, L., PERLMUTTER, S. & HORNER, P. 2008. No evidence for chronic demyelination in spared axons after spinal cord injury in a mouse. *J Neurosci*, 28, 3887-96.
- LEE, B. R. & DONG, Y. 2011. Cocaine-induced metaplasticity in the nucleus accumbens: silent synapse and beyond. *Neuropharmacology*, 61, 1060-9.
- LEUMANN, L., STERCHI, D., VOLLENWEIDER, F., LUDEWIG, K. & FRUH, H. 2001. A neural network approach to the acoustic startle reflex and prepulse inhibition. *Brain research bulletin*, 56, 101-110.
- LEVINE, R. A. 1999. Somatic (craniocervical) tinnitus and the dorsal cochlear nucleus hypothesis. *Am J Otolaryngol*, 20, 351-62.
- LEVINE, R. A., ABEL, M. & CHENG, H. 2003. CNS somatosensory-auditory interactions elicit or modulate tinnitus. *Exp Brain Res*, 153, 643-8.
- LIAO, D., HESSLER, N. A. & MALINOW, R. 1995. Activation of postsynaptically silent synapses during pairing-induced LTP in CA1 region of hippocampal slice. *Nature*, 375, 400-4.
- LIBERMAN, M. C. 1984. Single-neuron labeling and chronic cochlear pathology. I. Threshold shift and characteristic-frequency shift. *Hear Res*, 16, 33-41.
- LIBERMAN, M. C. & BEIL, D. G. 1979. Hair cell condition and auditory nerve response in normal and noise-damaged cochleas. *Acta Otolaryngol*, 88, 161-76.
- LIBERMAN, M. C. & DODDS, L. W. 1987. Acute ultrastructural changes in acoustic trauma: serial-section reconstruction of stereocilia and cuticular plates. *Hear Res*, 26, 45-64.
- LIBERMAN, M. C., GAO, J., HE, D. Z., WU, X., JIA, S. & ZUO, J. 2002. Prestin is required for electromotility of the outer hair cell and for the cochlear amplifier. *Nature*, 419, 300-4.

- LIN, H. W., FURMAN, A. C., KUJAWA, S. G. & LIBERMAN, M. C. 2011. Primary neural degeneration in the Guinea pig cochlea after reversible noise-induced threshold shift. *J Assoc Res Otolaryngol*, 12, 605-16.
- LISMAN, J. & RAGHAVACHARI, S. 2006. A unified model of the presynaptic and postsynaptic changes during LTP at CA1 synapses. *Sci STKE*, 2006, re11.
- LIU, Y. & FECHTER, L. D. 1996. Comparison of the effects of trimethyltin on the intracellular calcium levels in spiral ganglion cells and outer hair cells. *Acta Otolaryngol*, 116, 417-21.
- LOBARINAS, E., HAYES, S. H. & ALLMAN, B. L. 2013. The gap-startle paradigm for tinnitus screening in animal models: limitations and optimization. *Hear Res*, 295, 150-60.
- LOBARINAS, E., YANG, G., SUN, W., DING, D., MIRZA, N., DALBY-BROWN, W., HILCZMAYER, E., FITZGERALD, S., ZHANG, L. & SALVI, R. 2006. Salicylate- and quinine-induced tinnitus and effects of memantine. *Acta Otolaryngol Suppl*, 13-9.
- MA, W. L., HIDAKA, H. & MAY, B. J. 2006. Spontaneous activity in the inferior colliculus of CBA/J mice after manipulations that induce tinnitus. *Hear Res*, 212, 9-21.
- MADARA, J. C. & LEVINE, E. S. 2008. Presynaptic and postsynaptic NMDA receptors mediate distinct effects of brain-derived neurotrophic factor on synaptic transmission. *J Neurophysiol*, 100, 3175-84.
- MAGEE, J. C. 2000. Dendritic integration of excitatory synaptic input. *Nat Rev Neurosci*, 1, 181-90.
- MAISON, S. F. & LIBERMAN, M. C. 2000. Predicting vulnerability to acoustic injury with a noninvasive assay of olivocochlear reflex strength. *J Neurosci*, 20, 4701-7.
- MALENKA, R. C. & BEAR, M. F. 2004. LTP and LTD: an embarrassment of riches. *Neuron*, 44, 5-21.
- MALENKA, R. C. & NICOLL, R. A. 1999. Long-term potentiation--a decade of progress? *Science*, 285, 1870-4.
- MALINOW, R. & MALENKA, R. C. 2002. AMPA receptor trafficking and synaptic plasticity. *Annu Rev Neurosci*, 25, 103-26.
- MANIS, P. B. 1989. Responses to parallel fiber stimulation in the guinea pig dorsal cochlear nucleus in vitro. *J Neurophysiol*, 61, 149-61.
- MANIS, P. B. & MOLITOR, S. C. 1996. N-methyl-D-aspartate receptors at parallel fiber synapses in the dorsal cochlear nucleus. *J Neurophysiol*, 76, 1639-56.
- MANSCHOT, S. M., GISPEN, W. H., KAPPELLE, L. J. & BIESELS, G. J. 2003. Nerve conduction velocity and evoked potential latencies in streptozotocin-diabetic rats: effects of treatment with an angiotensin converting enzyme inhibitor. *Diabetes Metab Res Rev*, 19, 469-77.

- MANZOOR, N. F., CHEN, G. & KALTENBACH, J. A. 2013. Suppression of noise-induced hyperactivity in the dorsal cochlear nucleus following application of the cholinergic agonist, carbachol. *Brain Res*, 1523, 28-36.
- MANZOOR, N. F., LICARI, F. G., KLAPCHAR, M., ELKIN, R. L., GAO, Y., CHEN, G. & KALTENBACH, J. A. 2012. Noise-induced hyperactivity in the inferior colliculus: its relationship with hyperactivity in the dorsal cochlear nucleus. *J Neurophysiol*, 108, 976-88.
- MARKAND, O. N. 1994. Brainstem auditory evoked potentials. *J Clin Neurophysiol*, 11, 319-42.
- MATSUBARA, A., LAAKE, J. H., DAVANGER, S., USAMI, S. & OTTERSEN, O. P. 1996. Organization of AMPA receptor subunits at a glutamate synapse: a quantitative immunogold analysis of hair cell synapses in the rat organ of Corti. *J Neurosci*, 16, 4457-67.
- MAY, B. J. 2000. Role of the dorsal cochlear nucleus in the sound localization behavior of cats. *Hear Res*, 148, 74-87.
- MAYER, M. L., WESTBROOK, G. L. & GUTHRIE, P. B. 1984. Voltage-dependent block by Mg<sup>2+</sup> of NMDA responses in spinal cord neurones. *Nature*, 309, 261-3.
- MCINTYRE, C. C., RICHARDSON, A. G. & GRILL, W. M. 2002. Modeling the excitability of mammalian nerve fibers: influence of afterpotentials on the recovery cycle. *J Neurophysiol*, 87, 995-1006.
- MCLOUGHLIN, R. & MCQUILLAN, R. 1997. Transdermal fentanyl and respiratory depression. *Palliat Med*, 11, 419.
- MELIZA, C. D. & DAN, Y. 2006. Receptive-field modification in rat visual cortex induced by paired visual stimulation and single-cell spiking. *Neuron*, 49, 183-9.
- MENDELSON, J. R. & RICKETTS, C. 2001. Age-related temporal processing speed deterioration in auditory cortex. *Hear Res*, 158, 84-94.
- MENNERICK, S. & ZORUMSKI, C. F. 1995. Paired-pulse modulation of fast excitatory synaptic currents in microcultures of rat hippocampal neurons. *J Physiol*, 488 ( Pt 1), 85-101.
- MILLER, B., SARANTIS, M., TRAYNELIS, S. F. & ATTWELL, D. 1992. Potentiation of NMDA receptor currents by arachidonic acid. *Nature*, 355, 722-5.
- MILLER, R. J. 1998. Presynaptic receptors. *Annu Rev Pharmacol Toxicol*, 38, 201-27.
- MILLER, R. L., SCHILLING, J. R., FRANCK, K. R. & YOUNG, E. D. 1997. Effects of acoustic trauma on the representation of the vowel "eh" in cat auditory nerve fibers. *J Acoust Soc Am*, 101, 3602-16.
- MITCHELL, C. R., VERNON, J. A. & CREEDON, T. A. 1993. Measuring tinnitus parameters: loudness, pitch, and maskability. *J Am Acad Audiol*, 4, 139-51.
- MOLLER, A. R. 2007. Tinnitus: presence and future. *Prog Brain Res*, 166, 3-16.

- MOLNAR, E., PICKARD, L. & DUCKWORTH, J. K. 2002. Developmental changes in ionotropic glutamate receptors: lessons from hippocampal synapses. *Neuroscientist*, 8, 143-53.
- MORELL, P., GREENFIELD, S., COSTANTINO-CECCARINI, E. & WISNIEWSKI, H. 1972. Changes in the protein composition of mouse brain myelin during development. *J Neurochem*, 19, 2545-54.
- MOREST, D. K., KIM, J., POTASHNER, S. J. & BOHNE, B. A. 1998. Long-term degeneration in the cochlear nerve and cochlear nucleus of the adult chinchilla following acoustic overstimulation. *Microsc Res Tech*, 41, 205-16.
- MUGNAINI, E. 1985. GABA neurons in the superficial layers of the rat dorsal cochlear nucleus: light and electron microscopic immunocytochemistry. *J Comp Neurol*, 235, 61-81.
- MUGNAINI, E., DINO, M. R. & JAARSMA, D. 1997. The unipolar brush cells of the mammalian cerebellum and cochlear nucleus: cytology and microcircuitry. *Prog Brain Res*, 114, 131-50.
- MUGNAINI, E., WARR, W. B. & OSEN, K. K. 1980. Distribution and light microscopic features of granule cells in the cochlear nuclei of cat, rat, and mouse. *J Comp Neurol*, 191, 581-606.
- MULLER, M., FELMY, F. & SCHNEGGENBURGER, R. 2008. A limited contribution of Ca<sup>2+</sup> current facilitation to paired-pulse facilitation of transmitter release at the rat calyx of Held. *J Physiol*, 586, 5503-20.
- MULROY, M. J. & CURLEY, F. J. 1982. Stereociliary pathology and noise-induced threshold shift: a scanning electron microscopic study. *Scan Electron Microsc*, 1753-62.
- MULUK, N. B. & OGUZTURK, O. 2008. Occupational noise-induced tinnitus: does it affect workers' quality of life? *J Otolaryngol Head Neck Surg*, 37, 65-71.
- NEHER, E. & SAKMANN, B. 1992. The patch clamp technique. *Sci Am*, 266, 44-51.
- NELKEN, I. & YOUNG, E. D. 1994. Two separate inhibitory mechanisms shape the responses of dorsal cochlear nucleus type IV units to narrowband and wideband stimuli. *J Neurophysiol*, 71, 2446-62.
- NELSON, J. J. & CHEN, K. 2004. The relationship of tinnitus, hyperacusis, and hearing loss. *Ear Nose Throat J*, 83, 472-6.
- NICOLL, R. A. & MALENKA, R. C. 1999. Expression mechanisms underlying NMDA receptor-dependent long-term potentiation. *Ann N Y Acad Sci*, 868, 515-25.
- NIEDZIELSKI, A. S. & WENTHOLD, R. J. 1995. Expression of AMPA, kainate, and NMDA receptor subunits in cochlear and vestibular ganglia. *J Neurosci*, 15, 2338-53.
- NODAR, R. H. 1996. Tinnitus reclassified; new oil in an old lamp. *Otolaryngol Head Neck Surg*, 114, 582-5.

- NOGUCHI, Y., NISHIDA, H. & KOMATSUZAKI, A. 1999. A comparison of extratympanic versus transtympanic recordings in electrocochleography. *Audiology*, 38, 135-40.
- NORDMANN, A. S., BOHNE, B. A. & HARDING, G. W. 2000. Histopathological differences between temporary and permanent threshold shift. *Hear Res*, 139, 13-30.
- NORENA, A., MICHEYL, C., CHERY-CROZE, S. & COLLET, L. 2002. Psychoacoustic characterization of the tinnitus spectrum: implications for the underlying mechanisms of tinnitus. *Audiol Neurootol*, 7, 358-69.
- NORENA, A. J. 2011. An integrative model of tinnitus based on a central gain controlling neural sensitivity. *Neurosci Biobehav Rev*, 35, 1089-109.
- NORENA, A. J. & EGGERMONT, J. J. 2003. Changes in spontaneous neural activity immediately after an acoustic trauma: implications for neural correlates of tinnitus. *Hear Res*, 183, 137-53.
- NORENA, A. J. & EGGERMONT, J. J. 2005. Enriched acoustic environment after noise trauma reduces hearing loss and prevents cortical map reorganization. *J Neurosci*, 25, 699-705.
- NORENA, A. J. & FARLEY, B. J. 2013. Tinnitus-related neural activity: Theories of generation, propagation, and centralization. *Hear Res*, 295, 161-71.
- NORENA, A. J., MOFFAT, G., BLANC, J. L., PEZARD, L. & CAZALS, Y. 2010. Neural changes in the auditory cortex of awake guinea pigs after two tinnitus inducers: salicylate and acoustic trauma. *Neuroscience*, 166, 1194-209.
- NOWAK, L., BREGESTOVSKI, P., ASCHER, P., HERBET, A. & PROCHIANTZ, A. 1984. Magnesium gates glutamate-activated channels in mouse central neurones. *Nature*, 307, 462-5.
- OCHI, K., OHASHI, T. & KENMOCHI, M. 2003. Hearing impairment and tinnitus pitch in patients with unilateral tinnitus: comparison of sudden hearing loss and chronic tinnitus. *Laryngoscope*, 113, 427-31.
- OERTEL, D. & YOUNG, E. D. 2004. What's a cerebellar circuit doing in the auditory system? *Trends Neurosci*, 27, 104-10.
- OH, M. C., DERKACH, V. A., GUIRE, E. S. & SODERLING, T. R. 2006. Extrasynaptic membrane trafficking regulated by GluR1 serine 845 phosphorylation primes AMPA receptors for long-term potentiation. *J Biol Chem*, 281, 752-8.
- OHMORI, H. 1985. Mechano-electrical transduction currents in isolated vestibular hair cells of the chick. *J Physiol*, 359, 189-217.
- OLESKEVICH, S., CLEMENTS, J. & WALMSLEY, B. 2000. Release probability modulates short-term plasticity at a rat giant terminal. *J Physiol*, 524 Pt 2, 513-23.
- OLESKEVICH, S. & WALMSLEY, B. 2002. Synaptic transmission in the auditory brainstem of normal and congenitally deaf mice. *J Physiol*, 540, 447-55.
- OLIVER, D. L. 1984. Neuron types in the central nucleus of the inferior colliculus that project to the medial geniculate body. *Neuroscience*, 11, 409-24.

- OLIVER, D. L. & HALL, W. C. 1978. The medial geniculate body of the tree shrew, *Tupaia glis*. I. Cytoarchitecture and midbrain connections. *J Comp Neurol*, 182, 423-58.
- OSEN, K. K. 1969. The intrinsic organization of the cochlear nuclei. *Acta Otolaryngol*, 67, 352-9.
- PALMER, M. J., ISAAC, J. T. & COLLINGRIDGE, G. L. 2004. Multiple, developmentally regulated expression mechanisms of long-term potentiation at CA1 synapses. *J Neurosci*, 24, 4903-11.
- PENNER, M. J. 1983. Variability in matches to subjective tinnitus. *J Speech Hear Res*, 26, 263-7.
- PENNER, M. J. & BURNS, E. M. 1987. The dissociation of SOAEs and tinnitus. *J Speech Hear Res*, 30, 396-403.
- PETRALIA, R. S., WANG, Y. X., ZHAO, H. M. & WENTHOLD, R. J. 1996. Ionotropic and metabotropic glutamate receptors show unique postsynaptic, presynaptic, and glial localizations in the dorsal cochlear nucleus. *J Comp Neurol*, 372, 356-83.
- PETRENKO, A. B., YAMAKURA, T., BABA, H. & SHIMOJI, K. 2003. The role of N-methyl-D-aspartate (NMDA) receptors in pain: a review. *Anesth Analg*, 97, 1108-16.
- PHILLIPS, D. P. 1987. Stimulus intensity and loudness recruitment: neural correlates. *J Acoust Soc Am*, 82, 1-12.
- PHILPOT, B. D., ESPINOSA, J. S. & BEAR, M. F. 2003. Evidence for altered NMDA receptor function as a basis for metaplasticity in visual cortex. *J Neurosci*, 23, 5583-8.
- PIERI, L., SCHAFFNER, R., SCHERSCHLICHT, R., POLC, P., SEPINWALL, J., DAVIDSON, A., MOHLER, H., CUMIN, R., DA PRADA, M., BURKARD, W. P., KELLER, H. H., MULLER, R. K., GEROLD, M., PIERI, M., COOK, L. & HAEFELY, W. 1981. Pharmacology of midazolam. *Arzneimittelforschung*, 31, 2180-201.
- PILATI, N., BARKER, M., PANTELEIMONITIS, S., DONGA, R. & HAMANN, M. 2008. A rapid method combining Golgi and Nissl staining to study neuronal morphology and cytoarchitecture. *J Histochem Cytochem*, 56, 539-50.
- PILATI, N., ISON, M. J., BARKER, M., MULHERAN, M., LARGE, C. H., FORSYTHE, I. D., MATTHIAS, J. & HAMANN, M. 2012a. Mechanisms contributing to central excitability changes during hearing loss. *Proc Natl Acad Sci U S A*, 109, 8292-7.
- PILATI, N., LARGE, C., FORSYTHE, I. D. & HAMANN, M. 2012b. Acoustic over-exposure triggers burst firing in dorsal cochlear nucleus fusiform cells. *Hear Res*, 283, 98-106.
- POLAK, M., ESHRAGHI, A. A., NEHME, O., AHSAN, S., GUZMAN, J., DELGADO, R. E., HE, J., TELISCHI, F. F., BALKANY, T. J. & VAN DE WATER, T. R. 2004. Evaluation of hearing and auditory nerve function by combining ABR,

- DPOAE and eABR tests into a single recording session. *J Neurosci Methods*, 134, 141-9.
- POMA, R., CHAMBERS, H., DA COSTA, R. C., KONYER, N. B., NYKAMP, S., DOBSON, H. & MILGRAM, N. W. 2008. MRI measurement of the canine auditory pathways and relationship with brainstem auditory evoked responses. *Vet Comp Orthop Traumatol*, 21, 238-42.
- PUEL, J. L. 1995. Chemical synaptic transmission in the cochlea. *Prog Neurobiol*, 47, 449-76.
- PUEL, J. L., BOBBIN, R. P. & FALLON, M. 1988. An ipsilateral cochlear efferent loop protects the cochlea during intense sound exposure. *Hear Res*, 37, 65-9.
- PUEL, J. L. & GUITTON, M. J. 2007. Salicylate-induced tinnitus: molecular mechanisms and modulation by anxiety. *Prog Brain Res*, 166, 141-6.
- PUEL, J. L., SAFFIEDINE, S., GERVAIS D'ALDIN, C., EYBALIN, M. & PUJOL, R. 1995. Synaptic regeneration and functional recovery after excitotoxic injury in the guinea pig cochlea. *C R Acad Sci III*, 318, 67-75.
- QIAN, S. M. & DELANEY, K. R. 1997. Neuromodulation of activity-dependent synaptic enhancement at crayfish neuromuscular junction. *Brain Res*, 771, 259-70.
- QUINLAN, E. M., OLSTEIN, D. H. & BEAR, M. F. 1999. Bidirectional, experience-dependent regulation of N-methyl-D-aspartate receptor subunit composition in the rat visual cortex during postnatal development. *Proc Natl Acad Sci U S A*, 96, 12876-80.
- RECANZONE, G. H., SCHREINER, C. E. & MERZENICH, M. M. 1993. Plasticity in the frequency representation of primary auditory cortex following discrimination training in adult owl monkeys. *J Neurosci*, 13, 87-103.
- REID, C. A. & CLEMENTS, J. D. 1999. Postsynaptic expression of long-term potentiation in the rat dentate gyrus demonstrated by variance-mean analysis. *J Physiol*, 518 ( Pt 1), 121-30.
- REYMANN, K. G. & FREY, J. U. 2007. The late maintenance of hippocampal LTP: requirements, phases, 'synaptic tagging', 'late-associativity' and implications. *Neuropharmacology*, 52, 24-40.
- RICH, A. W., XIE, R. & MANIS, P. B. 2010. Hearing loss alters quantal release at cochlear nucleus stellate cells. *Laryngoscope*, 120, 2047-53.
- ROBERTS, L. E., EGGERMONT, J. J., CASPARY, D. M., SHORE, S. E., MELCHER, J. R. & KALTENBACH, J. A. 2010. Ringing ears: the neuroscience of tinnitus. *J Neurosci*, 30, 14972-9.
- ROBERTS, M. T. & TRUSSELL, L. O. 2010. Molecular layer inhibitory interneurons provide feedforward and lateral inhibition in the dorsal cochlear nucleus. *J Neurophysiol*, 104, 2462-73.
- ROBERTSON, D. 1983. Functional significance of dendritic swelling after loud sounds in the guinea pig cochlea. *Hear Res*, 9, 263-78.

- RODRIGUEZ-MORENO, A., BANERJEE, A. & PAULSEN, O. 2010. Presynaptic NMDA Receptors and Spike Timing-Dependent Depression at Cortical Synapses. *Front Synaptic Neurosci*, 2, 18.
- ROSE, J. E., GALAMBOS, R. & HUGHES, J. R. 1959. Microelectrode studies of the cochlear nuclei of the cat. *Bull Johns Hopkins Hosp*, 104, 211-51.
- ROSENHAMER, H. J., LINDSTROM, B. & LUNDBORG, T. 1981. On the use of click-evoked electric brainstem responses in audiological diagnosis. III. Latencies in cochlear hearing loss. *Scand Audiol*, 10, 3-11.
- ROSSI, G. T. & BRITT, R. H. 1984. Effects of hypothermia on the cat brain-stem auditory evoked response. *Electroencephalogr Clin Neurophysiol*, 57, 143-55.
- RUBEL, E. W. & FRITZSCH, B. 2002. Auditory system development: primary auditory neurons and their targets. *Annu Rev Neurosci*, 25, 51-101.
- RUTTIGER, L., CIUFFANI, J., ZENNER, H. P. & KNIPPER, M. 2003. A behavioral paradigm to judge acute sodium salicylate-induced sound experience in rats: a new approach for an animal model on tinnitus. *Hear Res*, 180, 39-50.
- RYDMARK, M. 1981. Nodal axon diameter correlates linearly with internodal axon diameter in spinal roots of the cat. *Neurosci Lett*, 24, 247-50.
- RYUGO, D. K., BAKER, C. A., MONTEY, K. L., CHANG, L. Y., COCO, A., FALLON, J. B. & SHEPHERD, R. K. 2010. Synaptic plasticity after chemical deafening and electrical stimulation of the auditory nerve in cats. *J Comp Neurol*, 518, 1046-63.
- SAFIEDDINE, S. & EYBALIN, M. 1992. Co-expression of NMDA and AMPA/kainate receptor mRNAs in cochlear neurones. *Neuroreport*, 3, 1145-8.
- SALIN, P. A., MALENKA, R. C. & NICOLL, R. A. 1996. Cyclic AMP mediates a presynaptic form of LTP at cerebellar parallel fiber synapses. *Neuron*, 16, 797-803.
- SALVI, R., HENDERSON, D., HAMERNIK, R. P. & PARKINS, C. 1980. VIII nerve response to click stimuli in normal and pathological cochleas. *Hear Res*, 2, 335-42.
- SALVI, R. J., SAUNDERS, S. S., GRATTON, M. A., AREHOLE, S. & POWERS, N. 1990. Enhanced evoked response amplitudes in the inferior colliculus of the chinchilla following acoustic trauma. *Hear Res*, 50, 245-57.
- SALVI, R. J., WANG, J. & DING, D. 2000. Auditory plasticity and hyperactivity following cochlear damage. *Hear Res*, 147, 261-74.
- SATAR, B., KAPKIN, O. & OZKAPTAN, Y. 2003. Evaluation of cochlear function in patients with normal hearing and tinnitus: a distortion product otoacoustic emission study. *Kulak Burun Bogaz Ihtis Derg*, 10, 177-82.
- SAUNDERS, J. C., SCHNEIDER, M. E. & DEAR, S. P. 1985. The structure and function of actin in hair cells. *J Acoust Soc Am*, 78, 299-311.
- SAVASTANO, M. 2008. Tinnitus with or without hearing loss: are its characteristics different? *Eur Arch Otorhinolaryngol*, 265, 1295-300.

- SCHEIBE, F., HAUPT, H., MAZUREK, B. & KONIG, O. 2001. Therapeutic effect of magnesium on noise-induced hearing loss. *Noise Health*, 3, 79-84.
- SCHNEGGENBURGER, R., SAKABA, T. & NEHER, E. 2002. Vesicle pools and short-term synaptic depression: lessons from a large synapse. *Trends Neurosci*, 25, 206-12.
- SCHONEWILLE, M., GAO, Z., BOELE, H. J., VELOZ, M. F., AMERIKA, W. E., SIMEK, A. A., DE JEU, M. T., STEINBERG, J. P., TAKAMIYA, K., HOEBEEK, F. E., LINDEN, D. J., HUGANIR, R. L. & DE ZEEUW, C. I. 2011. Reevaluating the role of LTD in cerebellar motor learning. *Neuron*, 70, 43-50.
- SCHREINER, C. E., READ, H. L. & SUTTER, M. L. 2000. Modular organization of frequency integration in primary auditory cortex. *Annu Rev Neurosci*, 23, 501-29.
- SCHULZ, P. E. 1997. Long-term potentiation involves increases in the probability of neurotransmitter release. *Proc Natl Acad Sci U S A*, 94, 5888-93.
- SCHWARZ, C. & THIER, P. 1999. Binding of signals relevant for action: towards a hypothesis of the functional role of the pontine nuclei. *Trends Neurosci*, 22, 443-51.
- SEKI, S. & EGGERMONT, J. J. 2003. Changes in spontaneous firing rate and neural synchrony in cat primary auditory cortex after localized tone-induced hearing loss. *Hear Res*, 180, 28-38.
- SHADDOCK PALOMBI, P., BACKOFF, P. M. & CASPARY, D. M. 2001. Responses of young and aged rat inferior colliculus neurons to sinusoidally amplitude modulated stimuli. *Hear Res*, 153, 174-80.
- SHEHATA, W. E., BROWNELL, W. E. & DIELER, R. 1991. Effects of salicylate on shape, electromotility and membrane characteristics of isolated outer hair cells from guinea pig cochlea. *Acta Otolaryngol*, 111, 707-18.
- SHEPHERD, R. K. & JAVEL, E. 1997. Electrical stimulation of the auditory nerve. I. Correlation of physiological responses with cochlear status. *Hear Res*, 108, 112-44.
- SHEPHERD, R. K., ROBERTS, L. A. & PAOLINI, A. G. 2004. Long-term sensorineural hearing loss induces functional changes in the rat auditory nerve. *Eur J Neurosci*, 20, 3131-40.
- SHORE, S. E. 2005. Multisensory integration in the dorsal cochlear nucleus: unit responses to acoustic and trigeminal ganglion stimulation. *The European journal of neuroscience*, 21, 3334-3348.
- SHORE, S. E., KOEHLER, S., OLDAKOWSKI, M., HUGHES, L. F. & SYED, S. 2008. Dorsal cochlear nucleus responses to somatosensory stimulation are enhanced after noise-induced hearing loss. *Eur J Neurosci*, 27, 155-68.
- SHORE, S. E., VASS, Z., WYS, N. L. & ALTSCHULER, R. A. 2000. Trigeminal ganglion innervates the auditory brainstem. *J Comp Neurol*, 419, 271-85.
- SHORE, S. E. & ZHOU, J. 2006. Somatosensory influence on the cochlear nucleus and beyond. *Hear Res*, 216-217, 90-9.

- SIMS, R. E. & HARTELL, N. A. 2005. Differences in transmission properties and susceptibility to long-term depression reveal functional specialization of ascending axon and parallel fiber synapses to Purkinje cells. *J Neurosci*, 25, 3246-57.
- SLEPECKY, N., HAMERNIK, R., HENDERSON, D. & COLING, D. 1982. Correlation of audiometric data with changes in cochlear hair cell stereocilia resulting from impulse noise trauma. *Acta Otolaryngol*, 93, 329-40.
- SMYDO, J. 1979. Delayed respiratory depression with fentanyl. *Anesth Prog*, 26, 47-8.
- SOHMER, H., FREEMAN, S., FRIEDMAN, I. & LIDAN, D. 1991. Auditory brainstem response (ABR) latency shifts in animal models of various types of conductive and sensori-neural hearing losses. *Acta Otolaryngol*, 111, 206-11.
- SONG, P., YANG, Y., BARNES-DAVIES, M., BHATTACHARJEE, A., HAMANN, M., FORSYTHE, I. D., OLIVER, D. L. & KACZMAREK, L. K. 2005. Acoustic environment determines phosphorylation state of the Kv3.1 potassium channel in auditory neurons. *Nat Neurosci*, 8, 1335-42.
- SOSSIN, W. S. 2008. Defining memories by their distinct molecular traces. *Trends Neurosci*, 31, 170-5.
- SPANGLER, K. M., CANT, N. B., HENKEL, C. K., FARLEY, G. R. & WARR, W. B. 1987. Descending projections from the superior olivary complex to the cochlear nucleus of the cat. *J Comp Neurol*, 259, 452-65.
- SPOENDLIN, H. 1971. Primary structural changes in the organ of Corti after acoustic overstimulation. *Acta Otolaryngol*, 71, 166-76.
- SPOENDLIN, H. & SCHROTT, A. 1989. Analysis of the human auditory nerve. *Hear Res*, 43, 25-38.
- STARR, A. & ACHOR, J. 1975. Auditory brain stem responses in neurological disease. *Arch Neurol*, 32, 761-8.
- STARR, A., PICTON, T. W., SININGER, Y., HOOD, L. J. & BERLIN, C. I. 1996. Auditory neuropathy. *Brain*, 119 ( Pt 3), 741-53.
- STENT, G. S. 1973. A physiological mechanism for Hebb's postulate of learning. *Proc Natl Acad Sci U S A*, 70, 997-1001.
- STOTLER, W. A. 1953. An experimental study of the cells and connections of the superior olivary complex of the cat. *J Comp Neurol*, 98, 401-31.
- STROUSE, A., ASHMEAD, D. H., OHDE, R. N. & GRANTHAM, D. W. 1998. Temporal processing in the aging auditory system. *J Acoust Soc Am*, 104, 2385-99.
- SULKOWSKI, W. 1988. [Electrophysiologic studies of hearing: current methods in clinical and occupational audiology. I. Brain stem evoked response audiometry (ABR)]. *Med Pr*, 39, 347-58.
- SUMNER, C. J., TUCCI, D. L. & SHORE, S. E. 2005. Responses of ventral cochlear nucleus neurons to contralateral sound after conductive hearing loss. *J Neurophysiol*, 94, 4234-43.

- SUN, W., TANG, L. & ALLMAN, B. L. 2011. Environmental noise affects auditory temporal processing development and NMDA-2B receptor expression in auditory cortex. *Behav Brain Res*, 218, 15-20.
- SUTHERLAND, D. P., GLENDENNING, K. K. & MASTERTON, R. B. 1998a. Role of acoustic striae in hearing: discrimination of sound-source elevation. *Hear Res*, 120, 86-108.
- SUTHERLAND, D. P., MASTERTON, R. B. & GLENDENNING, K. K. 1998b. Role of acoustic striae in hearing: reflexive responses to elevated sound-sources. *Behav Brain Res*, 97, 1-12.
- SZCZEPANIAK, W. S. & MOLLER, A. R. 1996. Evidence of neuronal plasticity within the inferior colliculus after noise exposure: a study of evoked potentials in the rat. *Electroencephalogr Clin Neurophysiol*, 100, 158-64.
- TABUCHI, K., OIKAWA, K., HOSHINO, T., NISHIMURA, B., HAYASHI, K., YANAGAWA, T., WARABI, E., ISHII, T., TANAKA, S. & HARA, A. 2010. Cochlear protection from acoustic injury by inhibitors of p38 mitogen-activated protein kinase and sequestosome 1 stress protein. *Neuroscience*, 166, 665-70.
- TEMMELE, A. F., KIERNER, A. C., STEURER, M., RIEDL, S. & INNITZER, J. 1999. Hearing loss and tinnitus in acute acoustic trauma. *Wien Klin Wochenschr*, 111, 891-3.
- THOMSON, A. M. 2000. Facilitation, augmentation and potentiation at central synapses. *Trends Neurosci*, 23, 305-12.
- THRELKELD, S. W., PENLEY, S. C., ROSEN, G. D. & FITCH, R. H. 2008. Detection of silent gaps in white noise following cortical deactivation in rats. *Neuroreport*, 19, 893-8.
- TONG, H., KOPP-SCHEINPFLUG, C., PILATI, N., ROBINSON, S. W., SINCLAIR, J. L., STEINERT, J. R., BARNES-DAVIES, M., ALLFREE, R., GRUBB, B. D., YOUNG, S. M., JR. & FORSYTHE, I. D. 2013. Protection from noise-induced hearing loss by kv2.2 potassium currents in the central medial olivocochlear system. *J Neurosci*, 33, 9113-21.
- TRUSSELL, L. O. 1999. Synaptic mechanisms for coding timing in auditory neurons. *Annu Rev Physiol*, 61, 477-96.
- TSUCHITANI, C. 1997. Input from the medial nucleus of trapezoid body to an interaural level detector. *Hear Res*, 105, 211-24.
- TSUPRUN, V. & SANTI, P. 2002. Structure of outer hair cell stereocilia side and attachment links in the chinchilla cochlea. *J Histochem Cytochem*, 50, 493-502.
- TUCKER, T. & FETTIPLACE, R. 1995. Confocal imaging of calcium microdomains and calcium extrusion in turtle hair cells. *Neuron*, 15, 1323-35.
- TUREYEN, K., VEMUGANTI, R., SAILOR, K. A., BOWEN, K. K. & DEMPSEY, R. J. 2004. Transient focal cerebral ischemia-induced neurogenesis in the dentate gyrus of the adult mouse. *J Neurosurg*, 101, 799-805.

- TURNER, J., LARSEN, D., HUGHES, L., MOECHARS, D. & SHORE, S. 2012. Time course of tinnitus development following noise exposure in mice. *J Neurosci Res*, 90, 1480-8.
- TURNER, J. G., BROZOSKI, T. J., BAUER, C. A., PARRISH, J. L., MYERS, K., HUGHES, L. F. & CASPARY, D. M. 2006. Gap detection deficits in rats with tinnitus: a potential novel screening tool. *Behavioral neuroscience*, 120, 188-195.
- TURRIGIANO, G. G. 1999. Homeostatic plasticity in neuronal networks: the more things change, the more they stay the same. *Trends in neurosciences*, 22, 221-227.
- TURRIGIANO, G. G. & NELSON, S. B. 2004. Homeostatic plasticity in the developing nervous system. *Nat Rev Neurosci*, 5, 97-107.
- TZOUNOPOULOS, T. 2008. Mechanisms of synaptic plasticity in the dorsal cochlear nucleus: plasticity-induced changes that could underlie tinnitus. *Am J Audiol*, 17, S170-5.
- TZOUNOPOULOS, T., KIM, Y., OERTEL, D. & TRUSSELL, L. O. 2004. Cell-specific, spike timing-dependent plasticities in the dorsal cochlear nucleus. *Nat Neurosci*, 7, 719-25.
- TZOUNOPOULOS, T., RUBIO, M. E., KEEN, J. E. & TRUSSELL, L. O. 2007. Coactivation of pre- and postsynaptic signaling mechanisms determines cell-specific spike-timing-dependent plasticity. *Neuron*, 54, 291-301.
- USUNOFF, K. G., MARANI, E. & SCHOEN, J. H. 1997. The trigeminal system in man. *Adv Anat Embryol Cell Biol*, 136, I-X, 1-126.
- VABNICK, I., MESSING, A., CHIU, S. Y., LEVINSON, S. R., SCHACHNER, M., RODER, J., LI, C., NOVAKOVIC, S. & SHRAGER, P. 1997. Sodium channel distribution in axons of hypomyelinated and MAG null mutant mice. *J Neurosci Res*, 50, 321-36.
- VALE, C. & SANES, D. H. 2002. The effect of bilateral deafness on excitatory and inhibitory synaptic strength in the inferior colliculus. *Eur J Neurosci*, 16, 2394-404.
- VAN DEN HONERT, C. & STYPULKOWSKI, P. H. 1984. Physiological properties of the electrically stimulated auditory nerve. II. Single fiber recordings. *Hear Res*, 14, 225-43.
- VARELA, J. A., SEN, K., GIBSON, J., FOST, J., ABBOTT, L. F. & NELSON, S. B. 1997. A quantitative description of short-term plasticity at excitatory synapses in layer 2/3 of rat primary visual cortex. *J Neurosci*, 17, 7926-40.
- VICKERS, C. A., DICKSON, K. S. & WYLLIE, D. J. 2005. Induction and maintenance of late-phase long-term potentiation in isolated dendrites of rat hippocampal CA1 pyramidal neurones. *J Physiol*, 568, 803-13.
- VORONIN, L. L. & CHERUBINI, E. 2004. 'Deaf, mute and whispering' silent synapses: their role in synaptic plasticity. *J Physiol*, 557, 3-12.
- WANG, C. Y. & DALLOS, P. 1972. Latency of whole-nerve action potentials: influence of hair-cell normalcy. *J Acoust Soc Am*, 52, 1678-86.

- WANG, H., BROZOSKI, T. J., TURNER, J. G., LING, L., PARRISH, J. L., HUGHES, L. F. & CASPARY, D. M. 2009. Plasticity at glycinergic synapses in dorsal cochlear nucleus of rats with behavioral evidence of tinnitus. *Neuroscience*, 164, 747-759.
- WANG, Y. & MANIS, P. B. 2005. Synaptic transmission at the cochlear nucleus endbulb synapse during age-related hearing loss in mice. *J Neurophysiol*, 94, 1814-24.
- WEHR, M. & ZADOR, A. M. 2003. Balanced inhibition underlies tuning and sharpens spike timing in auditory cortex. *Nature*, 426, 442-6.
- WEIL, D., BLANCHARD, S., KAPLAN, J., GUILFORD, P., GIBSON, F., WALSH, J., MBURU, P., VARELA, A., LEVILLIERS, J., WESTON, M. D. & ET AL. 1995. Defective myosin VIIA gene responsible for Usher syndrome type 1B. *Nature*, 374, 60-1.
- WEST, B. T. 2009. Analyzing longitudinal data with the linear mixed models procedure in SPSS. *Eval Health Prof*, 32, 207-28.
- WHITING, B., MOISEFF, A. & RUBIO, M. E. 2009. Cochlear nucleus neurons redistribute synaptic AMPA and glycine receptors in response to monaural conductive hearing loss. *Neuroscience*, 163, 1264-76.
- WILLOTT, J. F., PARHAM, K. & HUNTER, K. P. 1991. Comparison of the auditory sensitivity of neurons in the cochlear nucleus and inferior colliculus of young and aging C57BL/6J and CBA/J mice. *Hear Res*, 53, 78-94.
- WONG, J. C., MILLER, R. L., CALHOUN, B. M., SACHS, M. B. & YOUNG, E. D. 1998. Effects of high sound levels on responses to the vowel "eh" in cat auditory nerve. *Hear Res*, 123, 61-77.
- WRIGHT, E. F. & BIFANO, S. L. 1997. The Relationship between Tinnitus and Temporomandibular Disorder (TMD) Therapy. *The international tinnitus journal*, 3, 55-61.
- WU, C., GOPAL, K., GROSS, G. W., LUKAS, T. J. & MOORE, E. J. 2011. An in vitro model for testing drugs to treat tinnitus. *Eur J Pharmacol*, 667, 188-94.
- YANG, G., LOBARINAS, E., ZHANG, L., TURNER, J., STOLZBERG, D., SALVI, R. & SUN, W. 2007. Salicylate induced tinnitus: behavioral measures and neural activity in auditory cortex of awake rats. *Hear Res*, 226, 244-53.
- YANG, S., SU, W. & BAO, S. 2012. Long-term, but not transient, threshold shifts alter the morphology and increase the excitability of cortical pyramidal neurons. *J Neurophysiol*, 108, 1567-74.
- YANG, S., WEINER, B. D., ZHANG, L. S., CHO, S. J. & BAO, S. 2011. Homeostatic plasticity drives tinnitus perception in an animal model. *Proc Natl Acad Sci U S A*, 108, 14974-9.
- YATES, G. K., CODY, A. R. & JOHNSTONE, B. M. 1983. Recovery of eighth nerve action potential thresholds after exposure to short, intense pure tones: similarities with temporary threshold shift. *Hear Res*, 12, 305-22.

- YI, F., LIU, S. S., LUO, F., ZHANG, X. H. & LI, B. M. 2013. Signaling mechanism underlying alpha -adrenergic suppression of excitatory synaptic transmission in the medial prefrontal cortex of rats. *Eur J Neurosci*.
- ZAJACZKOWSKI, W., FRANKIEWICZ, T., PARSONS, C. G. & DANYSZ, W. 1997. Uncompetitive NMDA receptor antagonists attenuate NMDA-induced impairment of passive avoidance learning and LTP. *Neuropharmacology*, 36, 961-71.
- ZENG, C., NANNAPANENI, N., ZHOU, J., HUGHES, L. F. & SHORE, S. 2009. Cochlear damage changes the distribution of vesicular glutamate transporters associated with auditory and nonauditory inputs to the cochlear nucleus. *J Neurosci*, 29, 4210-7.
- ZENG, F. G., KONG, Y. Y., MICHALEWSKI, H. J. & STARR, A. 2005. Perceptual consequences of disrupted auditory nerve activity. *J Neurophysiol*, 93, 3050-63.
- ZHANG, J. & ZHANG, X. Electrical stimulation of the dorsal cochlear nucleus induces hearing in rats. *Brain Res*, 1311, 37-50.
- ZHANG, J. S. & KALTENBACH, J. A. 1998. Increases in spontaneous activity in the dorsal cochlear nucleus of the rat following exposure to high-intensity sound. *Neurosci Lett*, 250, 197-200.
- ZHANG, S. & OERTEL, D. 1993a. Giant cells of the dorsal cochlear nucleus of mice: intracellular recordings in slices. *J Neurophysiol*, 69, 1398-408.
- ZHANG, S. & OERTEL, D. 1993b. Tuberculoventral cells of the dorsal cochlear nucleus of mice: intracellular recordings in slices. *J Neurophysiol*, 69, 1409-21.
- ZHANG, S. & OERTEL, D. 1994. Neuronal circuits associated with the output of the dorsal cochlear nucleus through fusiform cells. *J Neurophysiol*, 71, 914-30.
- ZHAO, Y., RUBIO, M. E. & TZOUNOPOULOS, T. 2009. Distinct functional and anatomical architecture of the endocannabinoid system in the auditory brainstem. *J Neurophysiol*, 101, 2434-46.
- ZHAO, Y. & TZOUNOPOULOS, T. 2011. Physiological activation of cholinergic inputs controls associative synaptic plasticity via modulation of endocannabinoid signaling. *J Neurosci*, 31, 3158-68.
- ZHENG, Y., MCNAMARA, E., STILES, L., DARLINGTON, C. L. & SMITH, P. F. 2012. Evidence that Memantine Reduces Chronic Tinnitus Caused by Acoustic Trauma in Rats. *Front Neurol*, 3, 127.
- ZHOU, J., NANNAPANENI, N. & SHORE, S. 2007. Vesicular glutamate transporters 1 and 2 are differentially associated with auditory nerve and spinal trigeminal inputs to the cochlear nucleus. *J Comp Neurol*, 500, 777-87.
- ZHOU, J. & SHORE, S. 2004. Projections from the trigeminal nuclear complex to the cochlear nuclei: a retrograde and anterograde tracing study in the guinea pig. *J Neurosci Res*, 78, 901-7.

- ZHOU, J. & SHORE, S. 2006. Convergence of spinal trigeminal and cochlear nucleus projections in the inferior colliculus of the guinea pig. *J Comp Neurol*, 495, 100-12.
- ZORUMSKI, C. F. & IZUMI, Y. 2012. NMDA receptors and metaplasticity: mechanisms and possible roles in neuropsychiatric disorders. *Neurosci Biobehav Rev*, 36, 989-1000.
- ZUCKER, R. S. 1989. Short-term synaptic plasticity. *Annu Rev Neurosci*, 12, 13-31.
- ZUCKER, R. S. 1993. Calcium and transmitter release. *J Physiol Paris*, 87, 25-36.
- ZUCKER, R. S. & REGEHR, W. G. 2002. Short-term synaptic plasticity. *Annu Rev Physiol*, 64, 355-405.